

AD-A064 057

AIR FORCE INST OF TECH WRIGHT-PATTERSON AFB OHIO SCH--ETC F/6 20/8

X-RAY BUILD-UP FACTORS.(U)

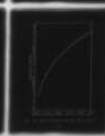
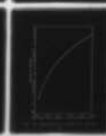
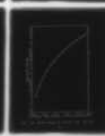
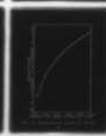
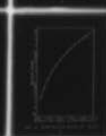
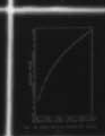
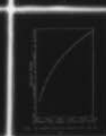
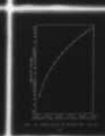
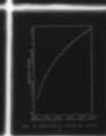
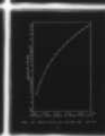
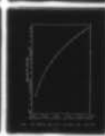
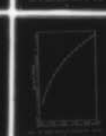
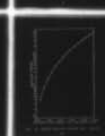
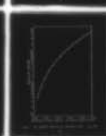
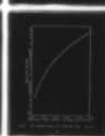
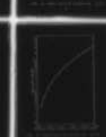
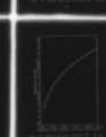
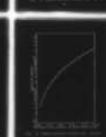
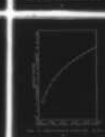
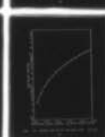
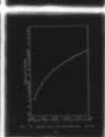
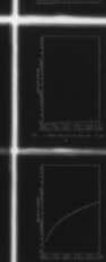
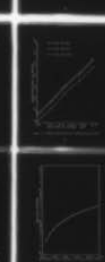
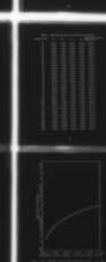
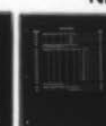
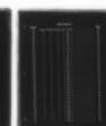
DEC 78 G M KALANSKY

AFIT/GNE/PH/78D-18

UNCLASSIFIED

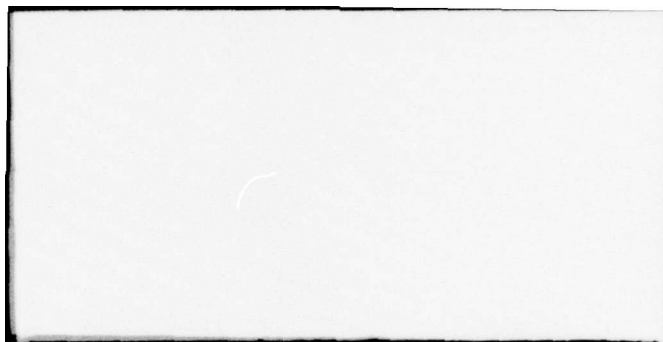
NL

1 OF 2  
AD  
A064 057









AFIT/GNE/PH/78D- 18

(1)

LEVEL

AA064057

DDC FILE COPY

DDC  
RECEIVED  
FEB 1 1979  
A

X-RAY BUILD-UP FACTORS

THESIS

AFIT/GNE/PH/78D- 18

Gary M. Kalansky  
2nd Lt. USAF

Approved for public release; distribution unlimited

14)

6

Presented to the Faculty of the School of Engineering  
of the Air Force Institute of Technology  
Air University  
in Partial Fulfillment of the  
Requirements for the Degree of  
Master of Science

9

12

10

Graduate Nuclear Engineering

11

ADDITION FOR

RTIS	White Section	<input checked="" type="checkbox"/>
BUC	Buff Section	<input type="checkbox"/>
UNANNOUNCED		<input type="checkbox"/>

JUSTIFICATION

BY

DISTRIBUTION/REGISTRATION CODE

DATE

Approved for public release; distribution unlimited.

012 225

Gu

### Preface

Although x-ray air build-up factors can be an extremely important tool in simplifying the x-ray air transport problem, no complete set of build-up factors exists in current literature. Many computer codes also exist to handle the x-ray air transport problem, but none have been used to calculate a complete set of build-up factors.

I have used the least expensive code which retains adequate accuracy to compile a complete set of x-ray air build-up factors. I must acknowledge the help of Dr. C. J. Bridgman for his help in guiding me in the correct direction for making this study a success. I also must acknowledge the help of Major Winfield S. Bigelow who was invaluable in getting the program to run successfully.

## Contents

Preface . . . . .	11
List of Figures . . . . .	v
Abstract. . . . .	ix
I. Introduction. . . . .	1
Purpose . . . . .	1
Theory of Build-up Factors. . . . .	1
Scope . . . . .	2
Plan of Development . . . . .	3
II. Computer Models . . . . .	4
Introduction. . . . .	4
Monte Carlo . . . . .	4
Discrete Ordinates Method . . . . .	6
Moments Method. . . . .	7
III. Program Used. . . . .	8
Literature Search . . . . .	8
Monte Carlo . . . . .	8
Discrete Ordinates Method . . . . .	9
Moments Method. . . . .	9
Description of PHOTDIS. . . . .	9
Input . . . . .	10
IV. Results . . . . .	11
Choice of Options . . . . .	11
Energies. . . . .	11
Ranges. . . . .	11
Graphs of Build-up Factors. . . . .	11
Empirical Build-up Factor Equation. . . . .	13
V. Discussion. . . . .	11
Intrinsic Estimate of the Accuracy. . . . .	121
Comparison of Results to Others . . . . .	121
Introduction. . . . .	121
Monte Carlo . . . . .	122
Discrete Ordinates Method . . . . .	137
Bigelow . . . . .	137
VI. Conclusion. . . . .	138
Purpose and Scope . . . . .	138
Results and Discussion. . . . .	138
Recommendations and Summary . . . . .	138
Bibliography. . . . .	142

## Contents

Appendix A: Solution of the Boltzmann Transport Equation by the Moments Method . . . . .	144
Appendix B: Sample Input and Program Listing . . . . .	150



# List of Figures

<u>Figure</u>		<u>Page</u>
0	Mean-free-paths for Various Altitudes . . . . .	15
1	Energy Build-up Factors for 12 keV. . . . .	16
2	" " " " 14 " . . . . .	17
3	" " " " 16 " . . . . .	18
4	" " " " 18 " . . . . .	19
5	" " " " 20 " . . . . .	20
6	" " " " 22 " . . . . .	21
7	" " " " 24 " . . . . .	22
8	" " " " 26 " . . . . .	23
9	" " " " 28 " . . . . .	24
10	" " " " 30 " . . . . .	25
11	" " " " 32 " . . . . .	26
12	" " " " 34 " . . . . .	27
13	" " " " 36 " . . . . .	28
14	" " " " 38 " . . . . .	29
15	" " " " 40 " . . . . .	30
16	" " " " 42 " . . . . .	31
17	" " " " 44 " . . . . .	32
18	" " " " 46 " . . . . .	33
19	" " " " 48 " . . . . .	34
20	" " " " 50 " . . . . .	35
21	" " " " 52 " . . . . .	36
22	" " " " 54 " . . . . .	37
23	" " " " 56 " . . . . .	38
24	" " " " 58 " . . . . .	39
25	" " " " 60 " . . . . .	40
26	" " " " 62 " . . . . .	41
27	" " " " 64 " . . . . .	42
28	" " " " 66 " . . . . .	43
29	" " " " 68 " . . . . .	44
30	" " " " 70 " . . . . .	45
31	" " " " 72 " . . . . .	46
32	" " " " 74 " . . . . .	47
33	" " " " 76 " . . . . .	48

# List of Figures

<u>Figure</u>		<u>Page</u>
34	Energy Build-up Factors for 78 keV. . . . .	49
35	" " " " 80 " . . . . .	50
36	" " " " 82 " . . . . .	51
37	" " " " 84 " . . . . .	52
38	" " " " 86 " . . . . .	53
39	" " " " 88 " . . . . .	54
40	" " " " 90 " . . . . .	55
41	" " " " 92 " . . . . .	56
42	" " " " 94 " . . . . .	57
43	" " " " 96 " . . . . .	58
44	" " " " 98 " . . . . .	59
45	" " " " 100 " . . . . .	60
46	" " " " 105 " . . . . .	61
47	" " " " 110 " . . . . .	62
48	" " " " 115 " . . . . .	63
49	" " " " 120 " . . . . .	64
50	" " " " 125 " . . . . .	65
51	" " " " 130 " . . . . .	66
52	" " " " 135 " . . . . .	67
53	" " " " 140 " . . . . .	68
54	" " " " 145 " . . . . .	69
55	" " " " 150 " . . . . .	70
56	" " " " 155 " . . . . .	71
57	" " " " 160 " . . . . .	72
58	" " " " 165 " . . . . .	73
59	" " " " 170 " . . . . .	74
60	" " " " 175 " . . . . .	75
61	" " " " 180 " . . . . .	76
62	" " " " 185 " . . . . .	77
63	" " " " 190 " . . . . .	78
64	" " " " 195 " . . . . .	79
65	" " " " 200 " . . . . .	80
66	" " " " 210 " . . . . .	81
67	" " " " 220 " . . . . .	82



# List of Figures

<u>Figure</u>		<u>Page</u>
68	Energy Build-up Factors for 230 keV. . . . .	83
69	" " " " 240 " . . . . .	84
70	" " " " 250 " . . . . .	85
71	" " " " 260 " . . . . .	86
72	" " " " 270 " . . . . .	87
73	" " " " 280 " . . . . .	88
74	" " " " 290 " . . . . .	89
75	" " " " 300 " . . . . .	90
76	" " " " 310 " . . . . .	91
77	" " " " 320 " . . . . .	92
78	" " " " 330 " . . . . .	93
79	" " " " 340 " . . . . .	94
80	" " " " 350 " . . . . .	95
81	" " " " 360 " . . . . .	96
82	" " " " 370 " . . . . .	97
83	" " " " 380 " . . . . .	98
84	" " " " 390 " . . . . .	99
85	" " " " 400 " . . . . .	100
86	" " " " 410 " . . . . .	101
87	" " " " 420 " . . . . .	102
88	" " " " 430 " . . . . .	103
89	" " " " 440 " . . . . .	104
90	" " " " 450 " . . . . .	105
91	" " " " 460 " . . . . .	106
92	" " " " 470 " . . . . .	107
93	" " " " 480 " . . . . .	108
94	" " " " 490 " . . . . .	109
95	" " " " 500 " . . . . .	110
96	" " " " 550 " . . . . .	111
97	" " " " 600 " . . . . .	112
98	" " " " 650 " . . . . .	113
99	" " " " 700 " . . . . .	114
100	" " " " 750 " . . . . .	115
101	" " " " 800 " . . . . .	116

# List of Figures

<u>Figure</u>		<u>Page</u>
102	Energy Build-up Factors for 850 keV . . . . .	117
103	" " " " 900 " . . . . .	118
104	" " " " 950 " . . . . .	119
105	" " " " 1000 " . . . . .	120
106	Comparison of Energy Build-up Factors at 10 Mean-free-paths. . . . .	123
107	Comparison of Energy Build-up Factors for 60 keV. . . . .	125
108	" " " " " " 20 " . . . . .	126
109	" " " " " " 40 " . . . . .	127
110	" " " " " " 100 " . . . . .	128
111	" " " " " " 20 " . . . . .	129
112	" " " " " " 40 " . . . . .	130
113	" " " " " " 60 " . . . . .	131
114	" " " " " " 90 " . . . . .	132
115	" " " " " " 120 " . . . . .	133
116	" " " " " " 150 " . . . . .	134
117	" " " " " " 200 " . . . . .	135
118	" " " " " " 300 " . . . . .	136
119	" " " " " " . . . . .	
	at 10 Mean-free-paths. . . . .	139
120	Energy Build-up Factors for 12-120 keV . . . . .	140
121	" " " " 150-1000 keV . . . . .	141

Abstract

↘ This report is a compilation of time integrated x-ray energy build-up factors from a monoenergetic point source in infinite homogeneous air. These factors were computed by the use of PHOTDIS, a moments method computer code, and performed on a CDC 6600. This code was chosen after a literature search and a review of many computer models. Energies from 12 keV to 1000 keV and ranges from 1 mean-free-path to 15 mean-free-paths are considered. All results are presented on semi-log graphs with each graph containing one energy. This program is estimated to have an error of at most 20%. The results are compared to Monte Carlo and Discrete Ordinates calculations. Even though the moments calculations do not completely agree with any of the Monte Carlo calculations, the moments calculation agree with the average of the Monte Carlo calculations. A complete derivation of the moments method from the Boltzmann Transport Equation is also included. ↙

## X-RAY BUILD-UP FACTORS

### I Introduction

#### Purpose

The purpose of this report is to provide one complete set of time integrated monoenergetic x-ray energy build-up factors in infinite homogeneous air. This study has used the moments method in the form of the program PHOTDIS (Ref 1). This program is written in Fortran and was run on the CDC 6600 of the Aeronautical Systems Division at Wright-Patterson Air Force Base, Ohio. This study was undertaken because of the lack of a complete set of these build-up factors.

#### Theory of Build-up Factors

The normal treatment of photon attenuation in an absorbing medium at range  $r$  from an isotropic monoenergetic point source is

$$F(r) = \frac{Se^{-\mu r}}{4\pi r^2} \quad (1)$$

where

$F(r)$  is the energy fluence at distance  $r$  in Joules/m<sup>2</sup> (or Cal/cm<sup>2</sup>)

$S$  is the total energy emitted by the monoenergetic source in Joules (or Calories)

$\mu$  is the total macroscopic cross section in m<sup>-1</sup> (or cm<sup>-1</sup>)

$r$  is the distance of interest in meters (or centimeters)

This equation accurately describes the fluence if the x-rays interact only by photoelectric absorption. So this equation is accurate for low energy x-rays, energy below about 12 keV where photoelectric absorption dominates.

For x-rays of energy above 12 keV, Compton scatter plays an increasingly important part. Therefore, Eq (1) must be modified to account for the Compton scatter. One possible modification is

$$F(r) = \frac{BSc^{-\mu r}}{4\pi r^2} \quad (2)$$

where B is the energy dependent build-up factor, or the correction factor to account for Compton scatter.

Eq (2) assumes a monoenergetic source which is not realistic in nuclear effects calculations. However the real polyenergetic sources can be treated by using Eq (2) in a multienergy group calculation:

$$F(r) = \sum \frac{B_i S_i e^{-\mu_i r}}{4\pi r^2} \quad (3)$$

where  $S_i$  represents the fraction of the continuous source energy spectra emitted within the bounds of energy group i. Eq (2) also assumes that the x-ray fluence varies only with one spatial coordinate which becomes increasingly invalid at larger energies and higher altitudes. This assumption is made to prevent the calculational complication of a two dimensional geometry. However, two dimensional effects can be approximated by rearranging Eq (3) into a  $4\pi r^2$  fluence and employing mass integral scaling (Ref 2):

$$4\pi r^2 F = \sum S_i B_i \exp\left(-\int_0^r \mu_i r' dr'\right) \quad (4)$$

These equations also ignore the time variable of the x-ray because most targets respond to total x-ray dose not x-ray dose rate. Finally, the calculations for build-up factors are presented in terms of mean-free-path which makes them applicable to homogeneous air at any altitude.

#### Scope

Due to the limits of the convergence of the moments method program, the



ranges considered were from one to 15 mean-free-paths of the source photon energy. The build-up factor for energies below about 12 keV is nearly one, so energies below 12 keV were not investigated. This program does not include pair production, so energies used in the calculations are all below 1000 keV. To facilitate the users' evaluation of the accuracy of the build-up factors presented here, comparison to other calculations are also included in this report.

#### Plan of Development

This report starts with an explanation of computer models which are used in x-ray transport problems. A discussion of the program PHOTDIS follows. The graphs of the build-up factors for each energy are the main portion of this report. The discussion of the results contain a comparison to others who have made x-ray transport calculations. Finally a detailed description of the derivation of the moments equation and the reconstruction of the energy fluence can be found in the appendix.

## II Computer Models

### Introduction

Three numerical models have evolved which are applicable to compute total fluence of x-rays where energy is greater than 12 keV. The three models are Monte Carlo, Discrete Ordinates, and the Moments Method. Each model has advantages and disadvantages which will be discussed along with a brief description of each method. Since the moments method was selected as the model used in this project, it will be presented in depth in Appendix A as well as the brief overview in this section.

### Monte Carlo

In the Monte Carlo method, a photon leaving the source is traced through the medium of interest. As the photon is traced, a record is kept of its energy, direction and position. Compton, pair production and photoelectric events are experienced by the photons in accordance with the cross sections for these events at a rate determined by statistical probability. The photon is followed until it is absorbed or until it passes out of the area of interest. Many photons are traced by this method. At a predetermined distance  $r$ , the energy of all the photons reaching that distance is added together and divided by  $4\pi r^2$ . This is the total energy fluence at that distance. To minimize computations without sacrificing accuracy, statistical improving schemes are used. These schemes are used to sample only "important" photons, which are determined by a "weight". The weight of a photon is an artificial biasing which is introduced while tracing the photon. Several statistical improving schemes are statistical estimations, exponential transformations, Russian Roulette and non-absorptive weighting. (Ref 3:19-20)

Statistical estimation may be a last-flight estimator which calculates

the probability that a photon which has just undergone a Compton event will travel a predetermined distance before absorption. Another statistical estimation scheme is next-event-estimator. This scheme calculates the probability that a photon which has just scattered will reach a predetermined distance after it is involved in another scatter. (Ref 3:20)

Exponential transformation biases the distance to the next event to increase the probability of a long flight. The weight associated with a photon is adjusted to correct for the bias. (Ref 3:21)

If a photon has lost so much of its weight through adjustment for biasing, Russian Roulette may be used. A random number is generated and compared with a survival probability, which is also less than one. If the random number, which is also less than one, is less than the survival probability, the weight is multiplied by the reciprocal of the survival probability and the tracking is continued. If the random number is greater than the survival probability, the tracking is discontinued. (Ref 3:21)

In non-absorptive weighting, at each event the photon's weight is scaled by a probability that the photon will not be absorbed. The scaling factor is the scattering cross section divided by the total cross section. When weight correction reduces the photon's ability to contribute to a very small amount, Russian Roulette is used. (Ref 3:22)

The accuracy of the answer depends on many factors. The statistical fluctuation produced by the stochastic nature of the method along with the type of weighting used are two major factors. Other factors affecting the accuracy are the cross sections and the number of photon tracked (histories). The number of histories is limited by the size of the computer and the amount of computer time and money spent on the problem. But the Monte Carlo method can treat a complex geometry consisting of many different materials.



### Discrete Ordinates Method

The Discrete Ordinates method deals with a numerical solution to the Boltzmann transport equation. The Boltzmann transport equation (which also describes time independent fluence) is

$$\Omega \cdot \nabla F(r, \Omega, E) + \mu^t F(r, \Omega, E) = S(r, \Omega, E) + \iint \mu^s F(r, \Omega', E') d\Omega' dE' \quad (5)$$

where

$F$  is the fluence

$\Omega$  is the direction vector

$r$  is the coordinates

$E$  is the energy

$S$  is the source function

$\mu^t$  is the total cross section

$\mu^s$  is the scatter cross section from direction  $\Omega'$  and energy  $E'$  to direction  $\Omega$  and energy  $E$

The most popular Discrete Ordinates programs solve the Boltzmann transport equation numerically by a method known as the  $S_N$  method. The  $S_N$  method expands the scatter cross section in the integral term in Legendre polynomials. By using the addition theorem for the Legendre polynomial, that integral reduces to one in energy and one in angle. Numerical quadrature is employed to evaluate the angle integral. The equation is separated into a group of equations by replacing the energy integral with a summation of group to group scatter terms. Since the resulting equations are differential equations, finite difference approximations are used to reduce these equations to a group of coupled algebraic equations. The numerical quadrature and finite difference approximations introduce truncation error. On the other hand if more terms in the quadrature and a finer mesh are used, round-off error is increased and the answer may not converge. So some error is unavoidable. The computation takes less time than Monte Carlo computations

but can not handle complex geometries.

#### Moments Method

The Moments method also produces a solution to the Boltzmann Transport Equation by numerical methods but involves more analytical reduction than does Discrete Ordinates. In this method, the scatter cross section and the fluence in all terms of Eq (5) are expanded in Legendre polynomials. Using the addition theorem, the scatter multiple integral reduces to a single integral in energy. By multiplying through the equation by the appropriate powerset directional angle factors and integrating each term over direction, the equation is reduced to a differential-integro equation set. By multiplying this set of equations by the spatial moments and integrating over all space, the equations reduce to the moments equations. The moments equations are recursive and because of the integration in energy, they must be evaluated by numerical quadrature in energy space. Once the moments have been calculated, the fluence is reconstructed by means of summing all the moments of a particular energy after they have been multiplied by a set of biorthogonal polynomials. A complete derivation of the moments equation and the reconstruction of the fluence is given in Appendix A. (Ref 1:3-14)

Since only a finite number of moments can be used, this method is also limited in accuracy. But depending on how many moments are used, the error can be limited. Thus a predetermined accuracy can be reached. This method is also limited to the time independent system and to a simple geometry and a homogeneous infinite medium. The time used to evaluate the fluence by this method is usually less than either Monte Carlo or Discrete Ordinates in such simple geometries.

### III Program Used

#### Literature Search

Monte Carlo. Many Monte Carlo programs were considered for this compilation of x-ray build-up factors. The MASTER program file (Ref 4) is a set of programs and cross section libraries used to solve radiation transport problems. The programs in this file are FASTER, BETA and TEMPER. All the programs can handle complex geometry, nonlinear and time dependent photon fluences. But the generality of this file makes it difficult for the user not acquainted with this file to provide data for a problem. The DART and DART II codes (Ref 5 and 6) are codes which handle time dependent photon transport in air. DART is a one dimensional code which assumes homogeneous air, while DART II assumes nonhomogeneous air and takes into account the curvature of the earth. DART II is especially suited for high altitude air transport. The THISTLE code (Ref 7) is a time dependent code which describes x-ray transport in exponential atmosphere.

The MORSE code (Ref 8) is a gamma ray transport code which uses multigroup cross sections. This code can handle three or one dimensional problems. It treats the atmosphere as a homogeneous medium and the answers are in a time dependent form. The HAM code (Ref 9) is a modified MORSE code which incorporates varying air density at high altitudes and to take into account the curvature of the earth. One of the most popular Monte Carlo codes used for x-ray radiation transport is the PHOTRAN code (Ref 10,11 and 12). This code handles time dependent radiation transport and calculates energy deposition, photon flux, electron flux or tissue equivalent dose. It can consider energies from zero to 100 MeV taking into account coherent and incoherent scattering, photoelectric effect, pair production, fluorescent and annihilation radiation. It can consider three dimensional geometry in

a homogeneous medium. ANDY is a series of transport codes (Ref 13) designed for time dependent photon transport which can handle three dimensional homogeneous atmosphere.

All the codes listed above were considered but rejected because of the amount of time and money involved in implementing and running these programs.

Discrete Ordinates. DTFXRAY is a one dimensional code (Ref 14) using Discrete Ordinates method of solution. This code does not treat time dependence and assumes a homogeneous atmosphere. ANISN is a Discrete Ordinates code (Ref 3) which treats a homogeneous atmosphere in one dimension. It does not handle time dependence.

Moments Method. PHOTDIS is a one dimensional code (Ref 1) for computing transport in a homogeneous atmosphere. It does not handle time dependence but it does compute the build-up factors. This program was selected because of the ease of input and the direct output of build-up factors. The speed of this program was another factor in its selection since time dependence and inhomogeneous atmosphere are not considered. Another factor for choosing a moments method program is the approximation of the error through convergence analysis which is not available from the other methods of solution.

#### Description of PHOTDIS

The program PHOTDIS consists of two phases, Phase I and Phase II. In Phase I, the moments for the scattered fluence are calculated. Most of Phase I is concerned with calculating the integral in Eq (28), which is found in Appendix A. Phase II reconstructs the fluence from the moments using Eqs (31), (32) and (33). The majority of Phase II is a numerical calculation of Eq (33), which is made difficult since only values of  $W_{ii}$  are known. At the end of Phase II, the build-up factor is calculated using Eqs (34), (35) and (36). A more complete description of the program can be



found in Ref 1.

### Input

The input to the program consists of 12 different sets of data. They are:

- 1) Klein-Nishina, Photoelectric and Compton scatter cross section as a function of energy.
- 2) Parameter determining if mesh parameters are to be input.
- 3) Altitude.
- 4) Density of the air at the altitude considered.
- 5) Energy above which no correction is to be made to the Klein-Nishina scattering equation.
- 6) Parameters determining which phases are to be run.
- 7) Number of space points, angular variables and a parameter determining if angular fluence is to be calculated.
- 8) Number of moments to be used.
- 9) Source energy and source strength.
- 10) Mesh parameters.
- 11) Angles at which the fluence is to be calculated.
- 12) Distance at which build-up factors are to be calculated.

The cross sections used for this study are from UCRL-50174 (Ref 13) and from AFWL-TR-67-11 (Ref 14). A listing of the code and a sample input are furnished in Appendix B.

## IV Results

### Choice of Options

Energies. As stated in Section I, the magnitude of the build-up factor is related to the amount of Compton scatter. For energies where Compton scatter is a major contributor to the total cross section, the build-up factor is greater than one. Therefore, this study begins at 12 keV since below that energy, Compton scatter is negligible. For energies below 12 keV, Eq (1) can be used since the build-up factor is approximately one. The Compton scatter cross section begins to decrease for energies above 100 keV. This decrease continues until the Compton scatter is very low, but is the only major contributor to the total cross section. Pair production, which is zero below 1020 keV, increases very rapidly just above 1020 keV and quickly becomes the major factor in the total cross section. Since the program does not handle pair production, this study terminates at 1000 keV.

Ranges. For each energy, calculations were made of the build-up factor for a distance from the source from one to 15 mean-free-paths in increments of one mean-free-path. The answers are not converged well beyond 15 mean-free-paths. The build-up factors at the various distances in mean-free-paths are valid at any altitude, but the mean-free-path varies with altitude. So at any altitude of interest, the build-up factor can be obtained for any distance in meters by converting the range in meters to mean-free-paths at any altitude. Fig 0 shows the variance of the mean-free-path with altitude for different energies.

### Graphs of Build-up Factors

Fig 1 to Fig 105 are the graphs of the build-up factors for various energies ranging from 12 keV to 1000 keV. For energies between 12 and 100

keV, the increment is 2 keV. For energies between 100 and 200 keV, the increment is 5 keV. For energies between 200 and 500 keV, the increment is 10 keV and for energies higher than 500 keV, the increment is 50 keV. On each graph, the points shown are the calculated results with the curve fitted by spline-fitting technique performed by the computer and drawn by a Calcomp plotter Model 765.

#### Empirical Build-up Factor Equation

Taylor (Ref 19) has developed a simple equation to describe build-up factors previously calculated. This equation is

$$B = A_1 e^{c_1 y} + A_2 e^{c_2 y} \quad (6)$$

where

y is number of mean-free-paths of source energy

$$A_2 = 1 - A_1$$

$A_1, c_1$  and  $c_2$  are constants to be determined from calculated Build-up factors.

A calculation was performed using the build-up factors obtained in this study to obtain these constants. A list of these constants and the maximum percent difference is shown in Table I. (Text continues on page 121)

Table I. Constants for empirical build-up factor equation

Energy in keV	$A_1$	$A_2$	$C_1$	$C_2$	Maximum % difference below 8 MFP
12	-0.227	1.227	-0.400	0.000	0.35 %
14	-0.370	1.370	-0.400	0.000	0.89 %
16	-0.323	1.323	-0.680	0.020	1.78 %
18	-0.634	1.634	-0.460	0.020	0.91 %
20	-1.072	2.072	-0.360	0.020	2.71 %
22	-1.048	2.048	-0.480	0.040	2.90 %
24	-1.740	2.748	-0.340	0.040	0.75 %
26	-2.673	3.673	-0.260	0.040	1.85 %
28	-2.664	3.664	-0.300	0.060	3.87 %
30	-6.038	7.038	-0.140	0.040	2.90 %
32	-8.805	9.805	-0.100	0.040	1.45 %
34	-8.504	9.504	-0.100	0.060	1.63 %
36	-75.83	76.83	0.000	0.020	0.97 %
38	-20.03	21.03	-0.020	0.060	3.77 %
40	-16.94	17.94	-0.020	0.080	6.93 %
45	14.59	-13.59	0.120	-0.020	13.7 %
50	11.31	-10.31	0.160	-0.040	21.1 %
55	109.2	-108.2	0.120	0.100	18.0 %
60	-11.05	12.05	0.000	0.200	26.6 %
70	-114.1	115.1	0.140	0.160	25.7 %
80	-113.1	114.1	0.160	0.180	27.6 %
100	-10.93	11.93	0.060	0.260	36.0 %
120	-8.153	9.153	0.020	0.280	39.1 %
150	13.14	-12.14	0.260	0.100	36.3 %
200	-88.92	89.92	0.180	0.200	33.1 %
250	-6.308	7.308	0.000	0.260	39.9 %
300	19.89	-18.89	0.200	0.120	33.1 %
350	72.37	-71.37	0.160	0.140	31.2 %
400	-6.063	7.063	0.000	0.220	35.1 %
500	16.29	-15.29	0.160	0.080	28.8 %
600	-57.58	57.58	0.100	0.120	25.7 %
750	-17.20	18.20	0.060	0.120	22.6 %



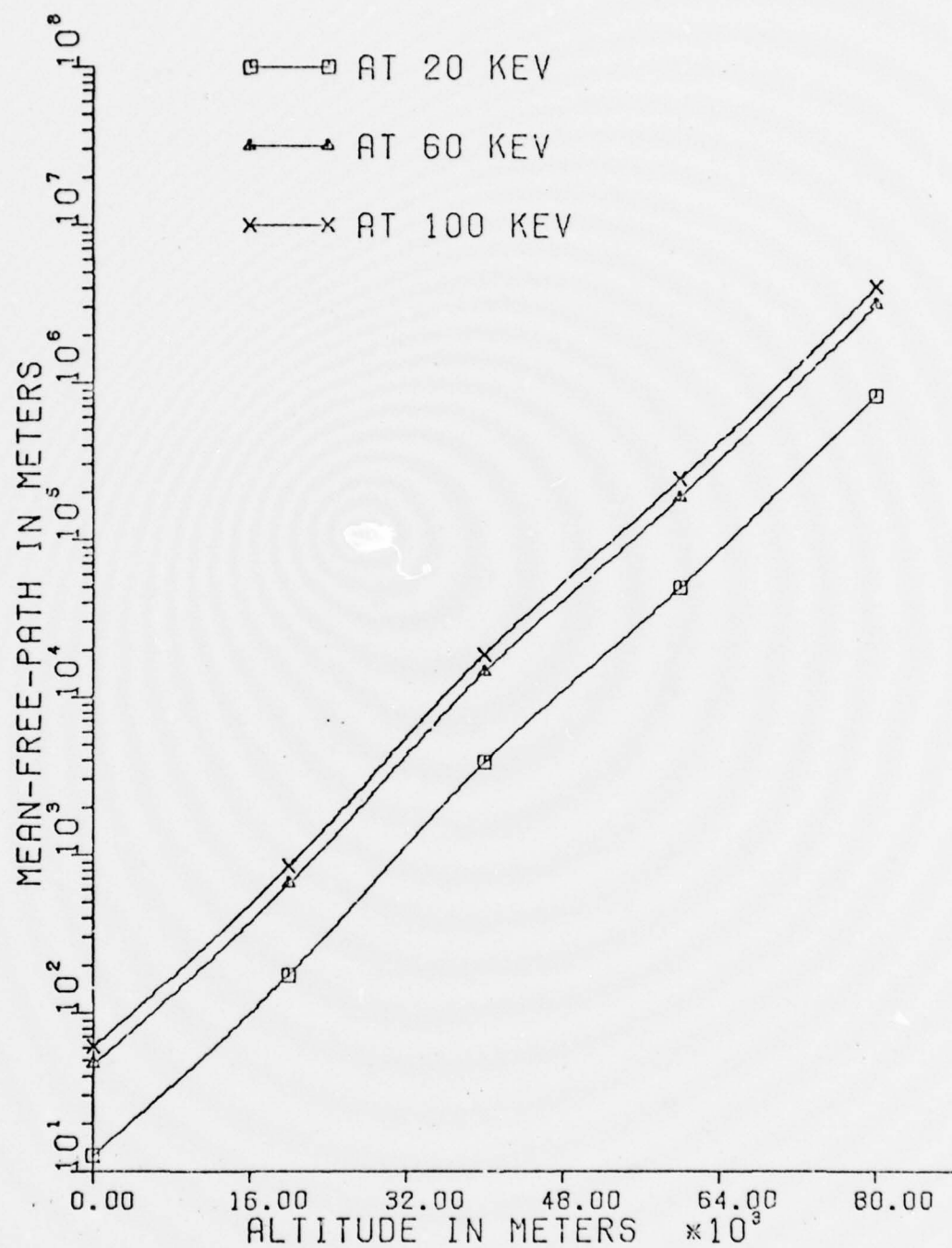


FIG. 0 MEAN-FREE-PATH AT VARIOUS ALTITUDE

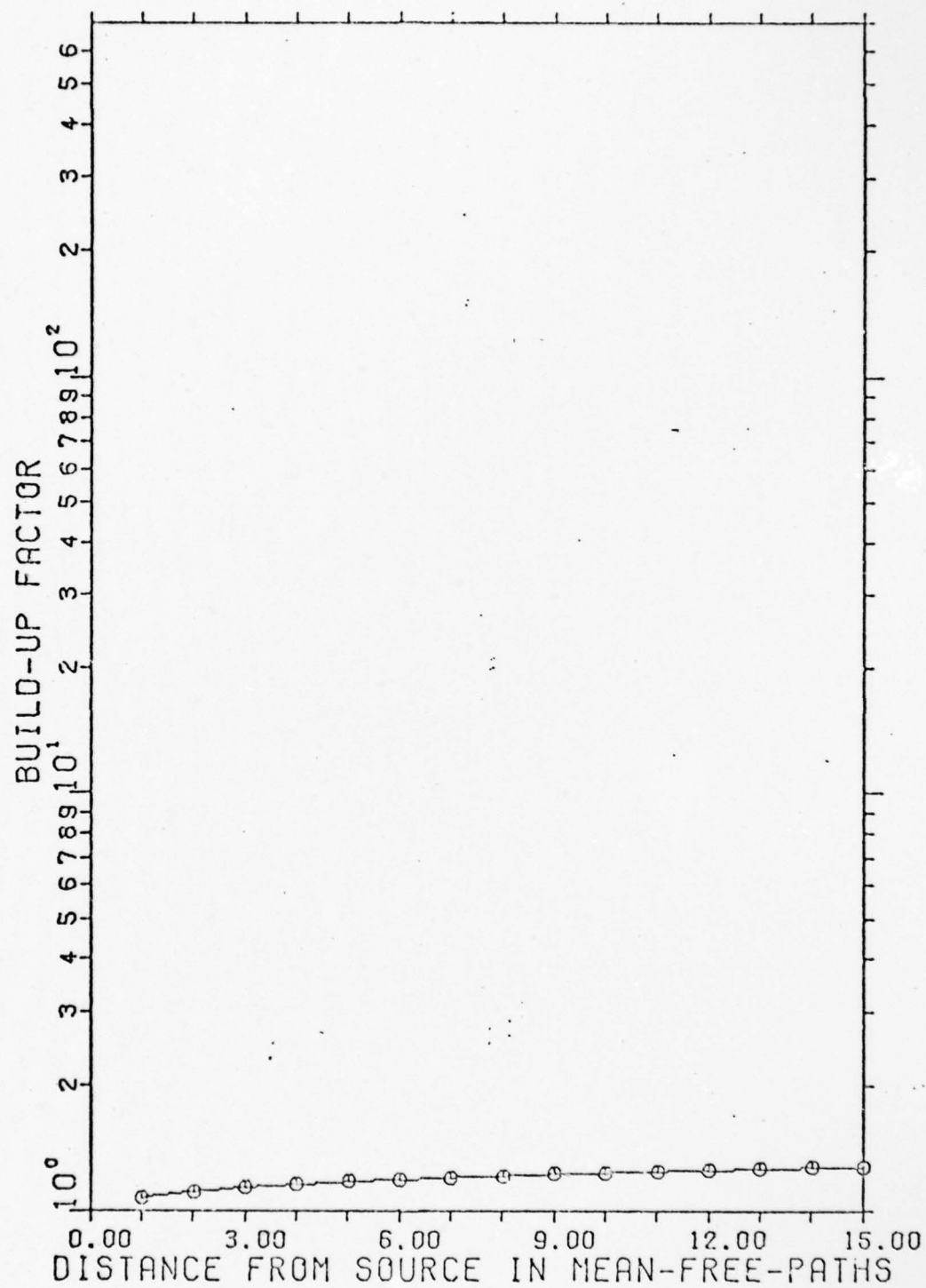


FIG. 1 ENERGY BUILD-UP FACTORS FOR 12 KEV

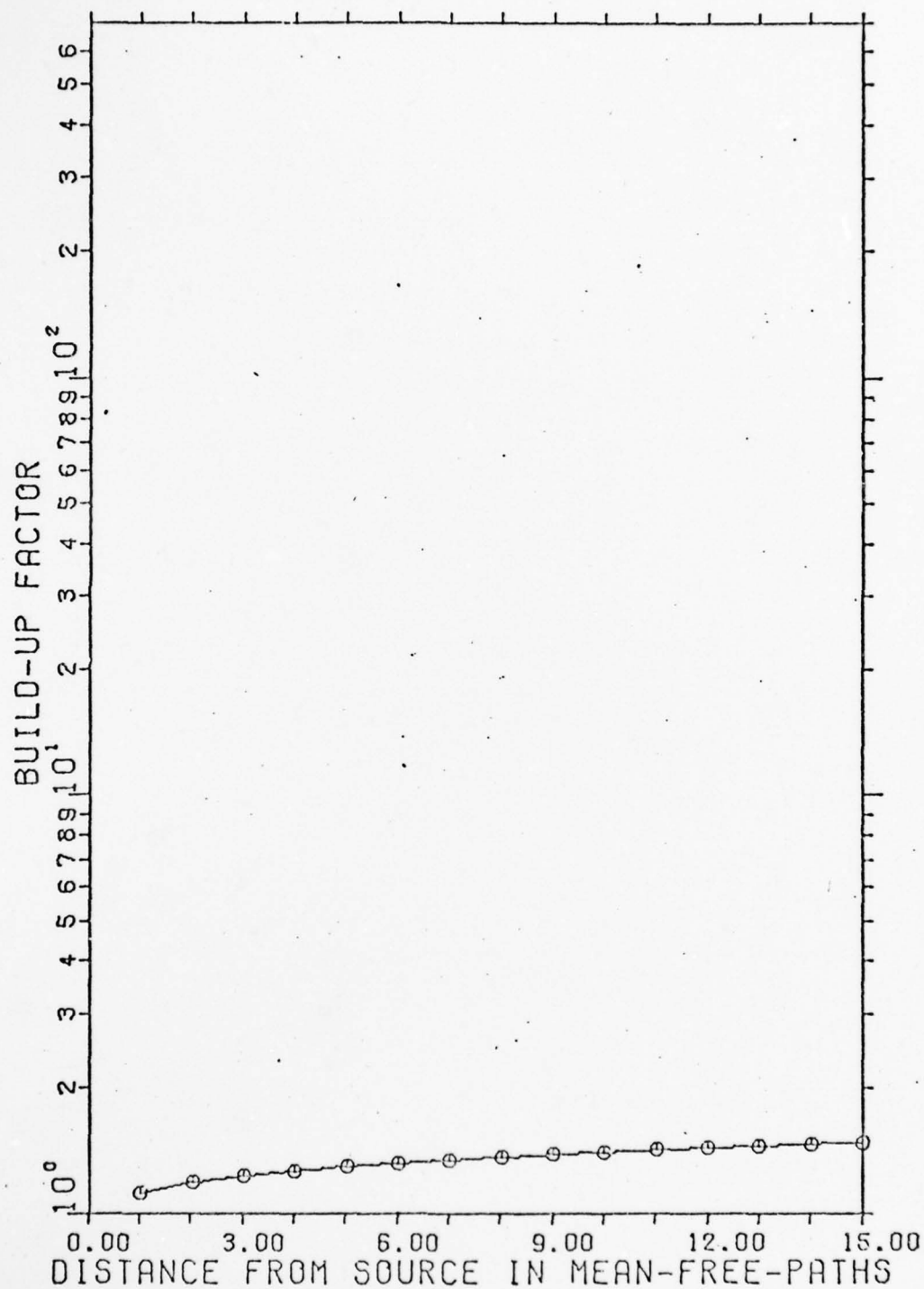


FIG. 2 ENERGY BUILD-UP FACTORS FOR 14 KEV

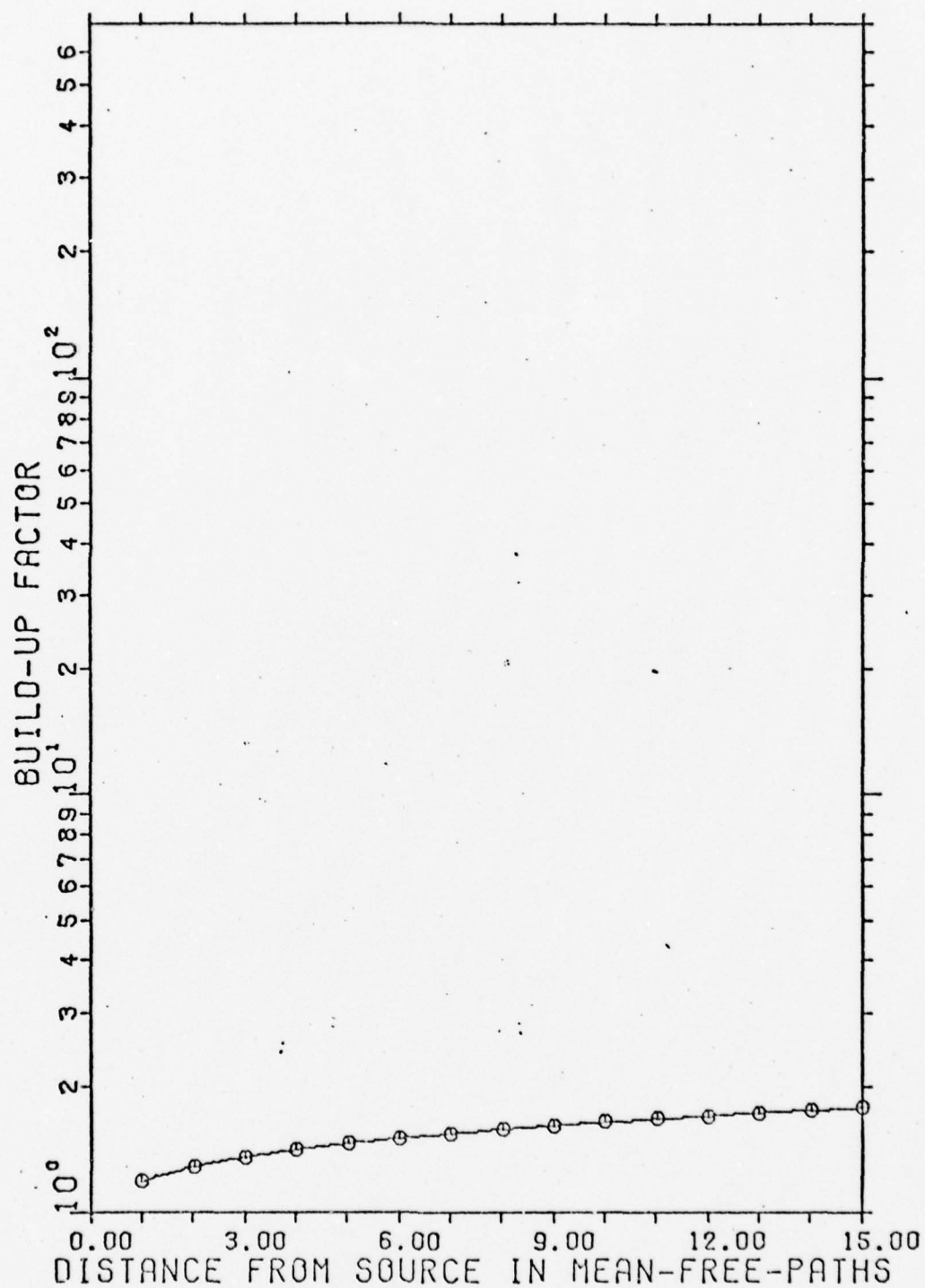


FIG. 3 ENERGY BUILD-UP FACTORS FOR 16 KEV

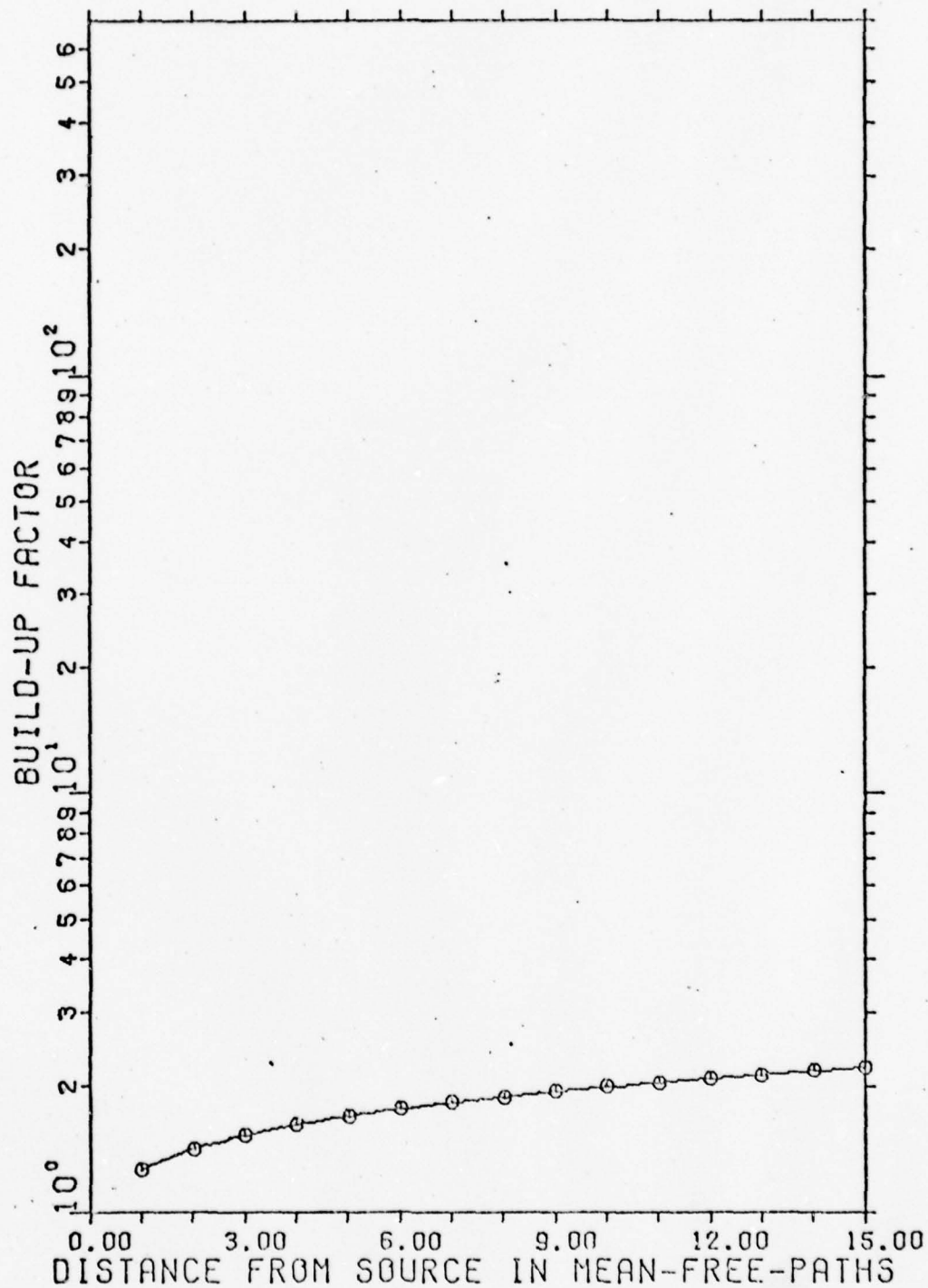


FIG. 4 ENERGY BUILD-UP FACTORS FOR 18 KEV

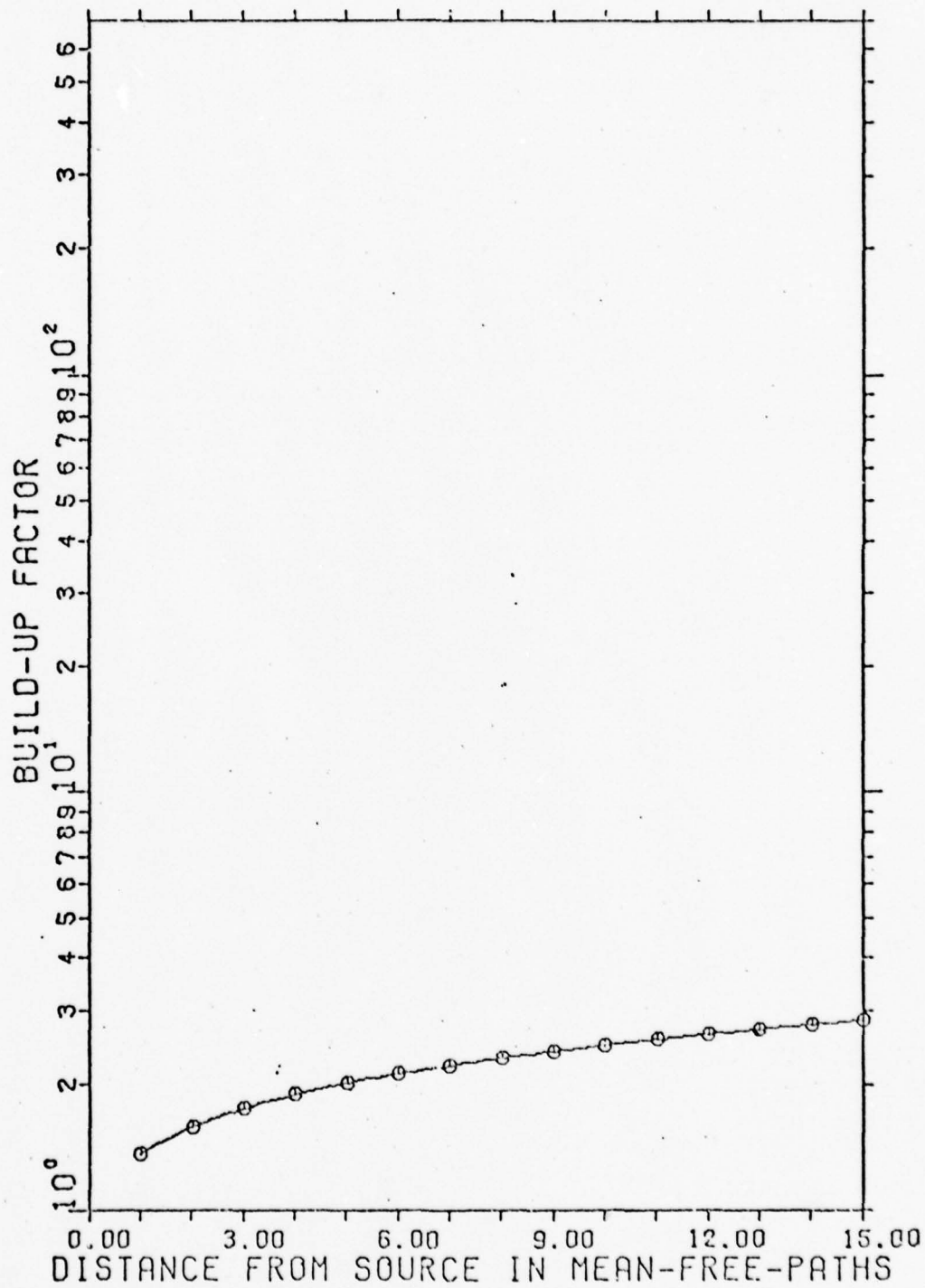


FIG. 5 ENERGY BUILD-UP FACTORS FOR 20 KEV



error is increased and the answer may not converge. The computation takes less time than Monte Carlo computations unavoidable. The computation takes less time than Monte Carlo computations

6

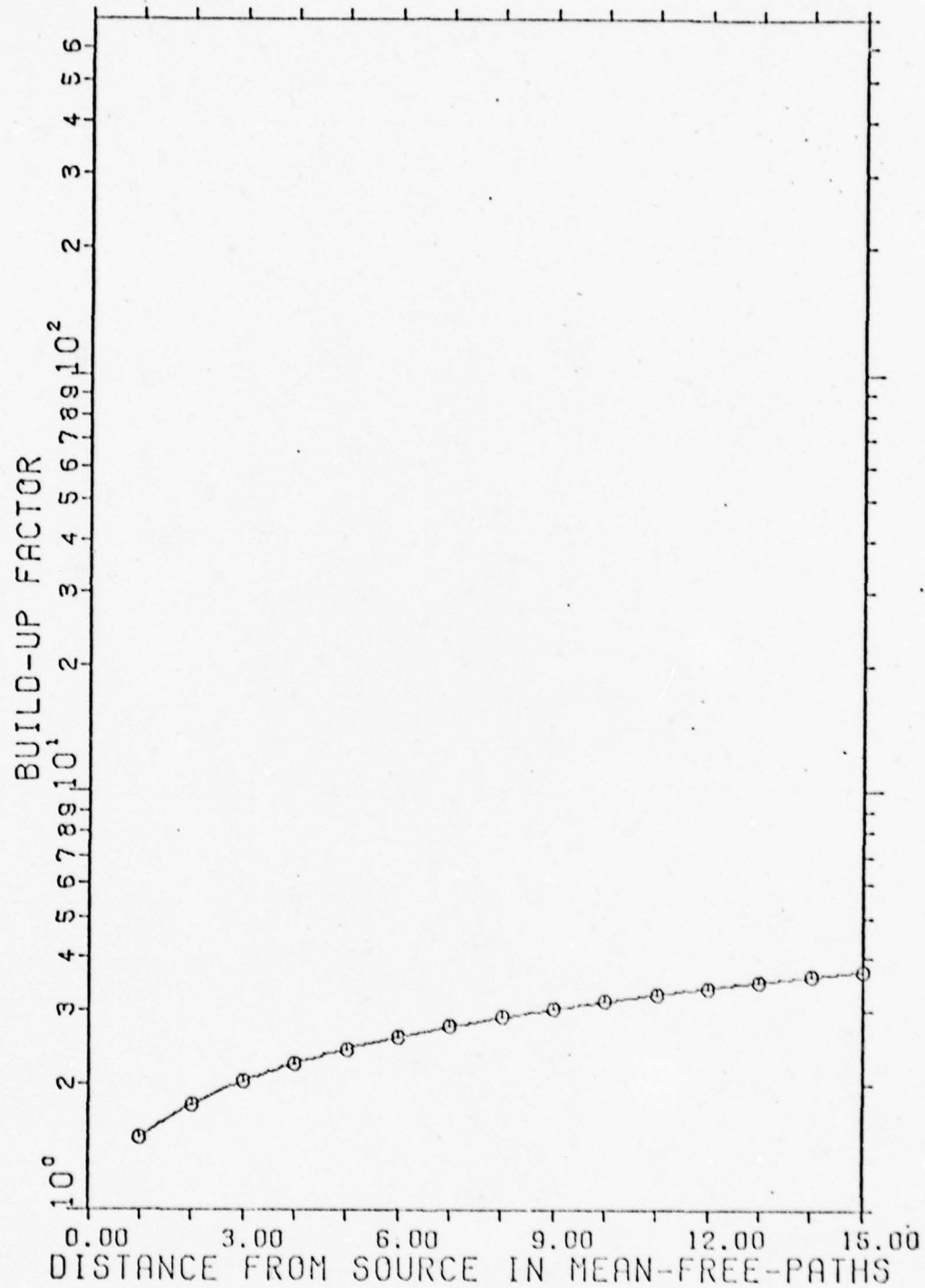


FIG. 6 ENERGY BUILD-UP FACTORS FOR 22 KEV

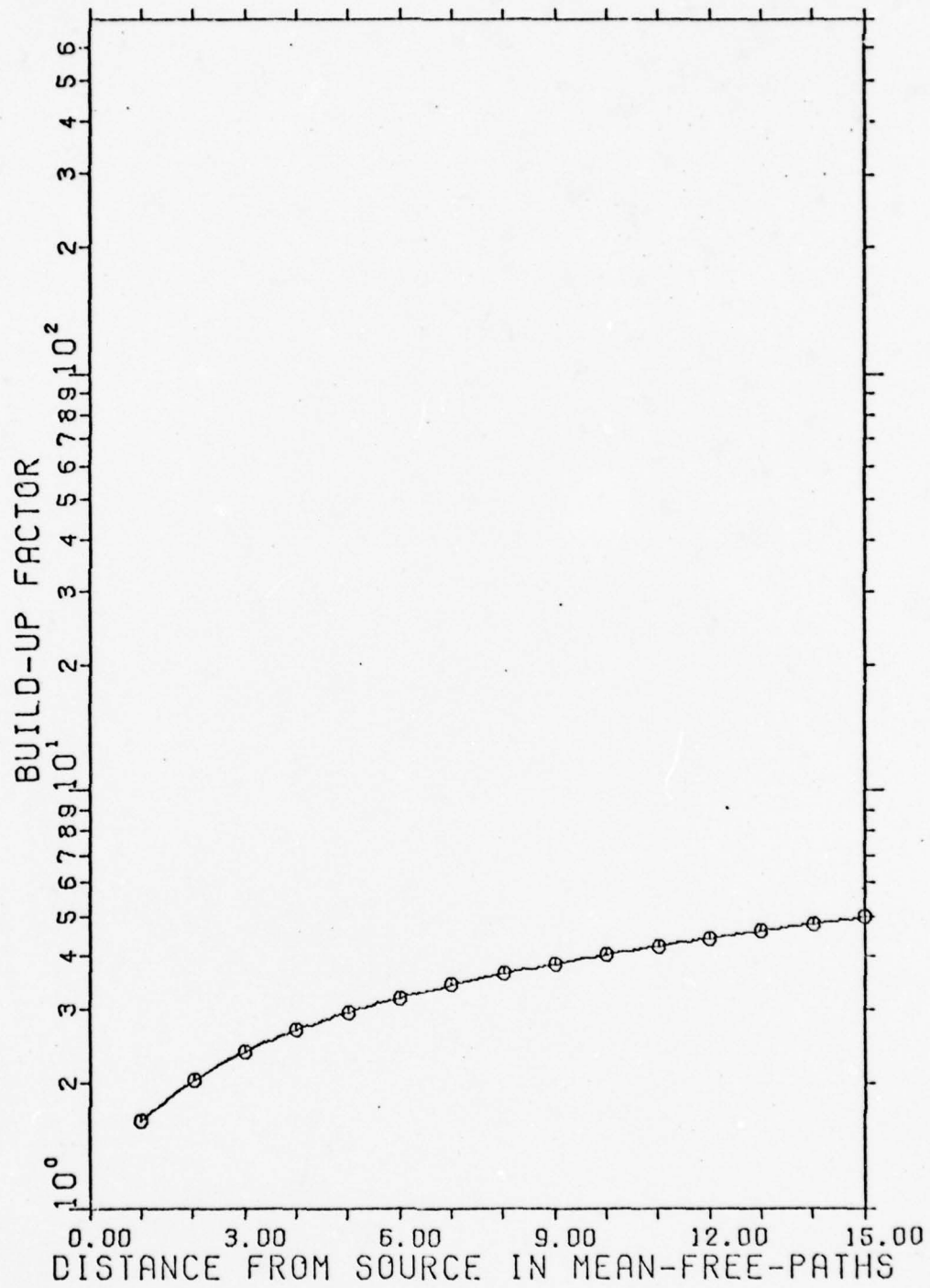


FIG. 7 ENERGY BUILD-UP FACTORS FOR 24 KEV



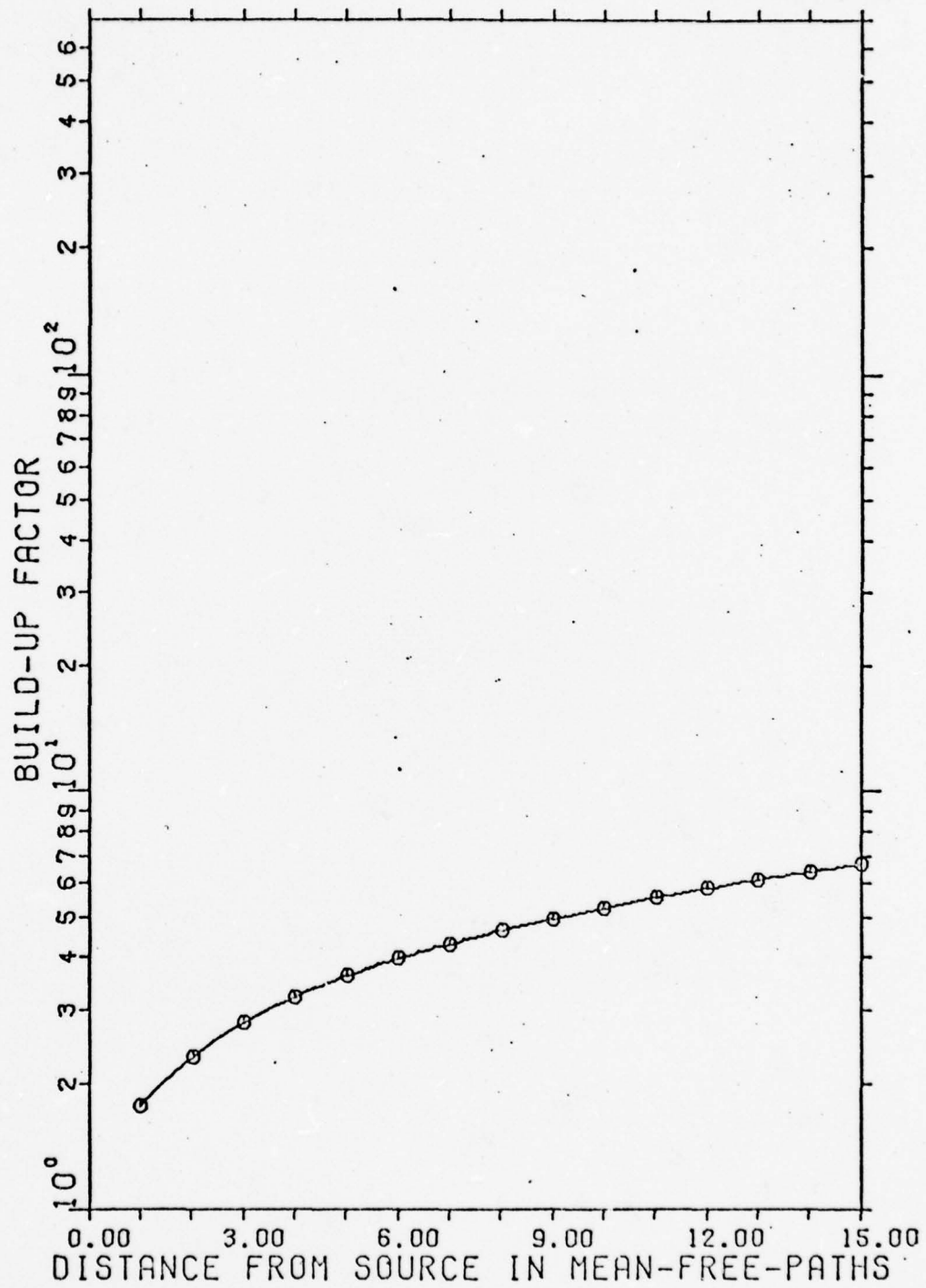


FIG. 8 ENERGY BUILD-UP FACTORS FOR 26 KEV

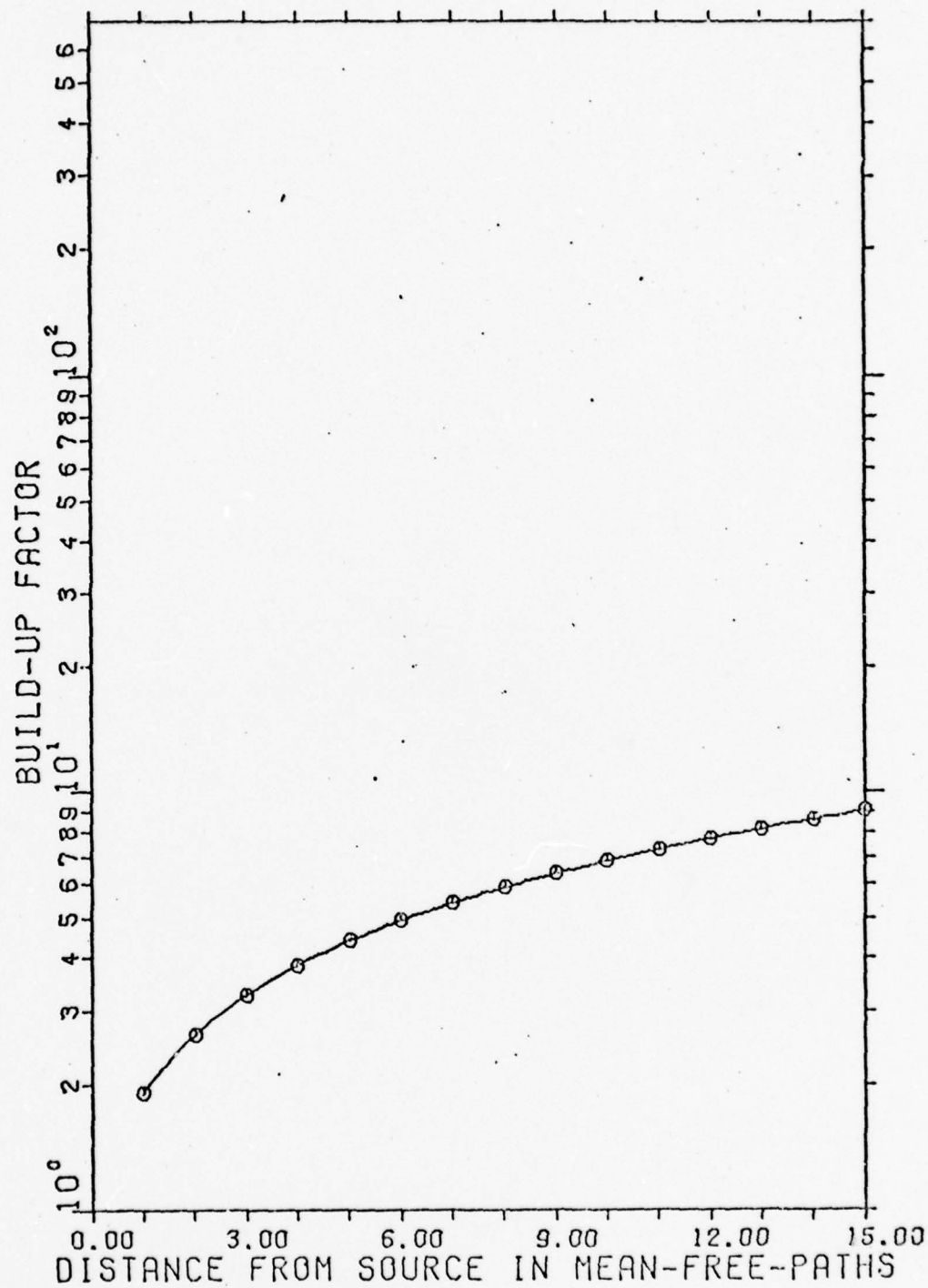


FIG. 9 ENERGY BUILD-UP FACTORS FOR 28 KEV

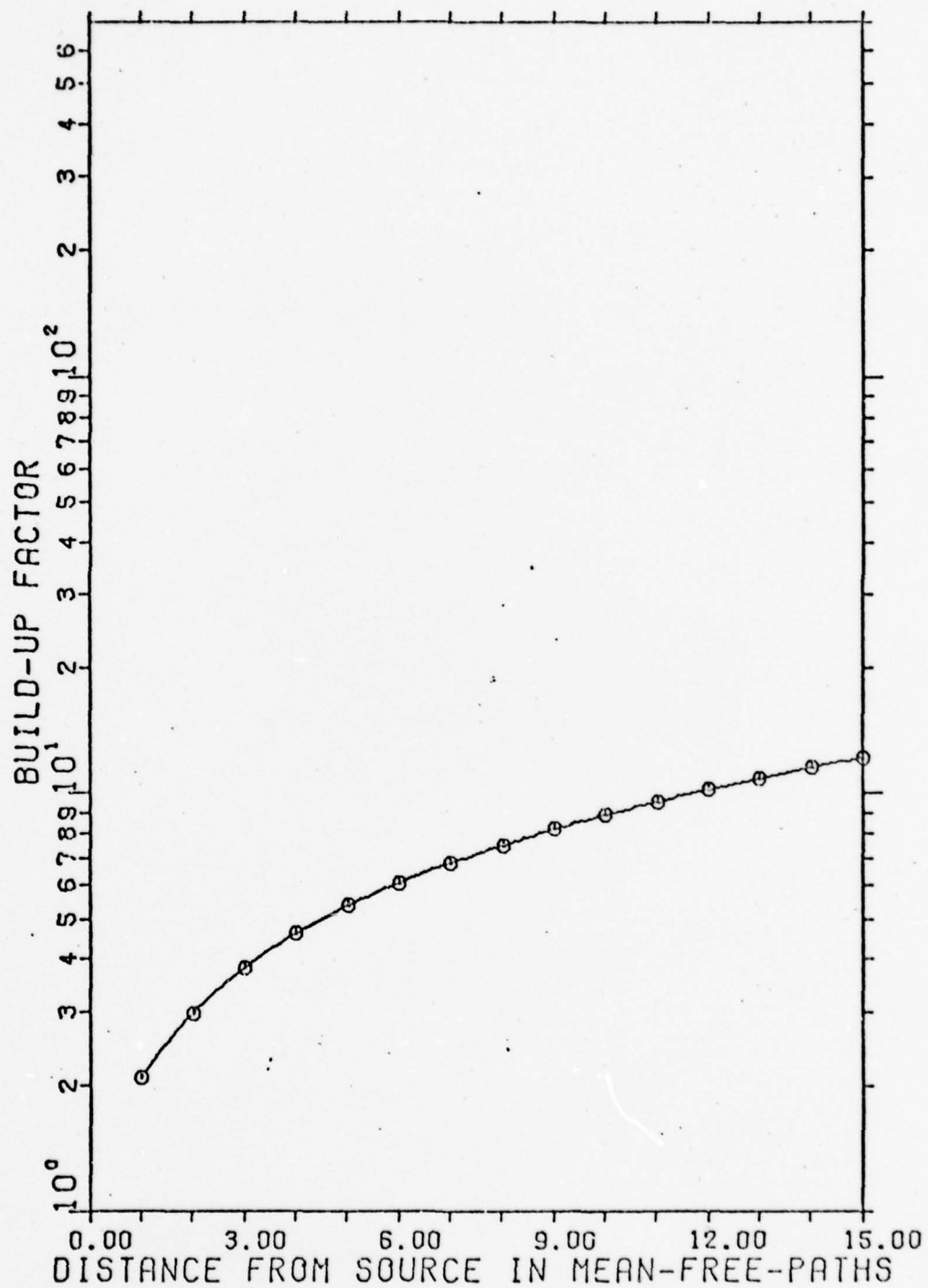


FIG. 10 ENERGY BUILD-UP FACTORS FOR 30 KEV

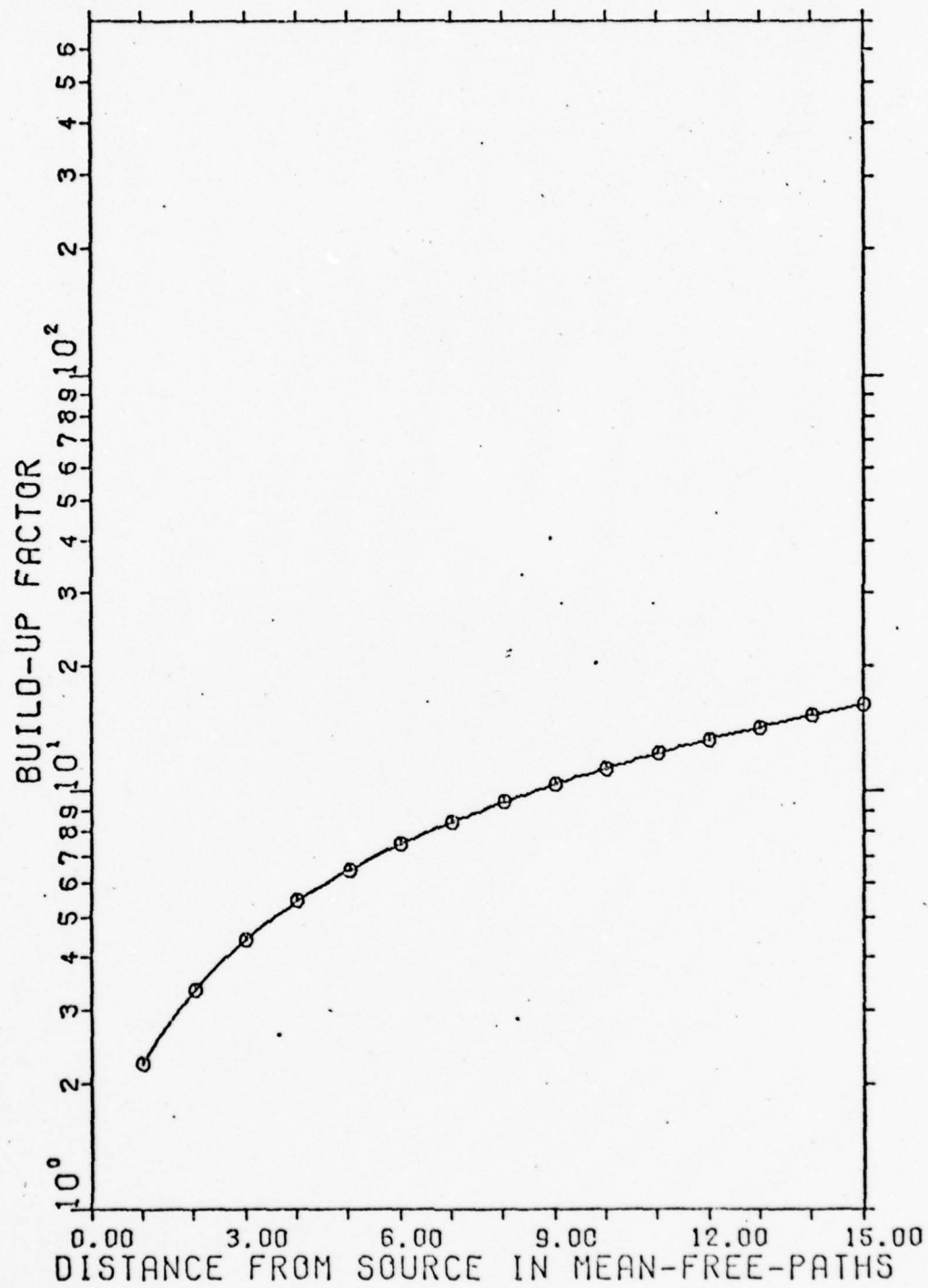


FIG. 11 ENERGY BUILD-UP FACTORS FOR 32 KEV

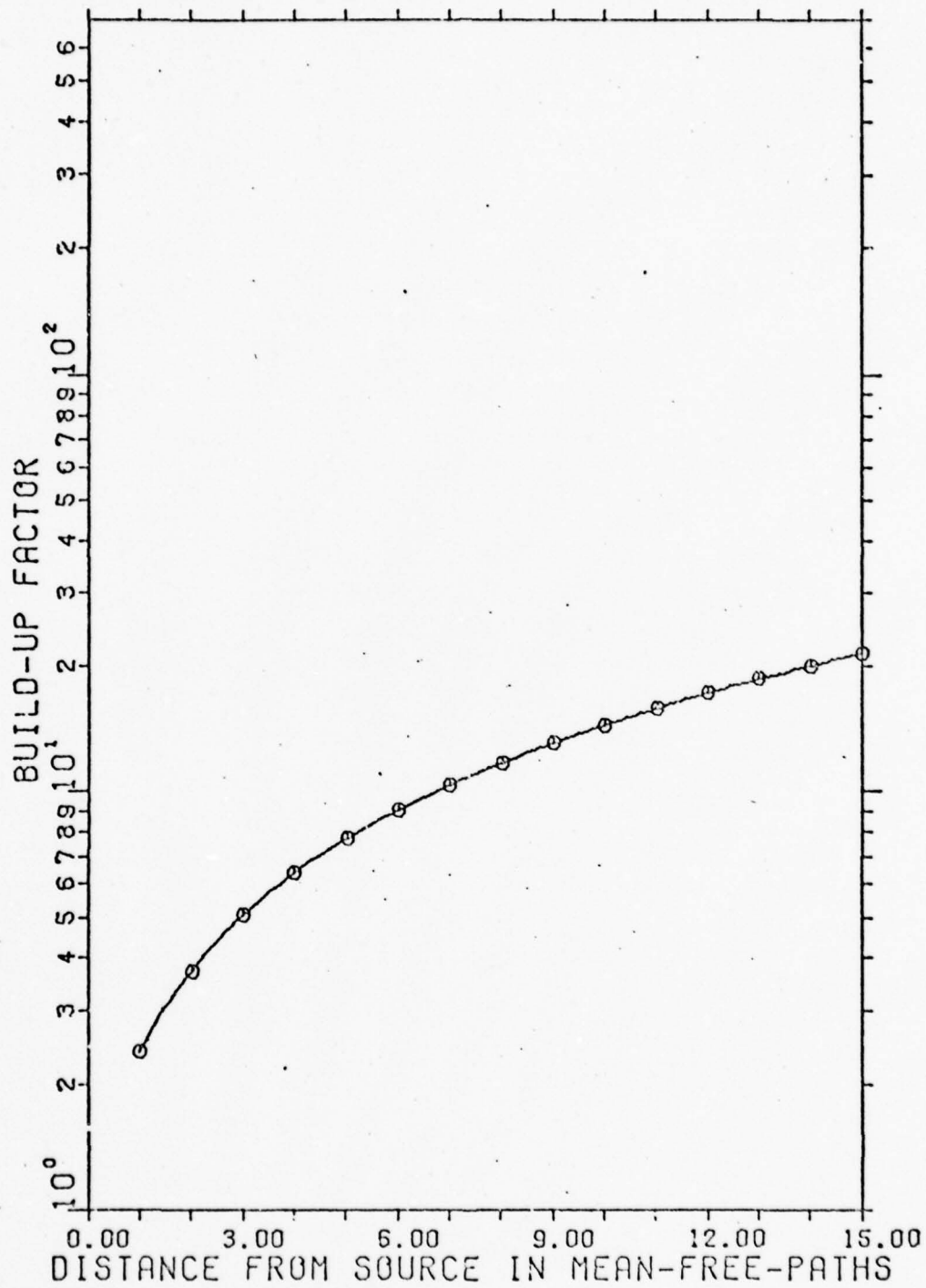


FIG. 12 ENERGY BUILD-UP FACTORS FOR 34 KEV



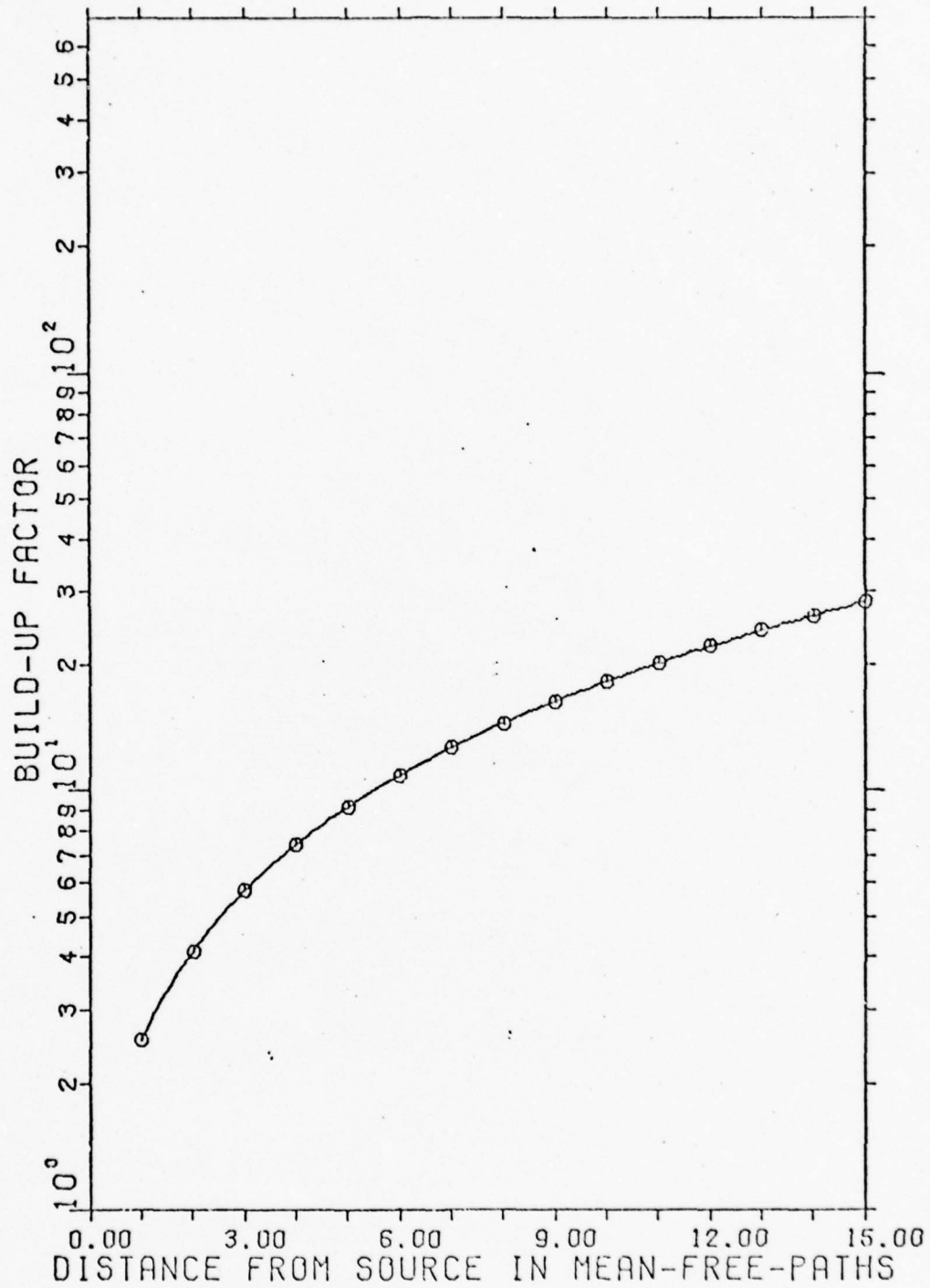


FIG. 13 ENERGY BUILD-UP FACTORS FOR 36 KEV

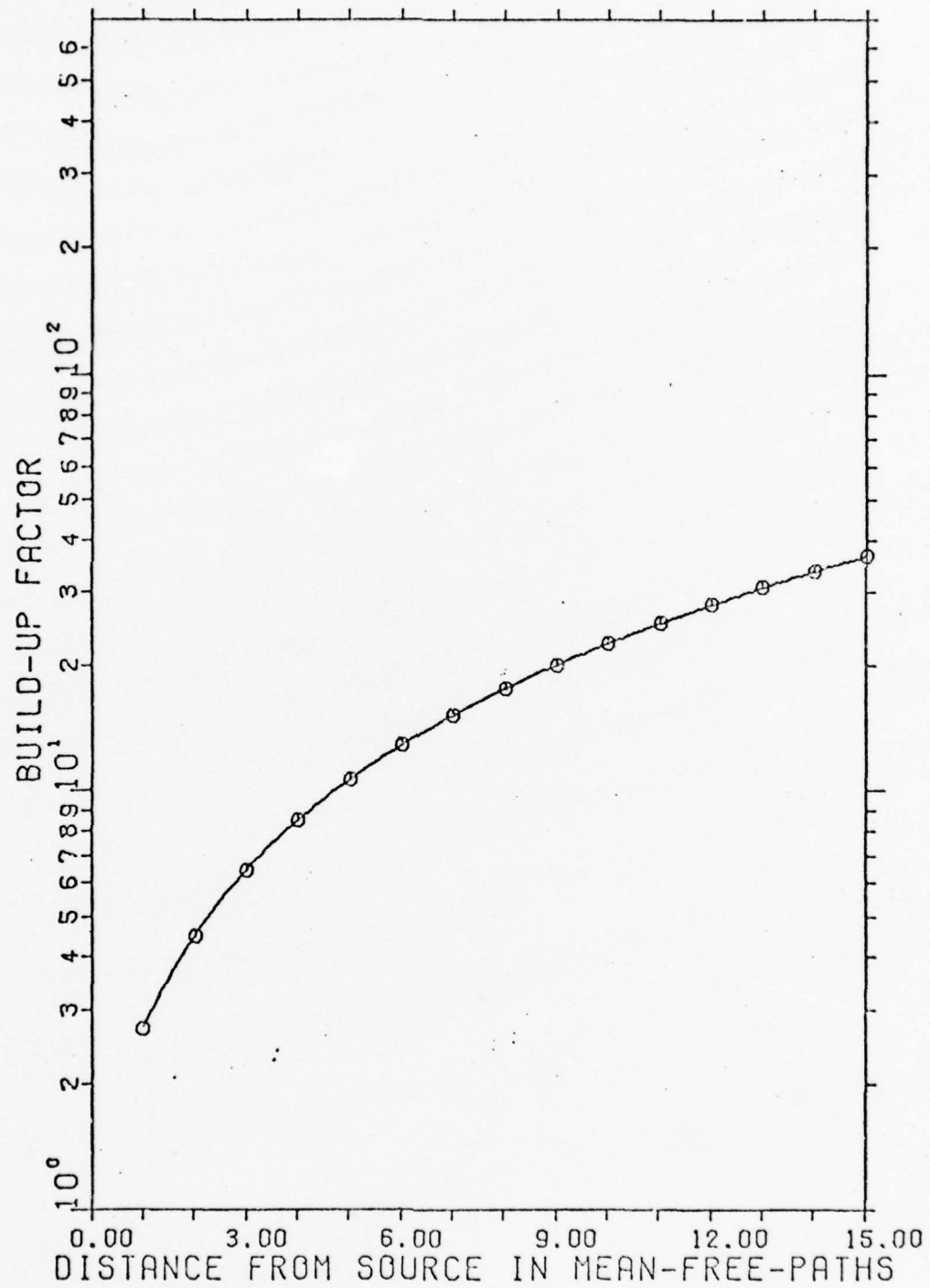


FIG. 14 ENERGY BUILD-UP FACTORS FOR 38 KEV

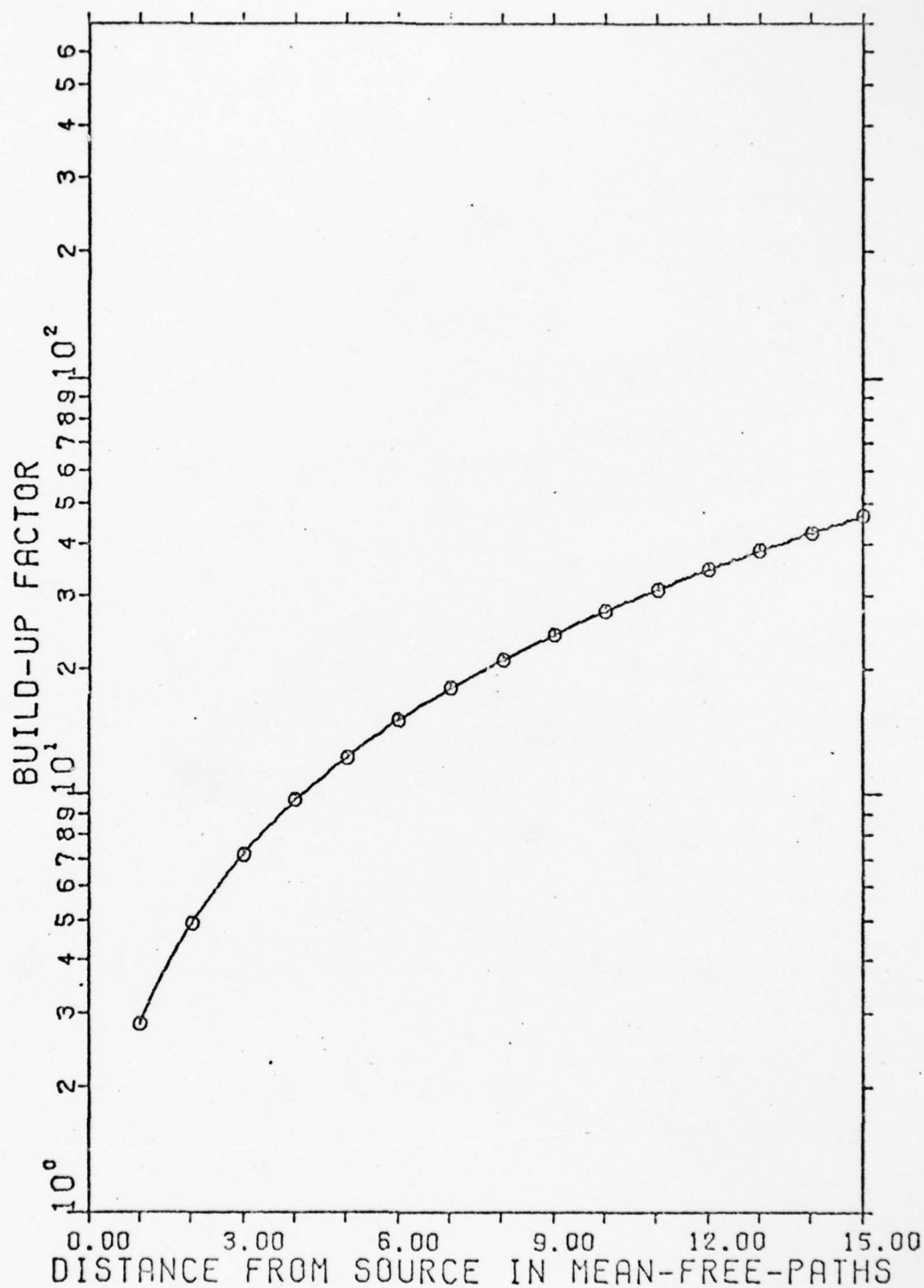


FIG. 15 ENERGY BUILD-UP FACTORS FOR 40 KEV

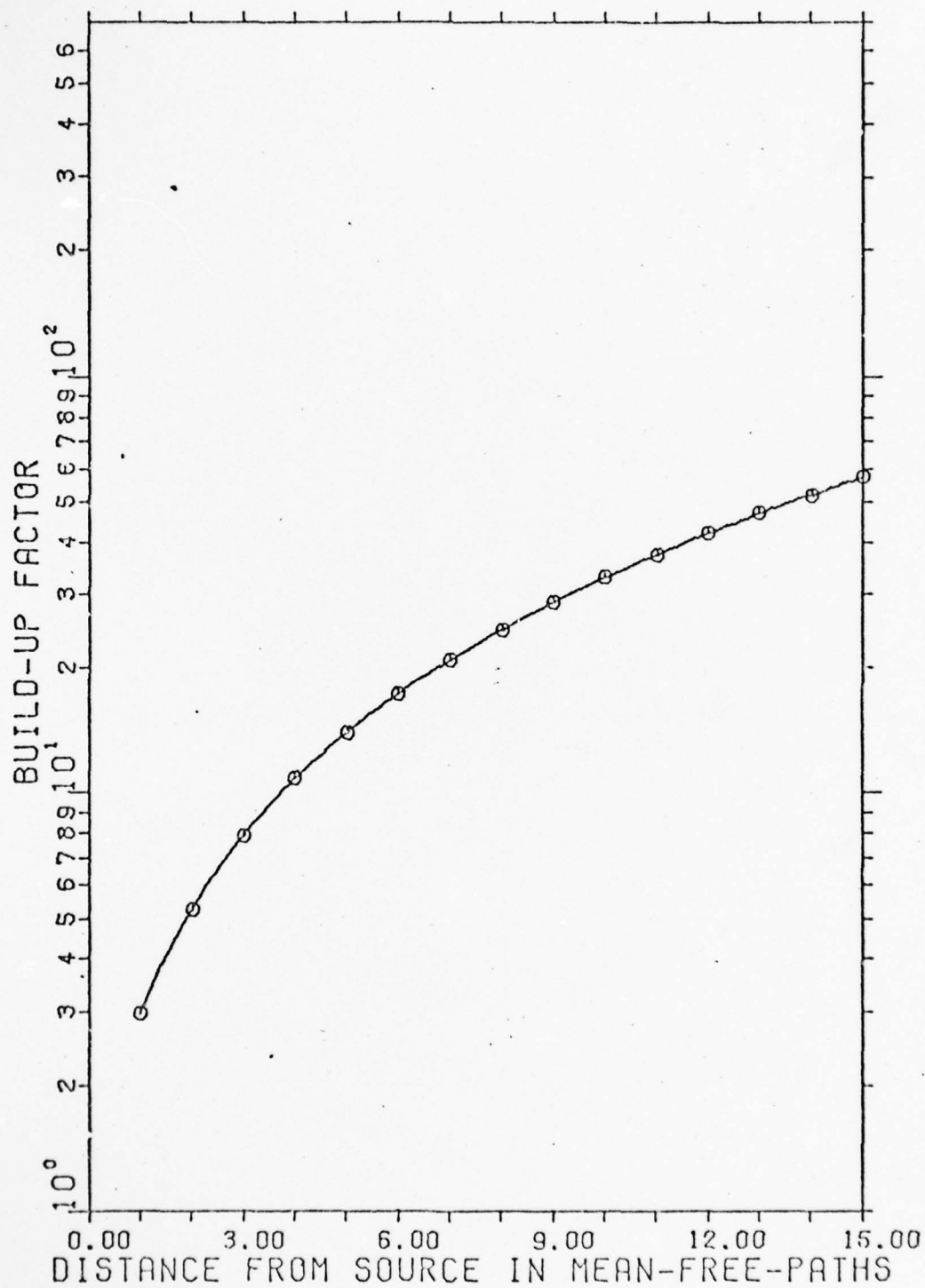


FIG. 16 ENERGY BUILD-UP FACTORS FOR 42 KEV

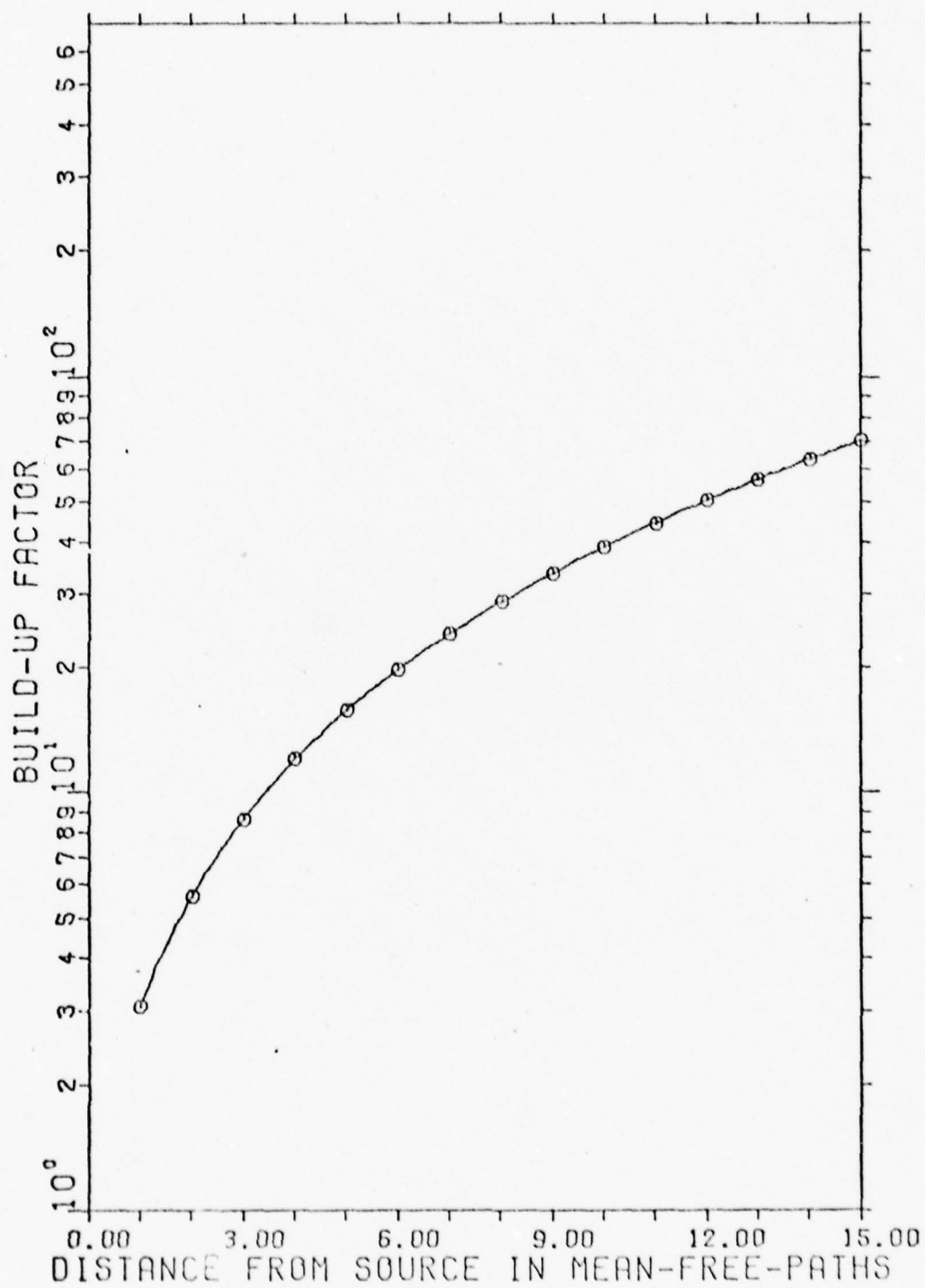


FIG. 17 ENERGY BUILD-UP FACTORS FOR 44 KEV



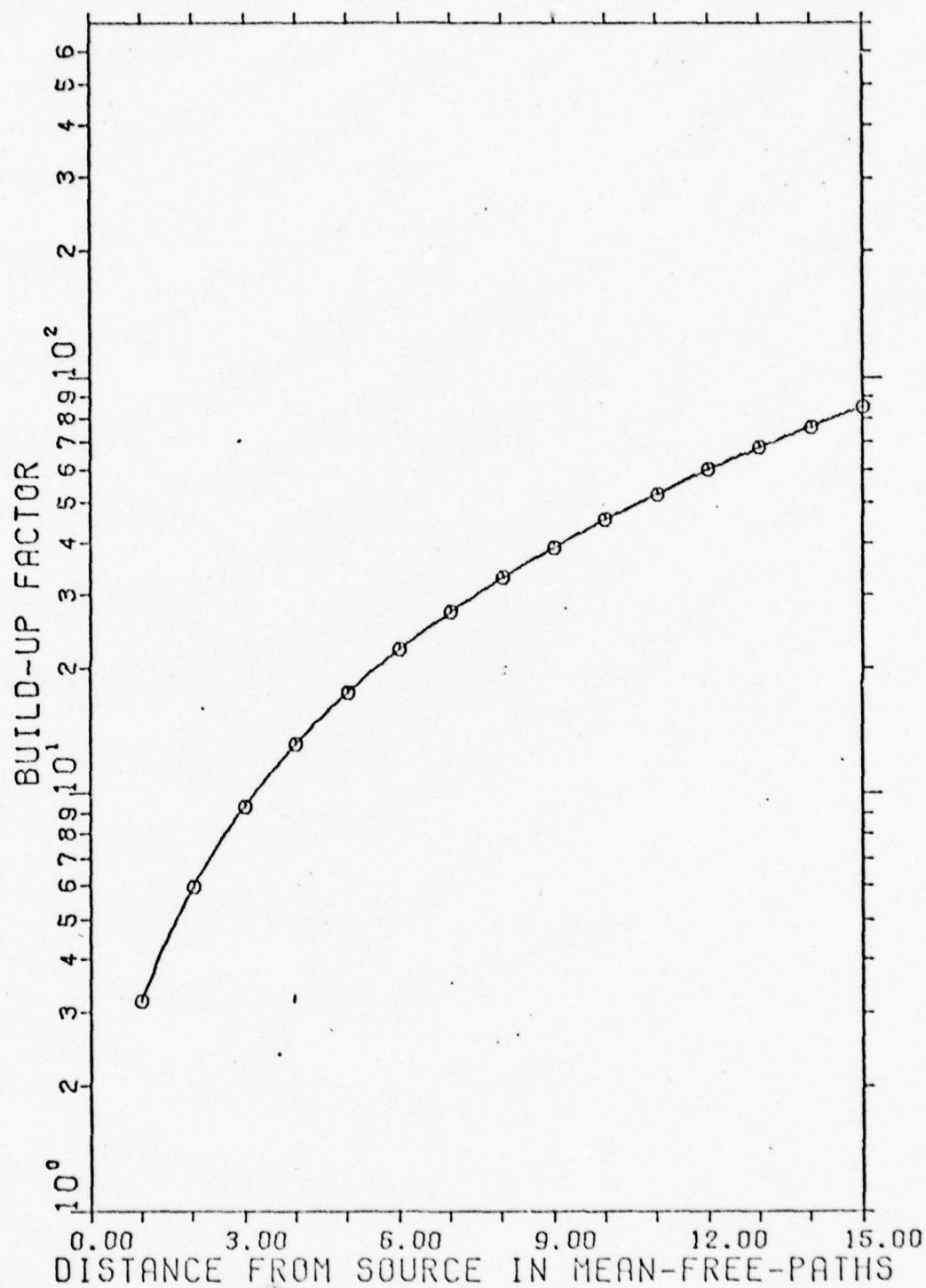


FIG. 18 ENERGY BUILD-UP FACTORS FOR 46 KEV

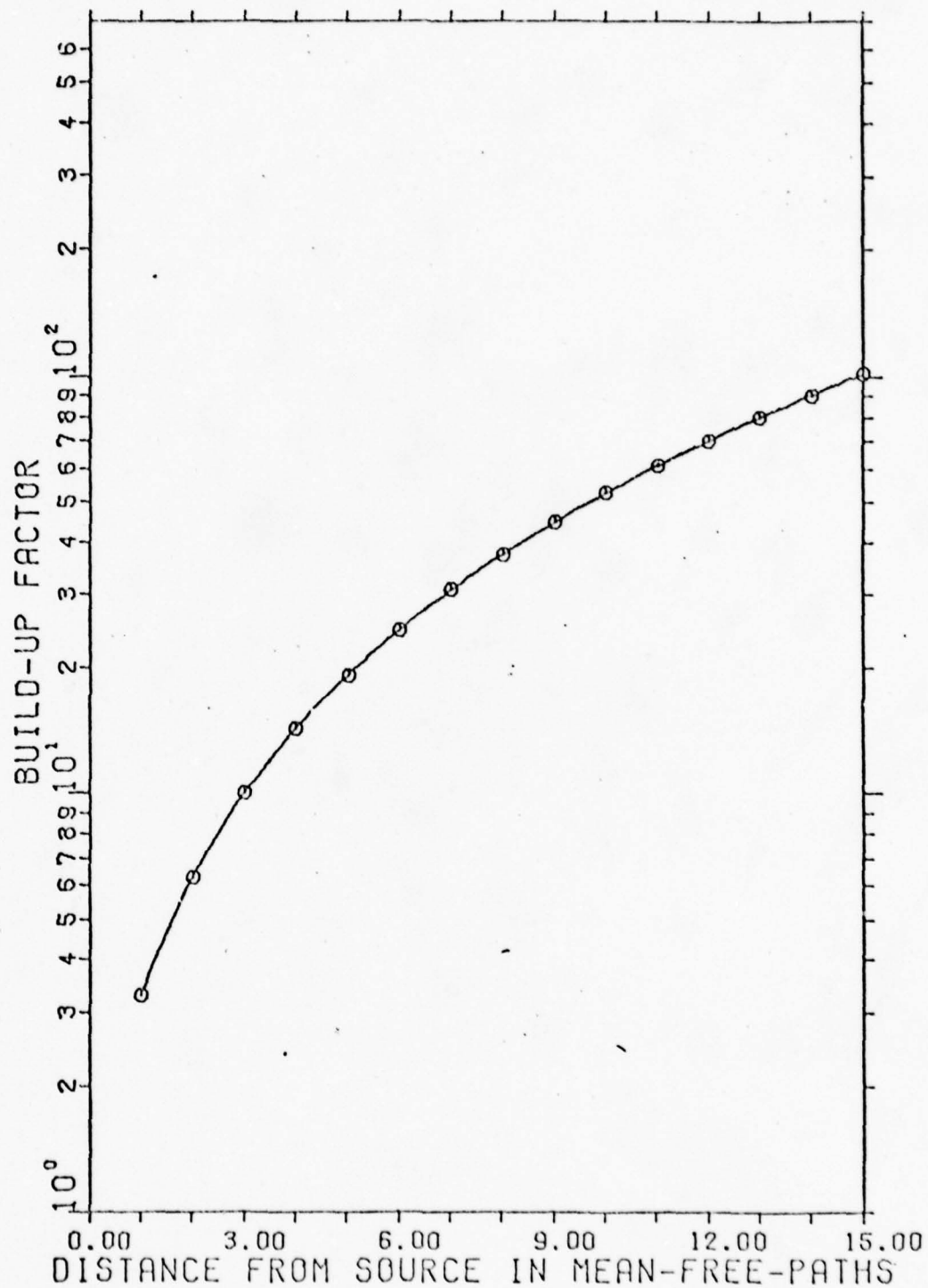


FIG. 19 ENERGY BUILD-UP FACTORS FOR 48 KEV

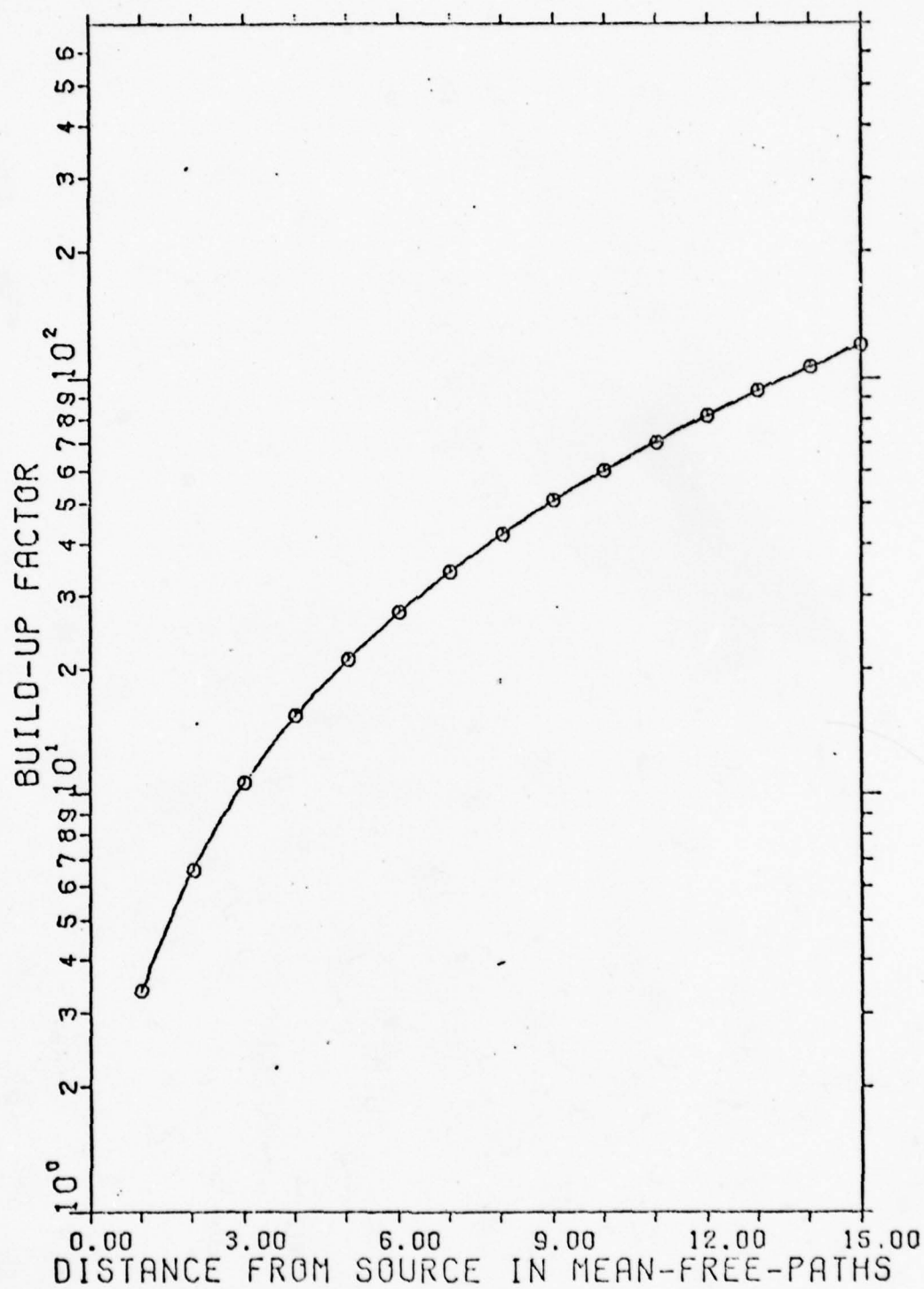


FIG. 20 ENERGY BUILD-UP FACTORS FOR 50 KEV

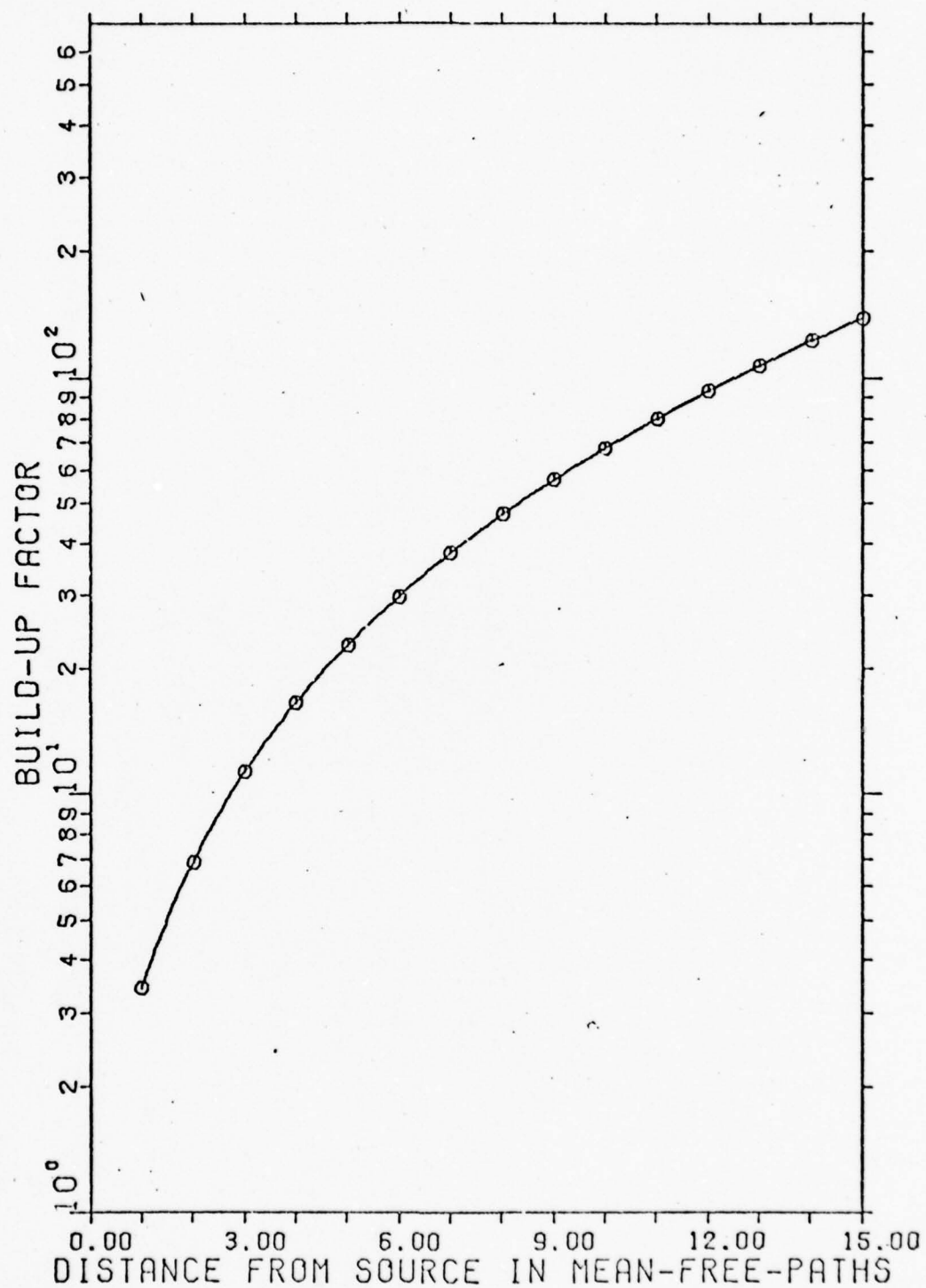


FIG. 21 ENERGY BUILD-UP FACTORS FOR 52 KEV

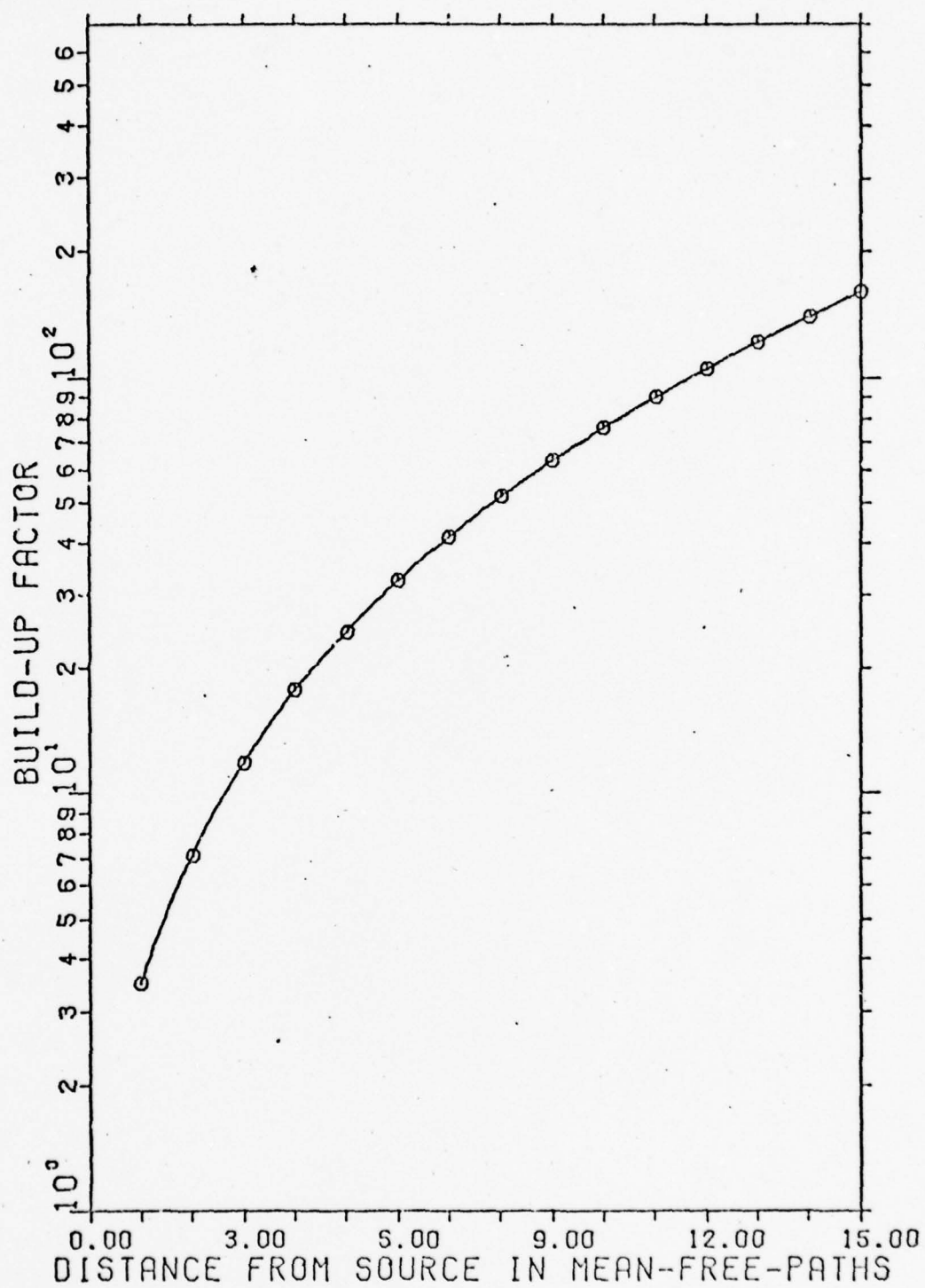


FIG. 22 ENERGY BUILD-UP FACTORS FOR 54 KEV



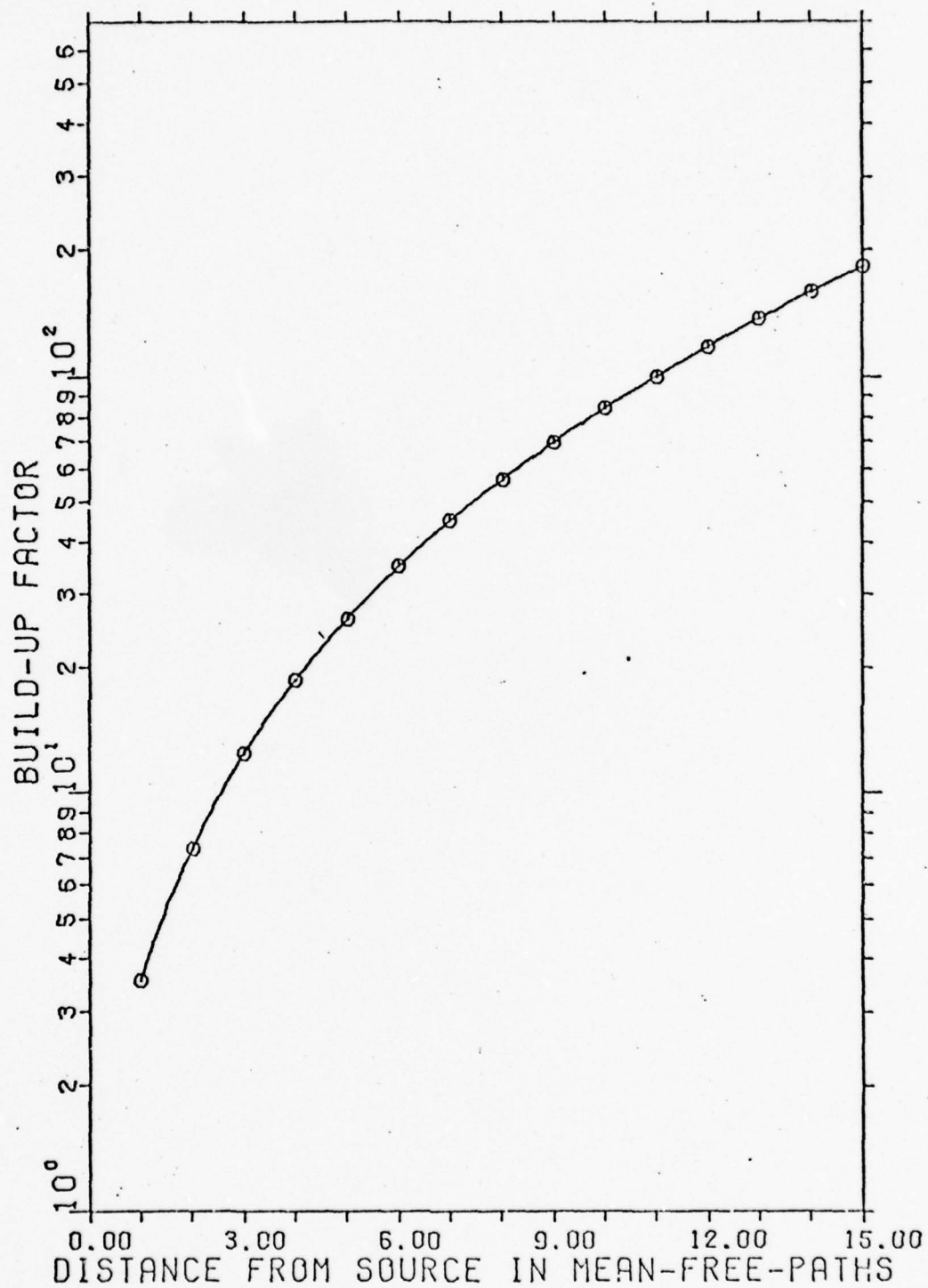


FIG. 23 ENERGY: BUILD-UP FACTORS FOR 56 KEV

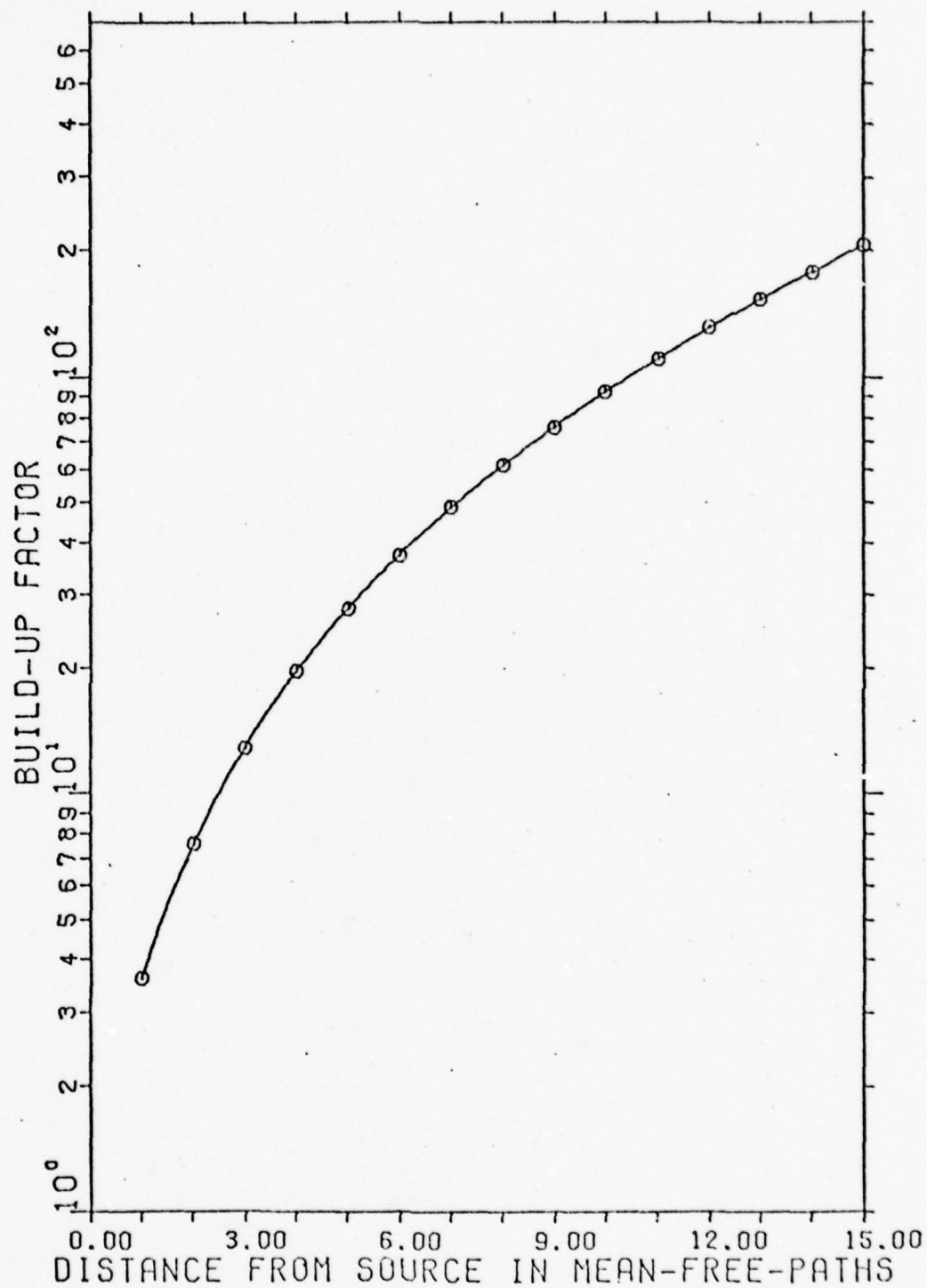


FIG. 24 ENERGY BUILD-UP FACTORS FOR 58 KEV

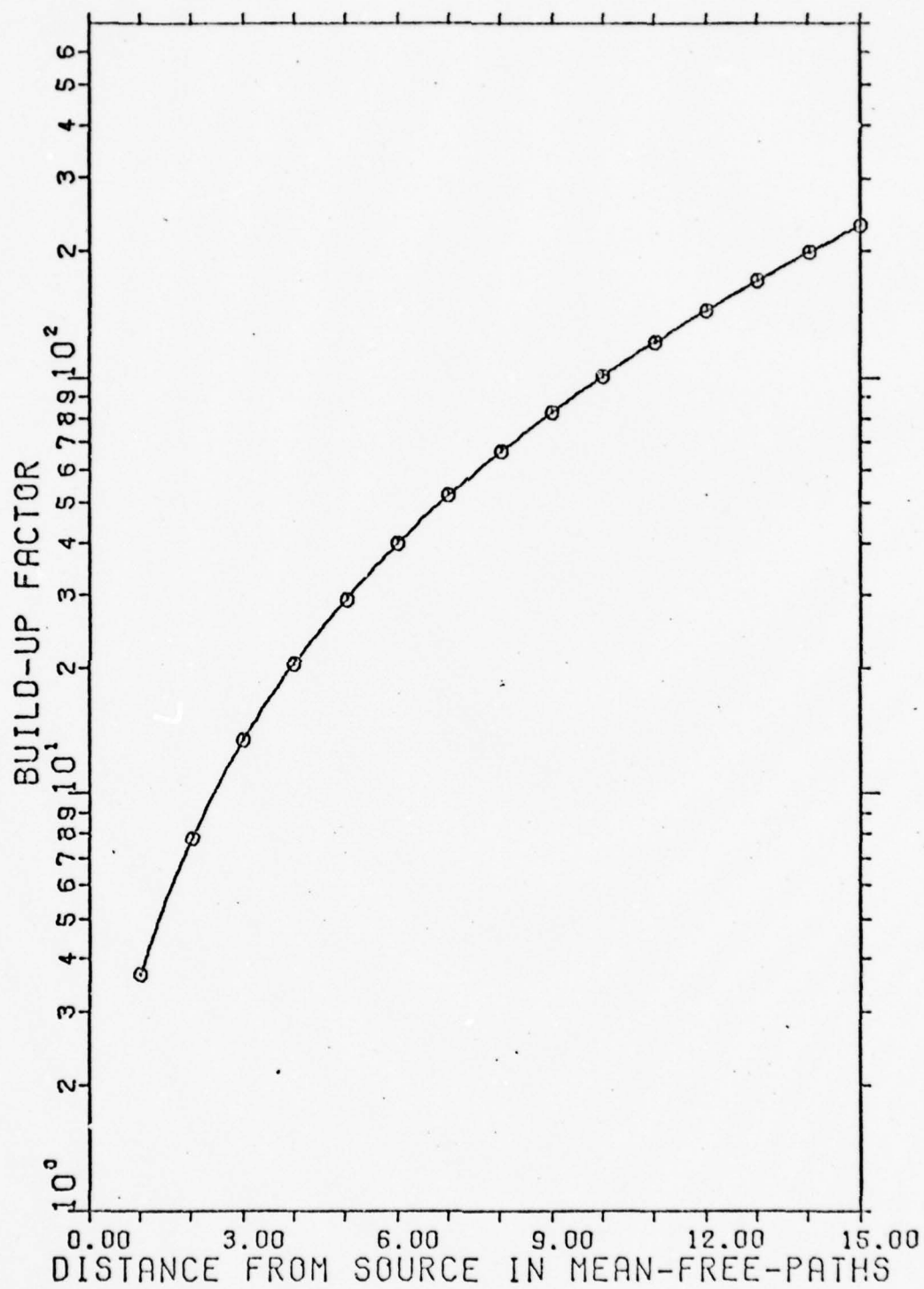


FIG. 25 ENERGY BUILD-UP FACTORS FOR 60 KEV

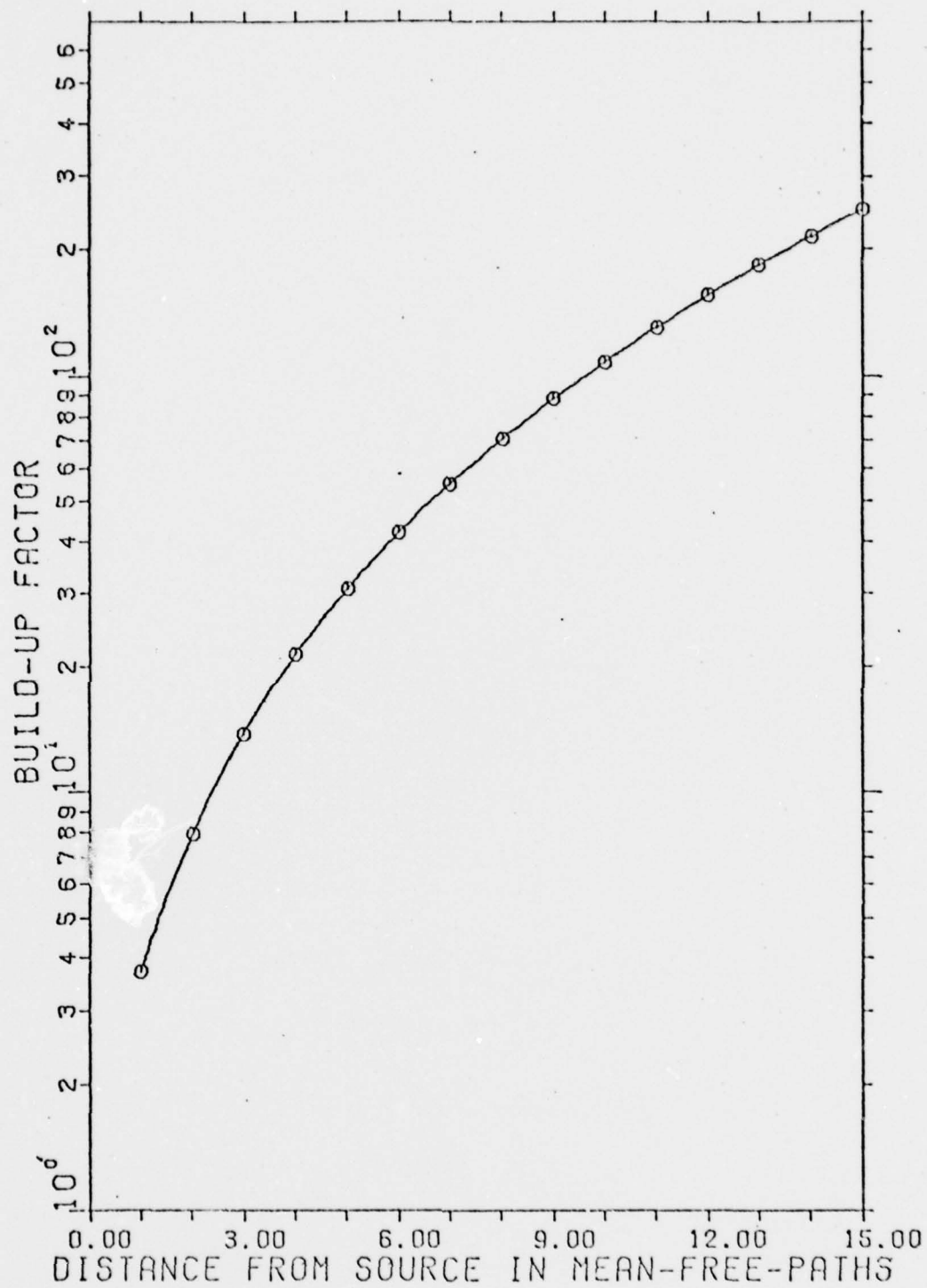


FIG. 26 ENERGY BUILD-UP FACTORS FOR 62 KEV

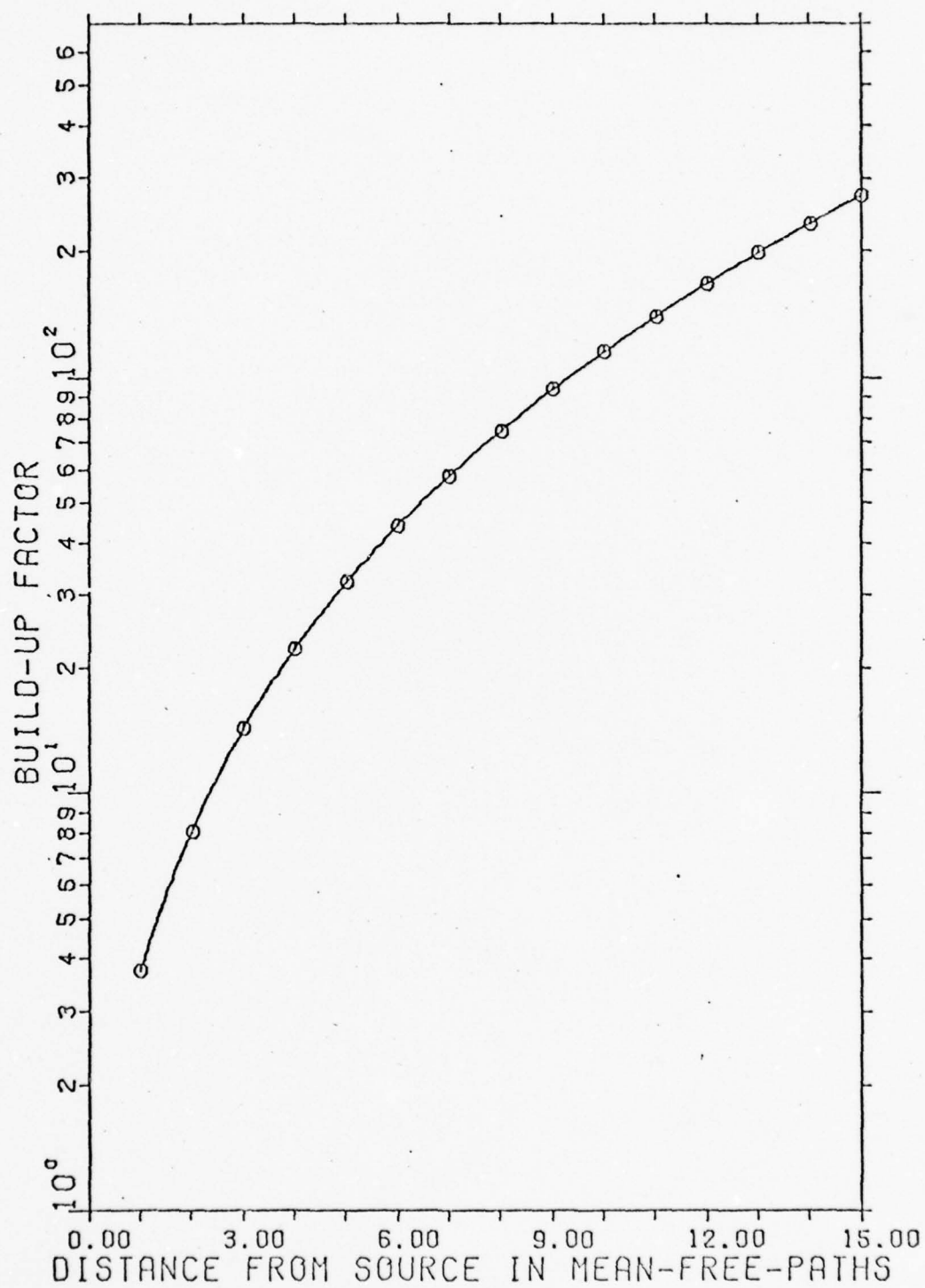


FIG. 27 ENERGY BUILD-UP FACTORS FOR 64 KEV



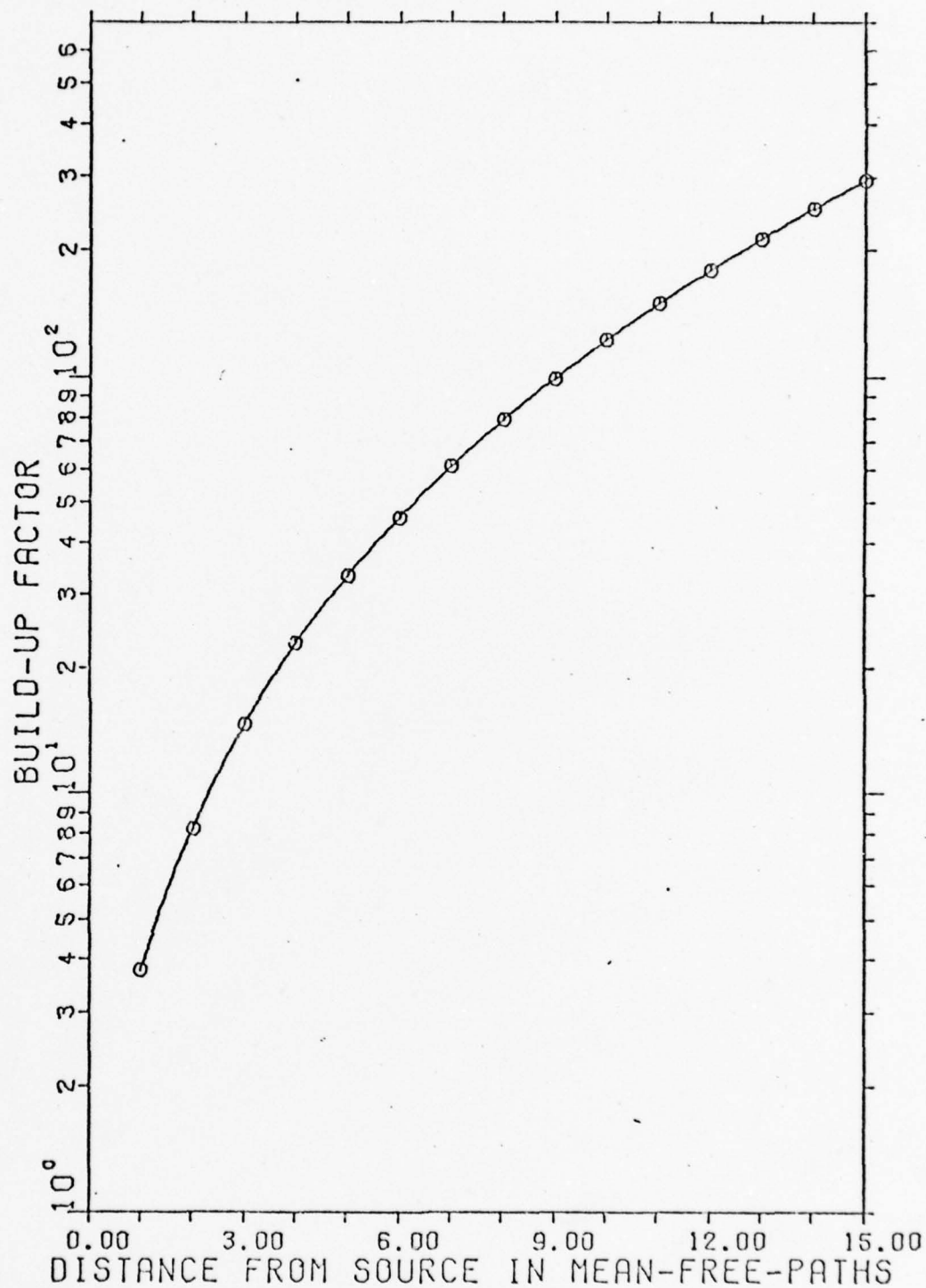


FIG. 28 ENERGY BUILD-UP FACTORS FOR 66 KEV

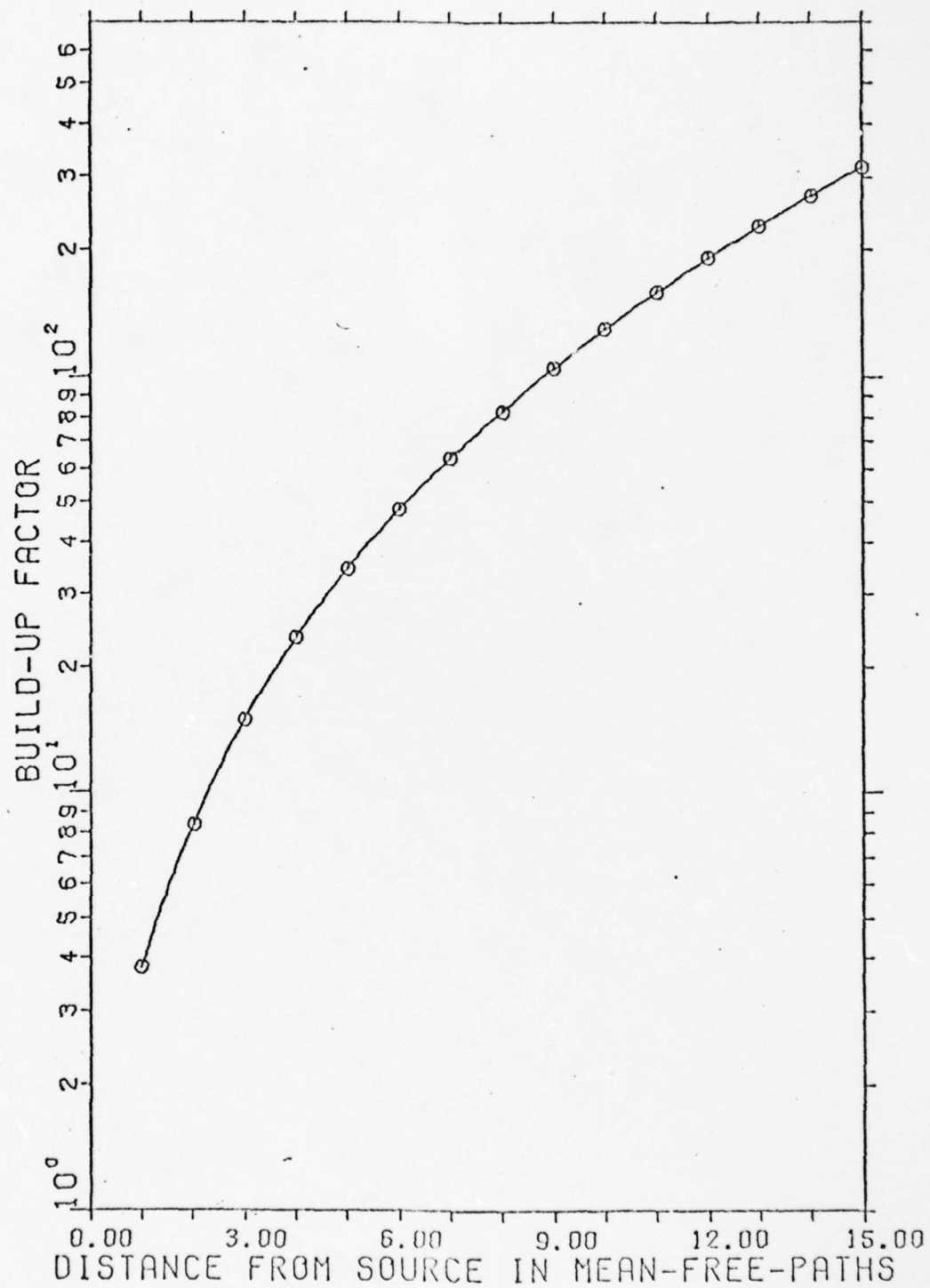


FIG. 29 ENERGY BUILD-UP FACTORS FOR 68 KEV

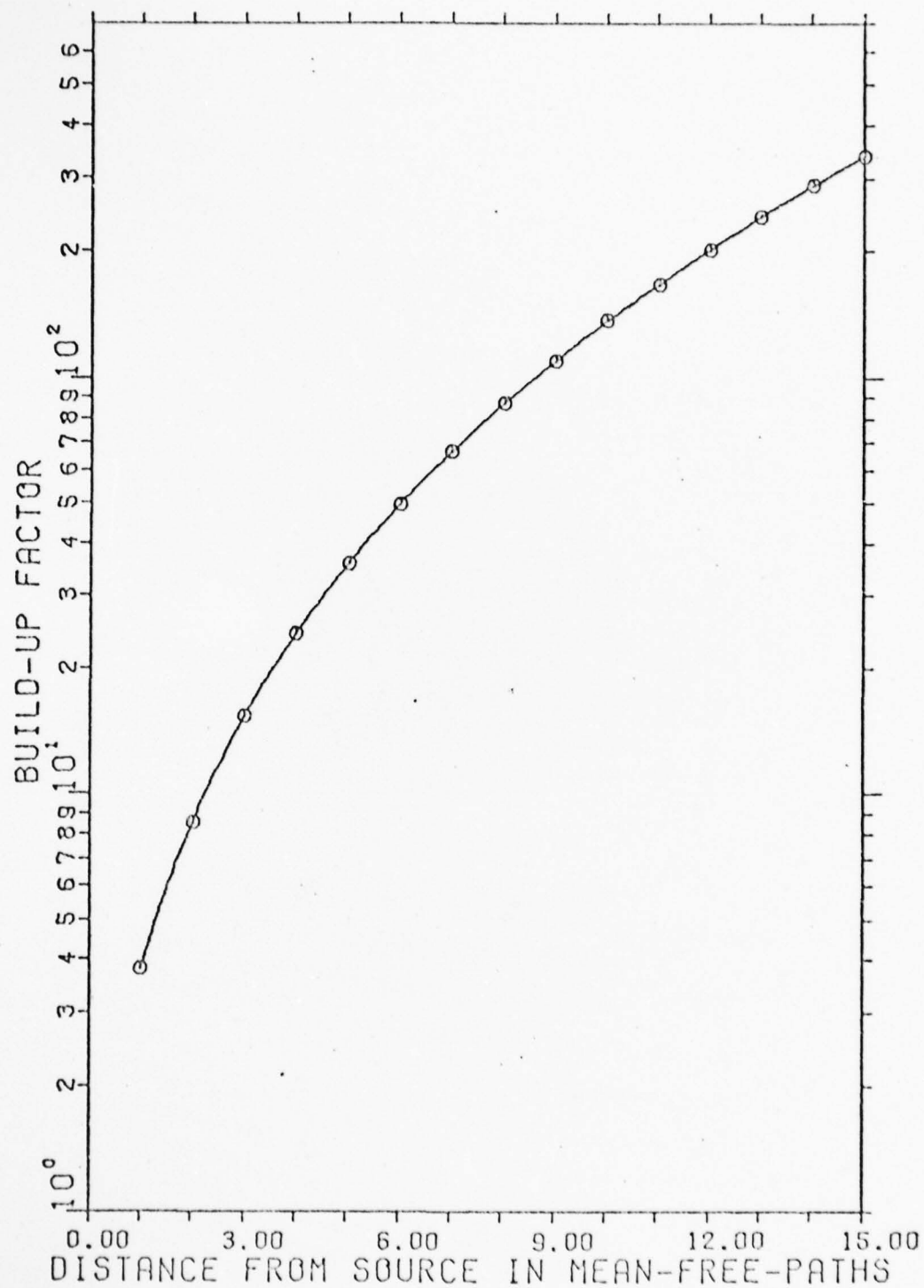


FIG. 30 ENERGY BUILD-UP FACTORS FOR 70 KEV

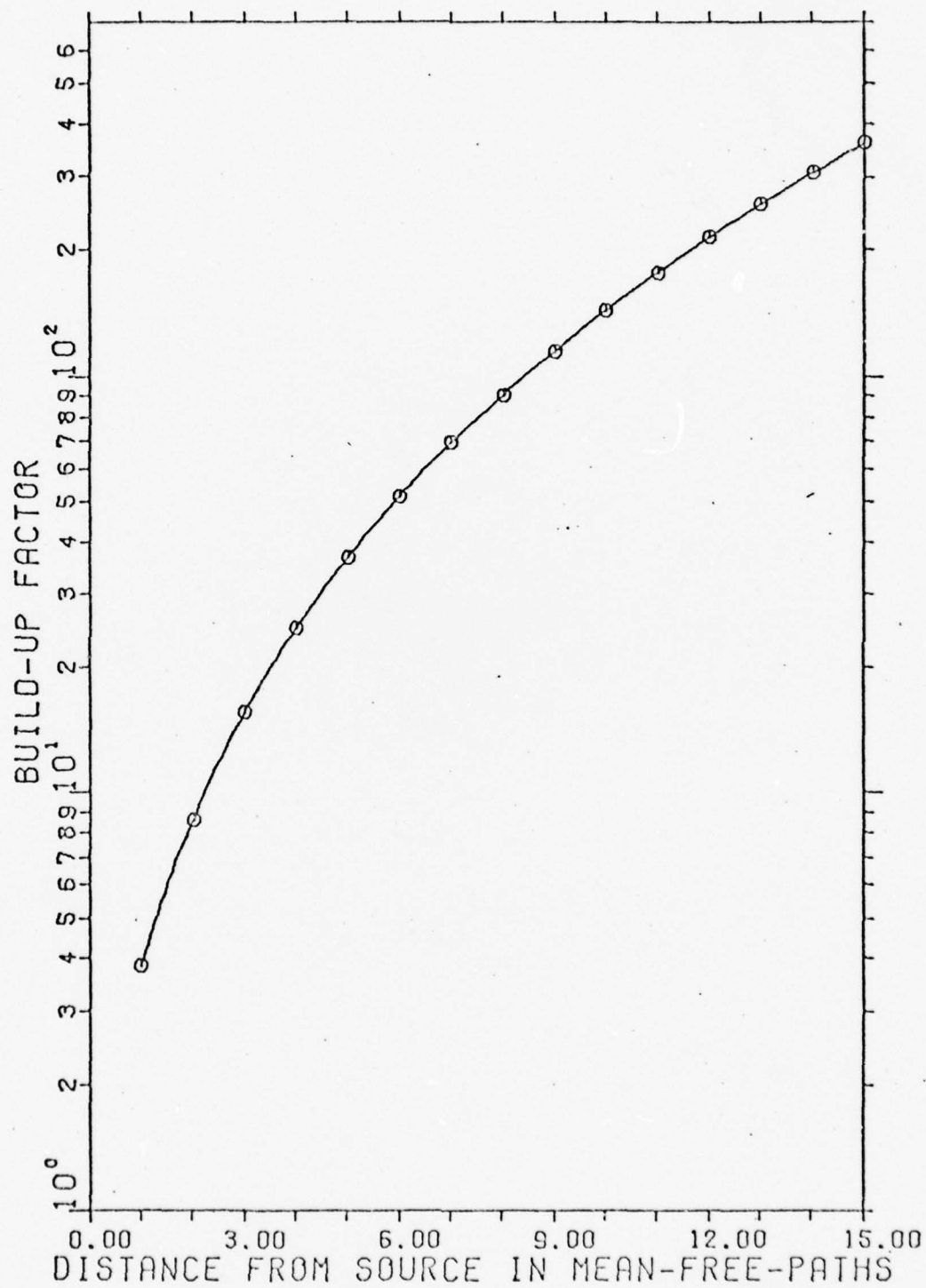


FIG. 31 ENERGY BUILD-UP FACTORS FOR 72 KEV

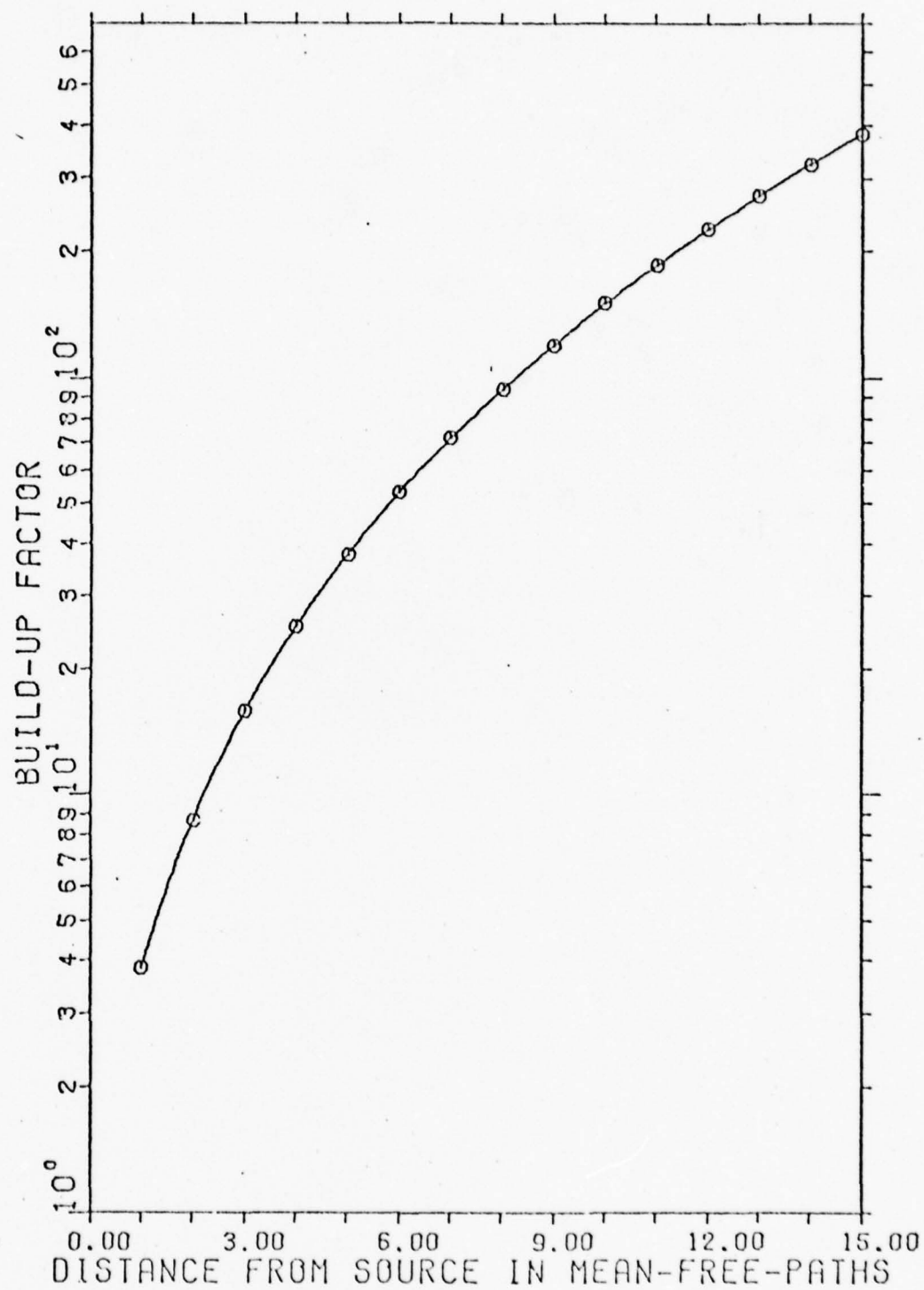


FIG. 32 ENERGY BUILD-UP FACTORS FOR 74 KEV



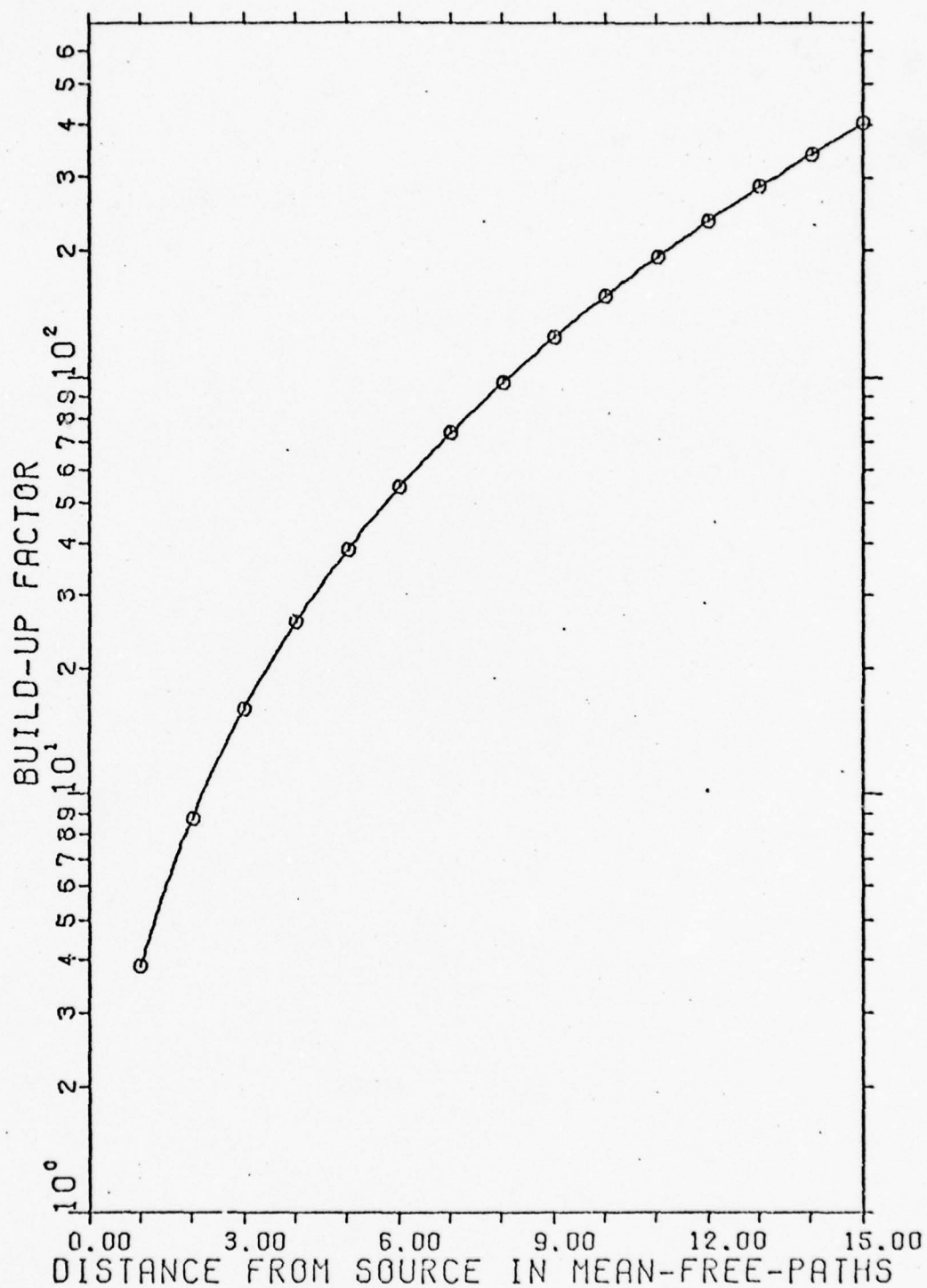


FIG. 33 ENERGY BUILD-UP FACTORS FOR 76 KEV

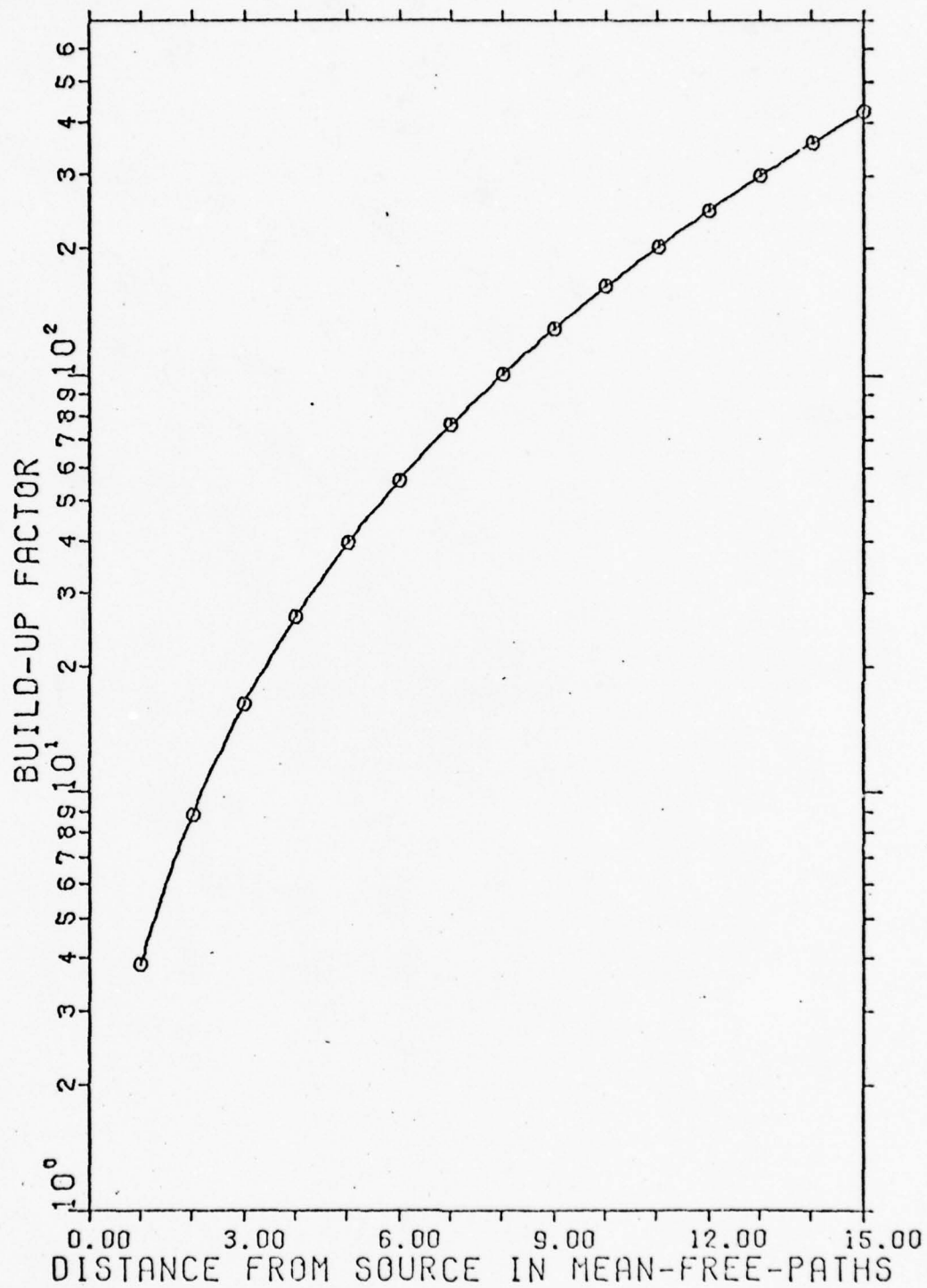


FIG. 34 ENERGY BUILD-UP FACTORS FOR 78 KEV

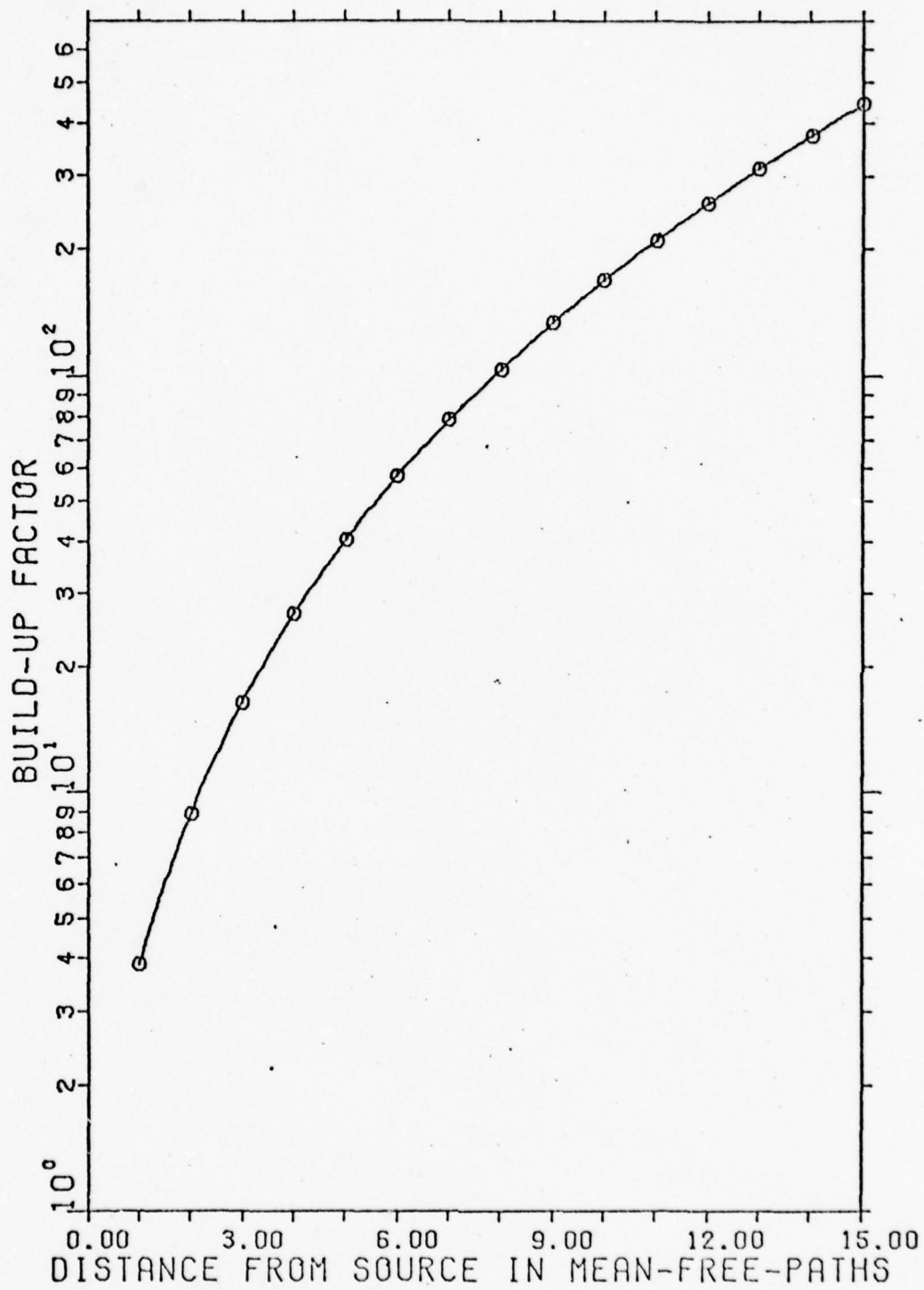


FIG. 35 ENERGY BUILD-UP FACTORS FOR 80 KEV

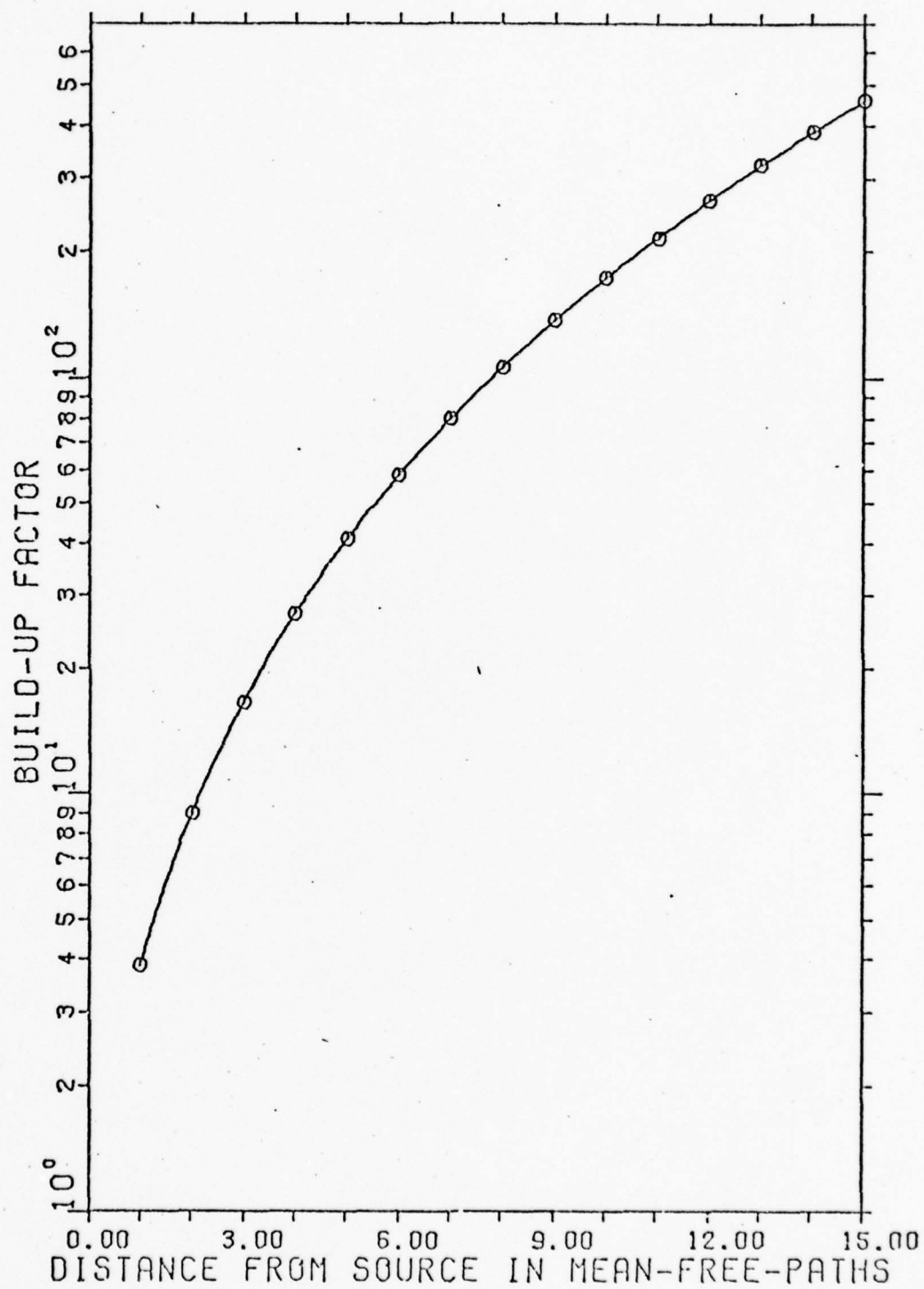


FIG. 36 ENERGY BUILD-UP FACTORS FOR 82 KEV

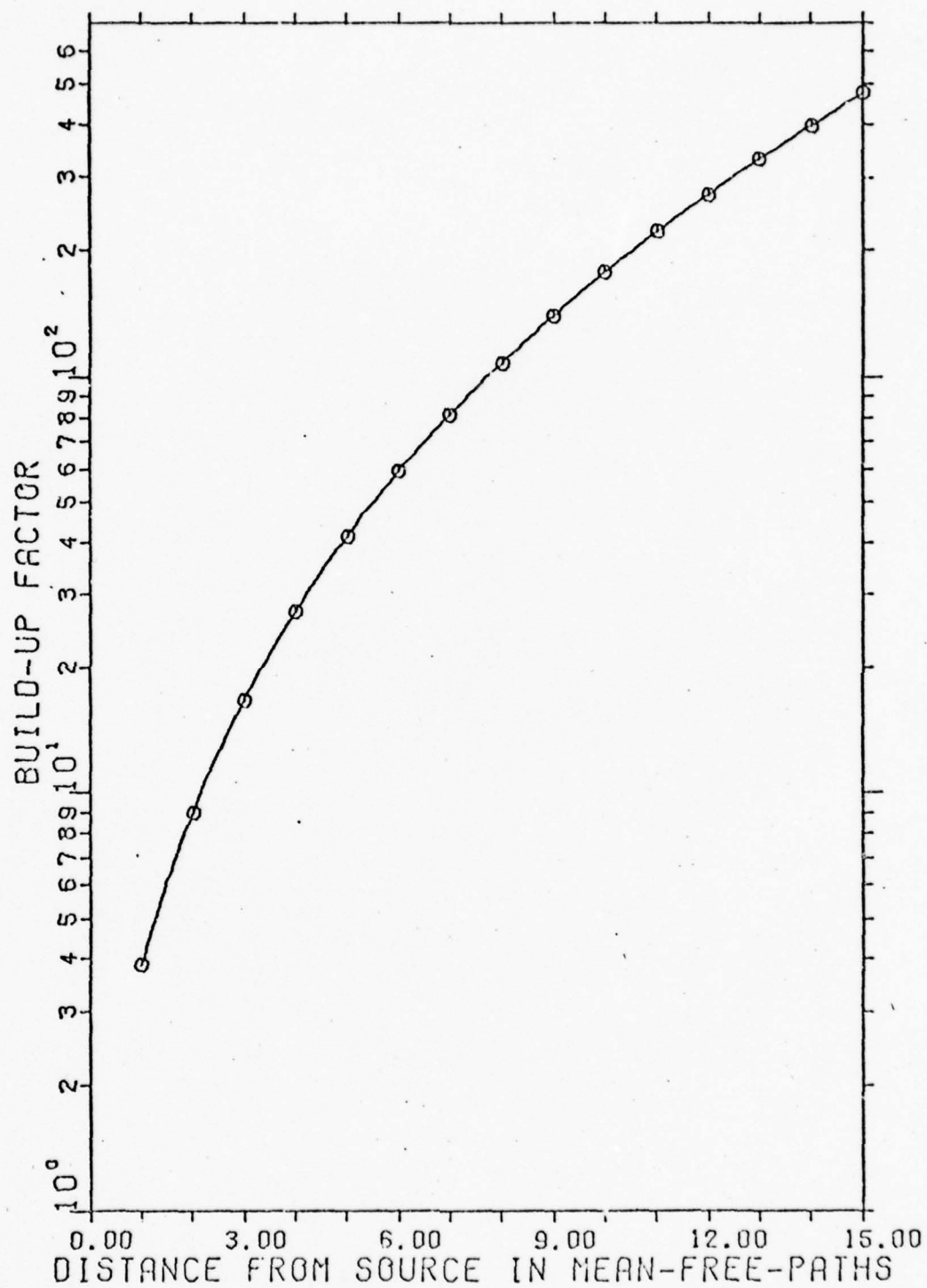


FIG. 37 ENERGY BUILD-UP FACTORS FOR 84 KEV



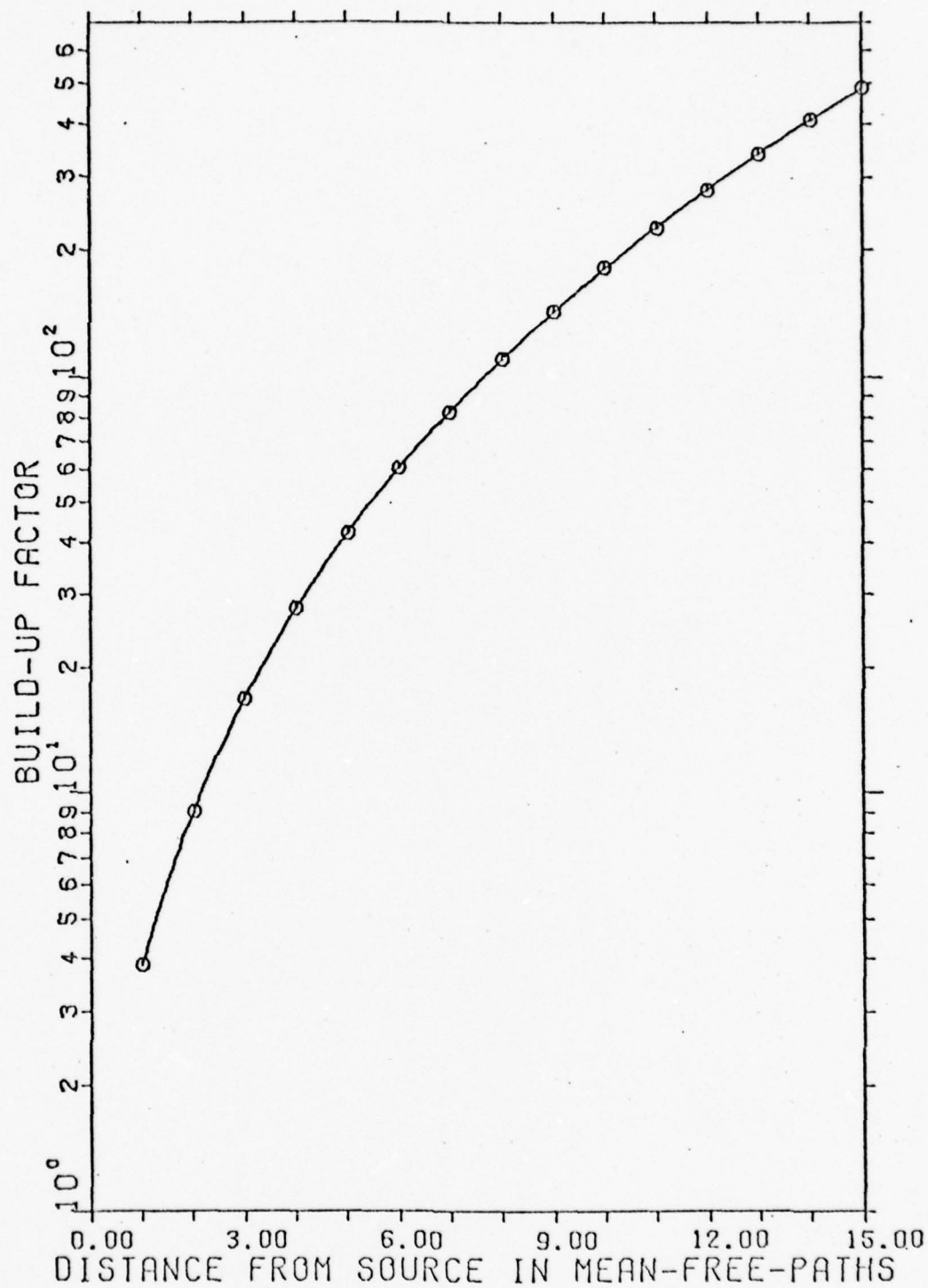


FIG. 38 ENERGY BUILD-UP FACTORS FOR 86 KEV

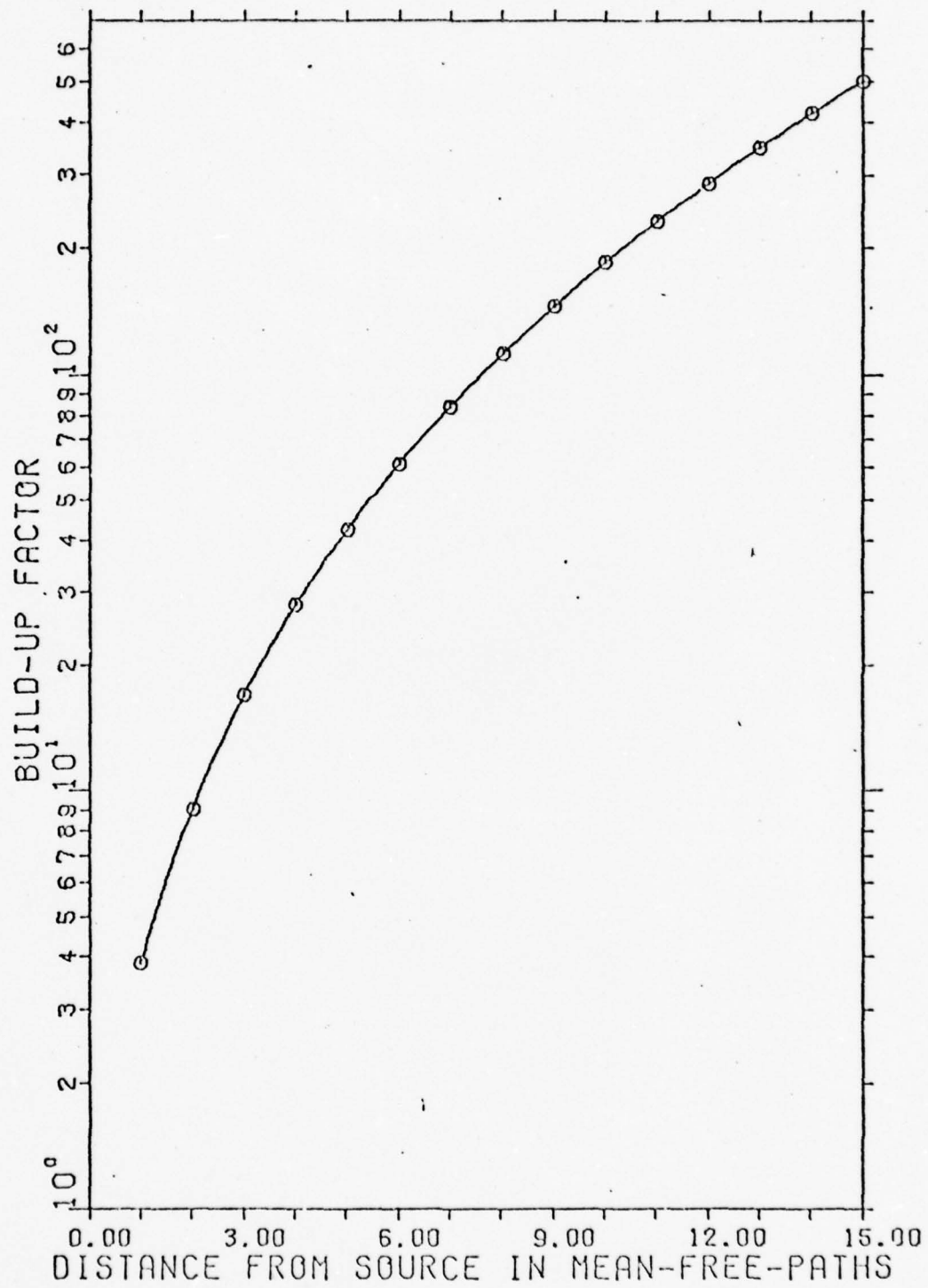


FIG. 39 ENERGY BUILD-UP FACTORS FOR 88 KEV

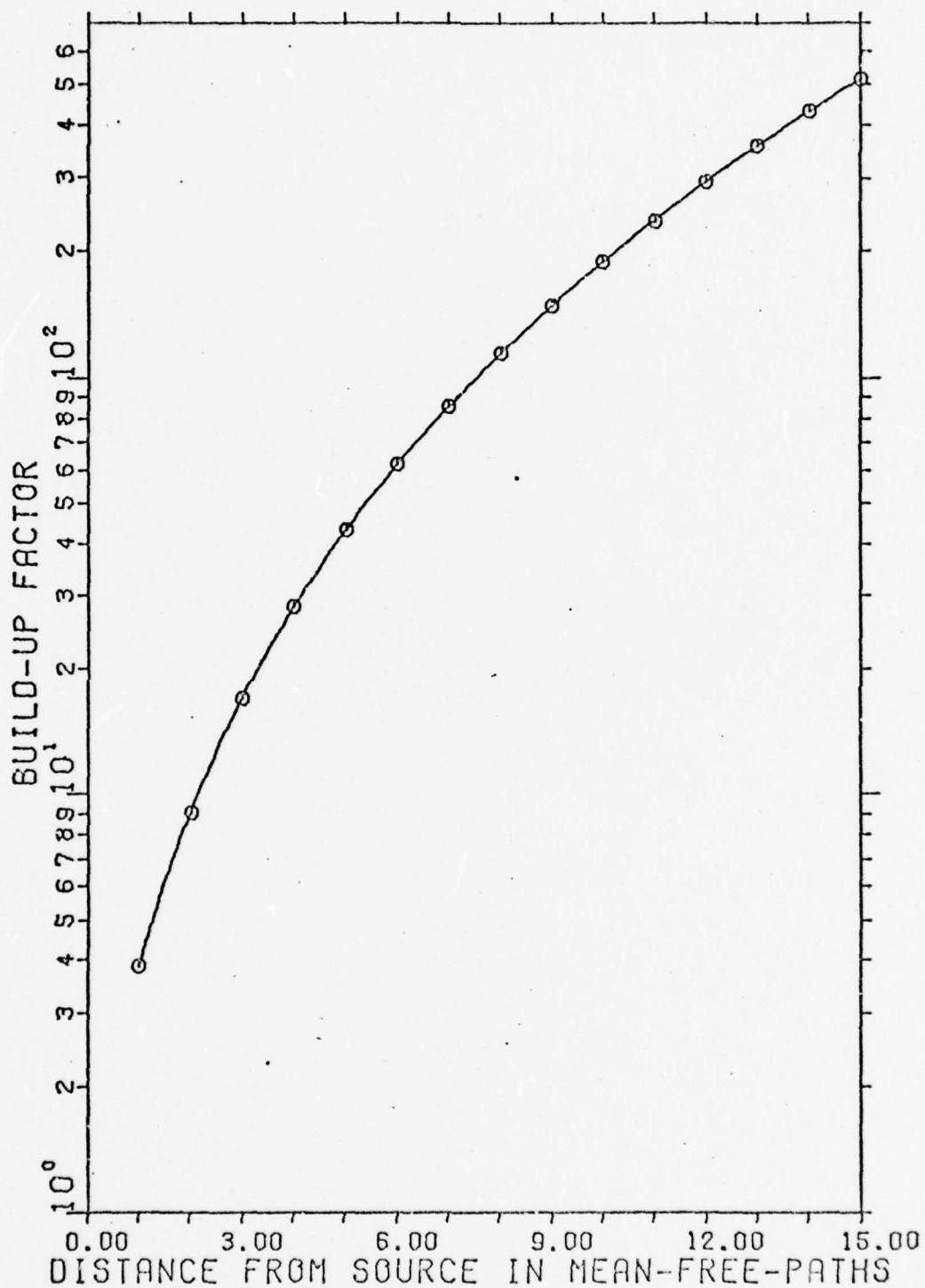


FIG. 40 ENERGY BUILD-UP FACTORS FOR 90 KEV

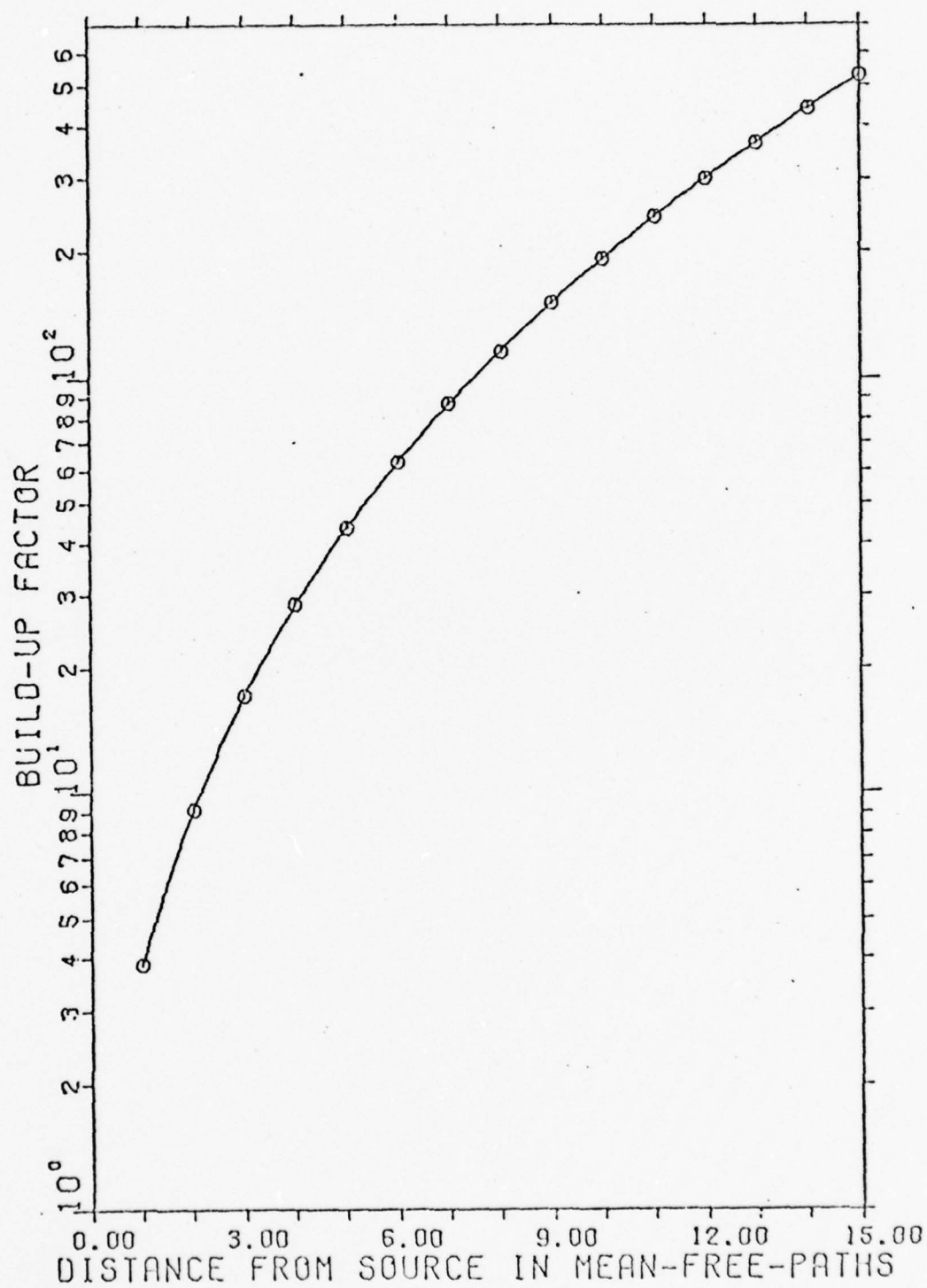


FIG. 41 ENERGY BUILD-UP FACTORS FOR 92 KEV

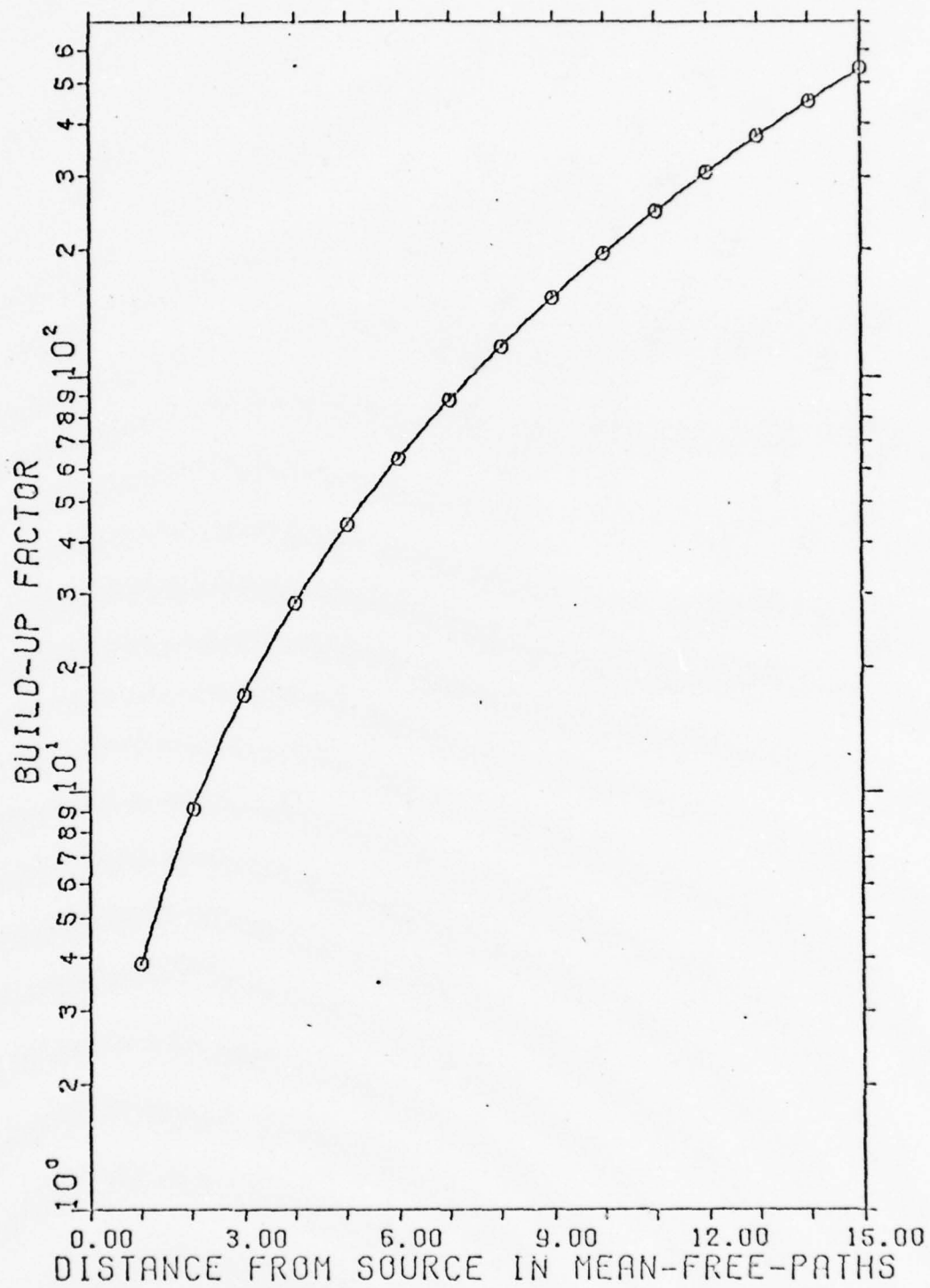


FIG. 42 ENERGY BUILD-UP FACTORS FOR 94 KEV



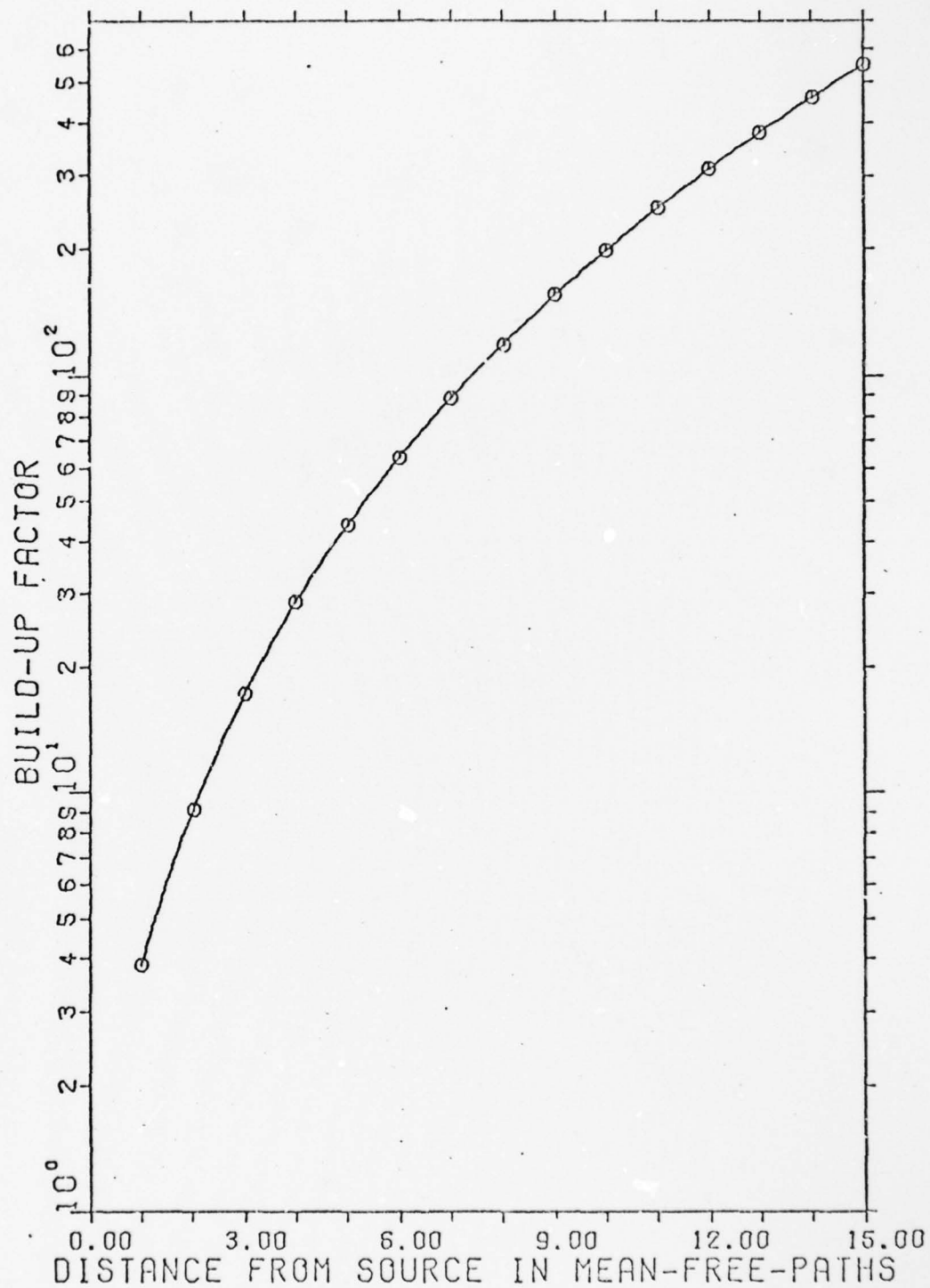


FIG. 43 ENERGY BUILD-UP FACTORS FOR 96 KEV

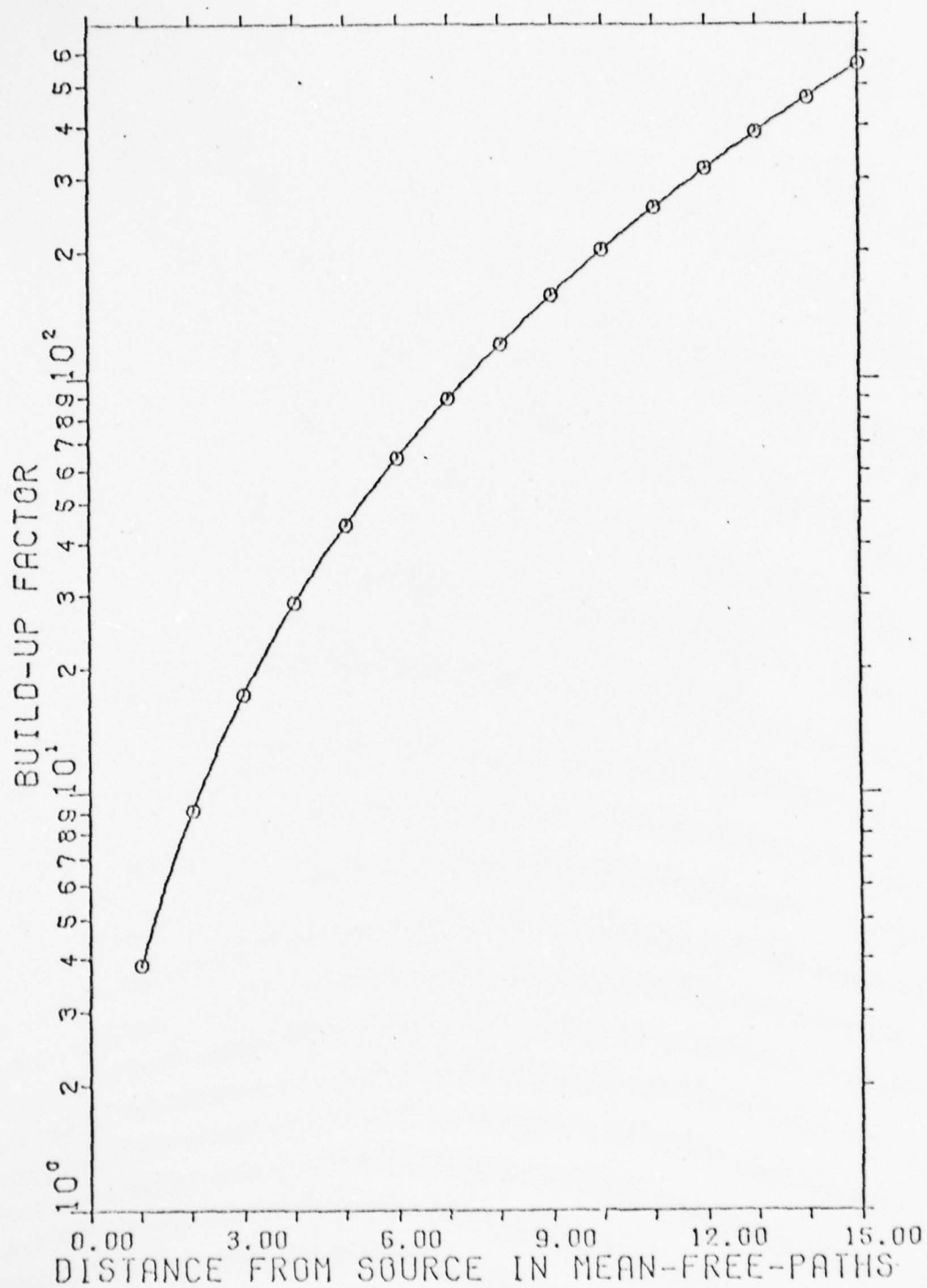


FIG. 44 ENERGY BUILD-UP FACTORS FOR 98 KEV

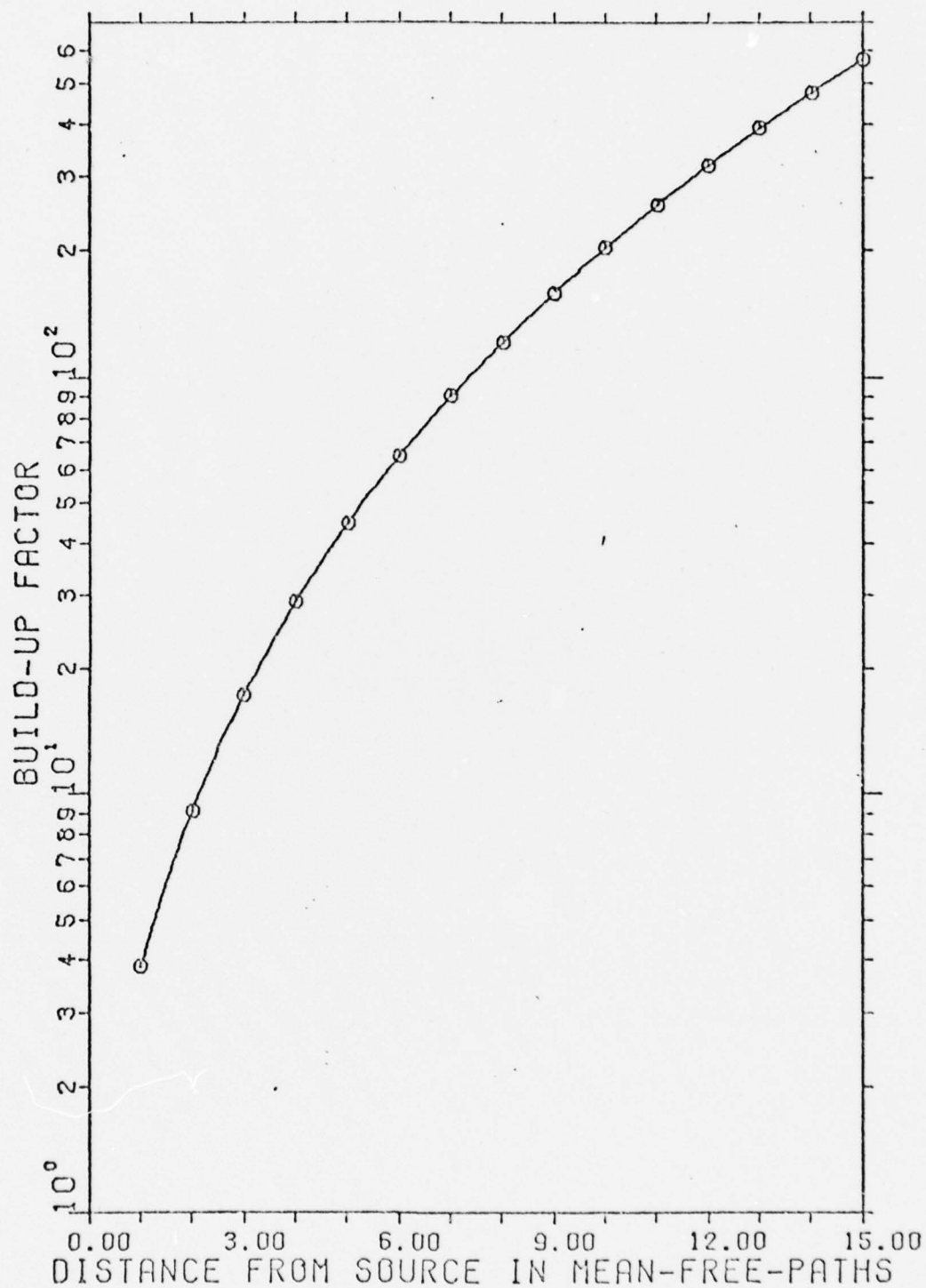


FIG. 45 ENERGY BUILD-UP FACTORS FOR 100 KEV

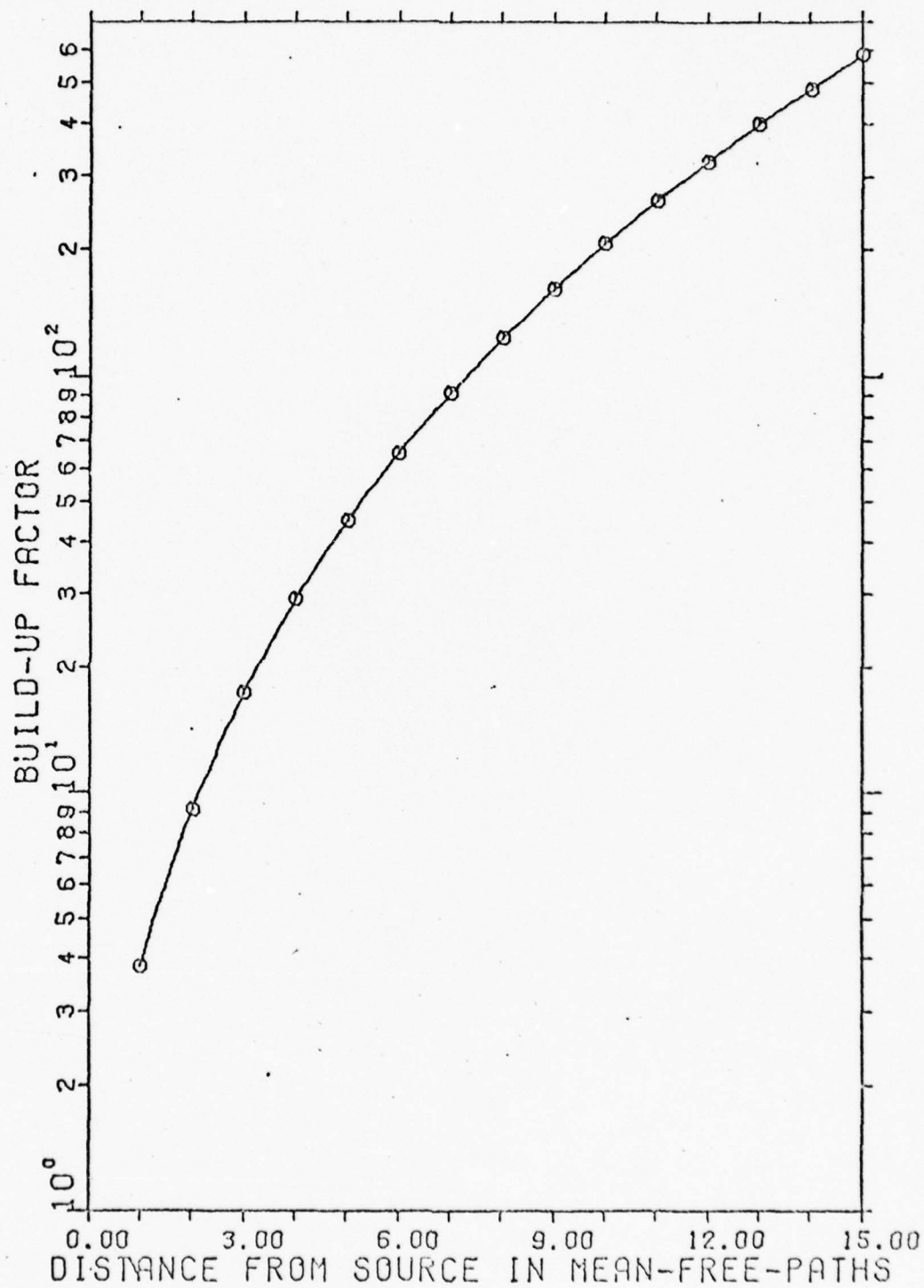


FIG. 46 ENERGY BUILD-UP FACTORS FOR 105 KEV

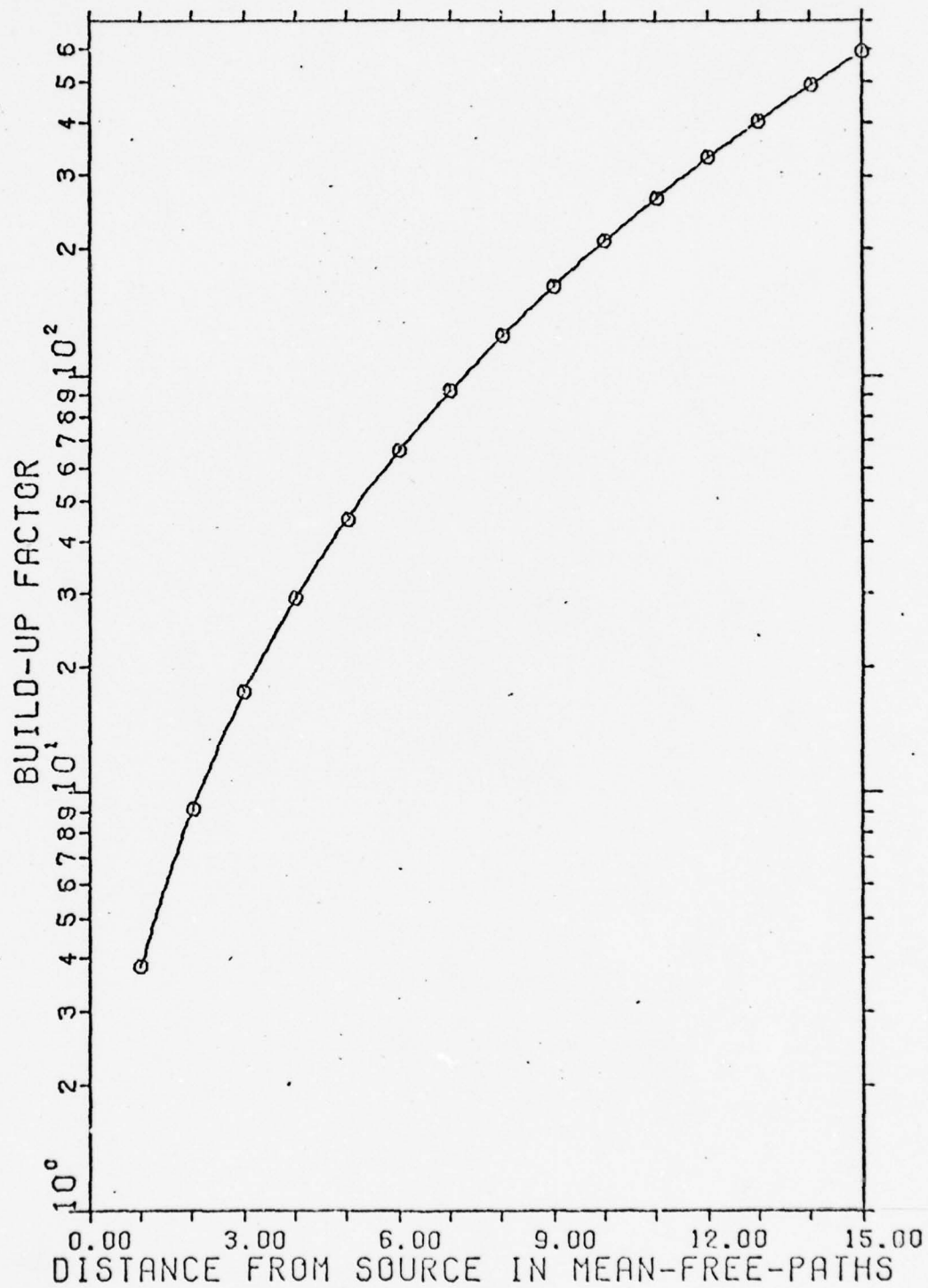


FIG. 47 ENERGY BUILD-UP FACTORS FOR 110 KEV



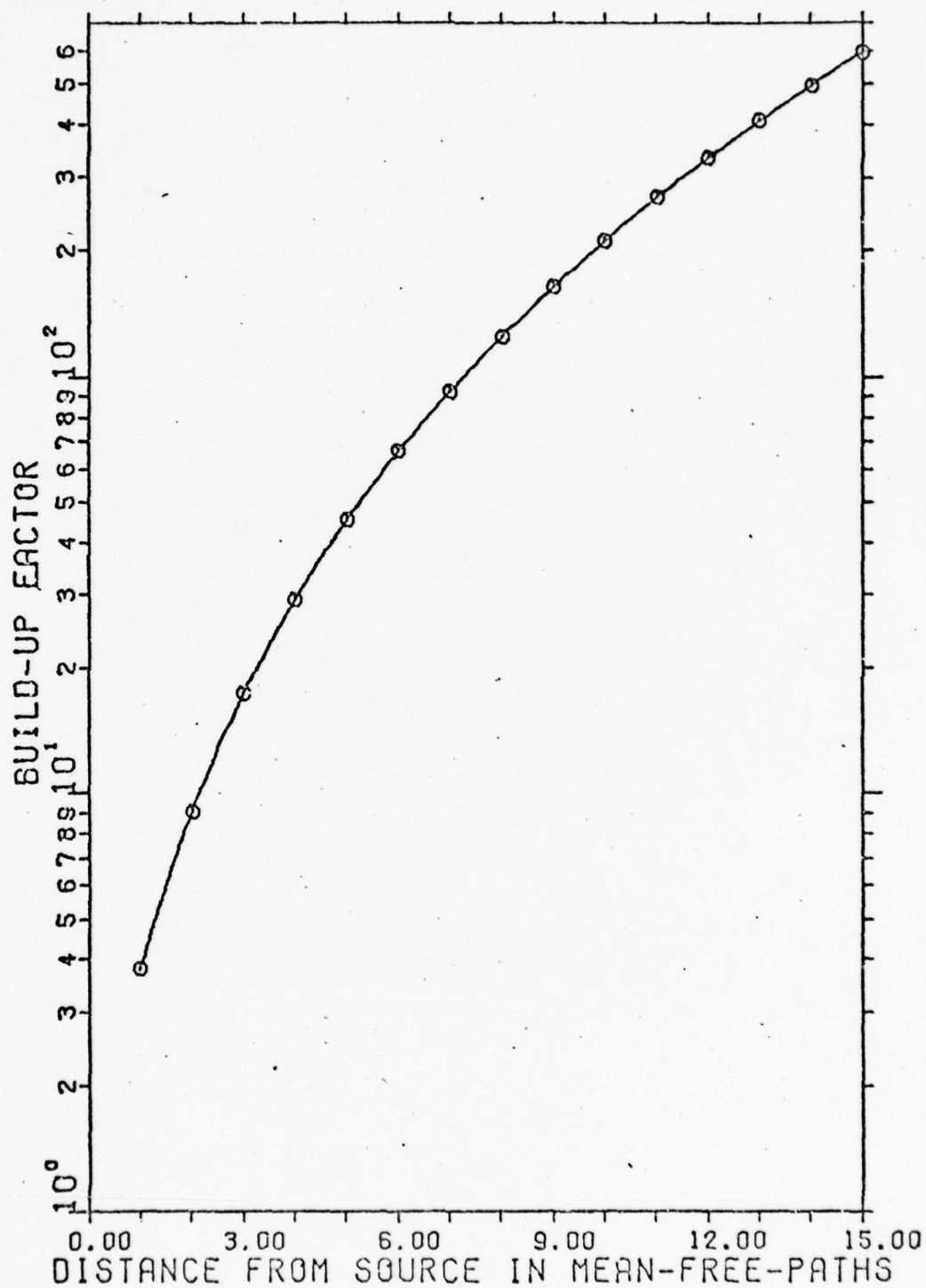


FIG. 48 ENERGY BUILD-UP FACTORS FOR 115 KEV

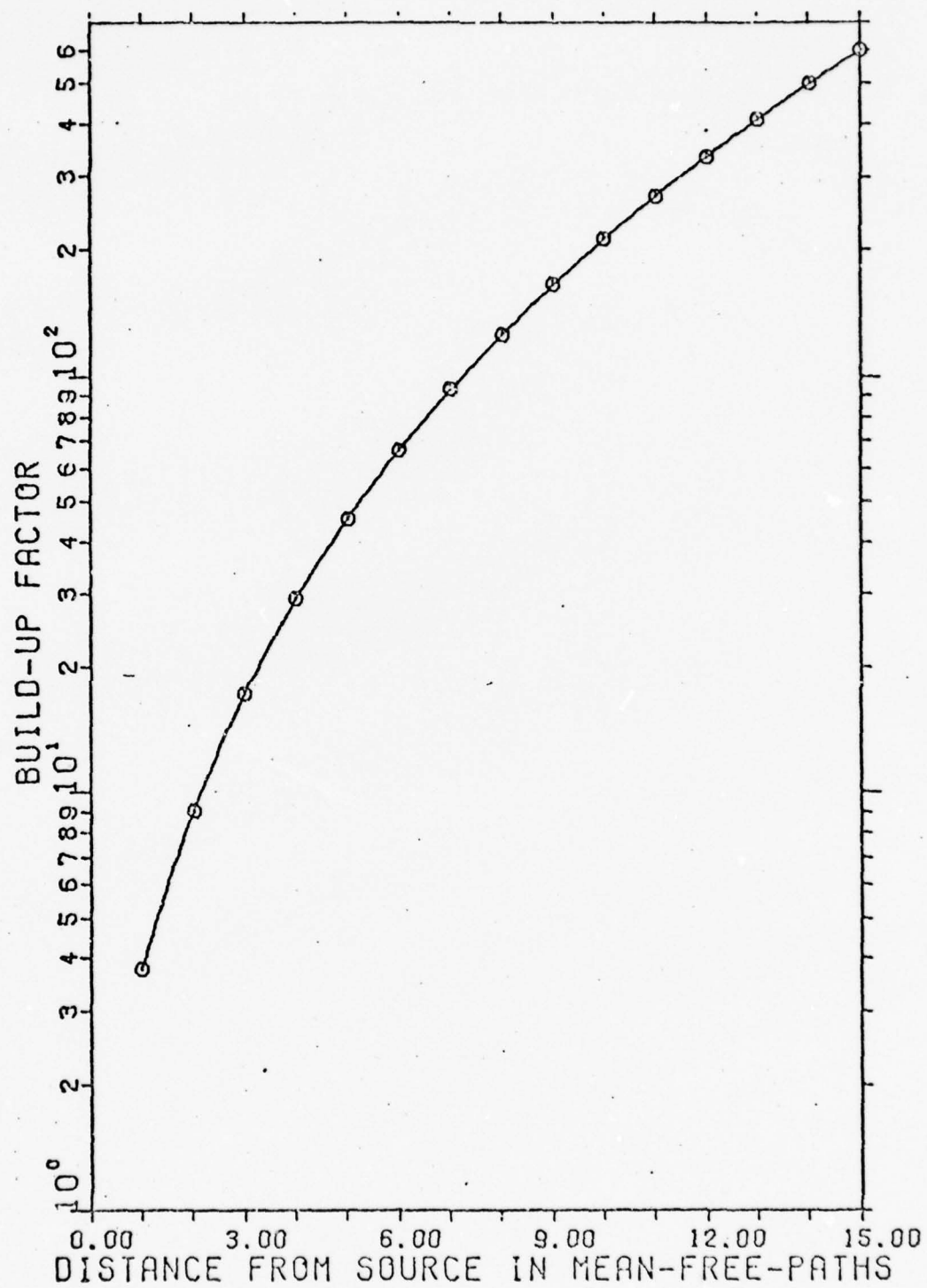


FIG. 49 ENERGY BUILD-UP FACTORS FOR 120 KEV

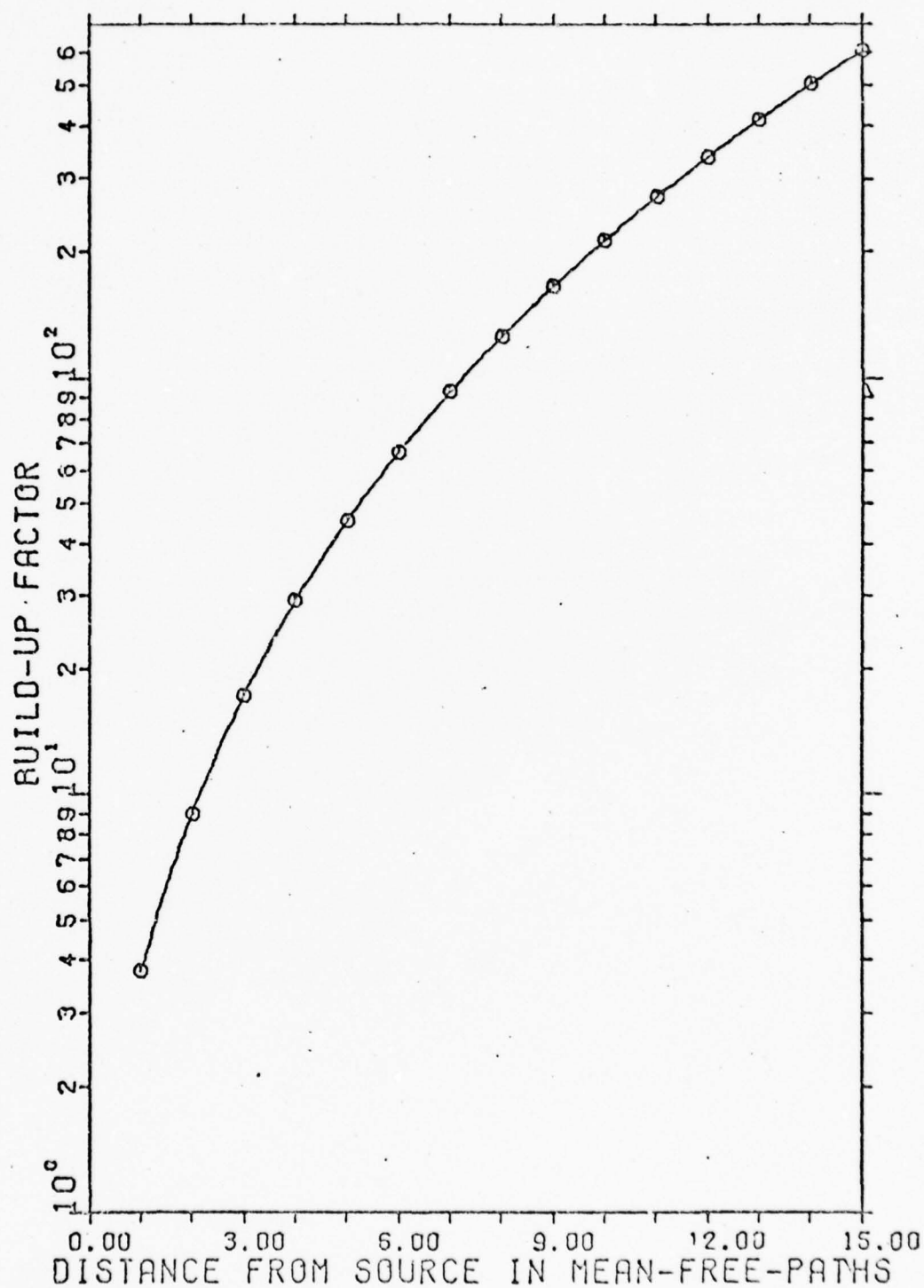


FIG. 50 ENERGY BUILD-UP FACTORS FOR 125 KEV

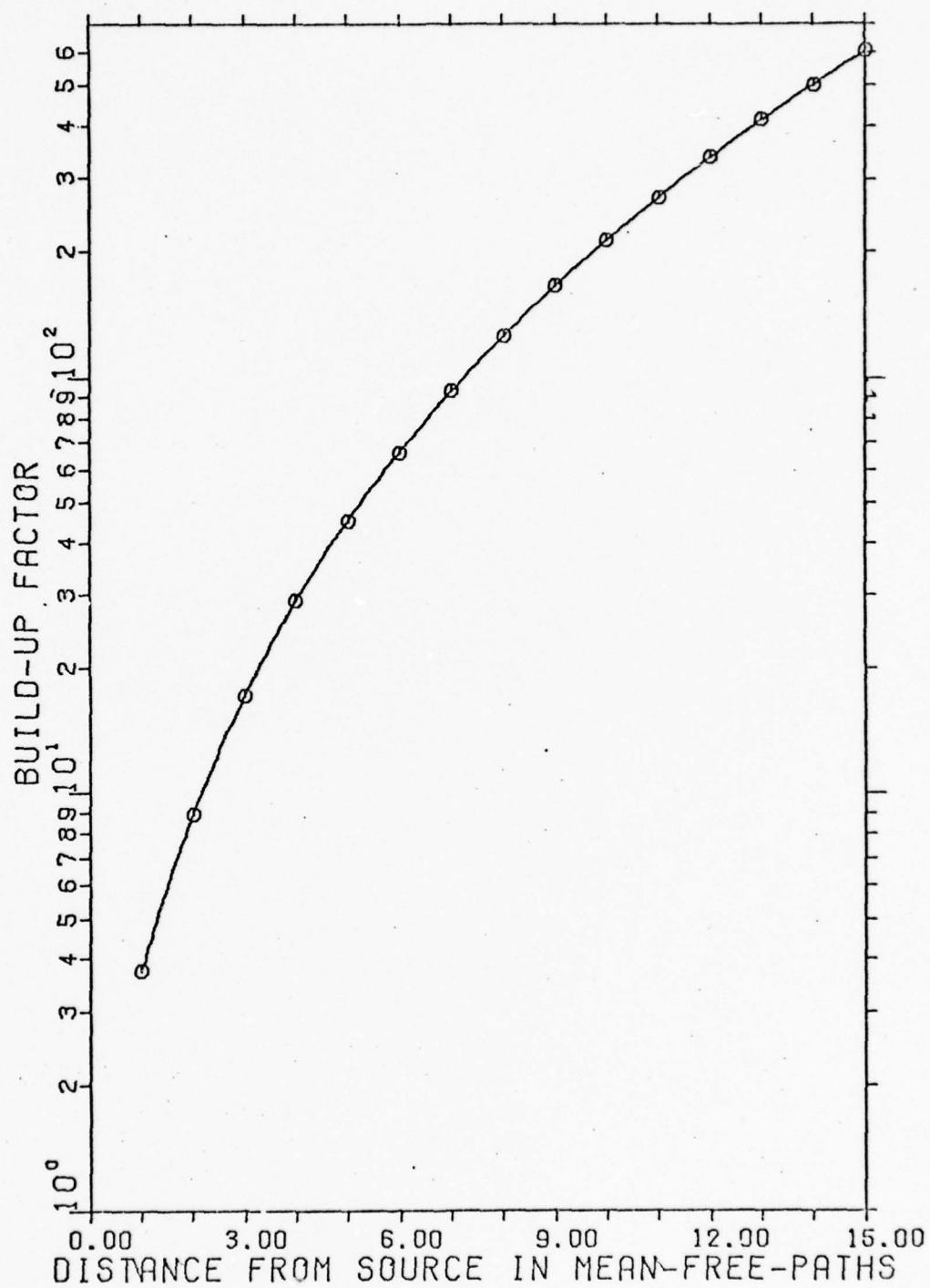


FIG. 51 ENERGY BUILD-UP FACTORS FOR 130 KEV

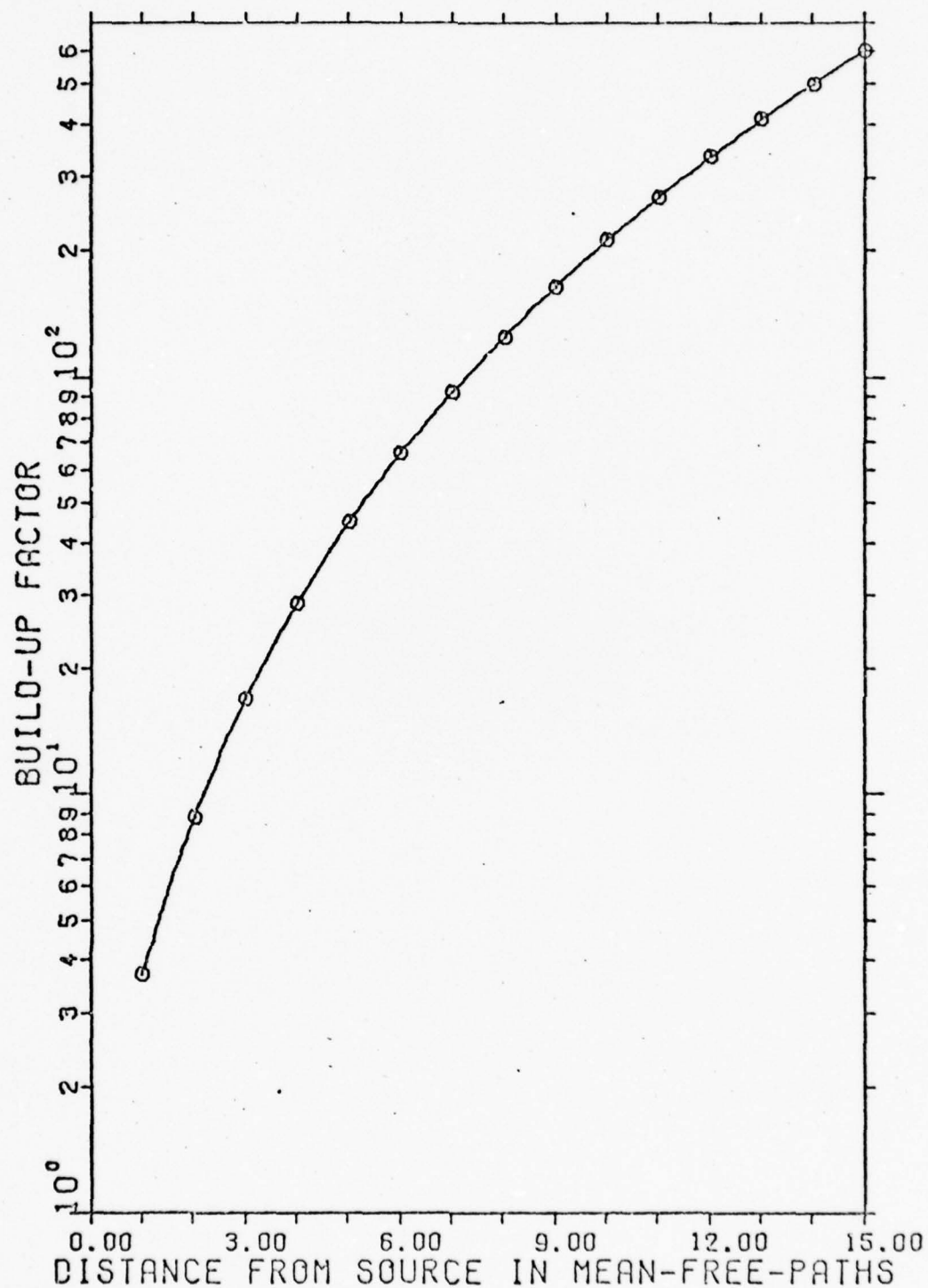


FIG. 52 ENERGY BUILD-UP FACTORS FOR 135 KEV

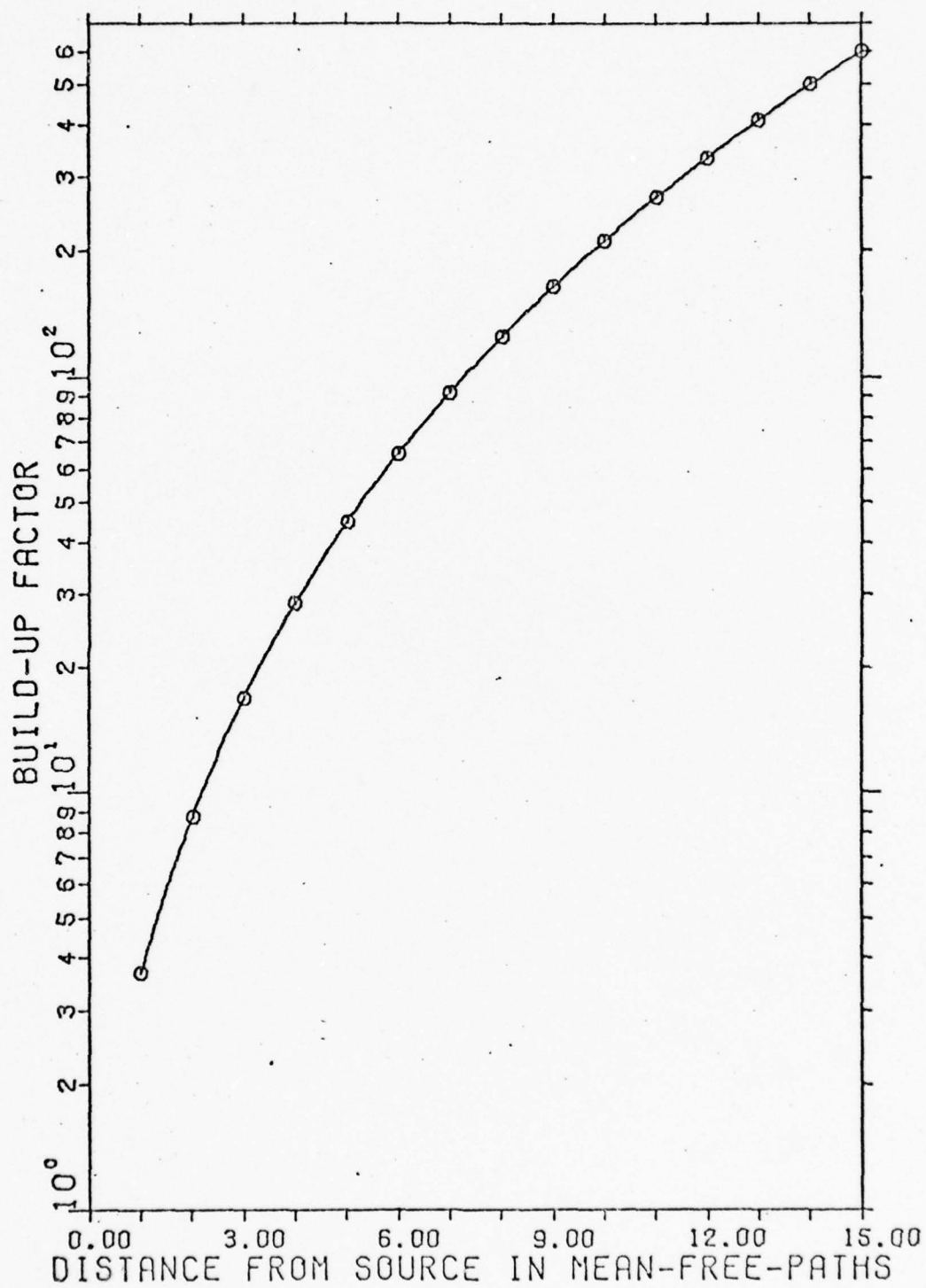


FIG. 53 ENERGY BUILD-UP FACTORS FOR 140 KEV



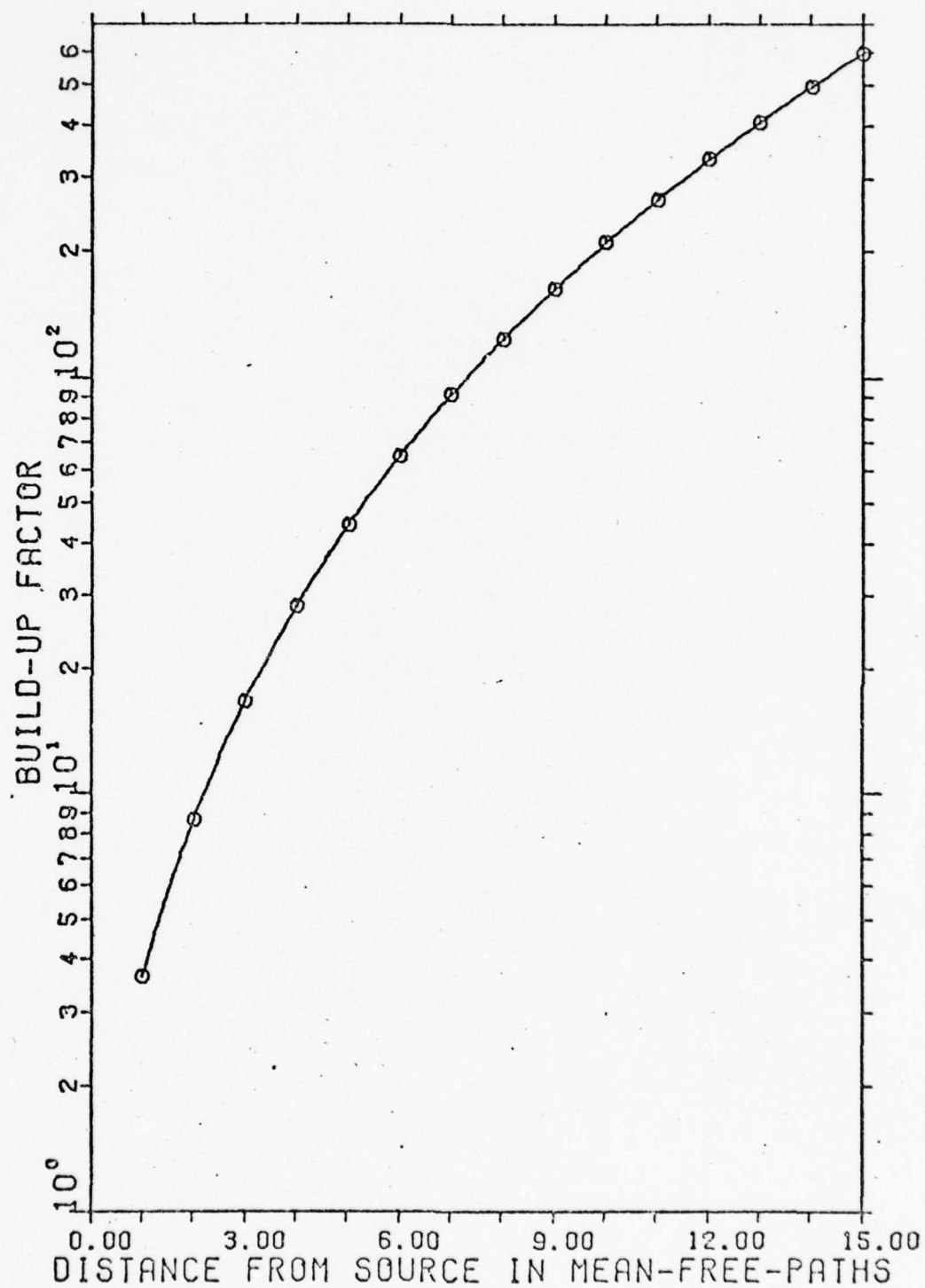


FIG. 54 ENERGY BUILD-UP FACTORS FOR 145 KEV

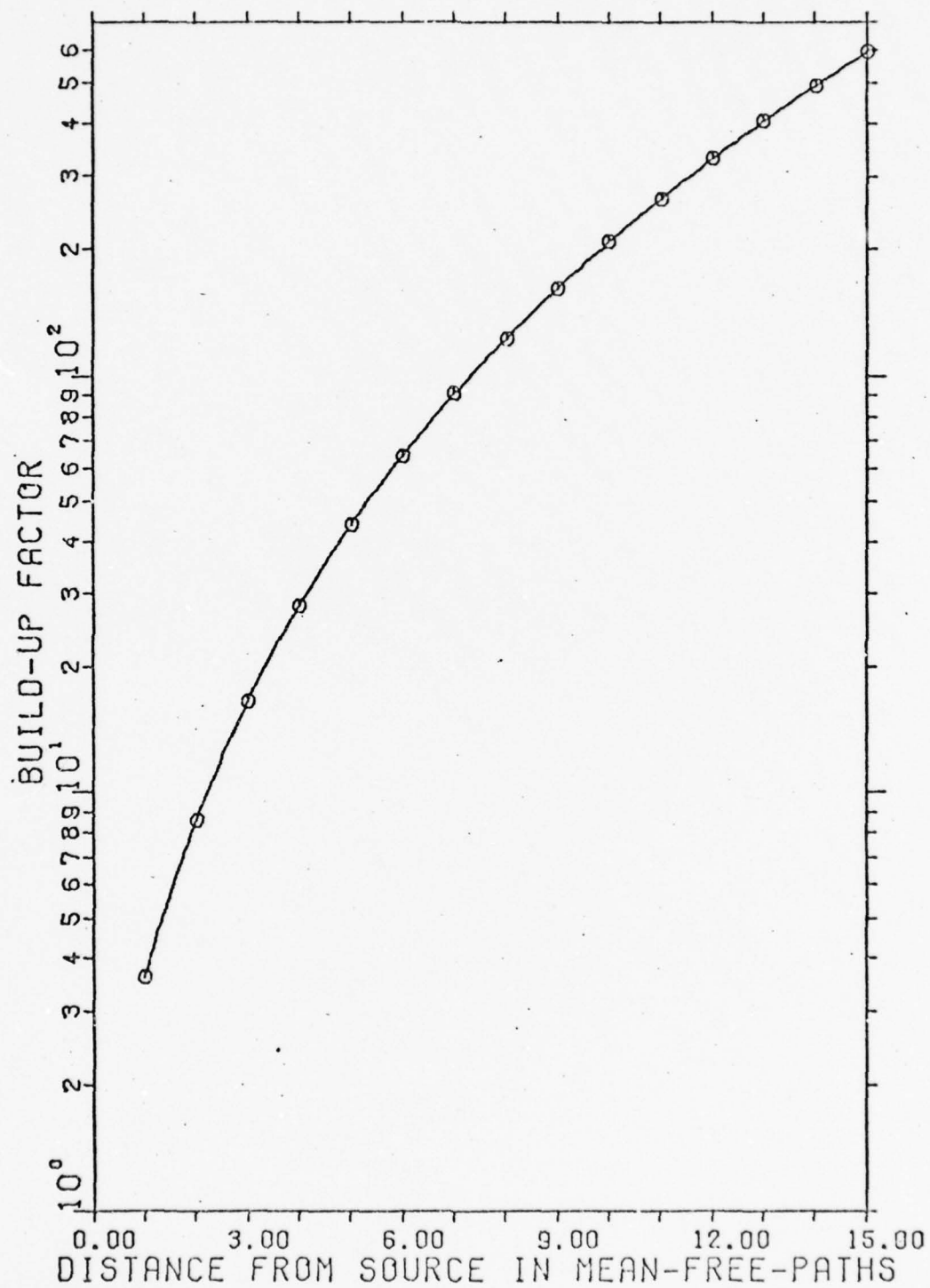


FIG. 55 ENERGY BUILD-UP FACTORS FOR 150 KEV

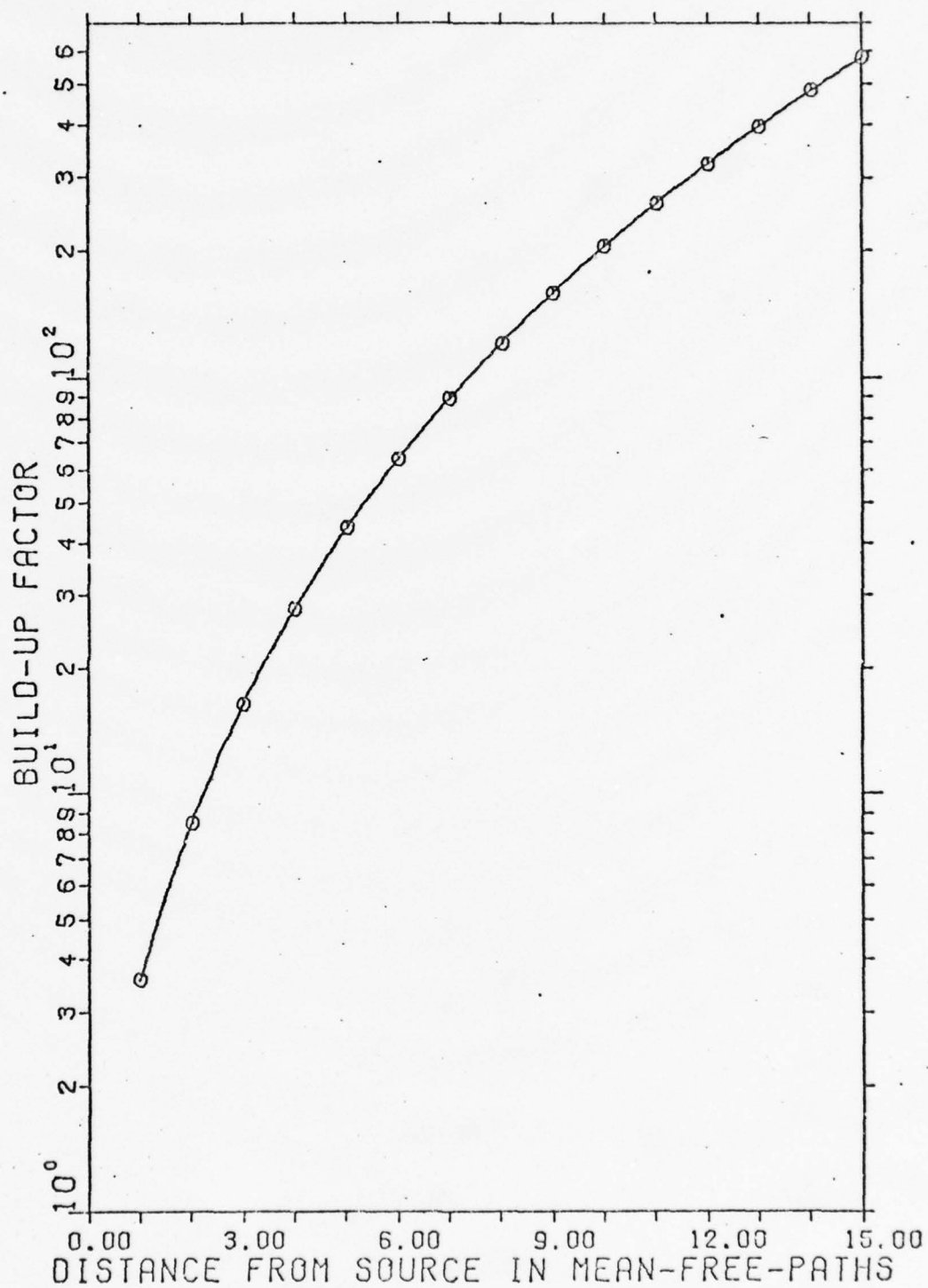


FIG. 56 ENERGY BUILD-UP FACTORS FOR 155 KEV

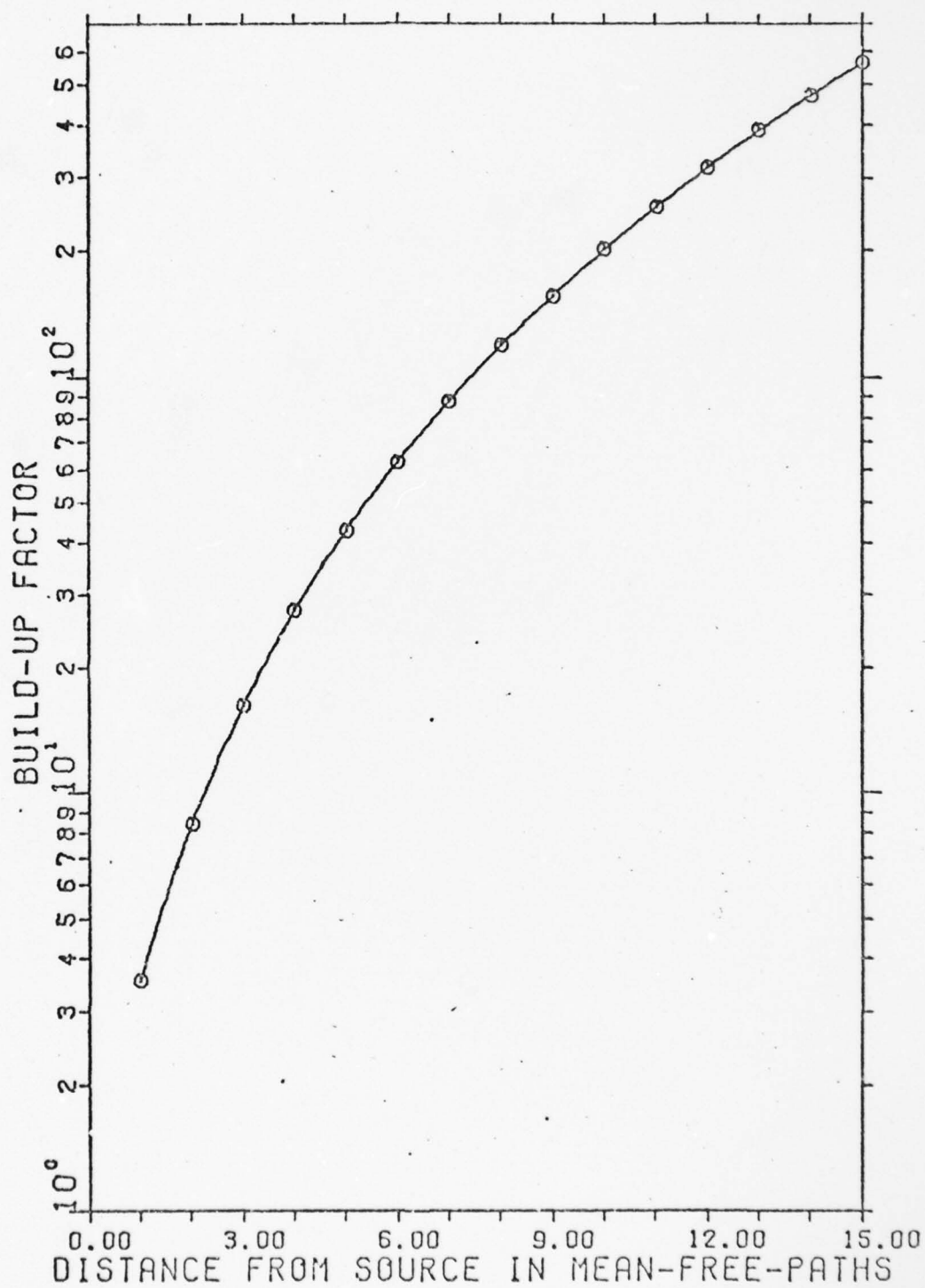


FIG. 57 ENERGY BUILD-UP FACTORS FOR 160 KEV

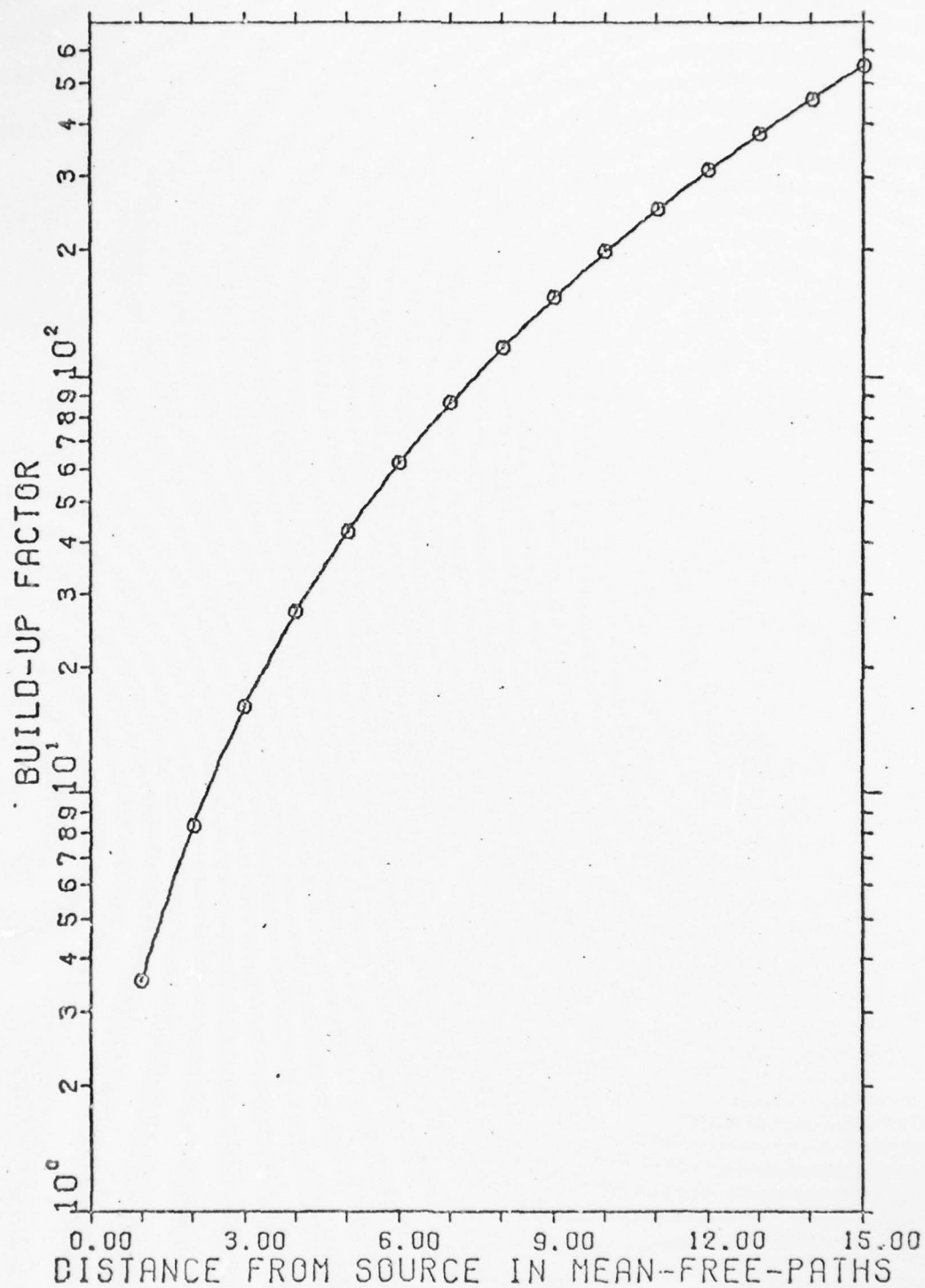


FIG. 58 ENERGY BUILD-UP FACTORS FOR 165 KEV

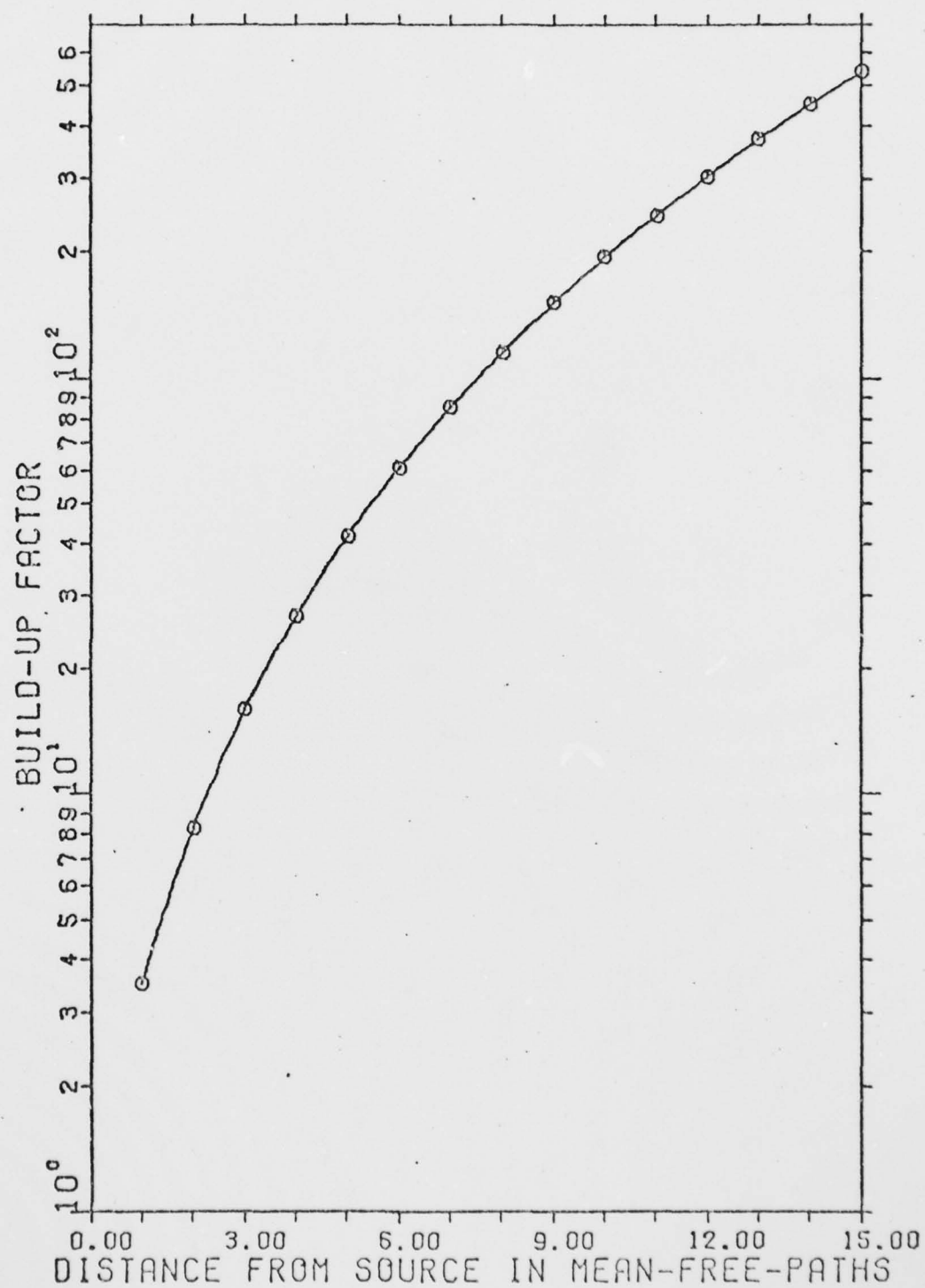


FIG. 59 ENERGY BUILD-UP FACTORS FOR 170 KEV



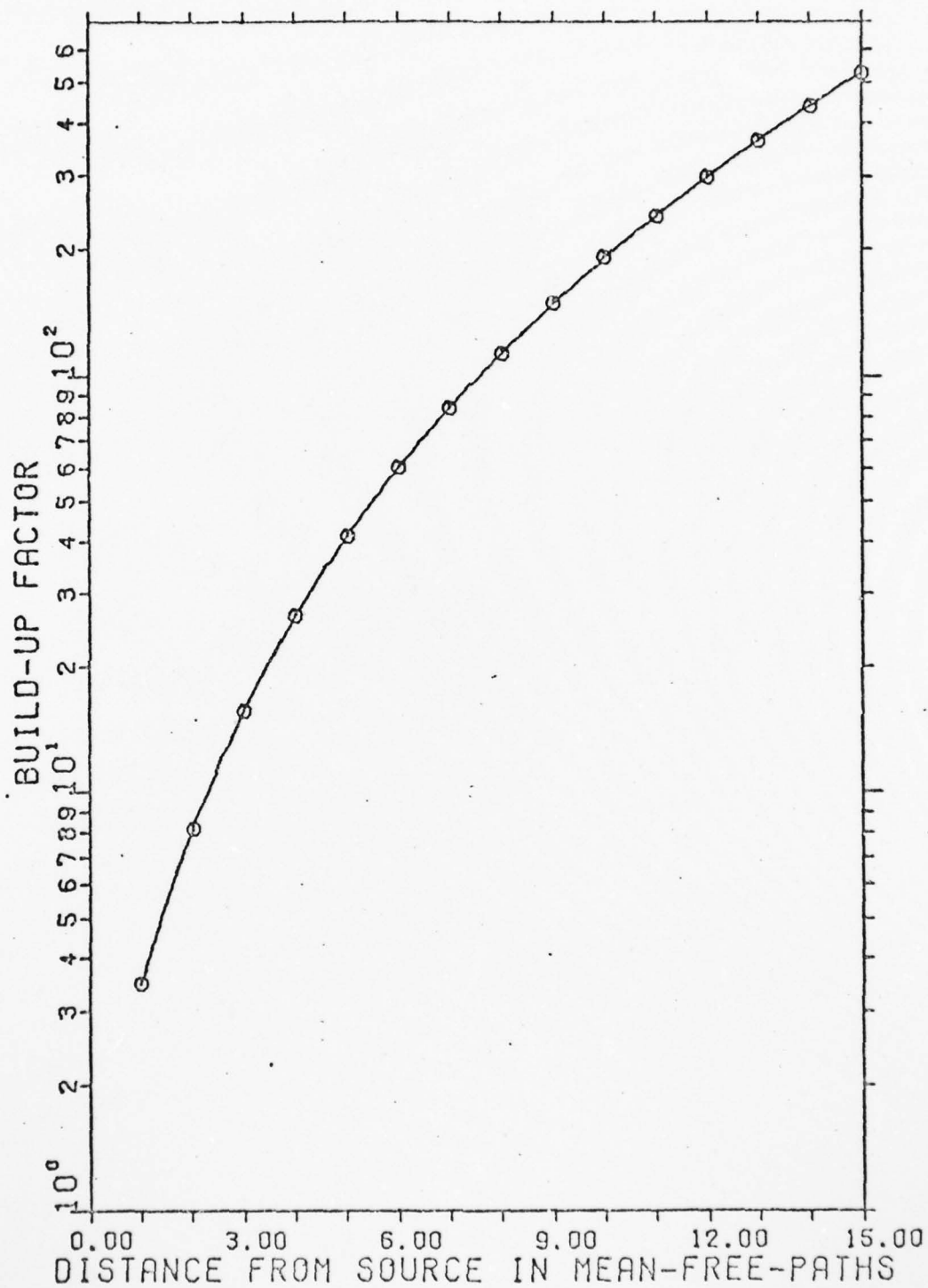


FIG. 60 ENERGY BUILD-UP FACTORS FOR 175 KEV

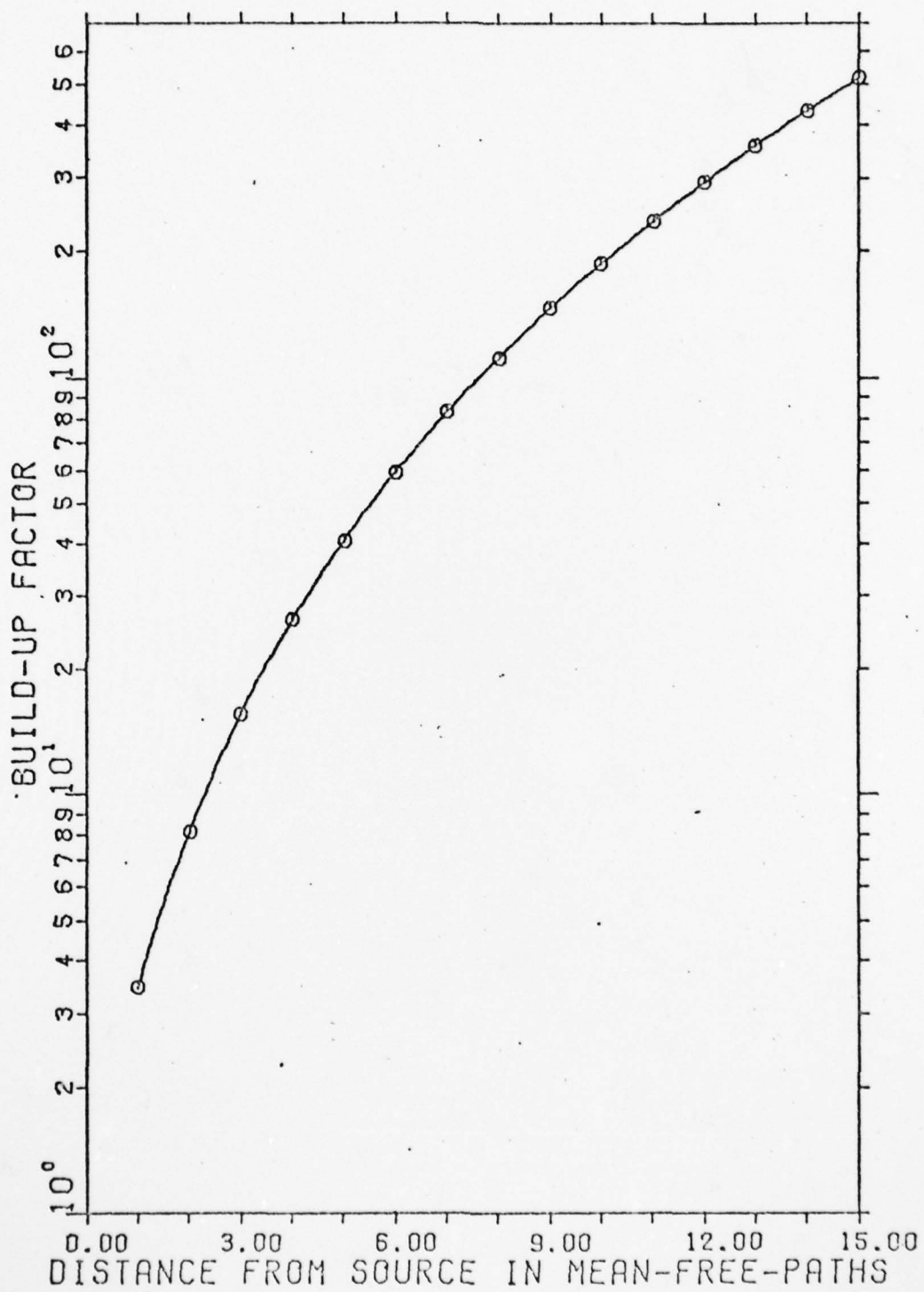


FIG. G1 ENERGY BUILD-UP FACTORS FOR 180 KEV

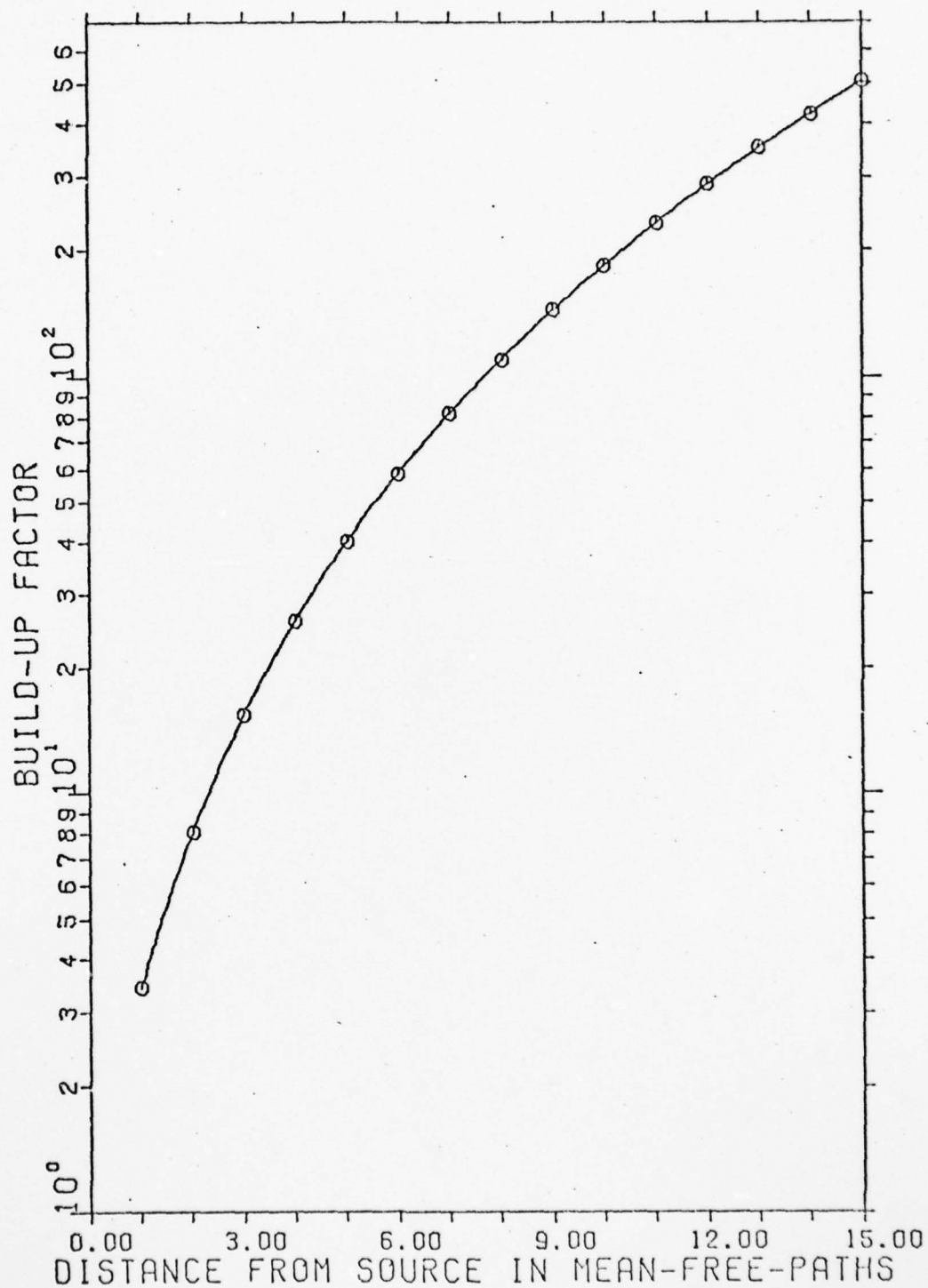


FIG. 62 ENERGY BUILD-UP FACTORS FOR 185 KEV

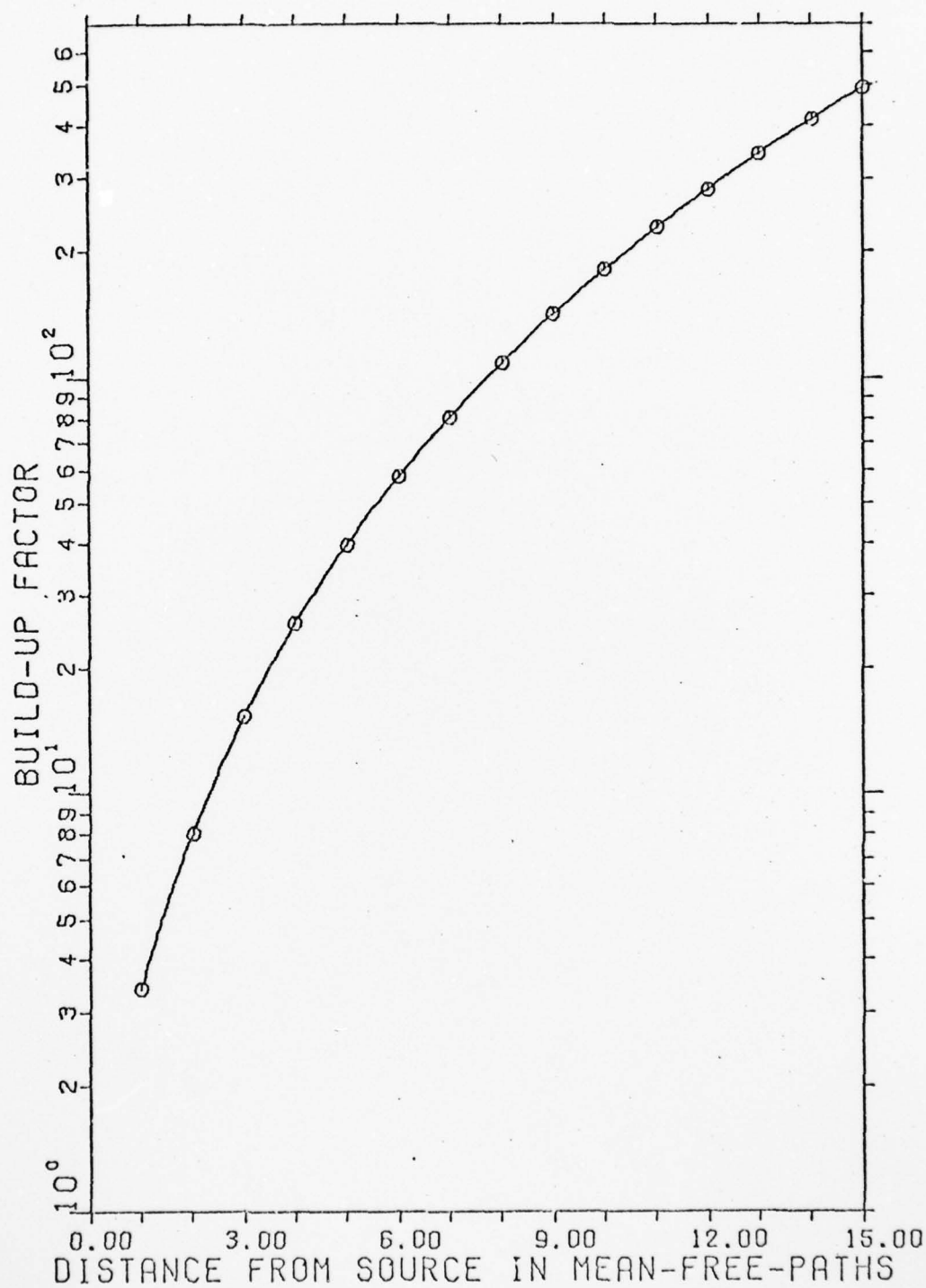


FIG. 63 ENERGY BUILD-UP FACTORS FOR 190 KEV

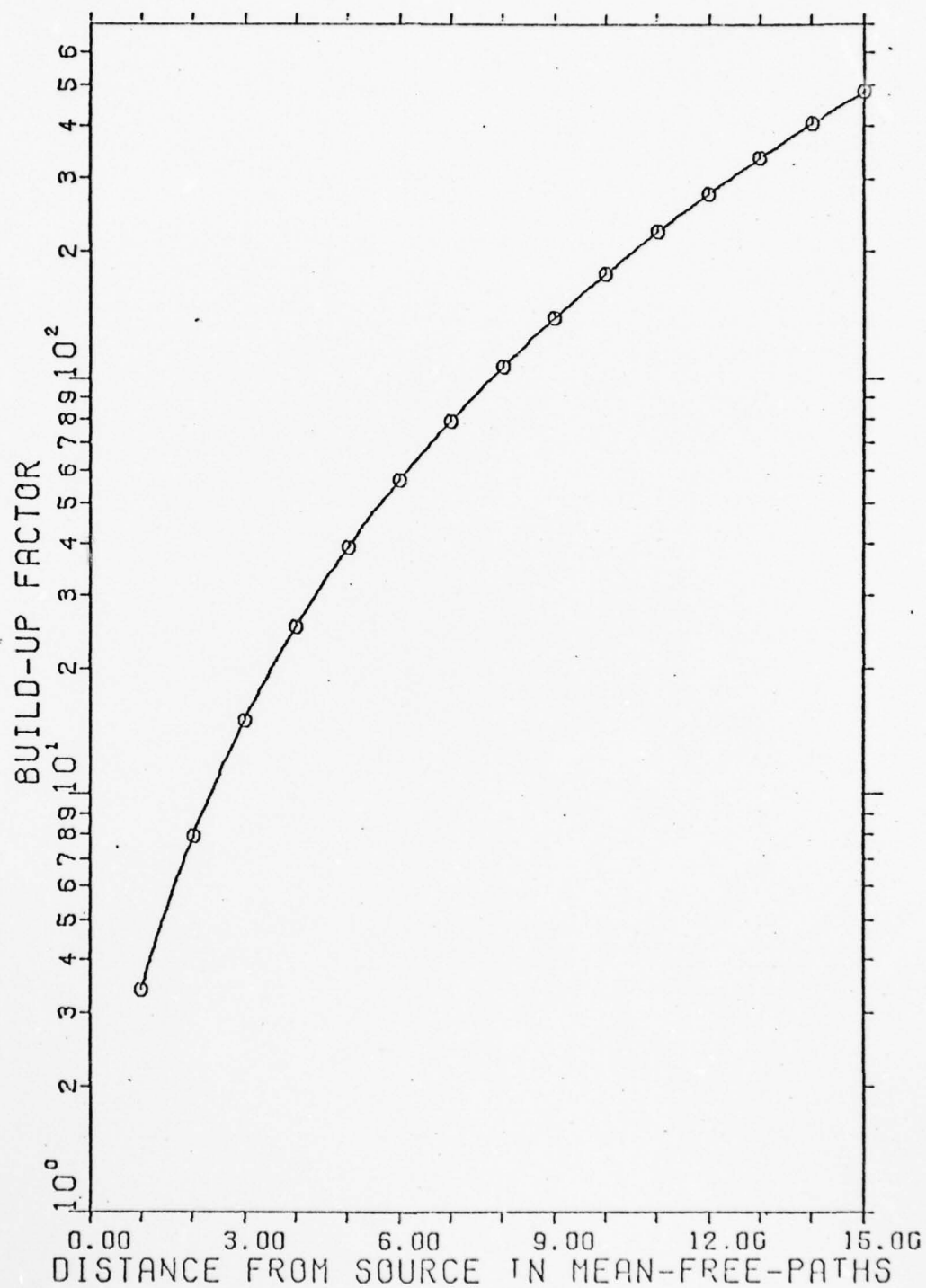


FIG. 64 ENERGY BUILD-UP FACTORS FOR 195 KEV

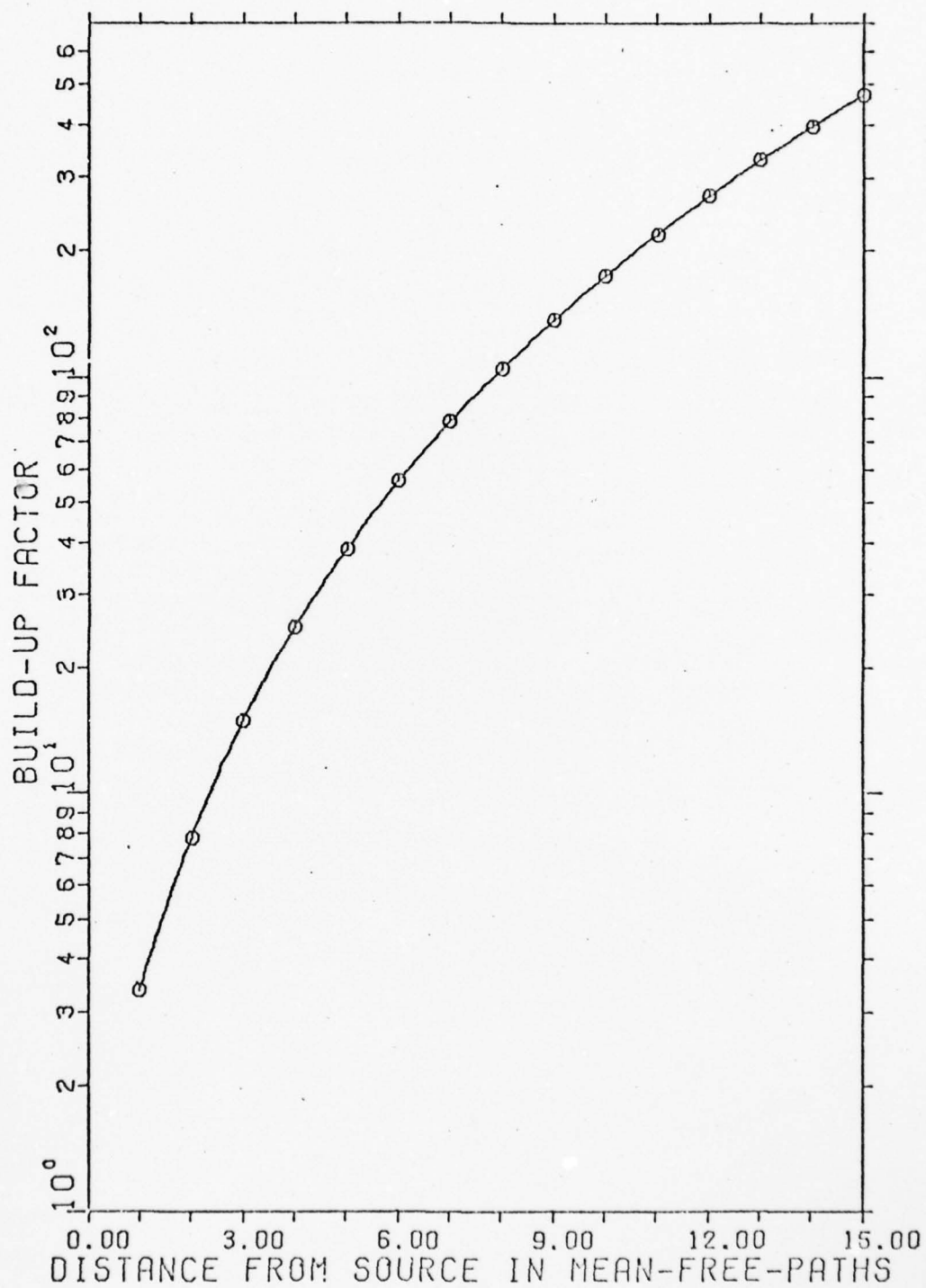


FIG. 65 ENERGY BUILD-UP FACTORS FOR 200 KEV



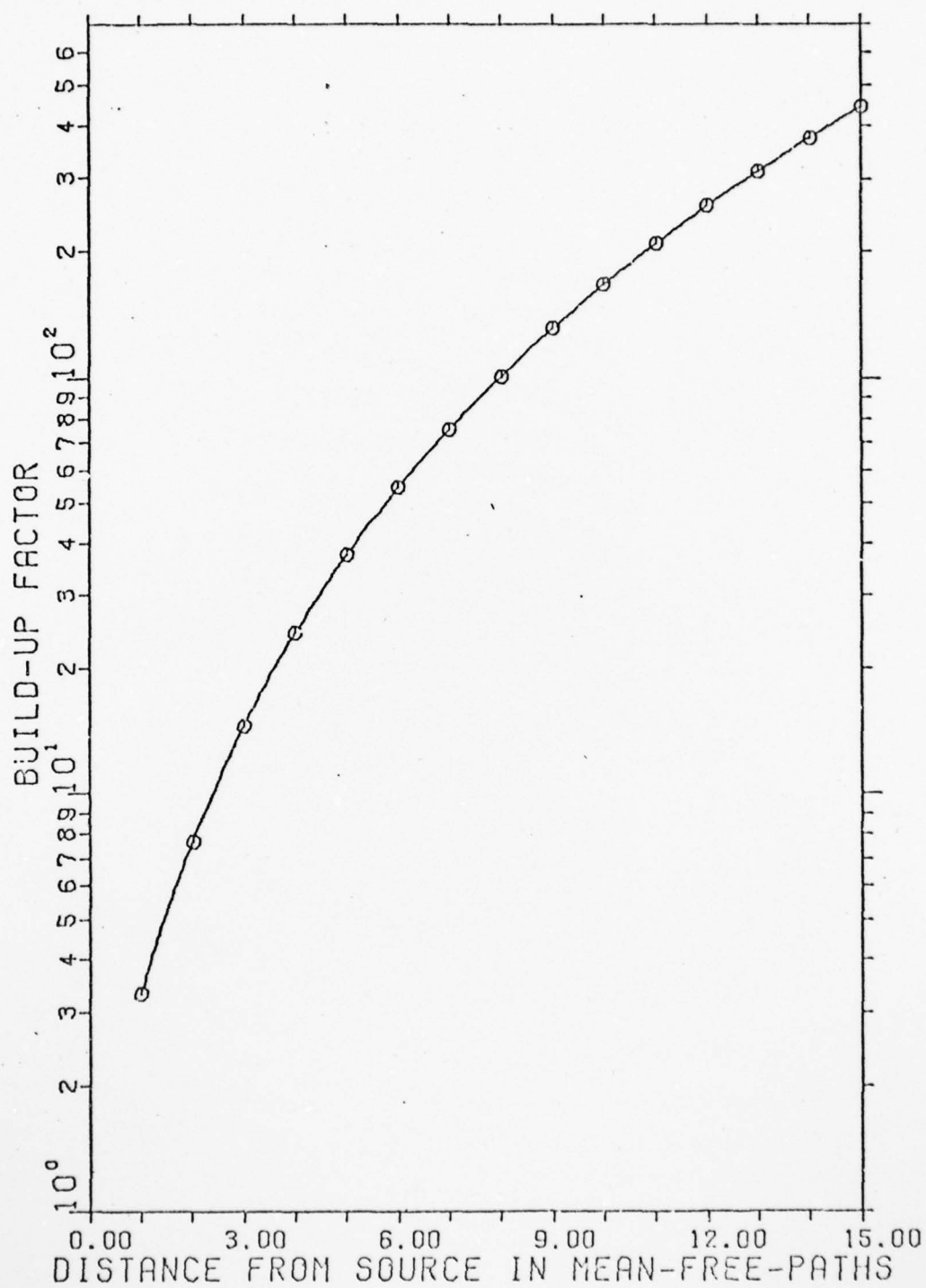


FIG. 66 ENERGY BUILD-UP FACTORS FOR 210 KEV

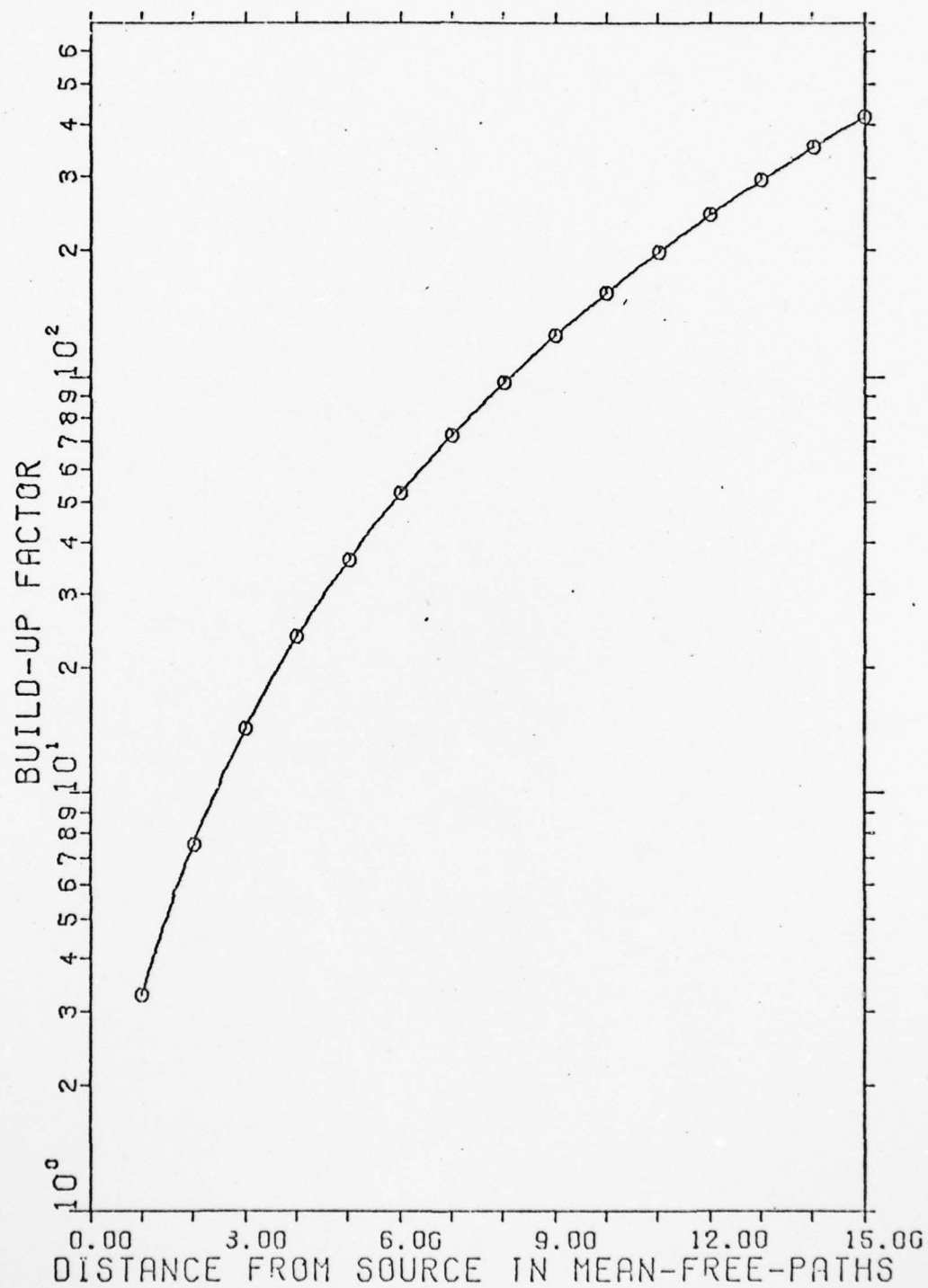


FIG. 67 ENERGY BUILD-UP FACTORS FOR 220 KEV

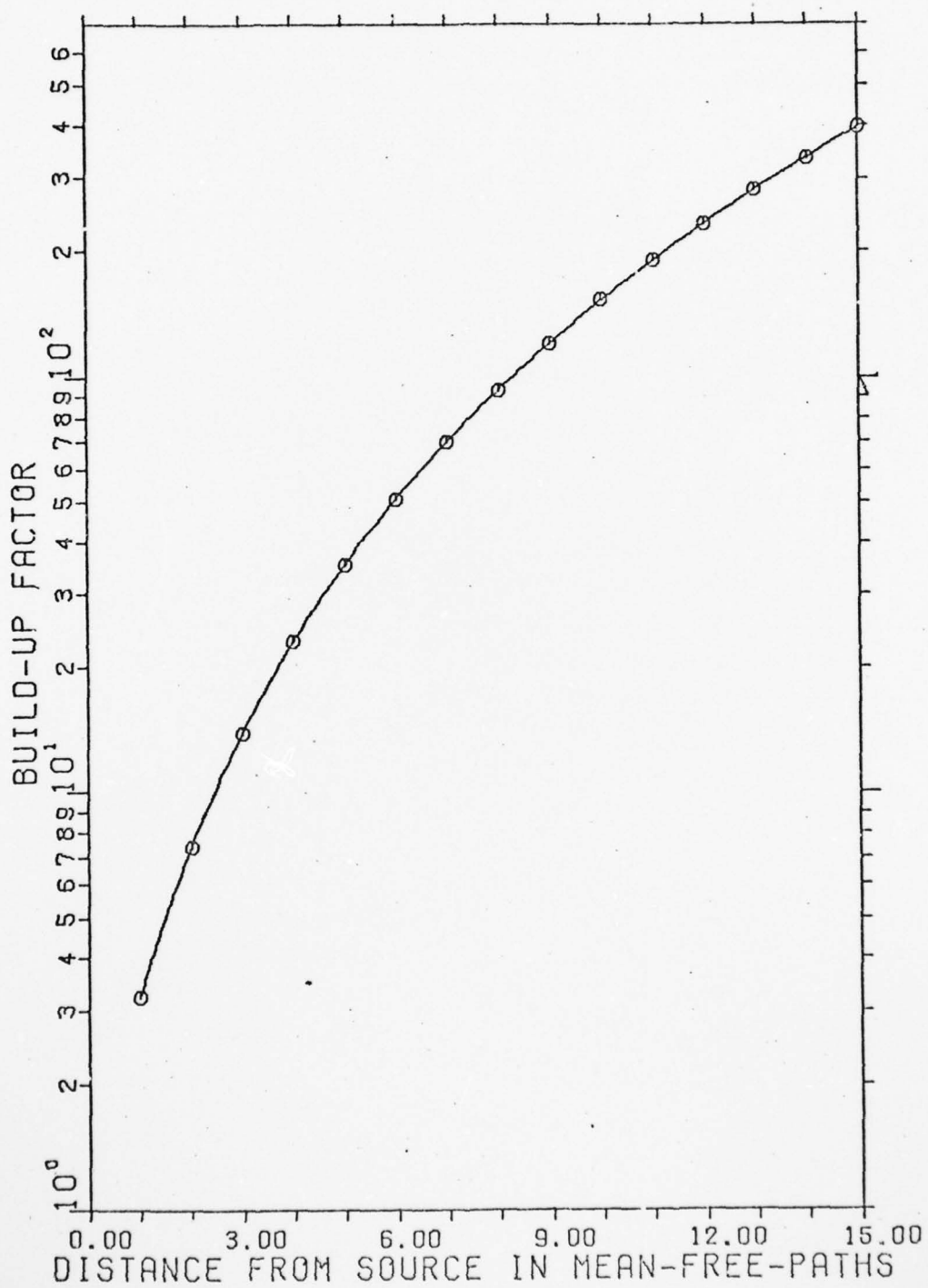


FIG. 68 ENERGY BUILD-UP FACTORS FOR 230 KEV

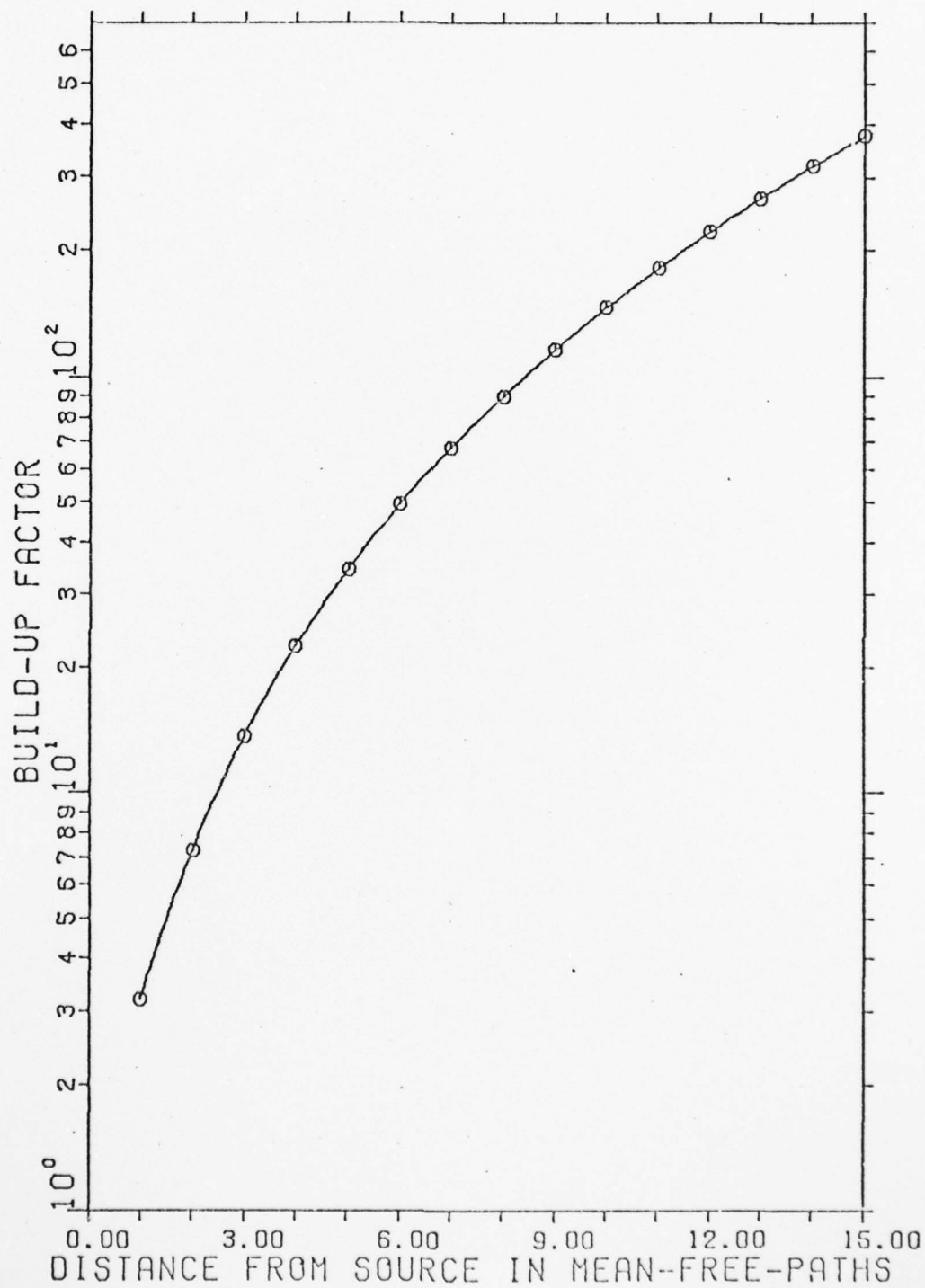


FIG. 69 ENERGY BUILD-UP FACTORS FOR 240 KEV

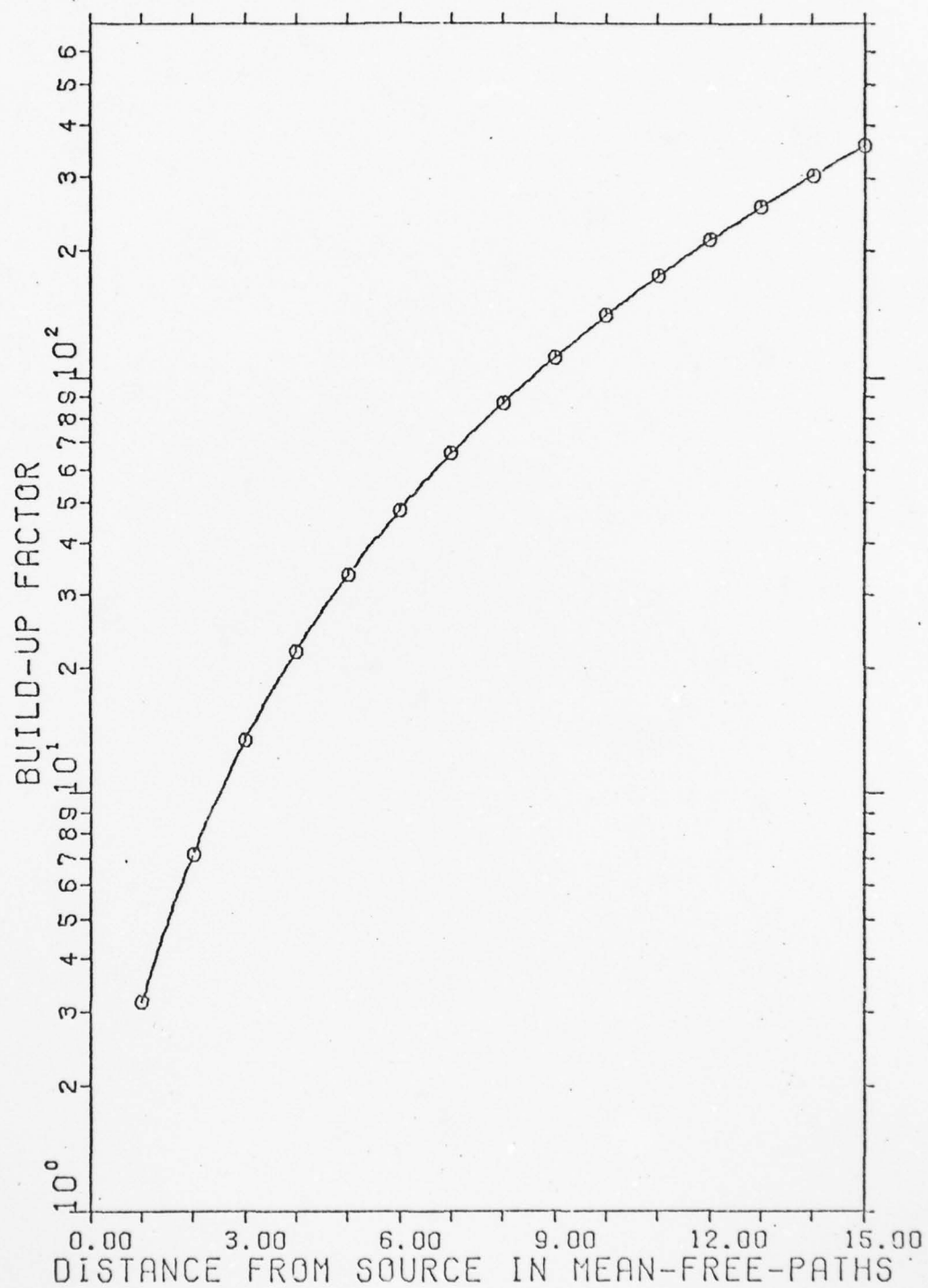


FIG. 70 ENERGY BUILD-UP FACTORS FOR 250 KEV

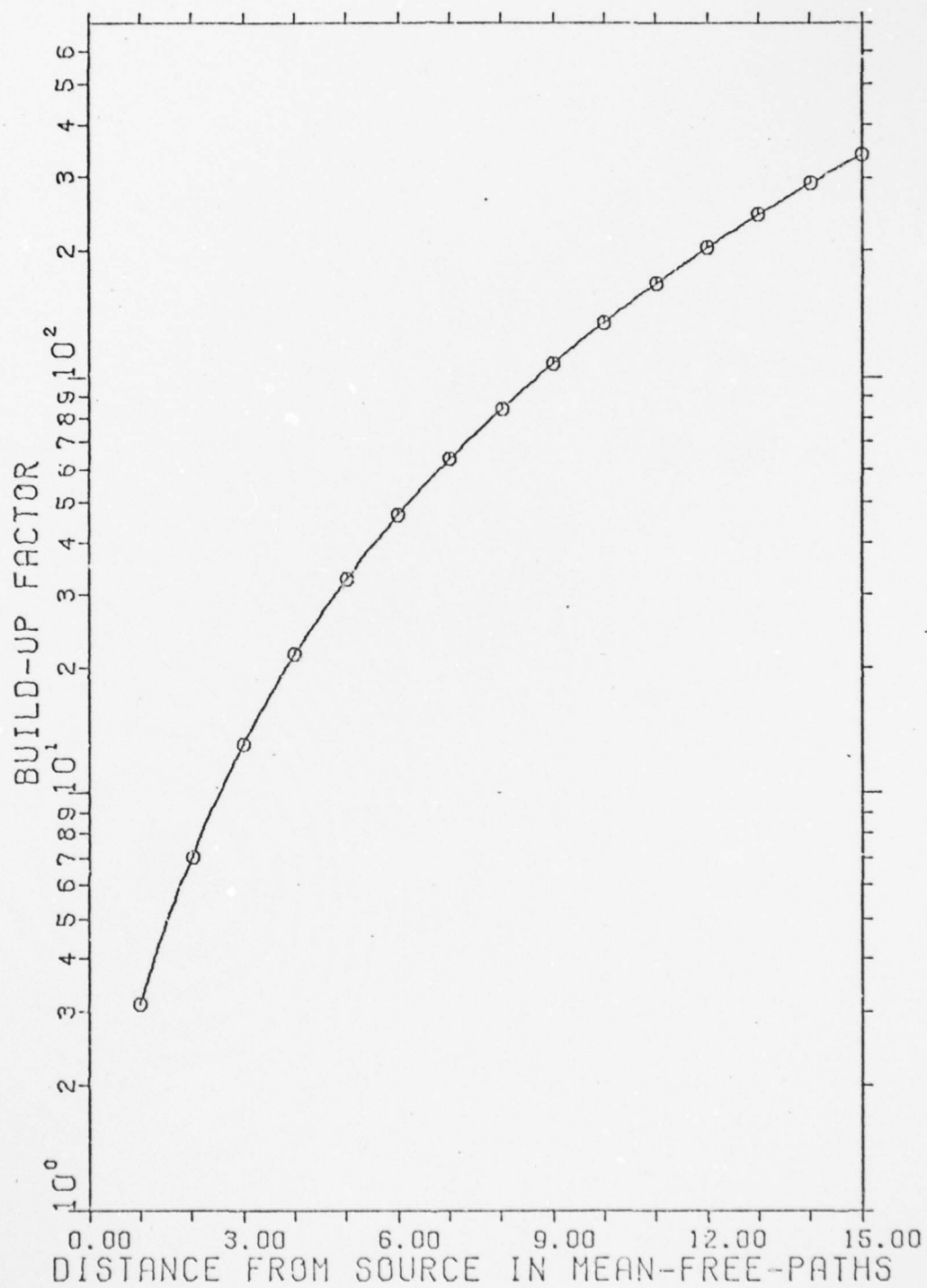


FIG. 71 ENERGY BUILD-UP FACTORS FOR 260 KEV

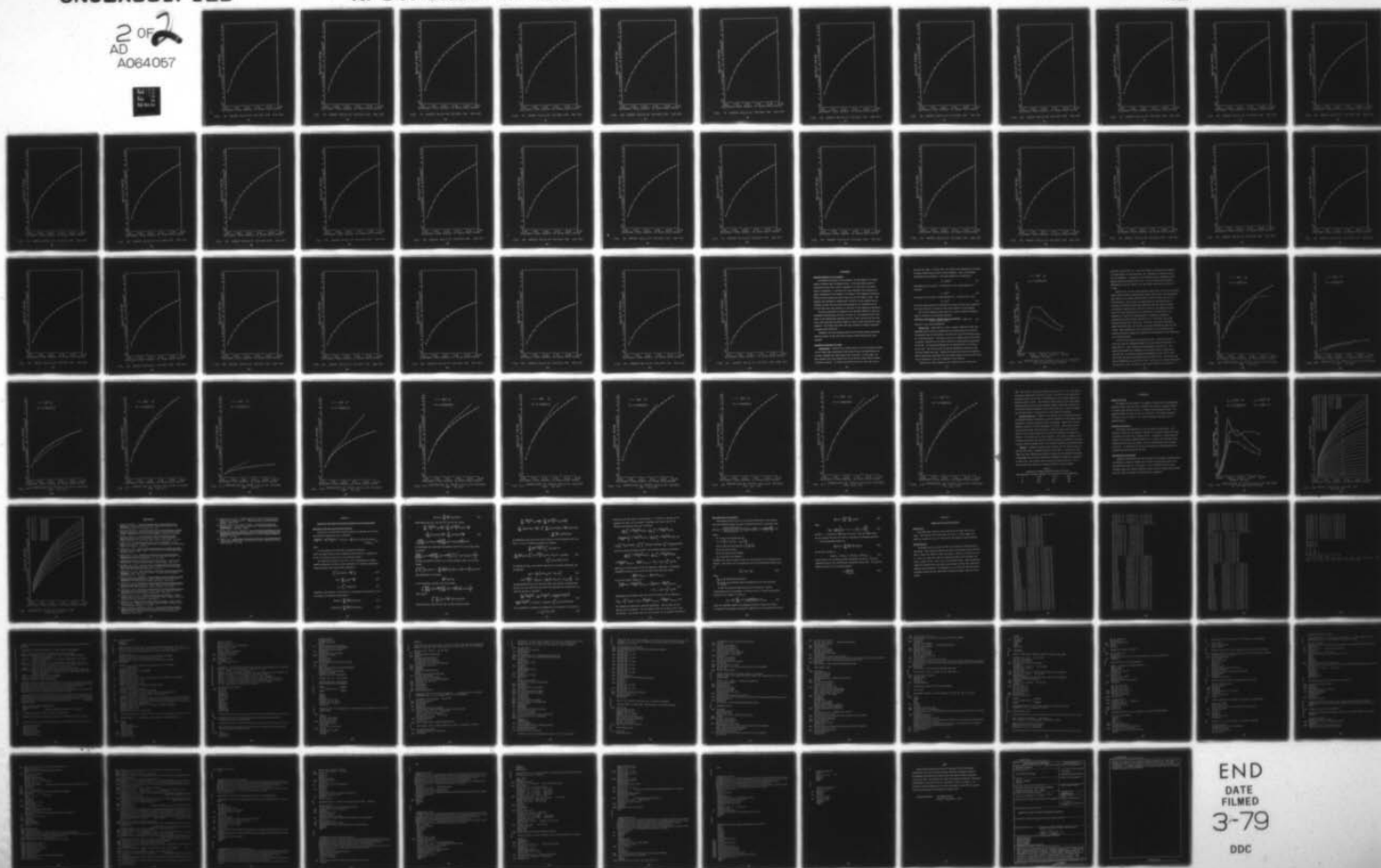


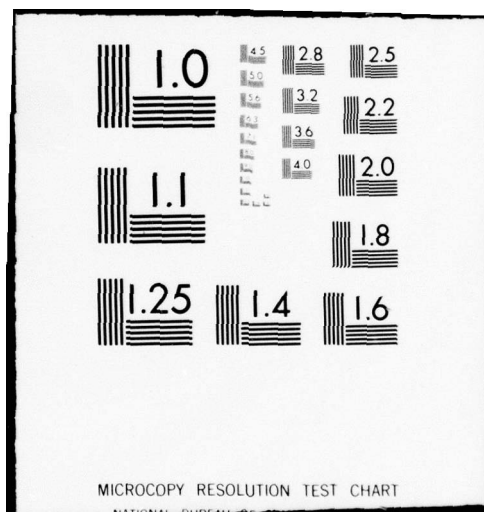
AD-A064 057 AIR FORCE INST OF TECH WRIGHT-PATTERSON AFB OHIO SCH--ETC F/6 20/8  
X-RAY BUILD-UP FACTORS, (U)  
DEC 78 G M KALANSKY

UNCLASSIFIED AFIT/GNE/PH/78D-18

NL

2 OF 2  
AD  
A064057





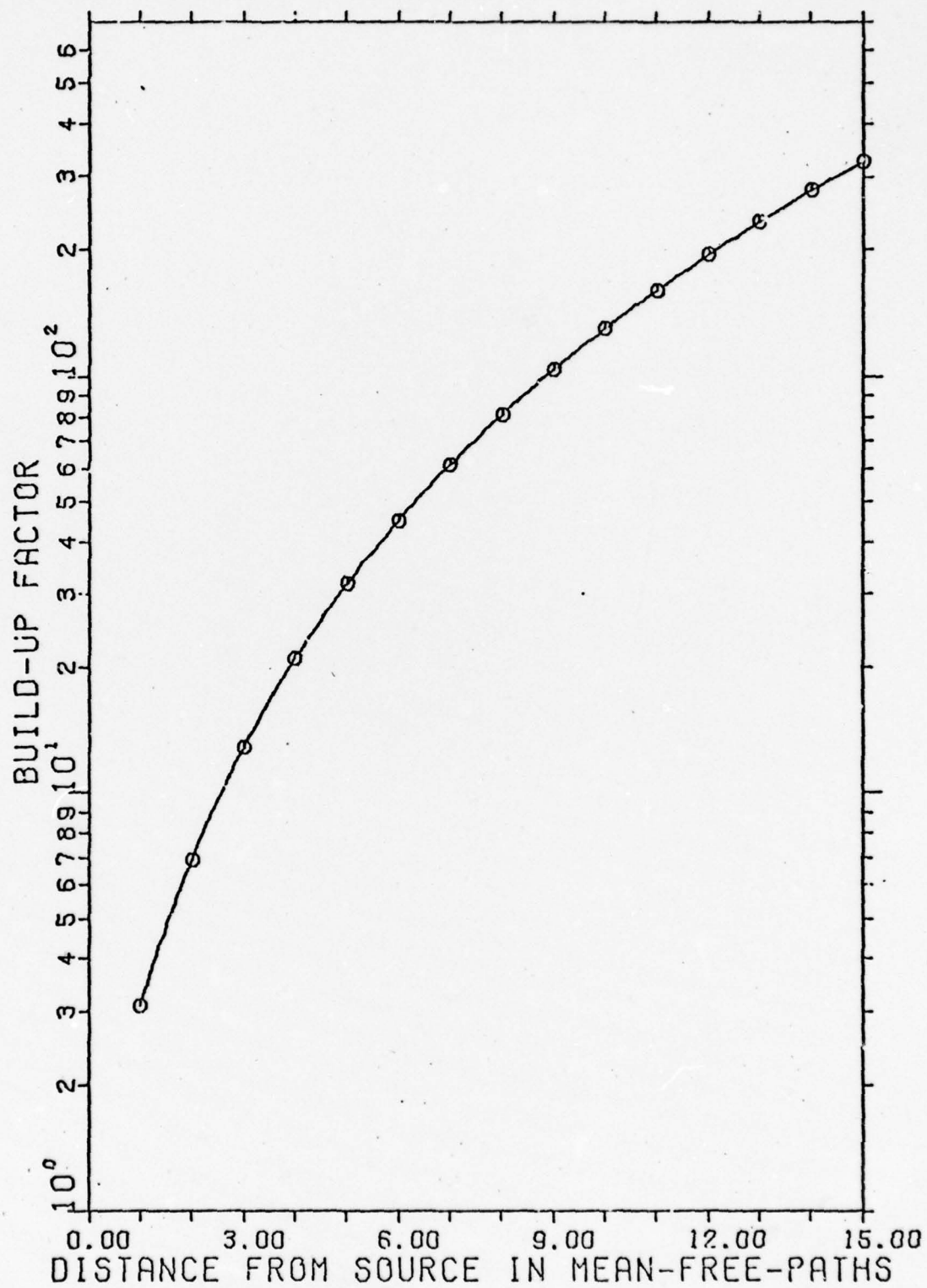


FIG. 72 ENERGY BUILD-UP FACTORS FOR 270 KEV

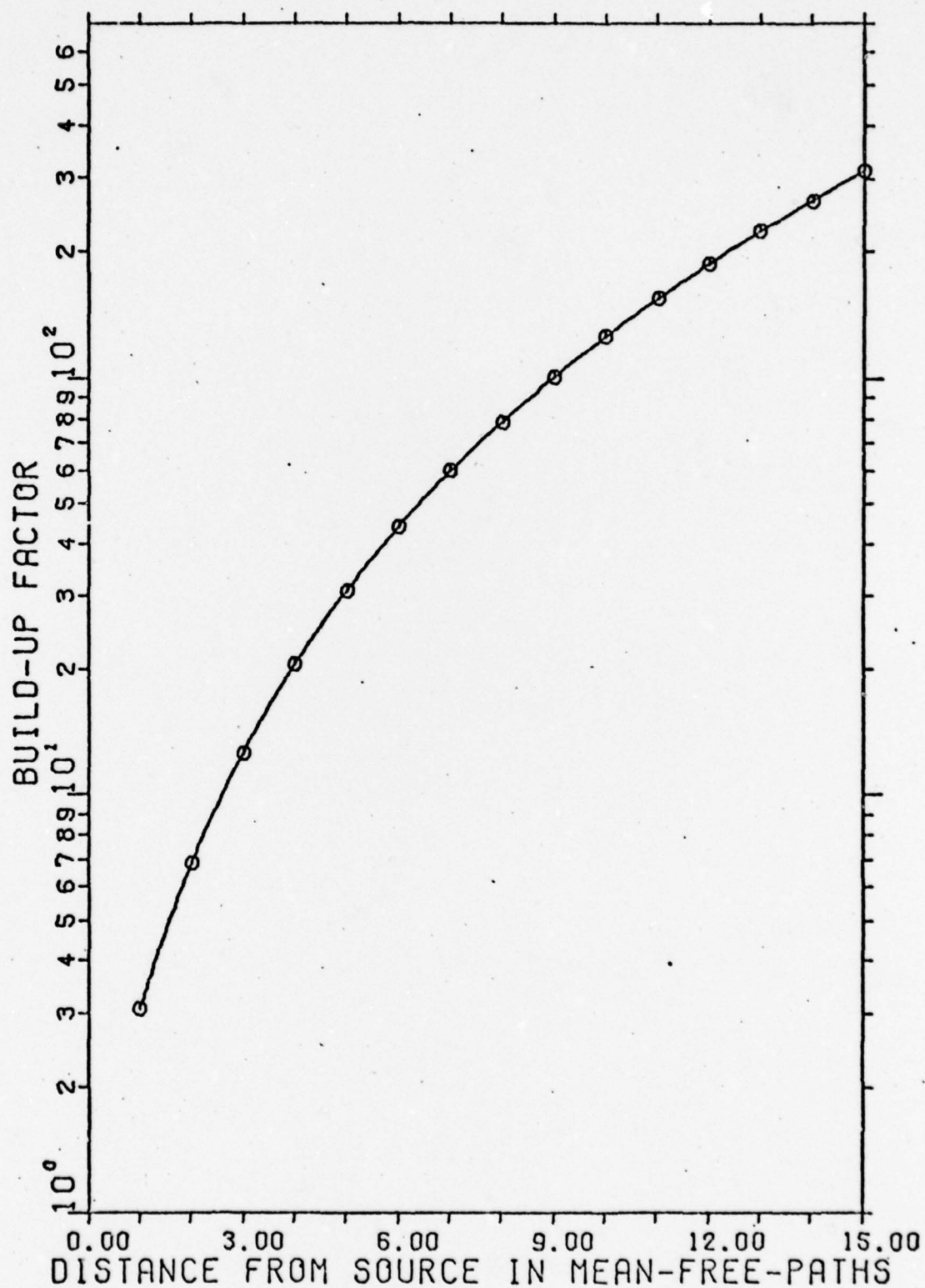


FIG. 73 ENERGY BUILD-UP FACTORS FOR 280 KEV

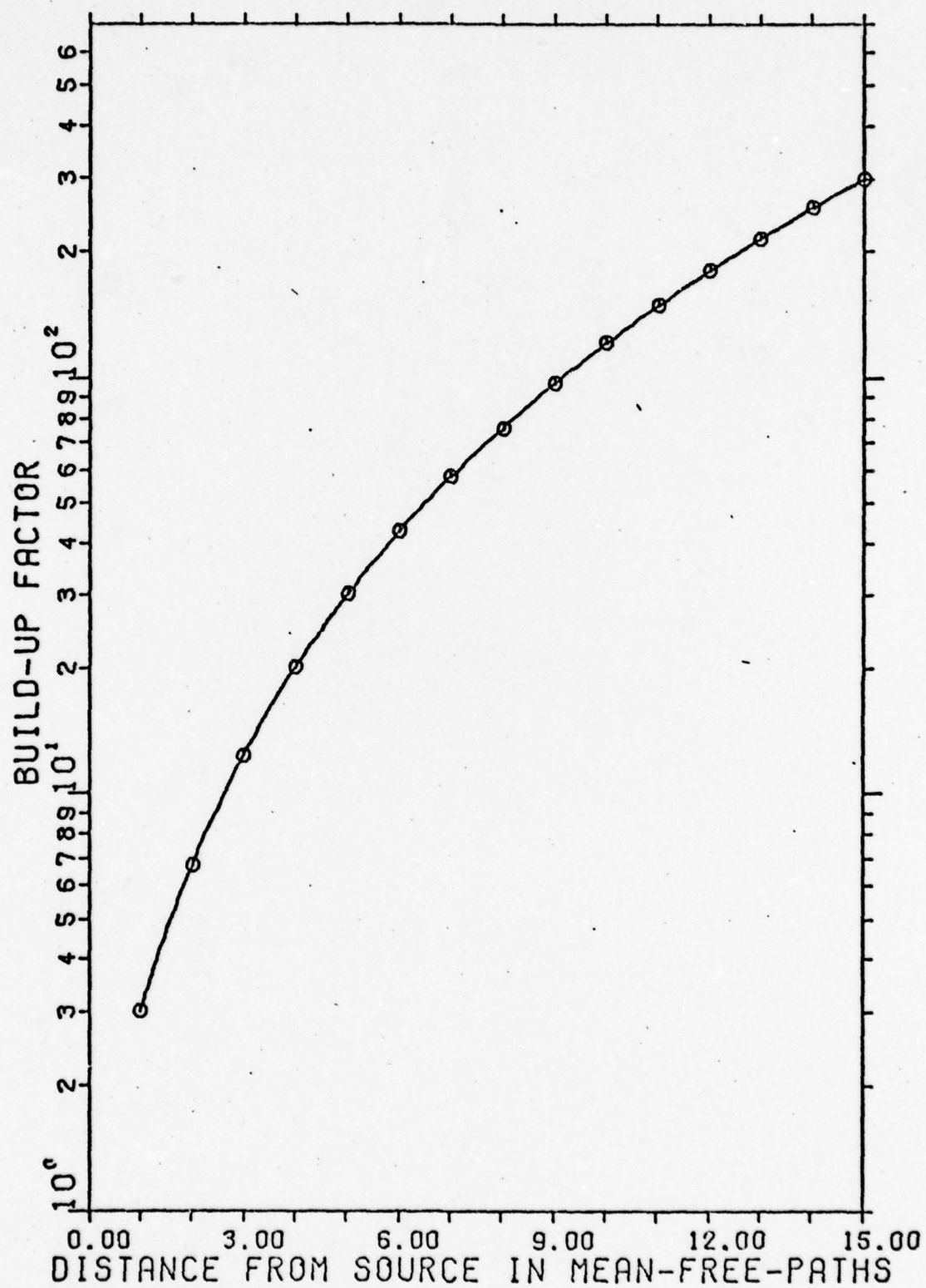


FIG. 74 ENERGY BUILD-UP FACTORS FOR 290 KEV



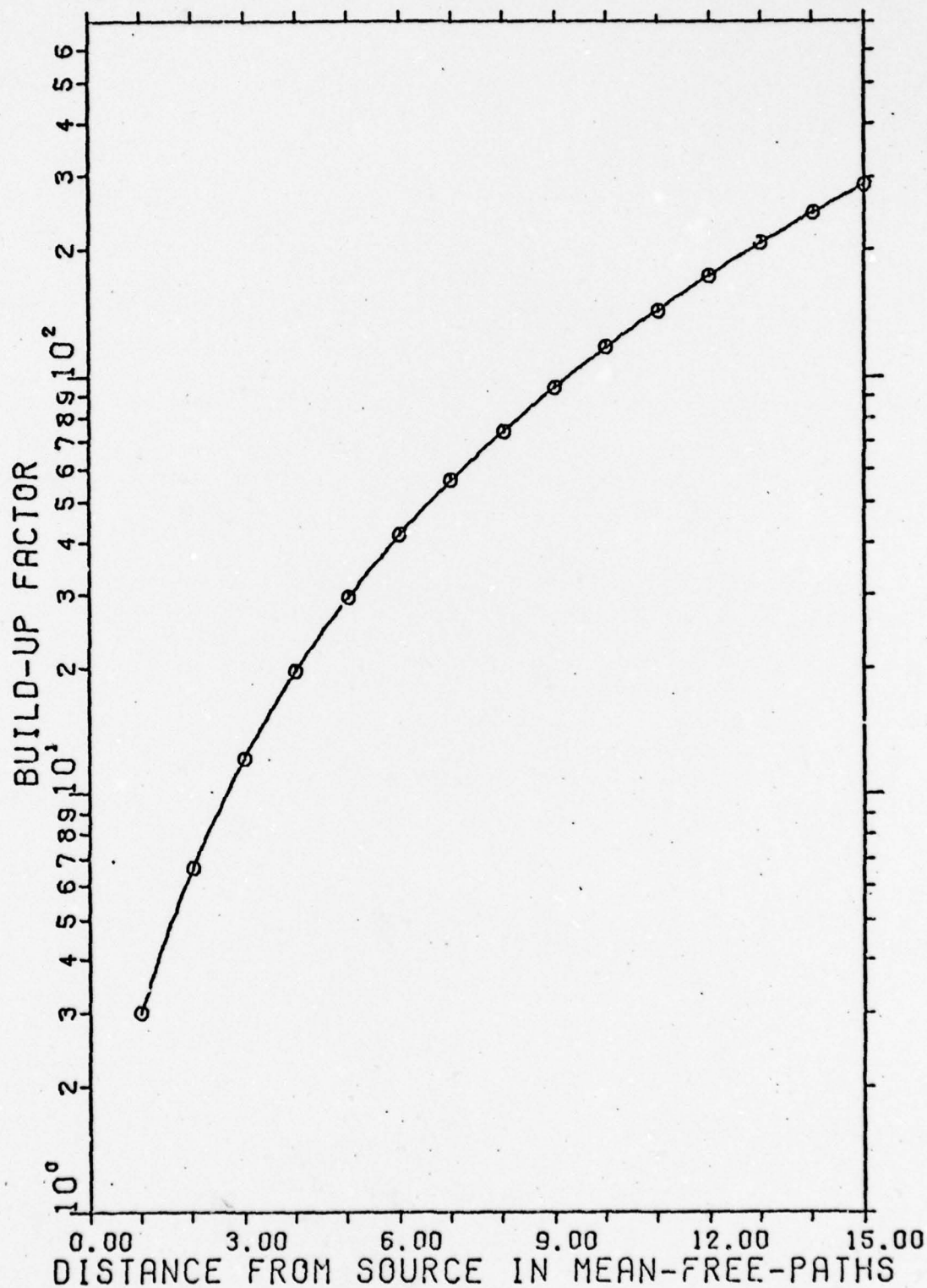


FIG. 75 ENERGY BUILD-UP FACTORS FOR 300 KEV



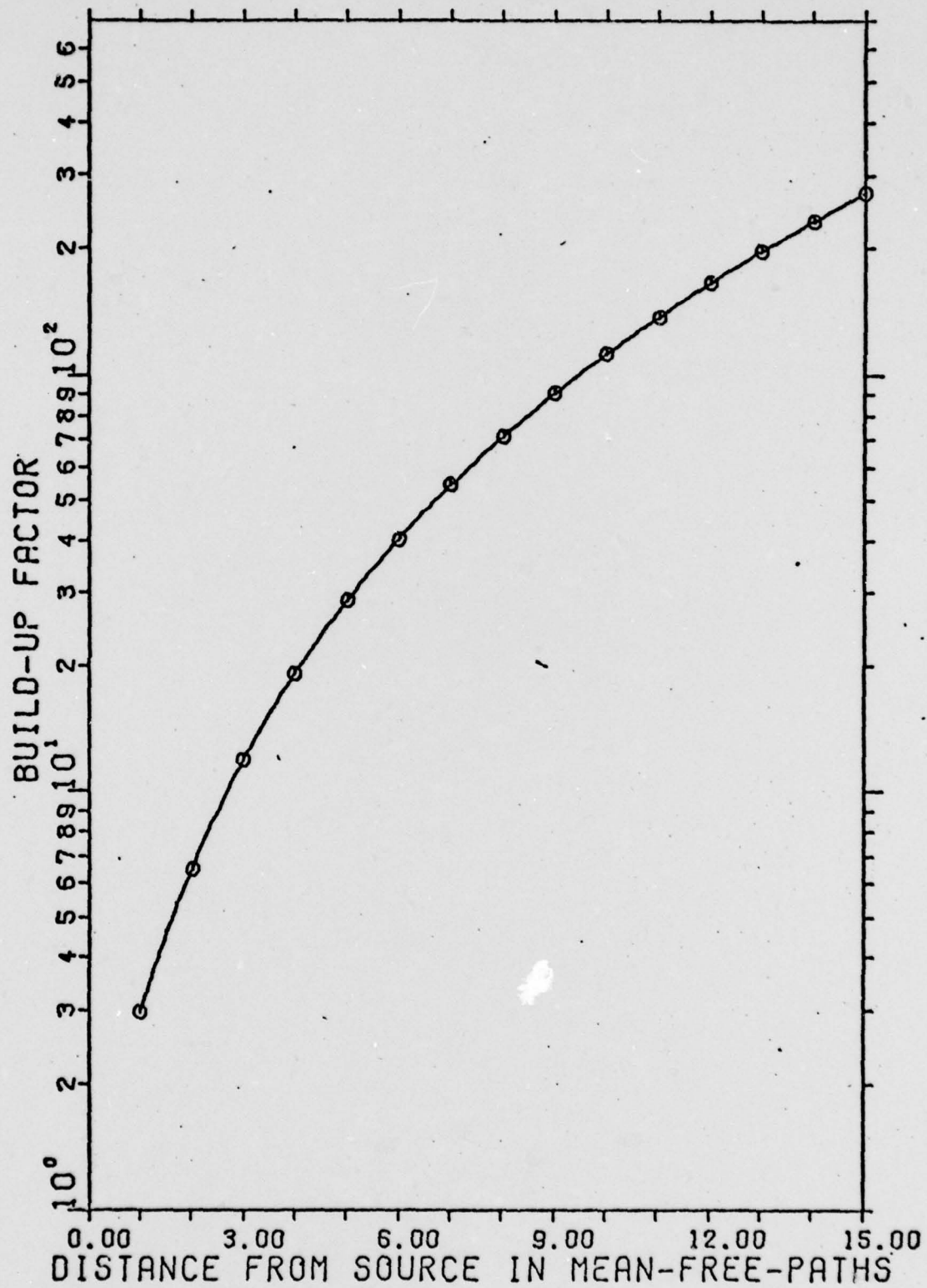


FIG. 76 ENERGY BUILD-UP FACTORS FOR 310 KEV

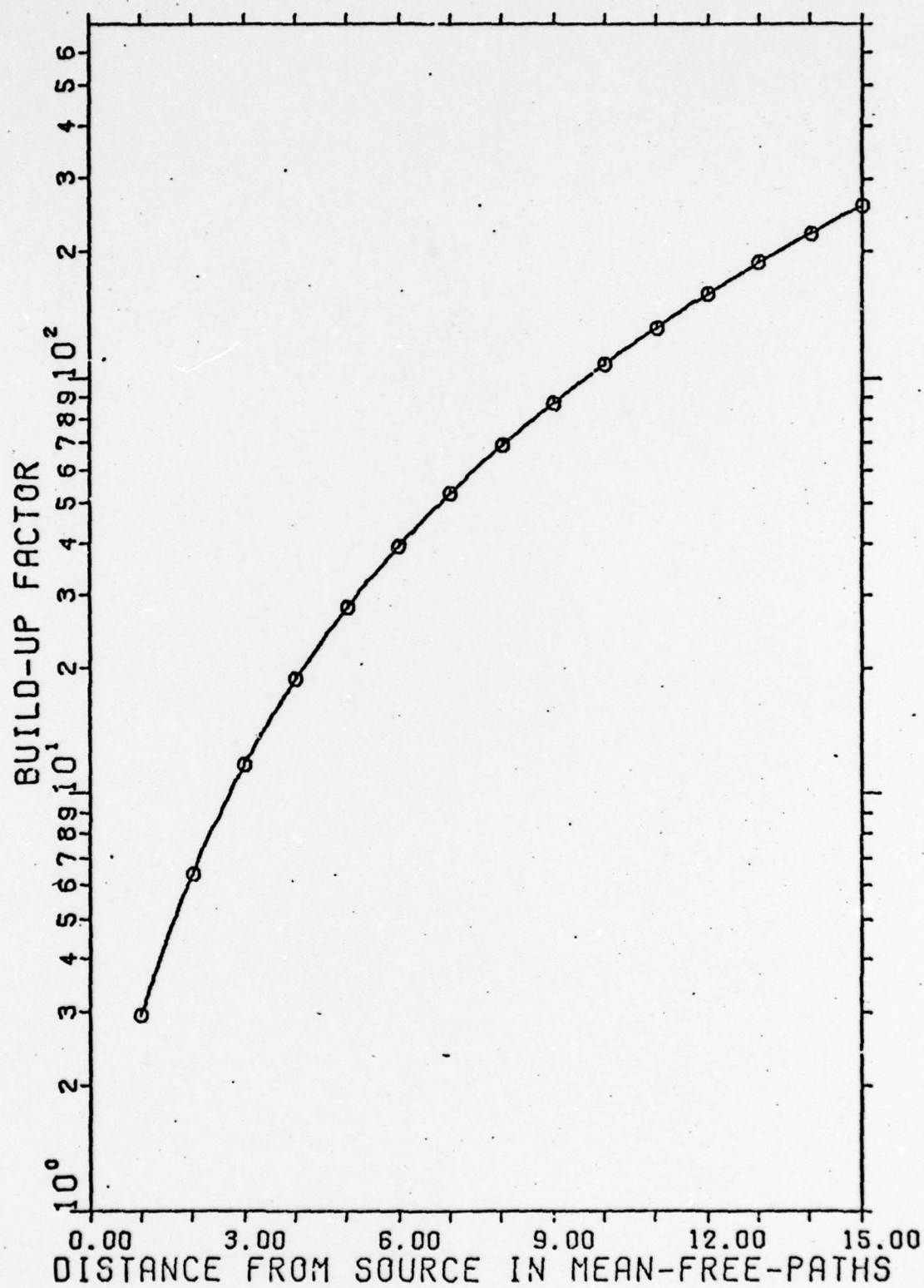


FIG. 77 ENERGY BUILD-UP FACTORS FOR 320 KEV

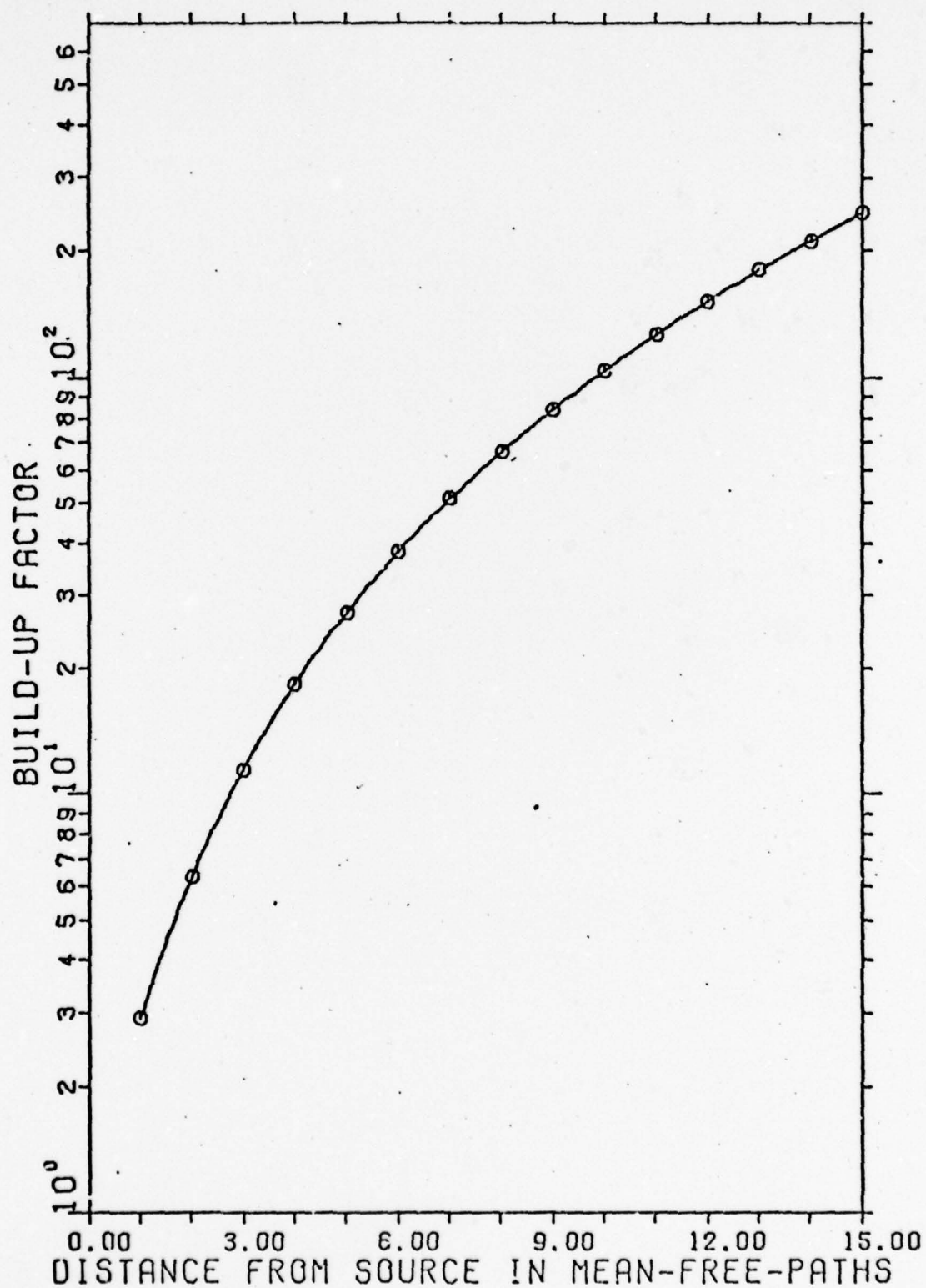


FIG. 78 ENERGY BUILD-UP FACTORS FOR 330 KEV

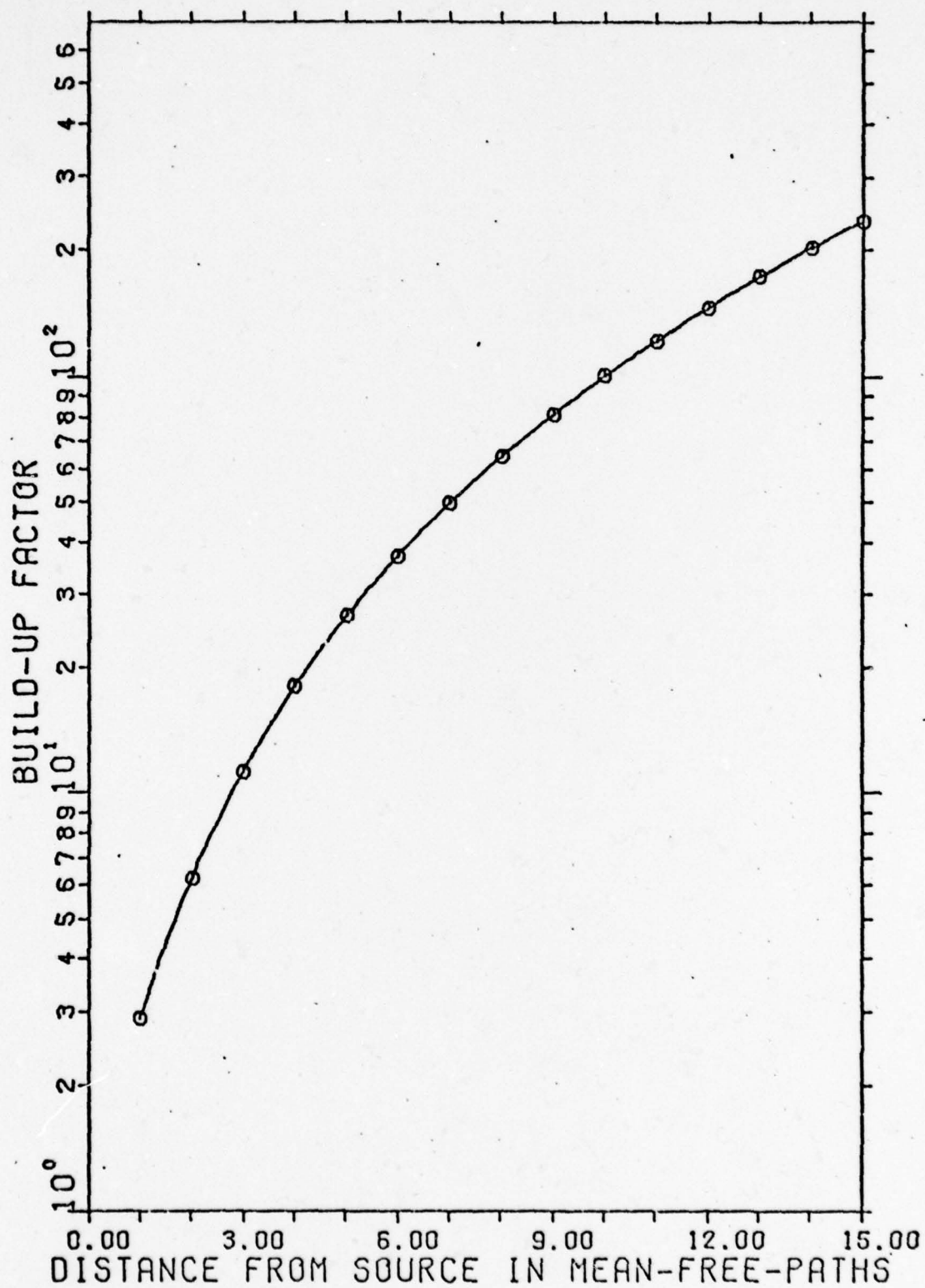


FIG. 79 ENERGY BUILD-UP FACTORS FOR 340 KEV



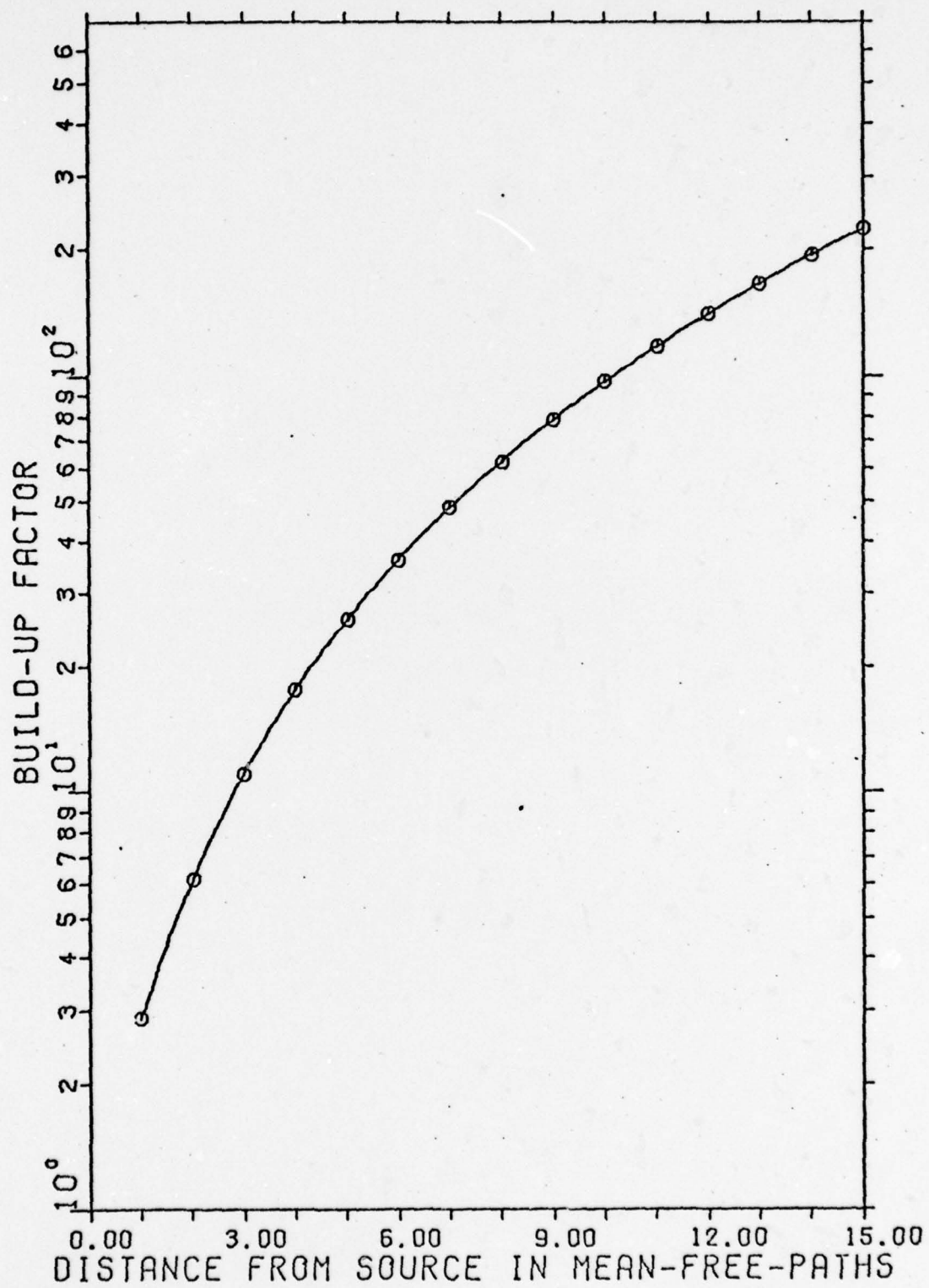


FIG. 80 ENERGY BUILD-UP FACTORS FOR 350 KEV

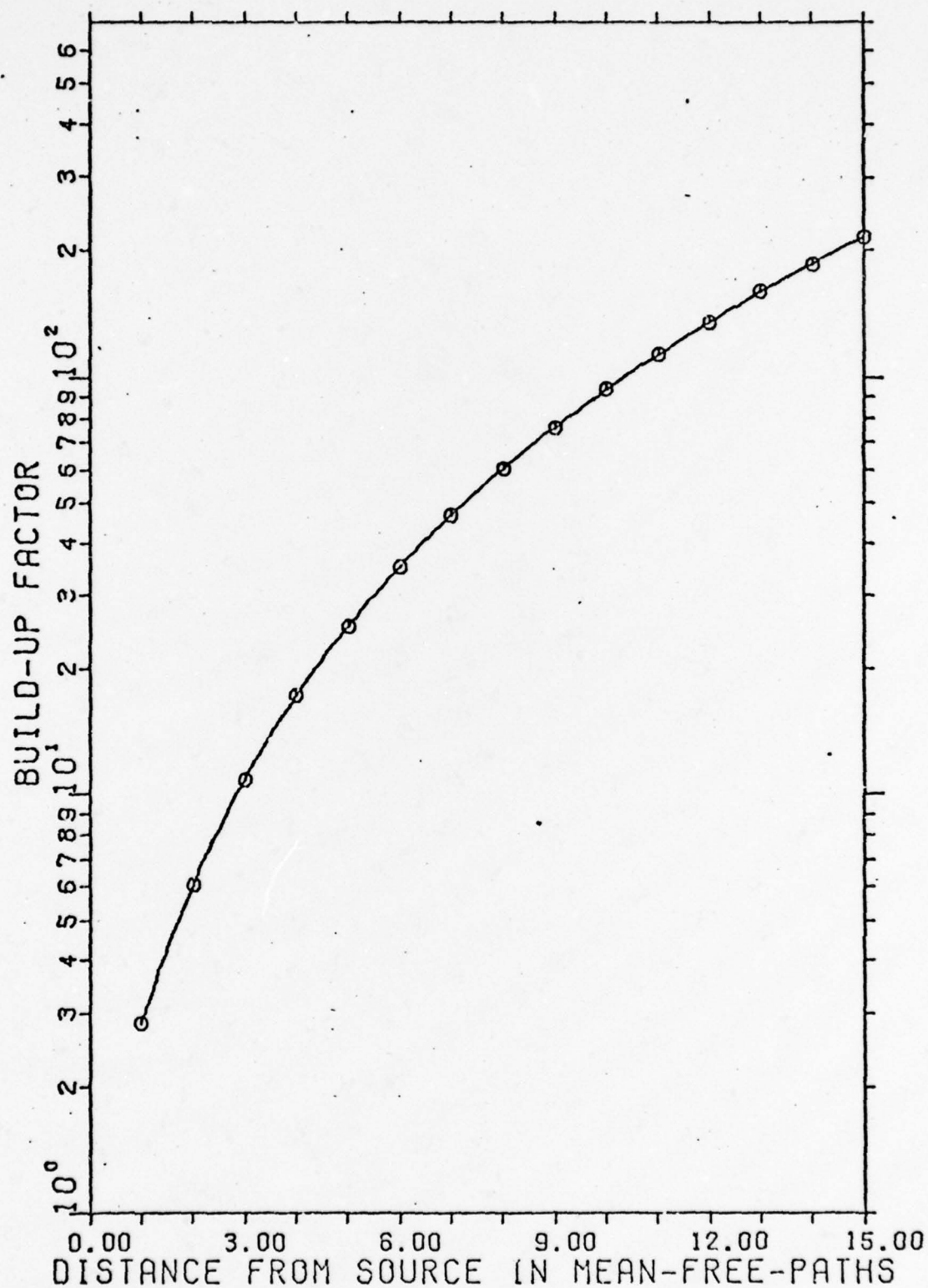


FIG. 81 ENERGY BUILD-UP FACTORS FOR 360 KEV



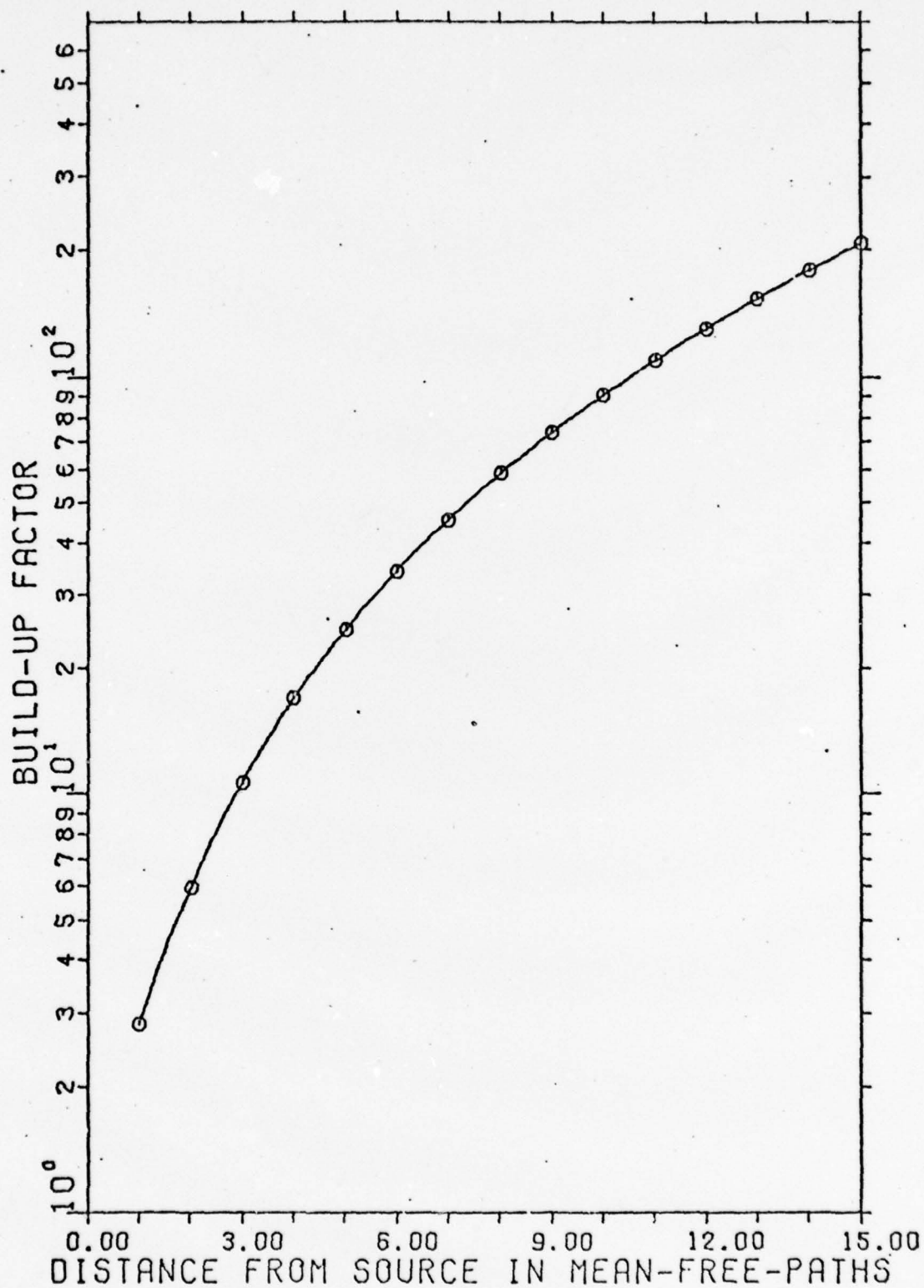


FIG. 82 ENERGY BUILD-UP FACTORS FOR 370 KEV

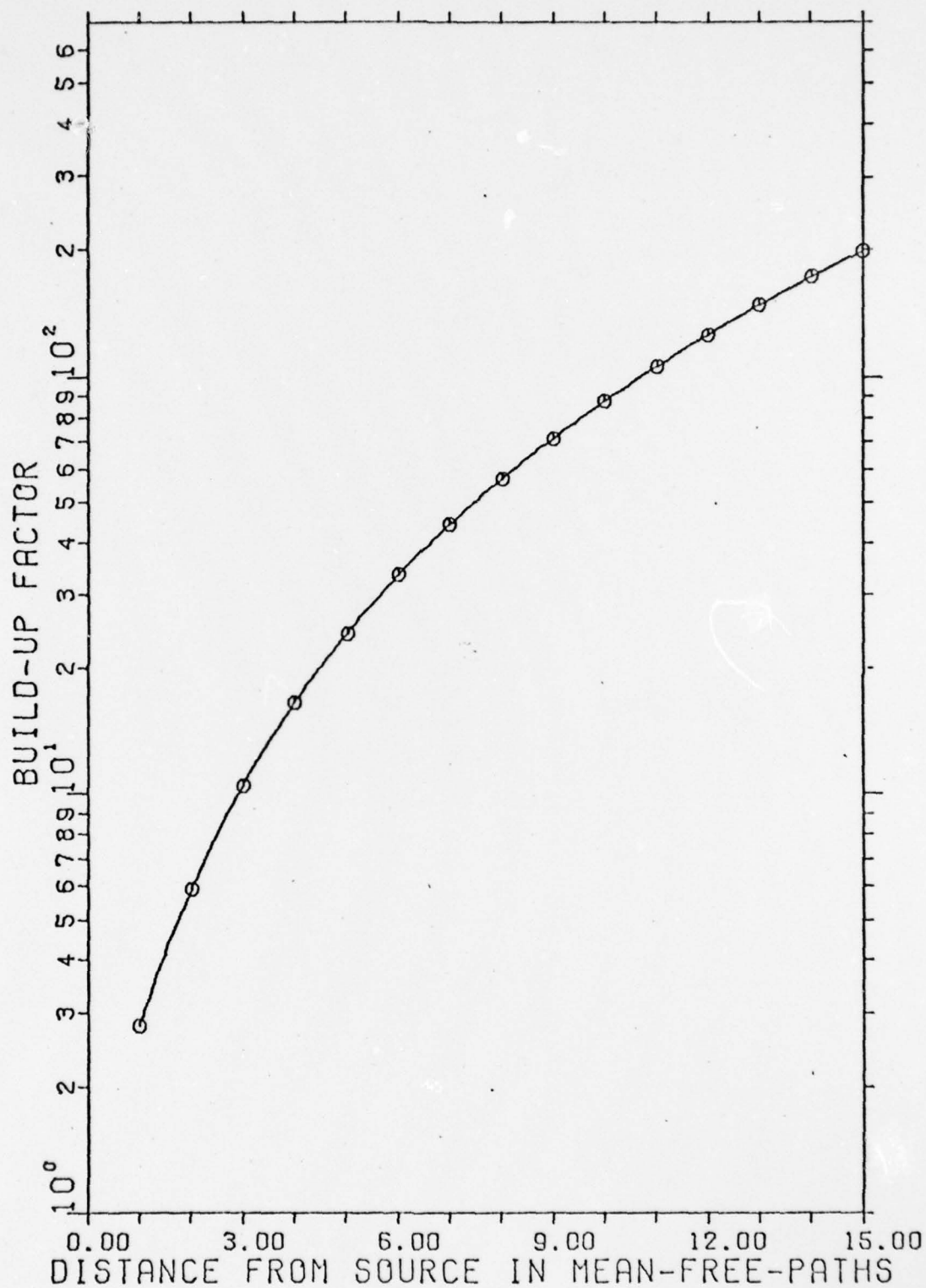


FIG. 83 ENERGY BUILD-UP FACTORS FOR 380 KEV

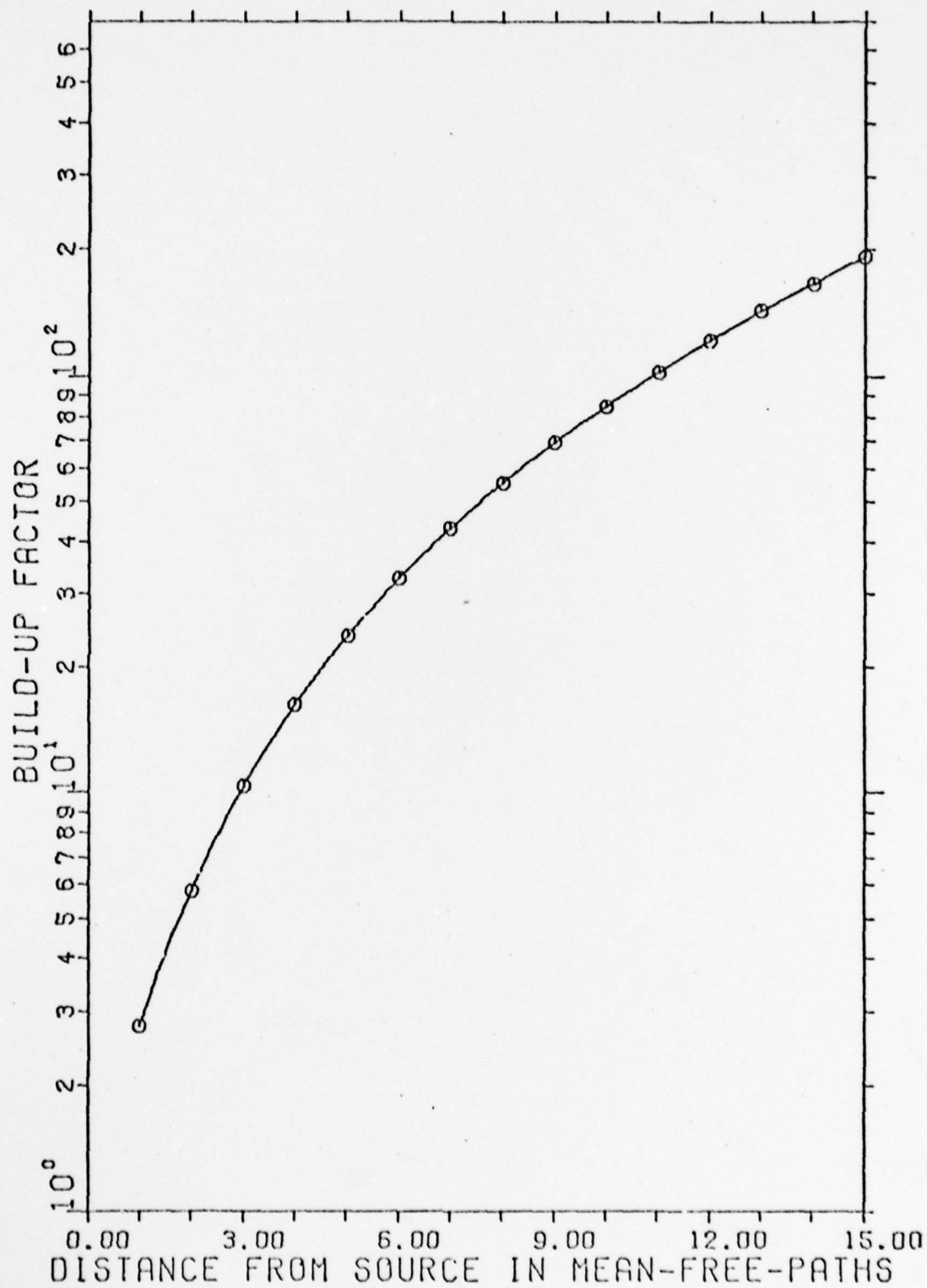


FIG. 84 ENERGY BUILD-UP FACTORS FOR 390 KEV

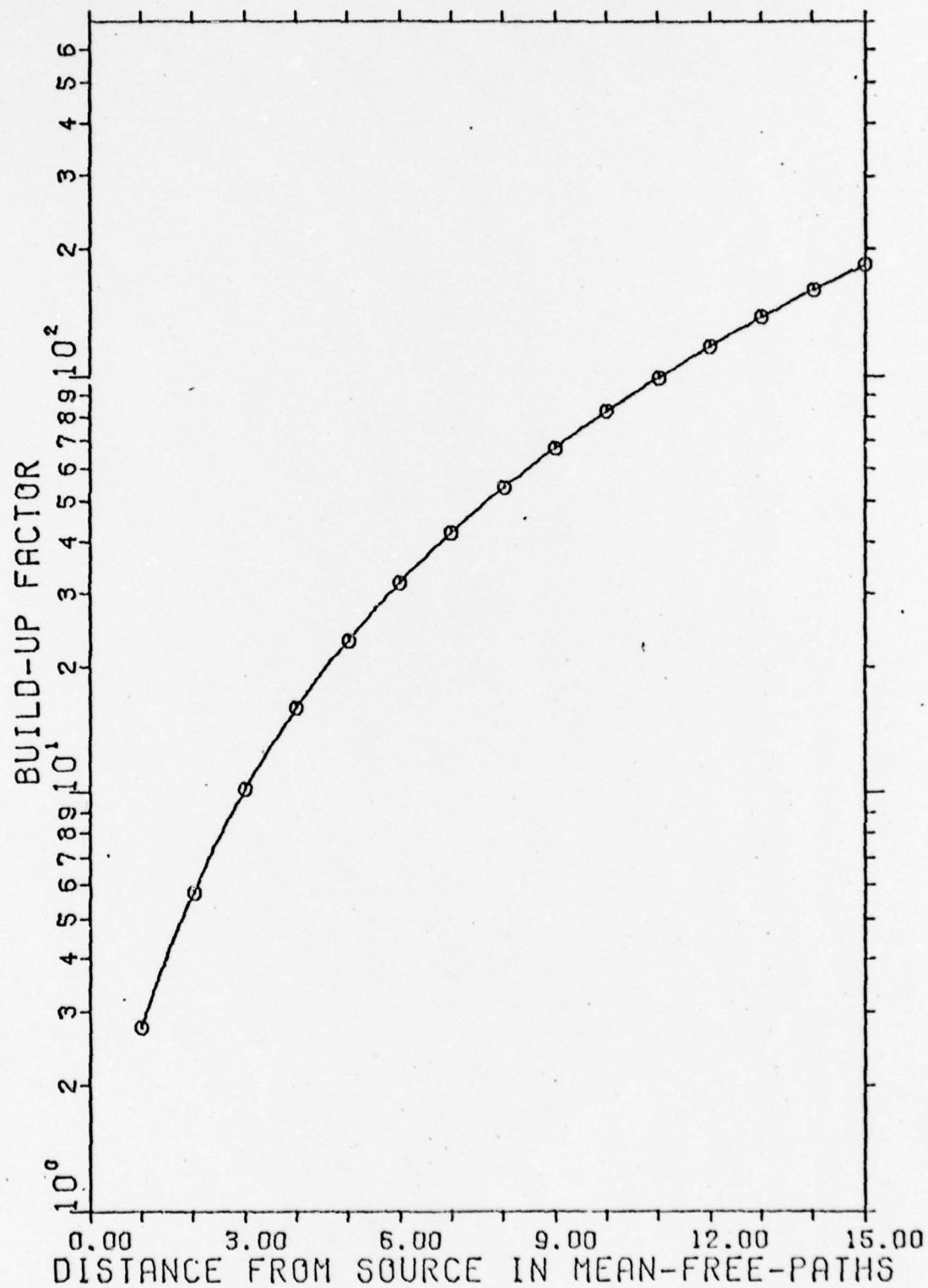


FIG. 85 ENERGY BUILD-UP FACTORS FOR 400 KEV

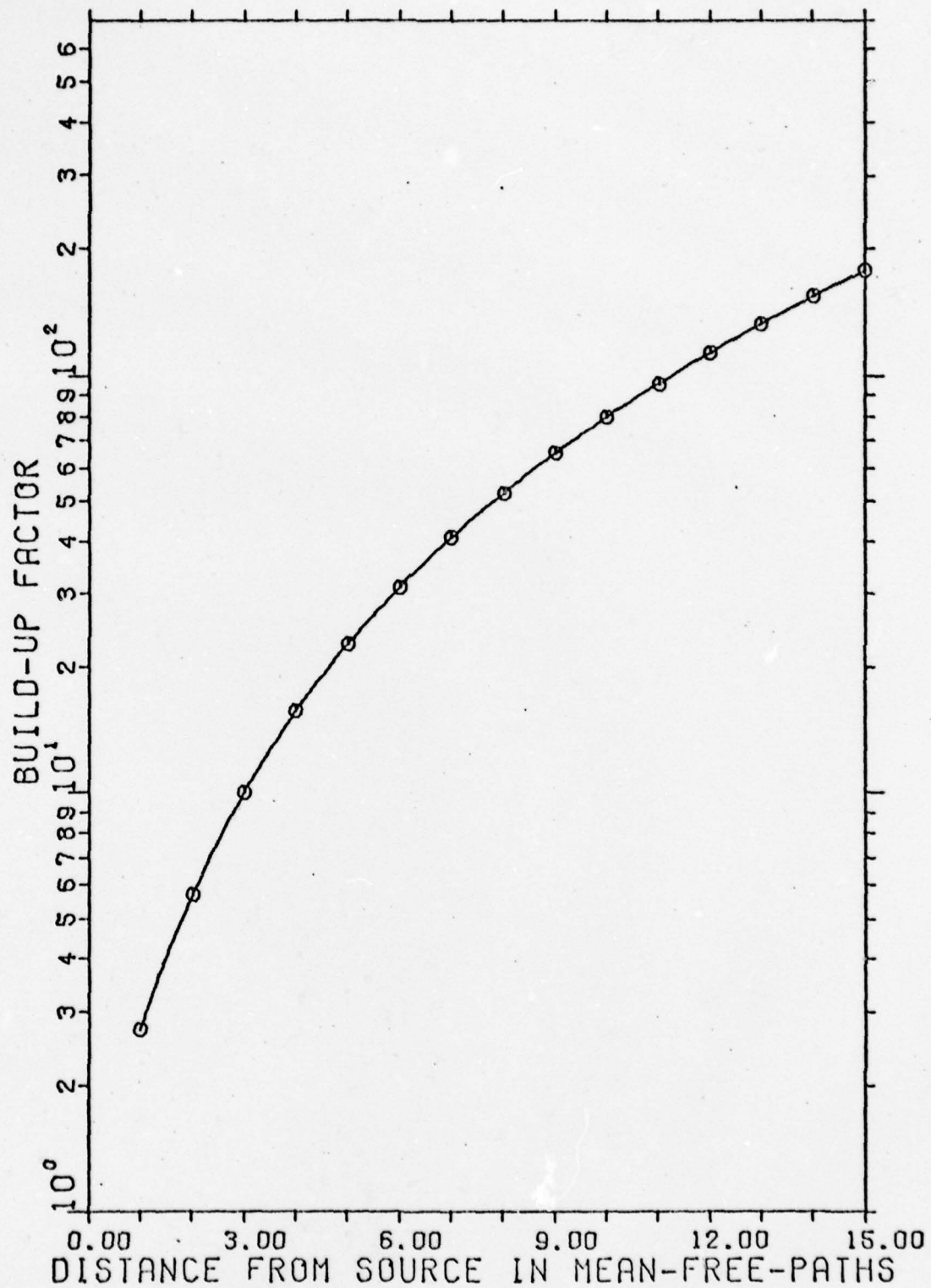


FIG. 86 ENERGY BUILD-UP FACTORS FOR 410 KEV



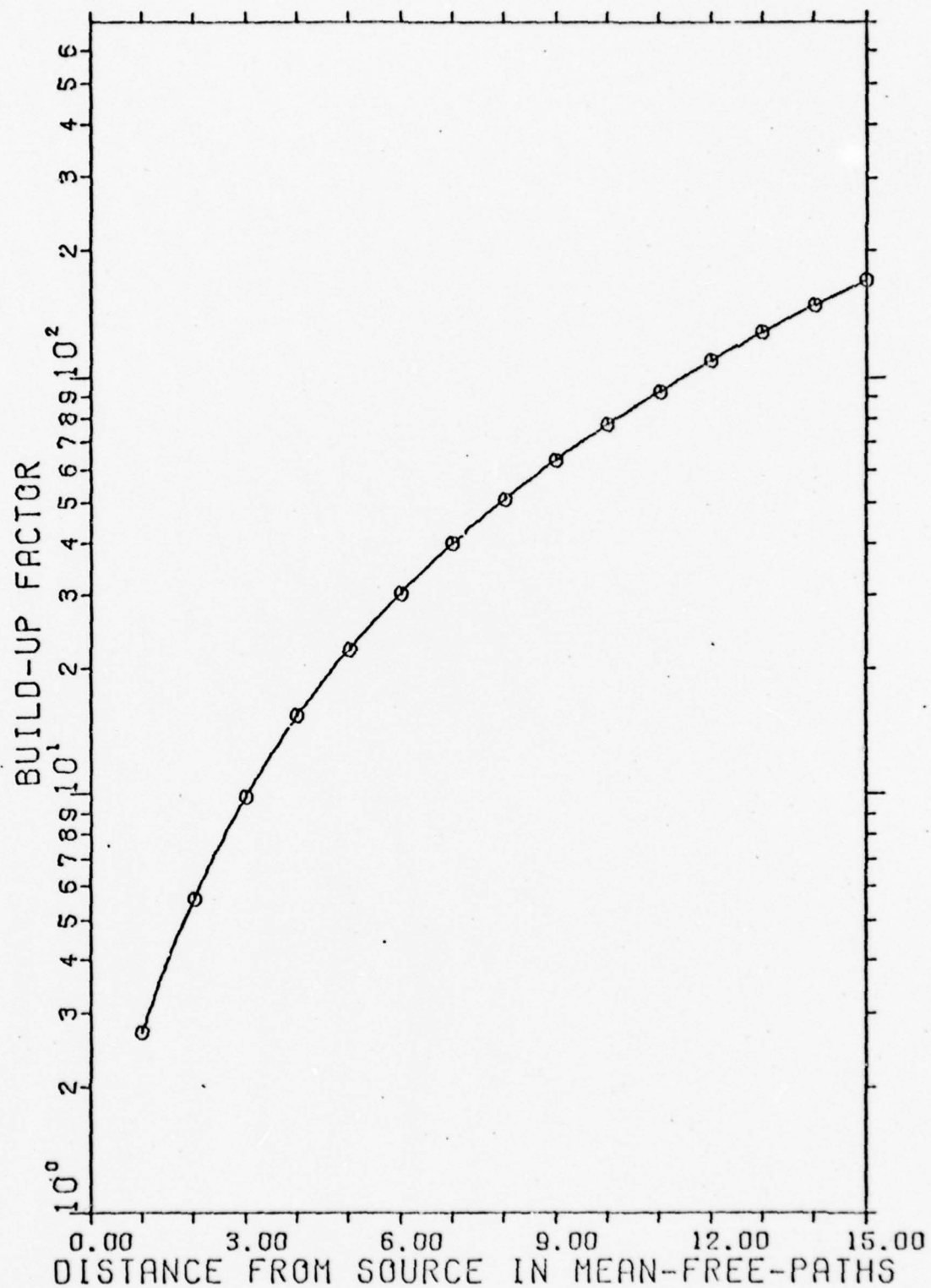


FIG. 87 ENERGY BUILD-UP FACTORS FOR 420 KEV



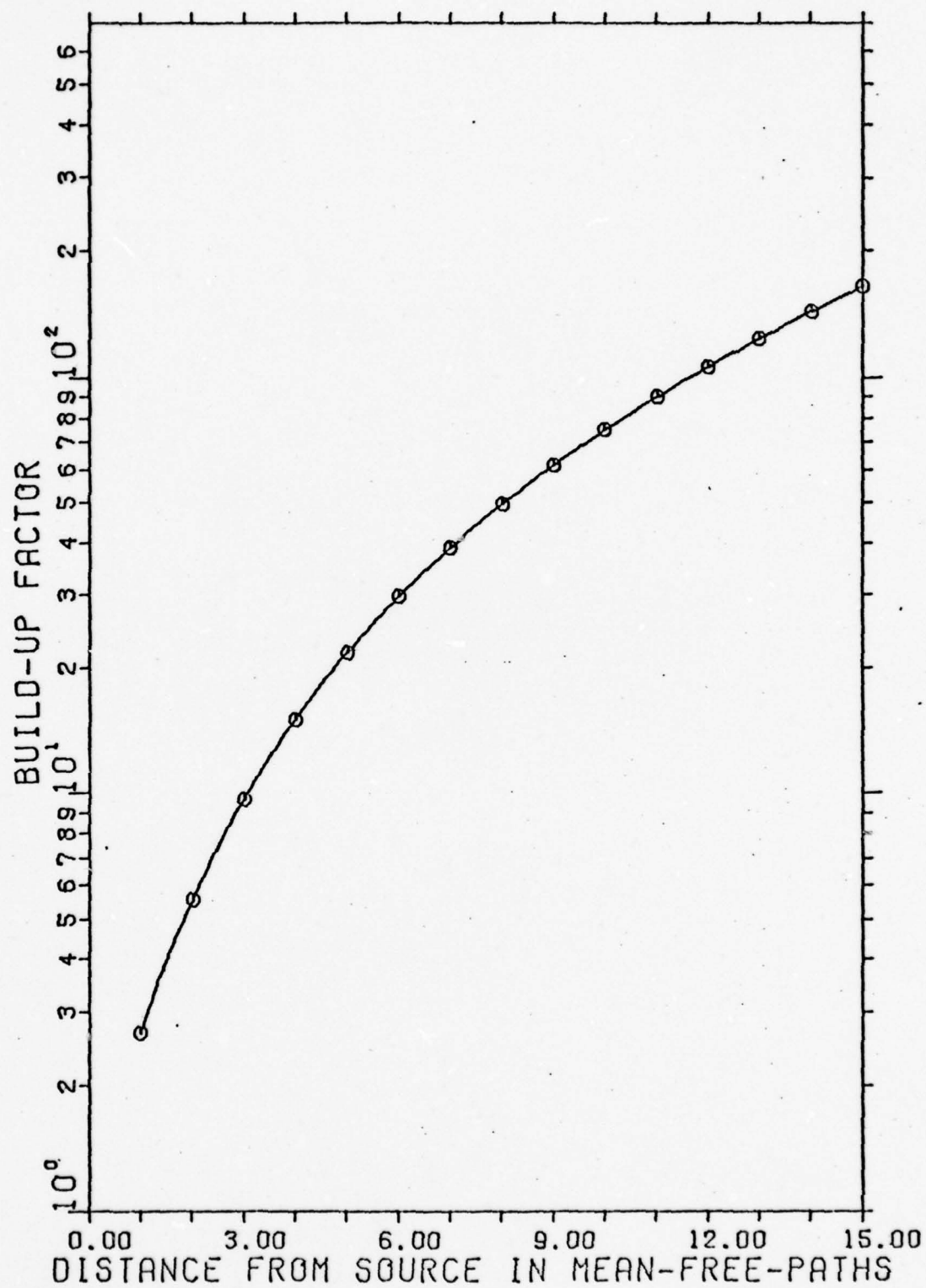


FIG. 88 ENERGY BUILD-UP FACTORS FOR 430 KEV

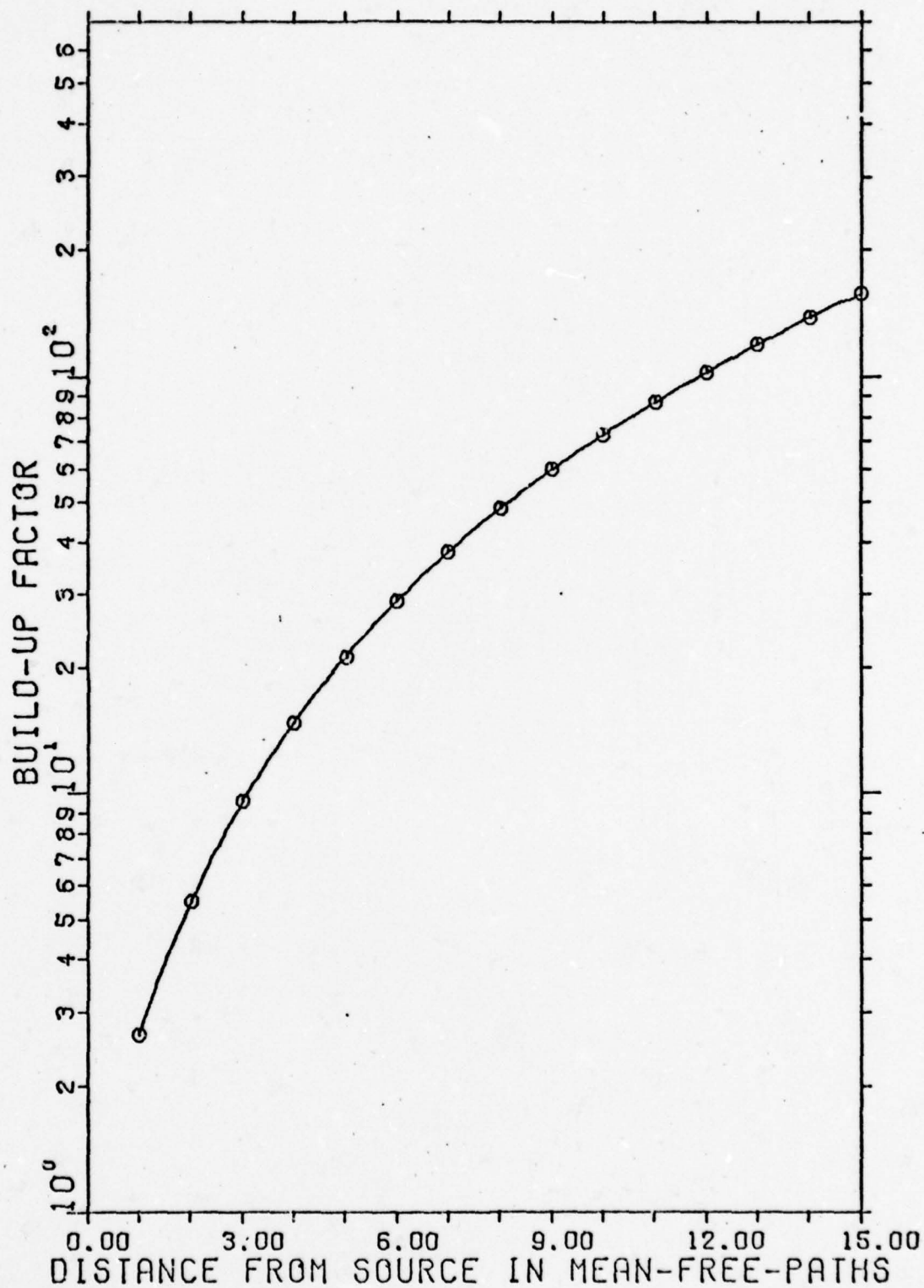


FIG. 89 ENERGY BUILD-UP FACTORS FOR 440 KEV

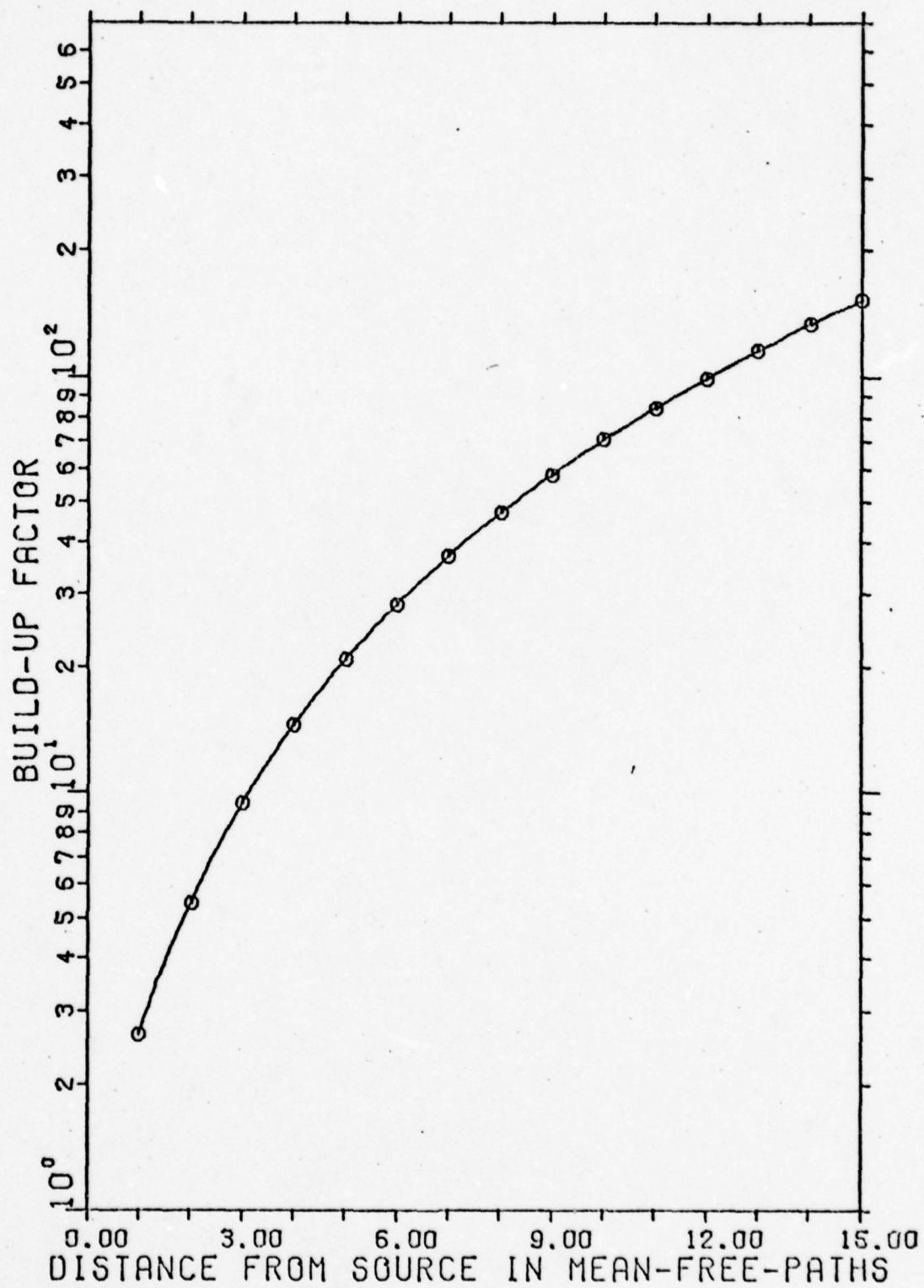


FIG. 90 ENERGY BUILD-UP FACTORS FOR 450 KEV

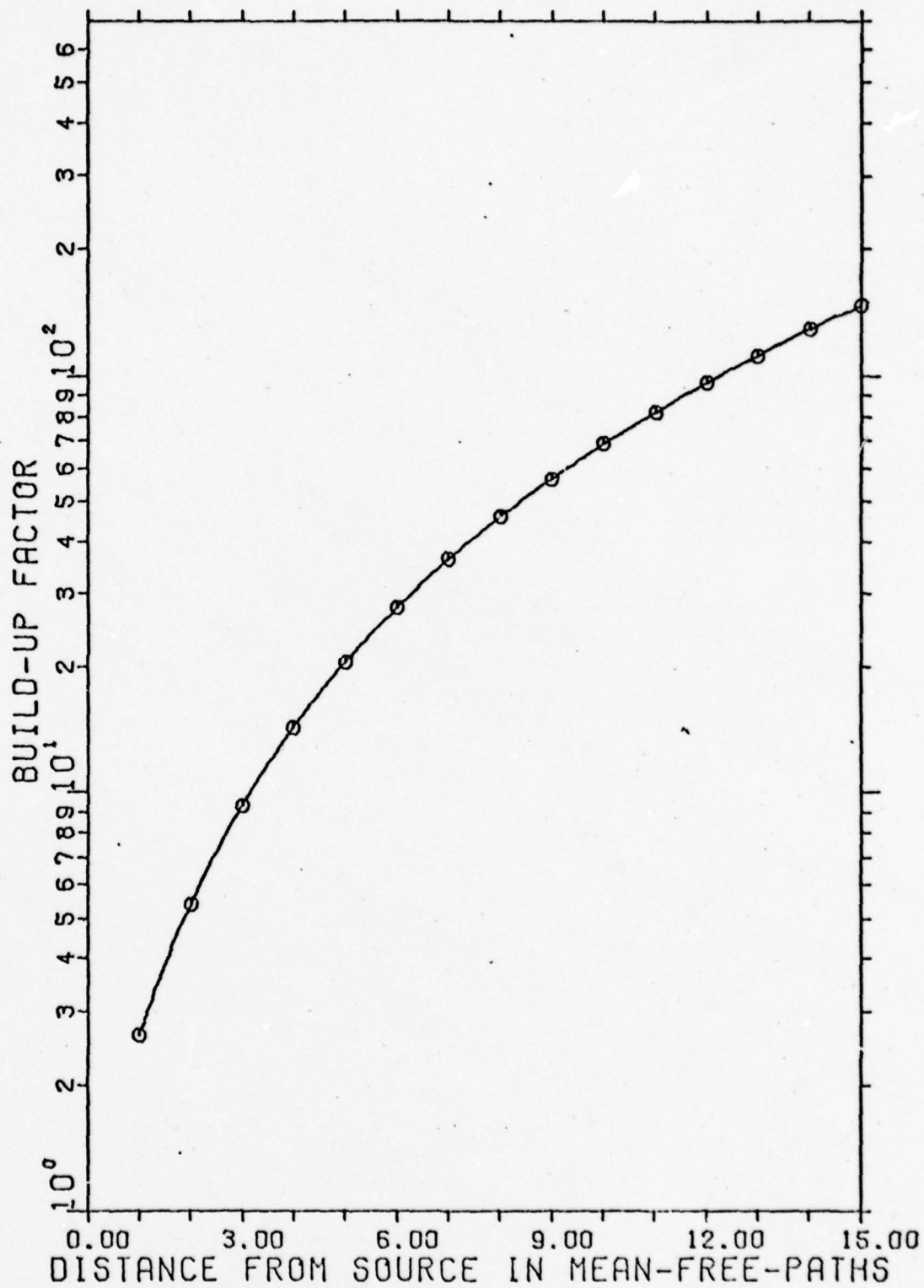


FIG. 91 ENERGY BUILD-UP FACTORS FOR 460 KEV

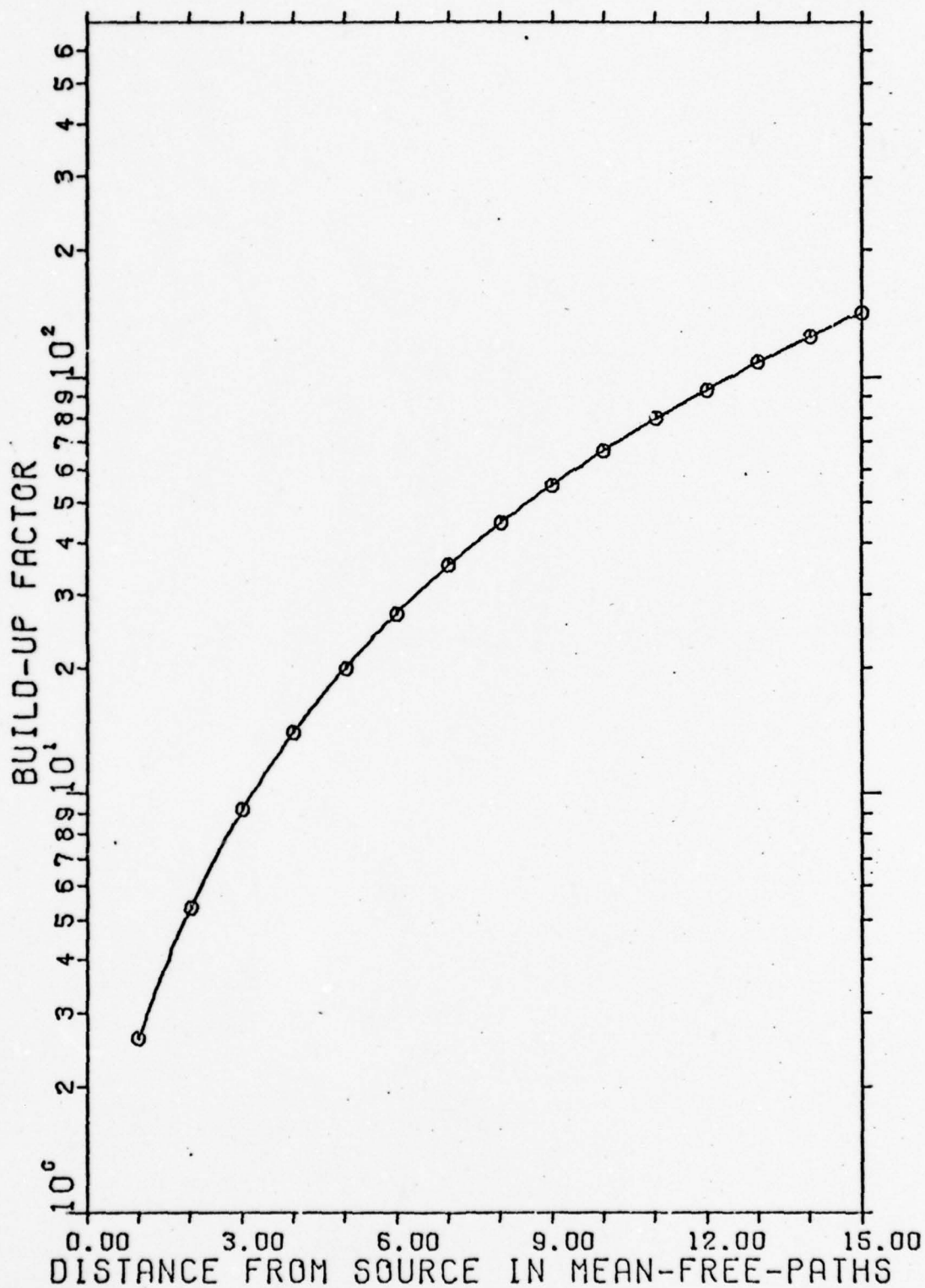


FIG. 92 ENERGY BUILD-UP FACTORS FOR 470 KEV



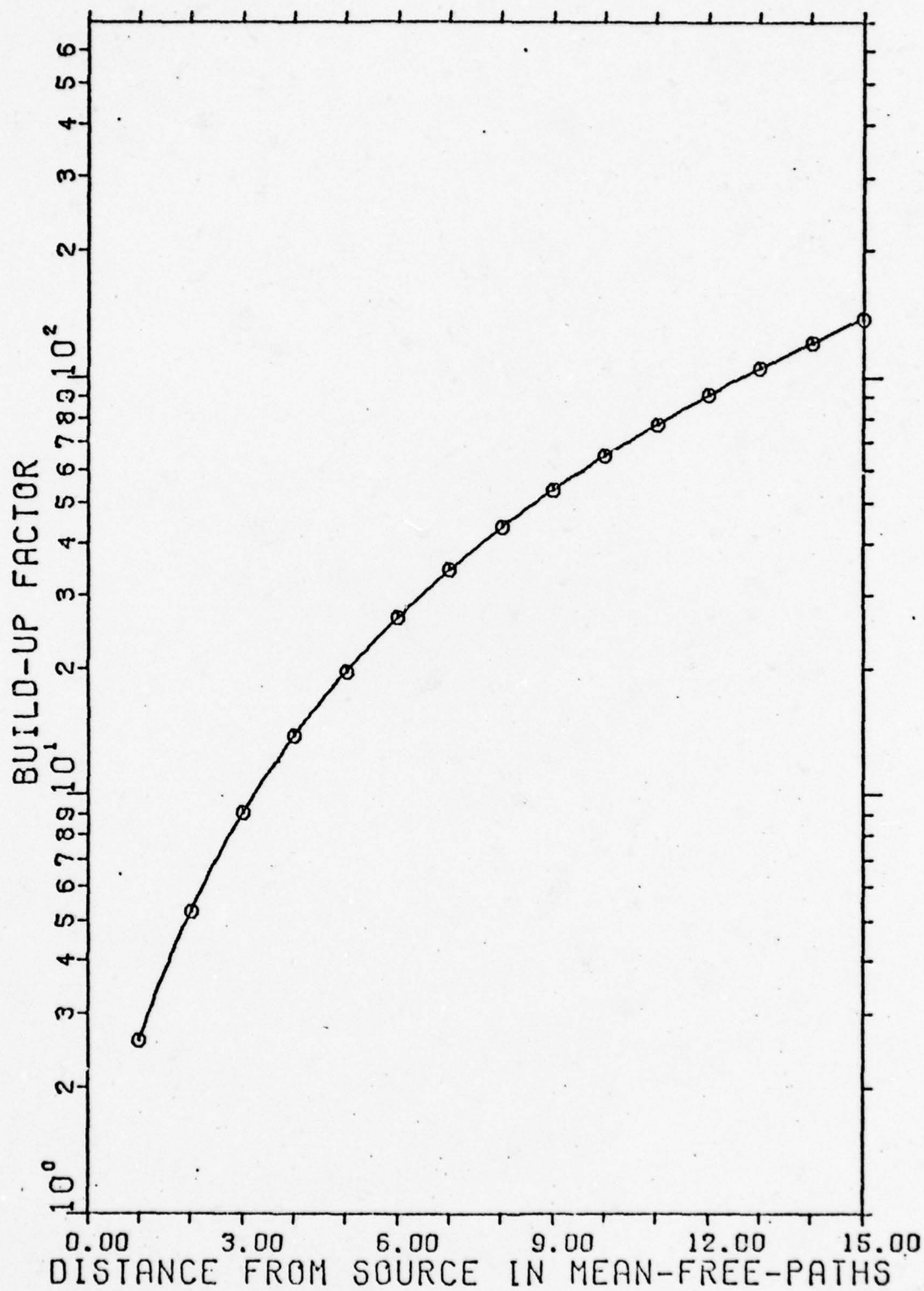


FIG. 93 ENERGY BUILD-UP FACTORS FOR 480 KEV



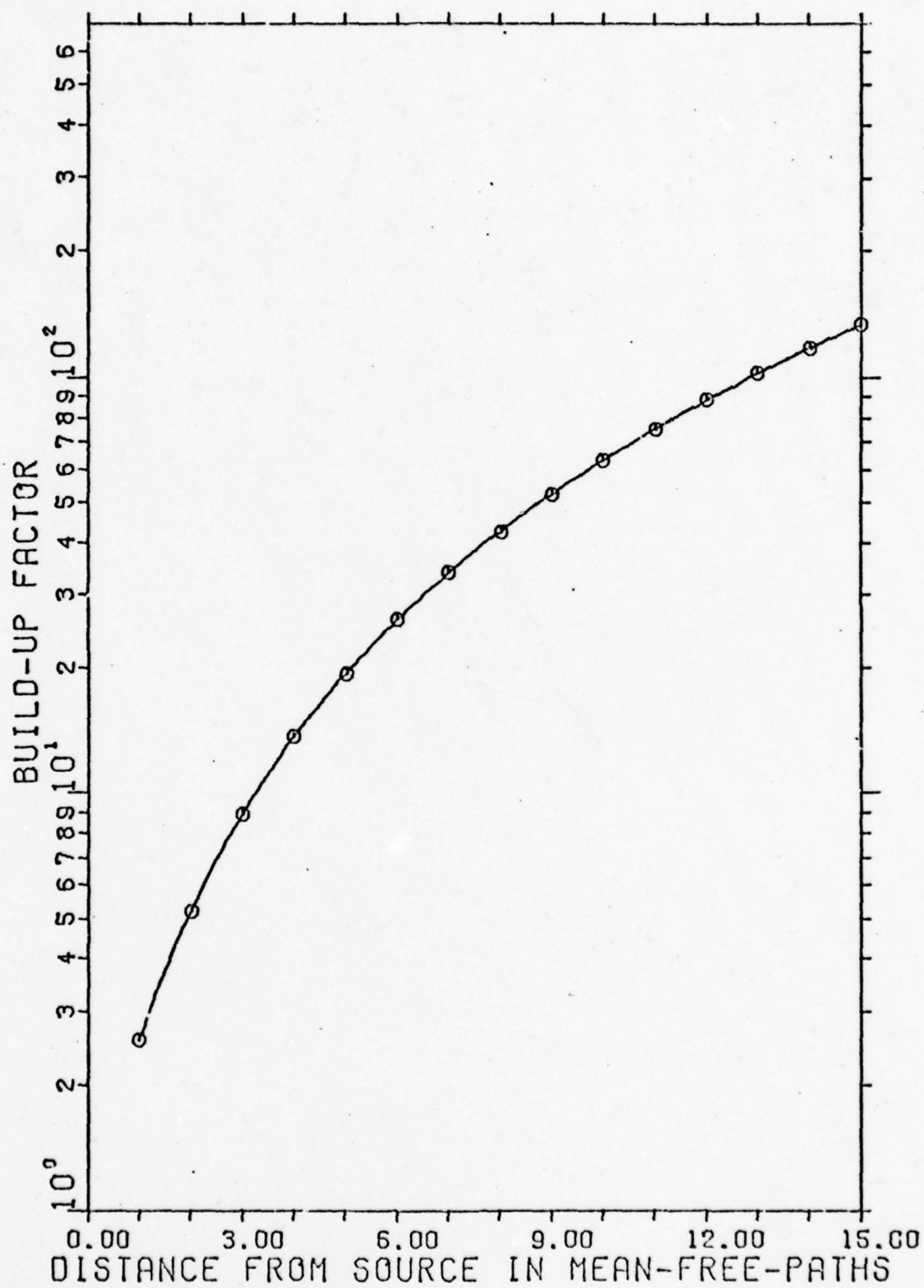


FIG. 94 ENERGY BUILD-UP FACTORS FOR 490 KEV

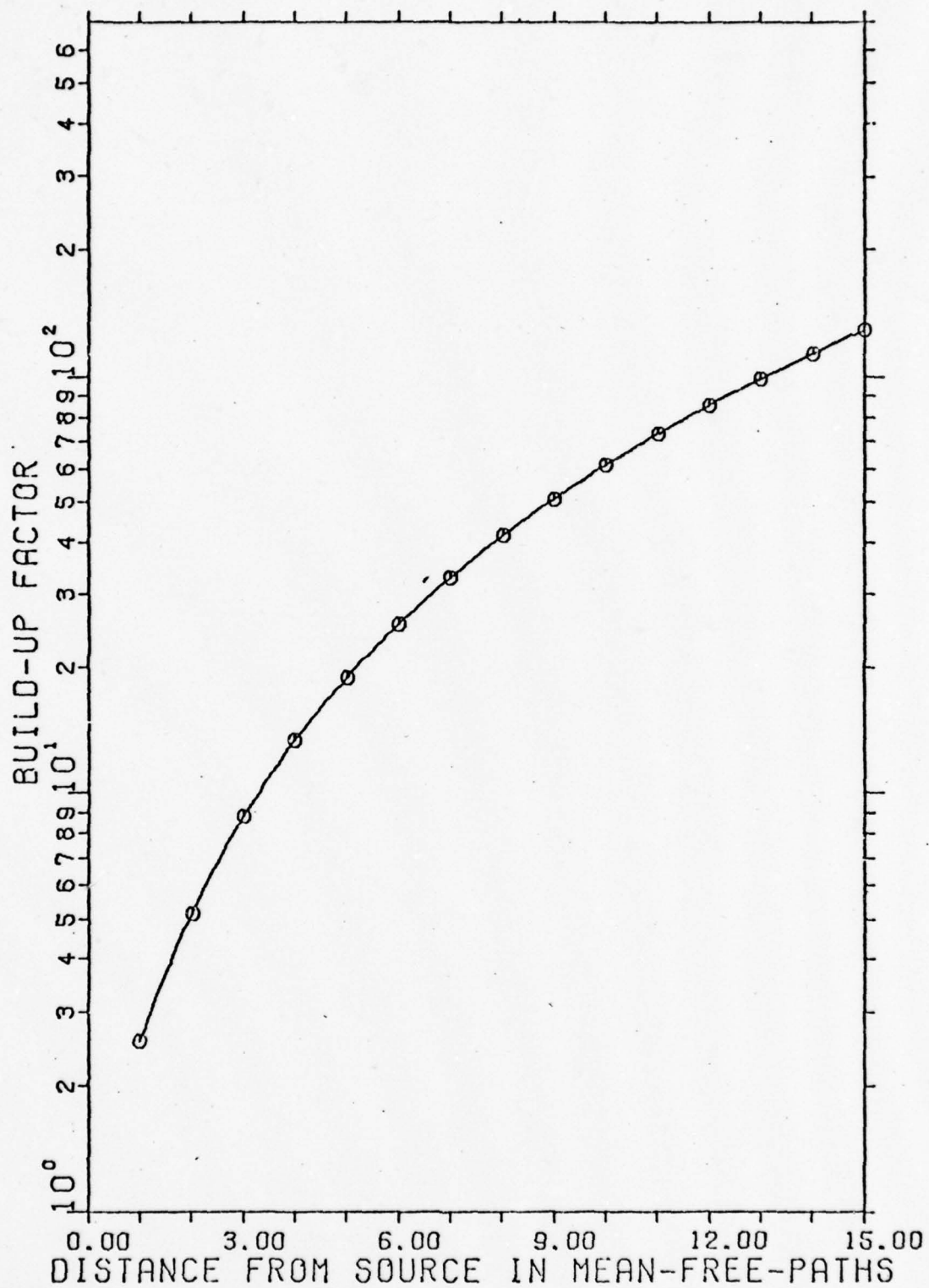


FIG. 95 ENERGY BUILD-UP FACTORS FOR 500 KEV

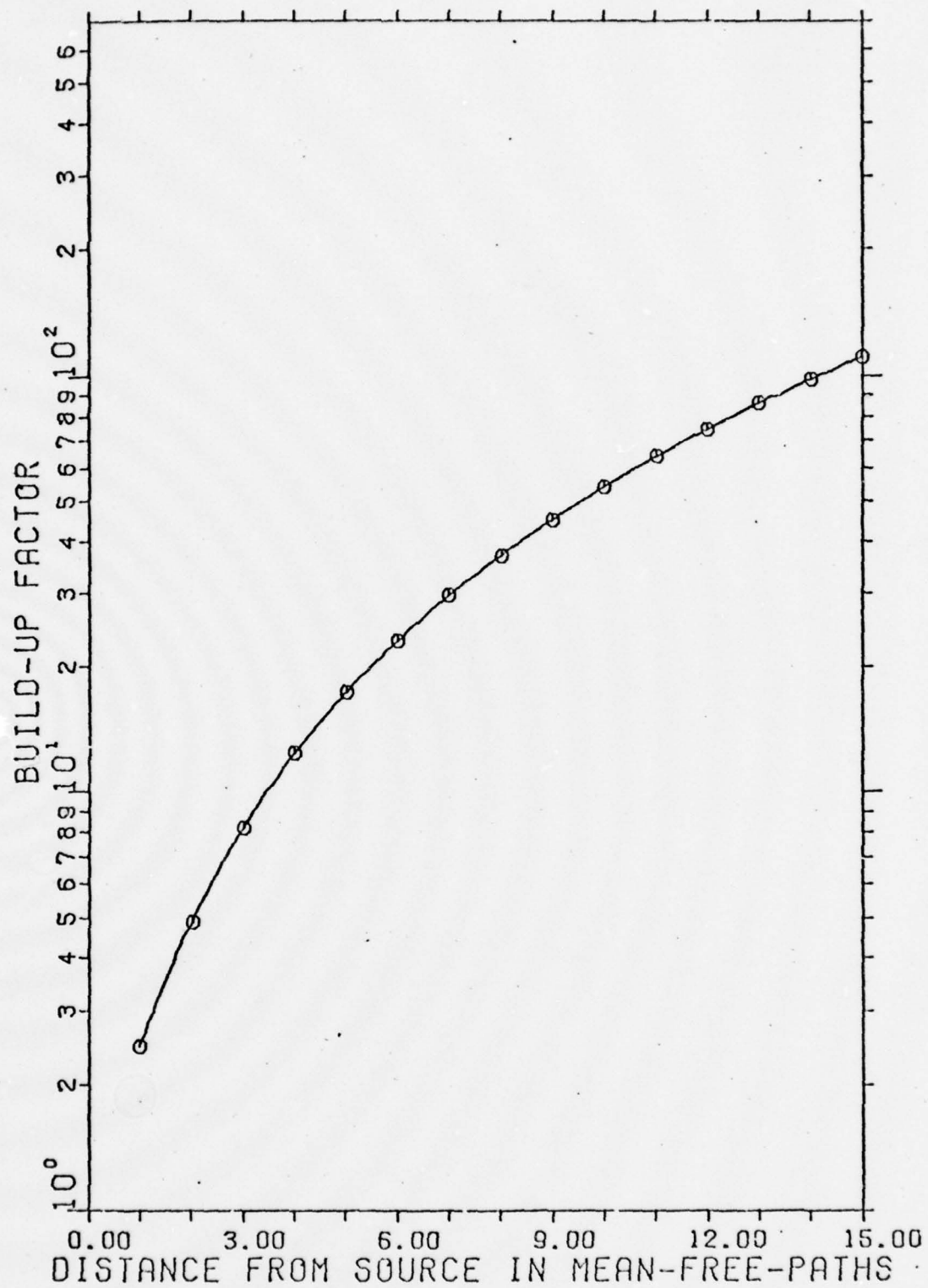


FIG. 96 ENERGY BUILD-UP FACTORS FOR 550 KEV

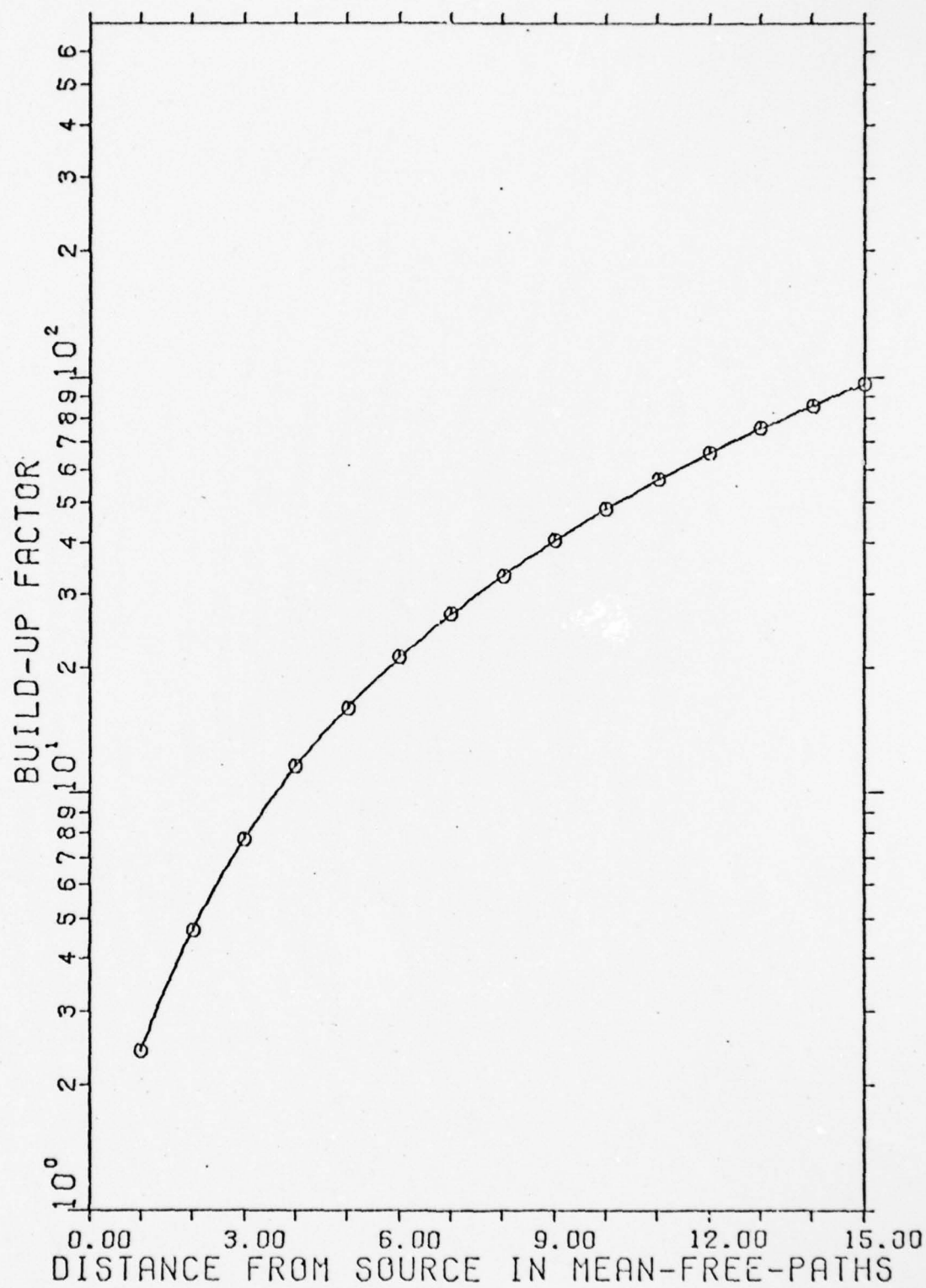


FIG. 97 ENERGY BUILD-UP FACTORS FOR 600 KEV

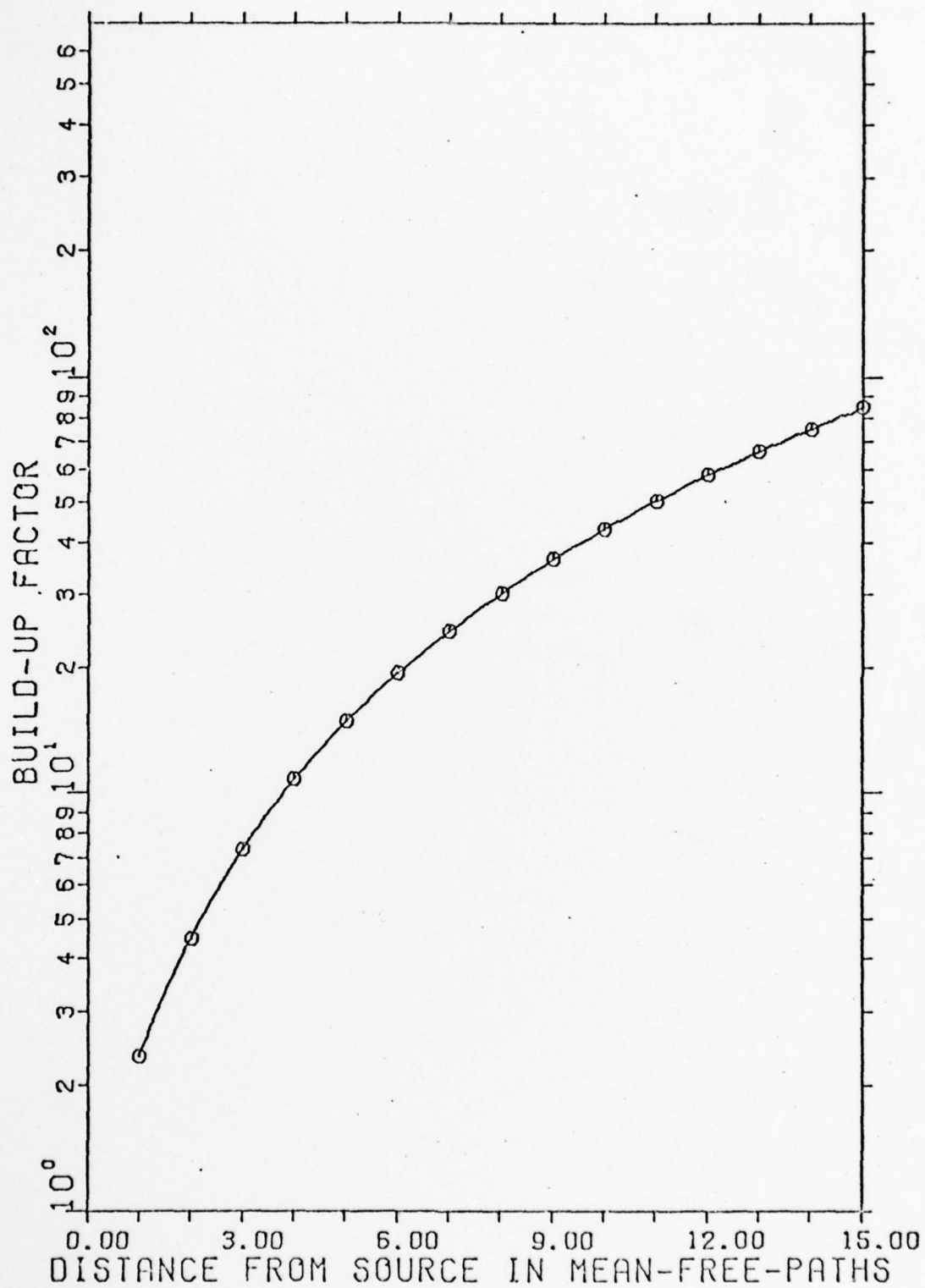


FIG. 98 ENERGY BUILD-UP FACTORS FOR 650 KEV



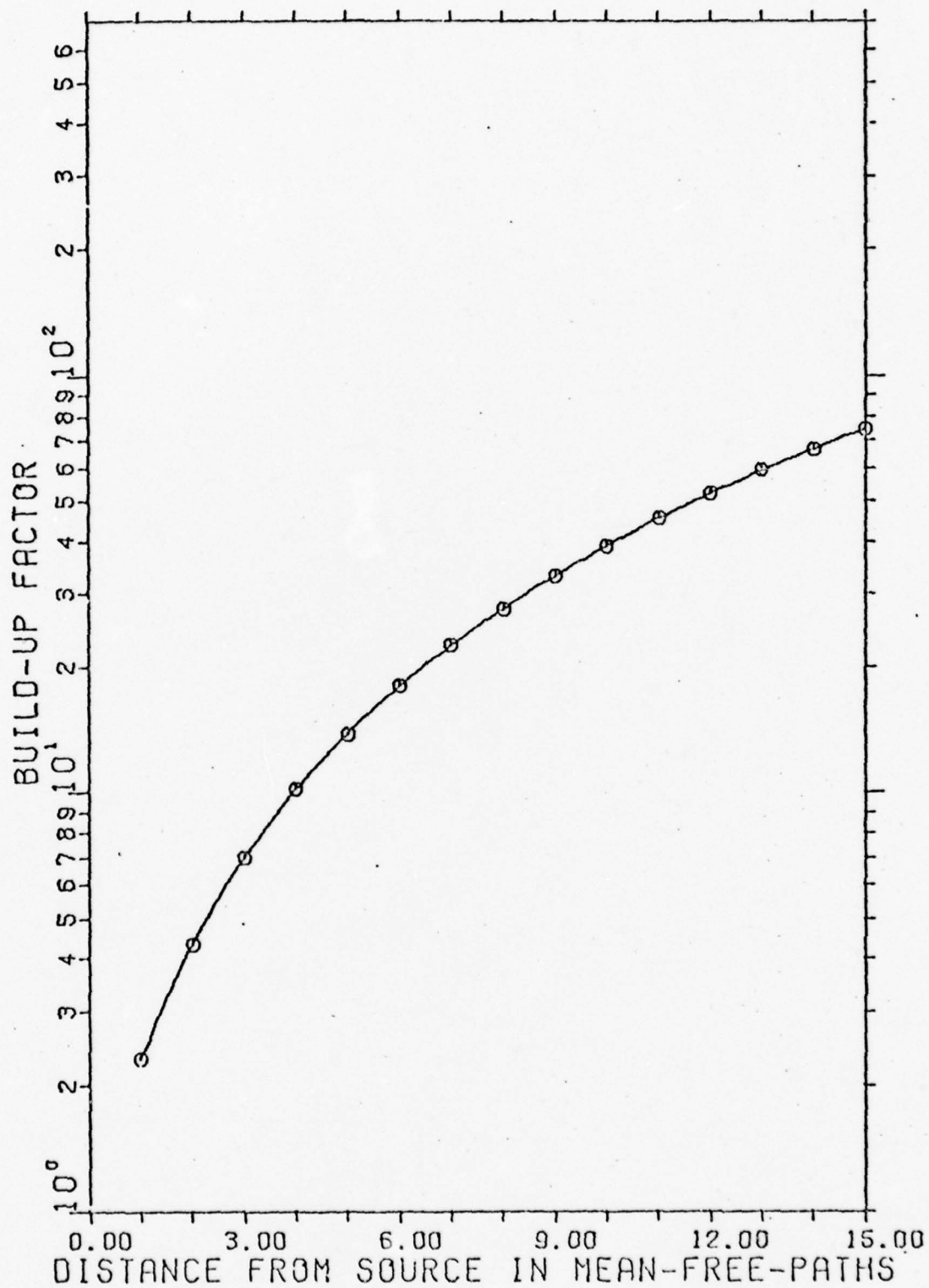


FIG. 99 ENERGY BUILD-UP FACTORS FOR 700 KEV



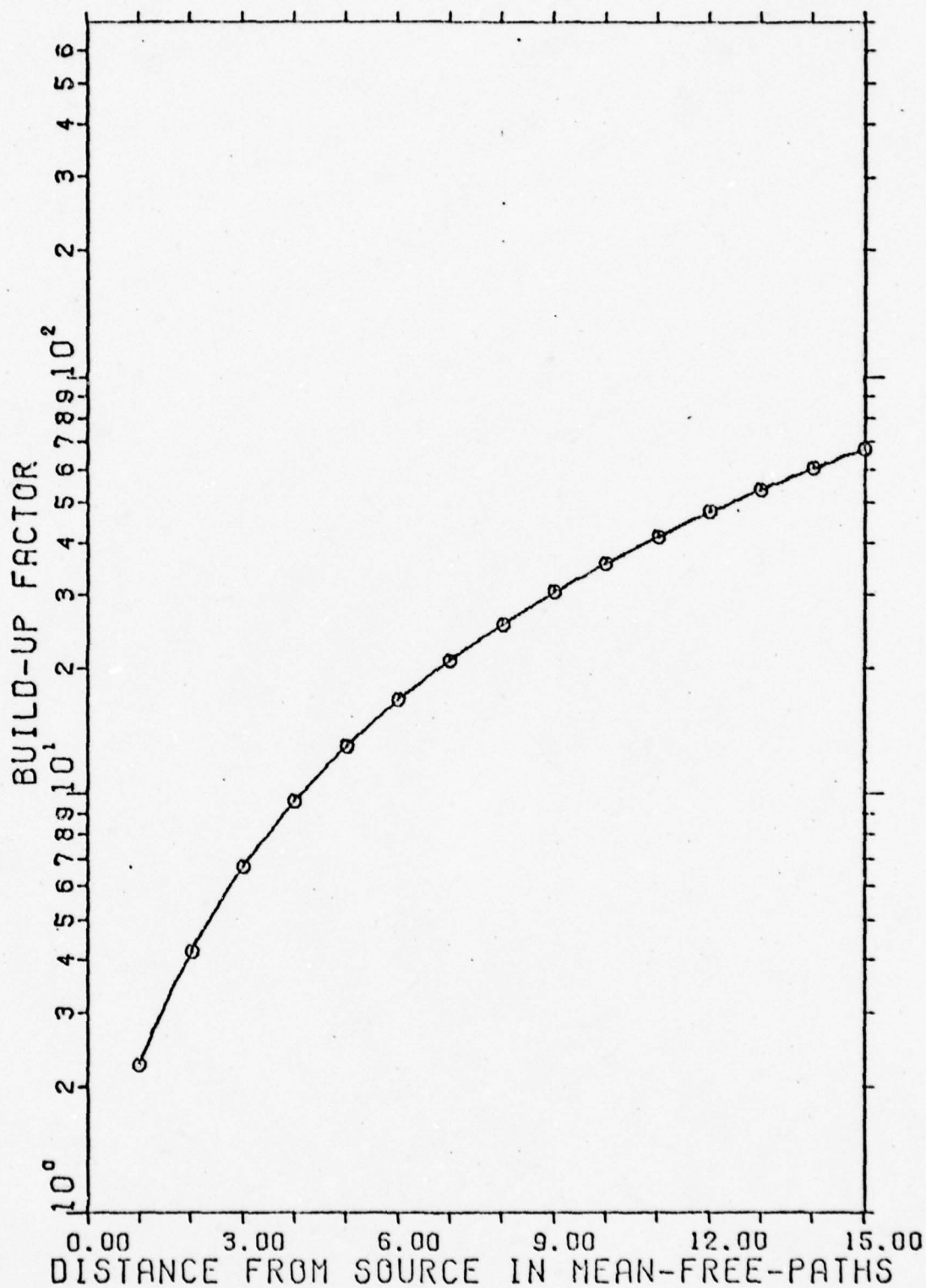


FIG. 100 ENERGY BUILD-UP FACTORS FOR 750 KEV

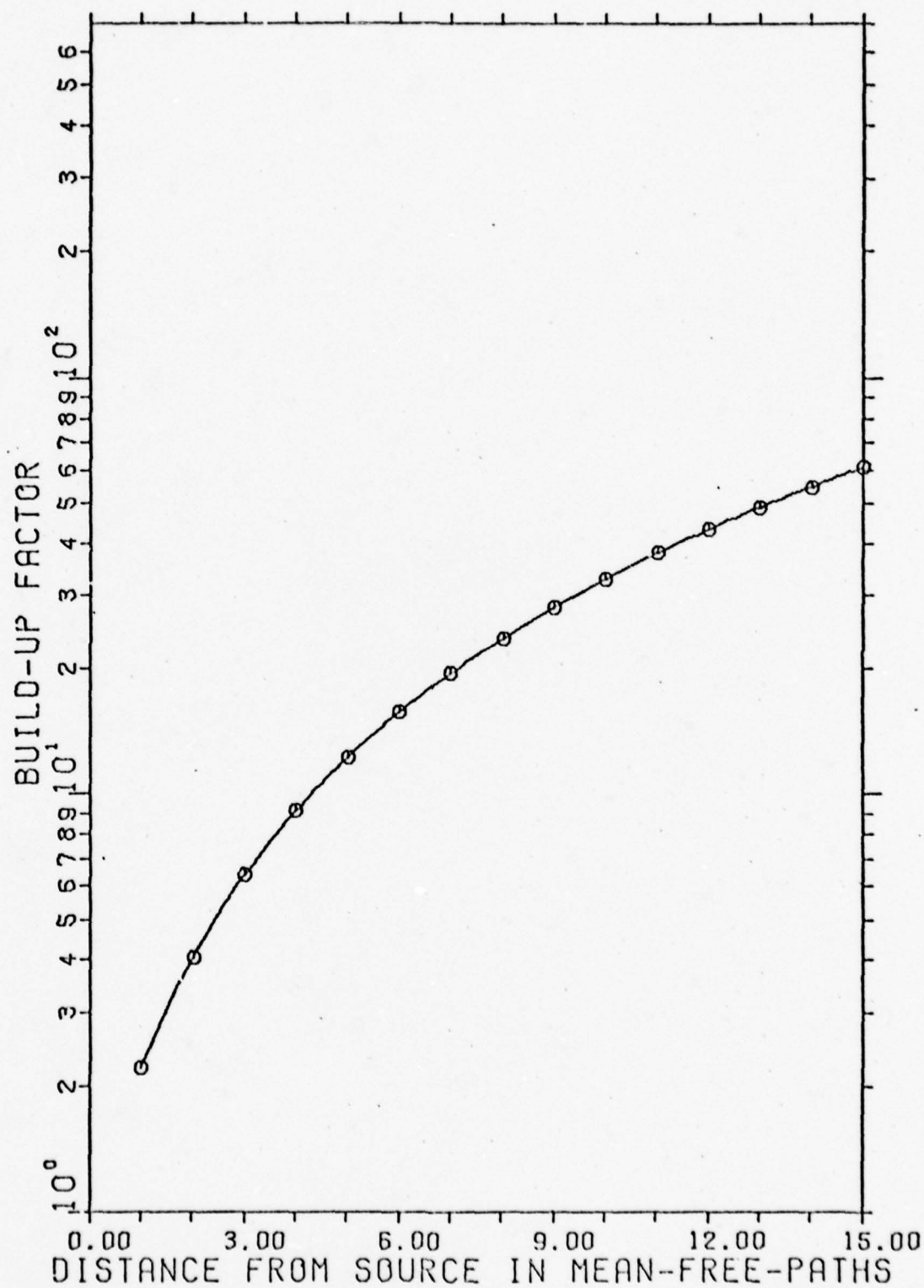


FIG. 101 ENERGY BUILD-UP FACTORS FOR 800 KEV

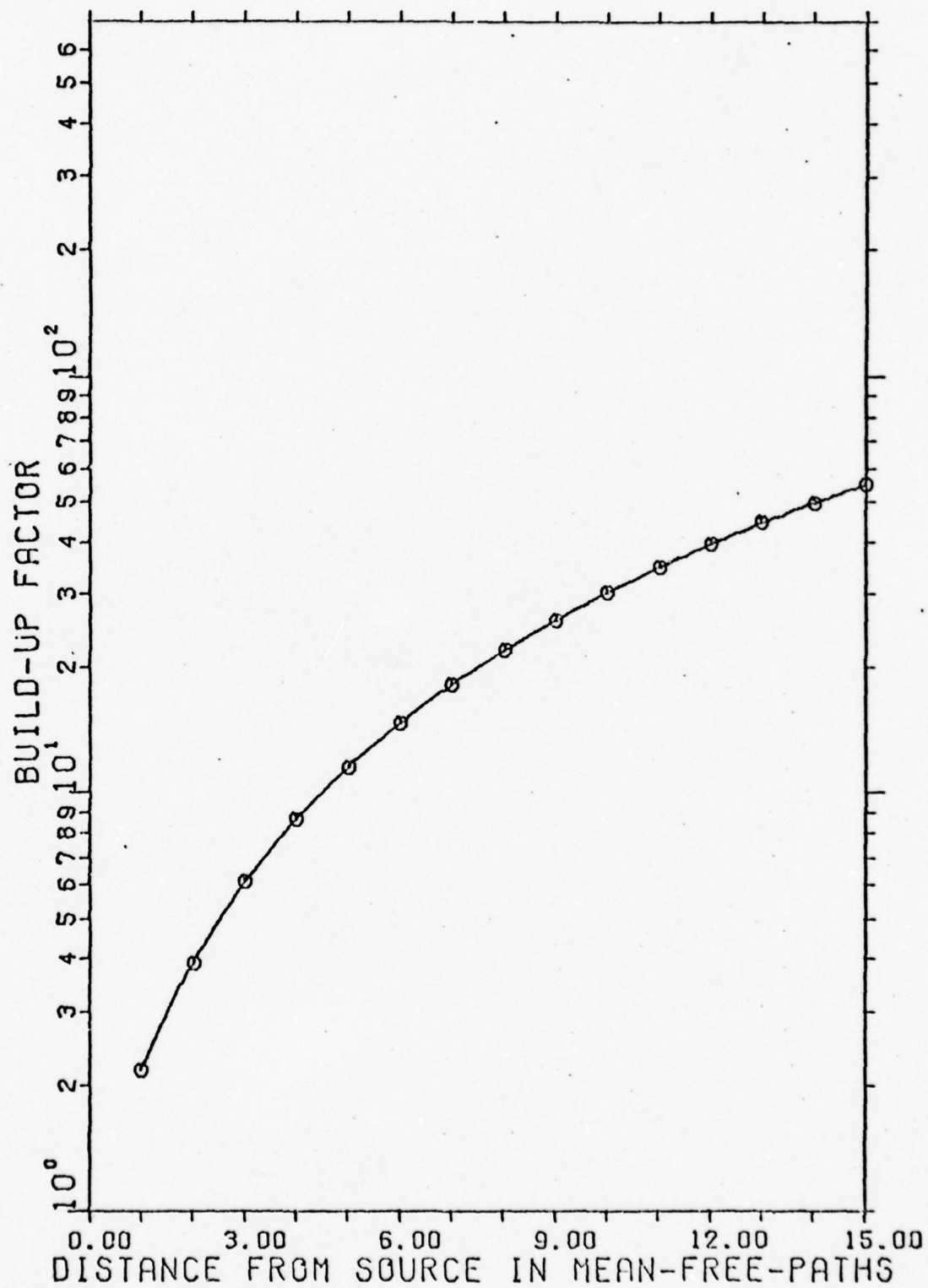


FIG. 102 ENERGY BUILD-UP FACTORS FOR 850 KEV

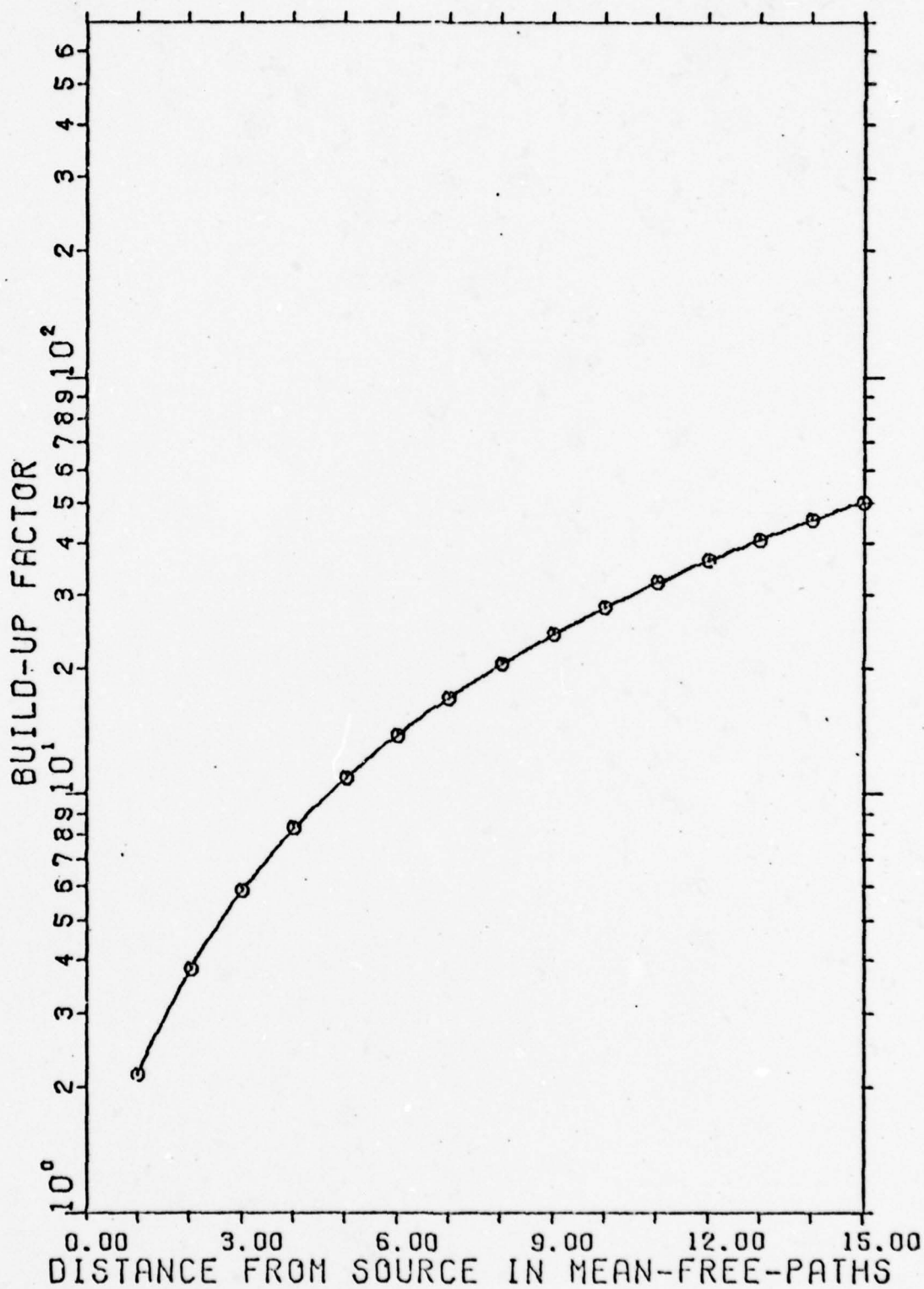


FIG. 103 ENERGY BUILD-UP FACTORS FOR 900 KEV

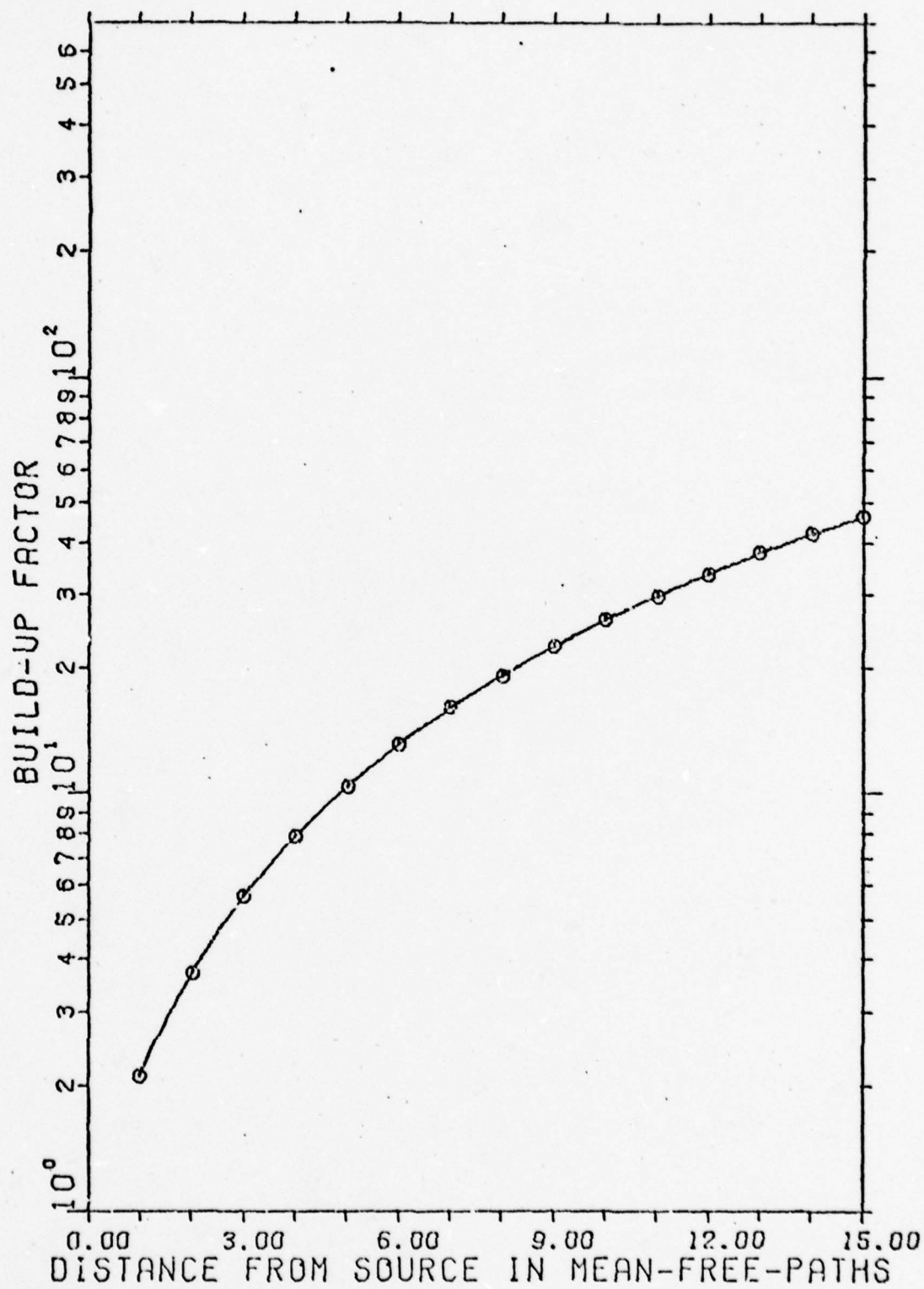


FIG. 104 ENERGY BUILD-UP FACTORS FOR 950 KEV



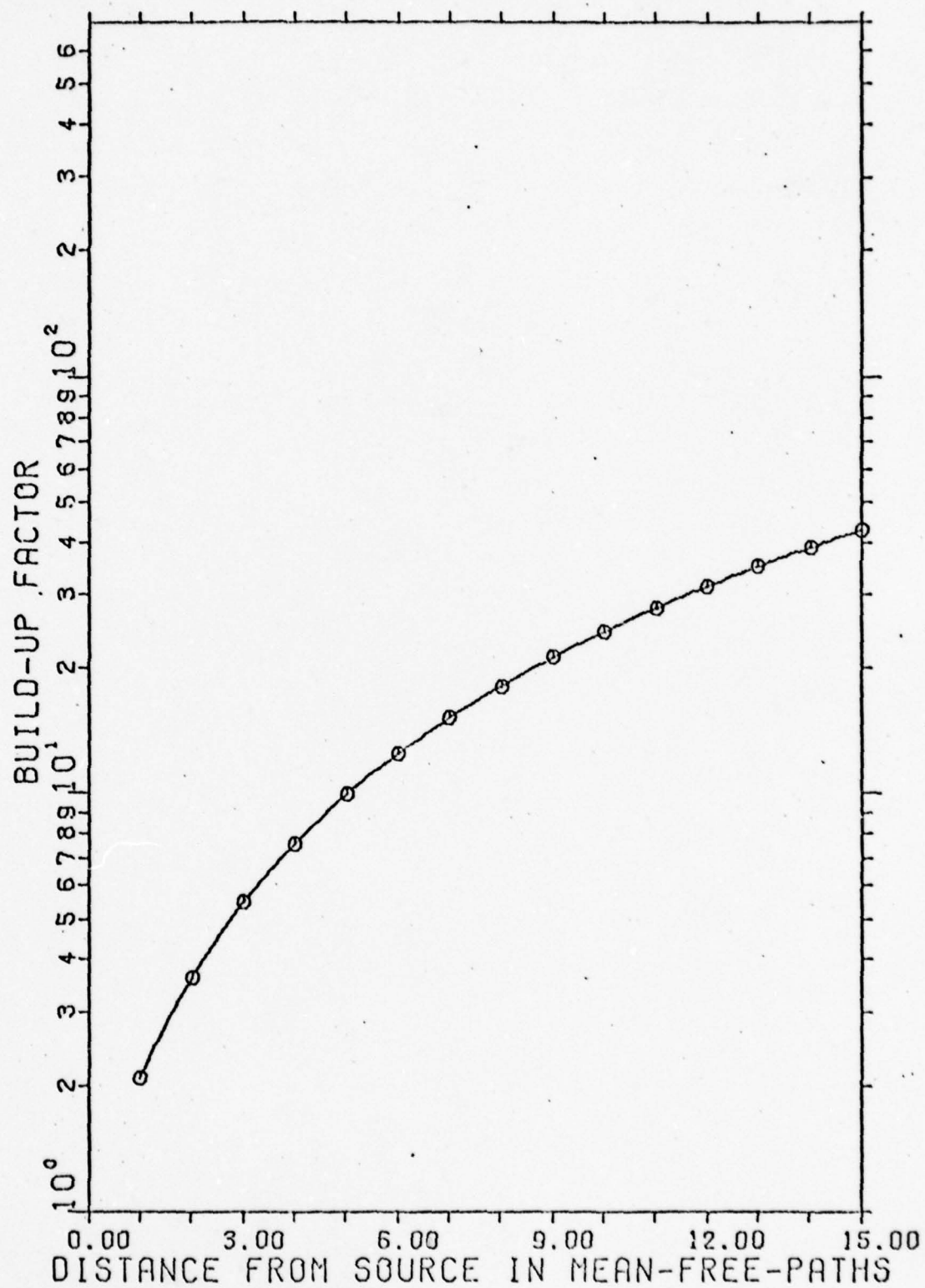


FIG. 105 ENERGY BUILD-UP FACTORS FOR 1000 KEV



## V Discussion

### Intrinsic Estimate of the Accuracy

To examine the accuracy of this program, the convergence of a finite number of moments must be examined first. If all the moments could be calculated from Eq (28), found in Appendix A, no error from this source would be introduced. To estimate the error injected by the truncation of terms, examination of the change of the values of the expansion coefficient  $F^m(r,E)$  as more moments are used in Eqs (31) and (32) would be used. This analysis was performed by Bigelow (Ref 1:116-119) on this program and his findings indicate that the total error produced by the truncation of all but the first nine terms results in a 5% error in the expansion coefficients.

The error introduced by calculating the scattered fluence by using the polynomial reconstruction, Eq (34), is about 1%. The numerical error introduced by the calculations performed in Eq (1), (29), (35) and (36) are from 1% at small distances for small energies to 15% at large distances for large energies. The figures used above were also obtained by analysis performed by Bigelow (Ref 1:126-127).

Therefore, the total maximum error for the build-up factors introduced from all sources is 20%, which only occurs at large distances for large energies.

### Comparison of Results to Others

Introduction. Because of the limited amount of data for build-up factors of the energy range considered in this study for air, some modification of the data obtained from other sources had to be made. In some cases, the data obtained from other sources were in the form of energy fluence instead of build-up factors. To obtain the build-up factors in this case, Eqs (1)

and (36) were used. In other cases, the results were presented as a fraction of vacuum fluence that reached a certain distance. Then, the following calculations were performed. The vacuum fluence can be defined as

$$F^V = S/4\pi r^2 \quad (7)$$

By dividing Eq (2) by Eq (7) the fraction of the vacuum fluence  $V$  is obtained:

$$V = Be^{-\mu r} \quad (8)$$

$\mu r$  is equal to the number of mean-free-paths  $y$ . Solving Eq (8) for  $B$

$$B = V/e^{-y} \quad (9)$$

So for any mean-free-path of interest, the build-up factor can be extracted from data giving only fraction of the vacuum fluence to that distance.

All of the comparisons made below are in terms of percent difference which is defined by the following equation:

$$\frac{(\text{Moments-method result}) - (\text{Result used in comparison})}{(\text{Moments method result})} \cdot 100\% = PD \quad (10)$$

where PD is the percent difference.

Monte Carlo. Banks (Ref 15), using a modified CGRE Monte Carlo code, performed photon transport calculations for energies from 20 to 300 keV. He presented some of the results in the form of a graph of build-up factors at 10 mean-free-paths. This graph as well as a similar graph of the build-up factors calculated by the moments method are superimposed and presented in Fig 106. The percent difference for the energies below 50 keV are as low as -47%. But above 50 keV, the percent differences range up to 26% with the average being 23%. Taking into account the error of the build-up factor calculation associated with the moments method, the rest of the error can be attributed to the use of different cross sections.

Coleman did a study computing x-ray transport and the results are

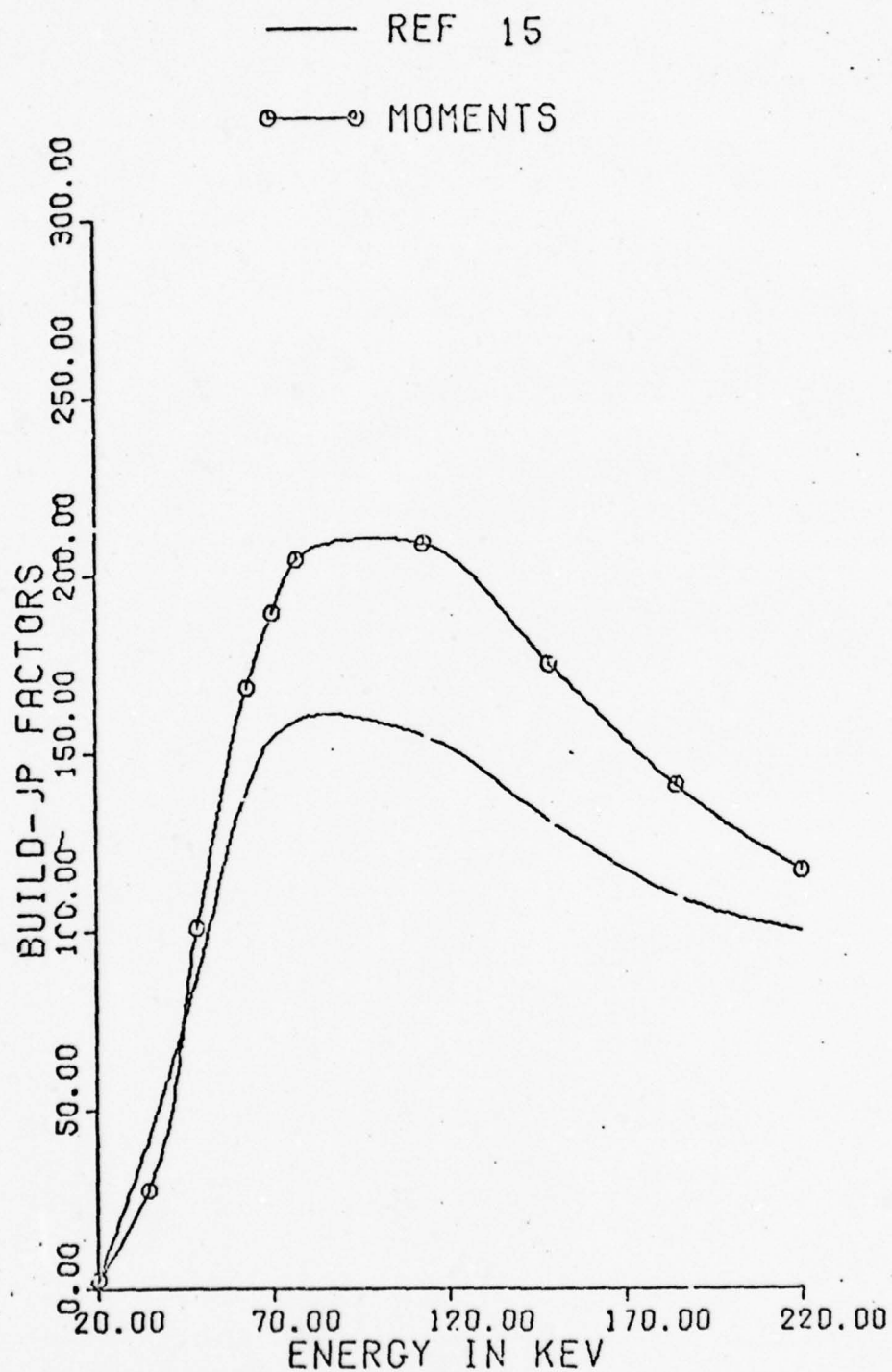


FIG. 106 COMPARISON OF ENERGY BUILD-UP FACTORS  
AT 10 MEAN-FREE-PATHS

presented in Banks (Ref 15). Since the results are presented as a fraction of vacuum fluence in mean-free-paths, the conversion to build-up factors must be performed. A comparison to the build-up factors calculated by the moments method is presented in Fig 107. It can be seen that the percent differences for 60 keV, which is the only energy range given, are from 17% to 52%.

Krumbein (Ref 16) using SAGE performed calculations of x-ray air transport. SAGE is United Nuclear's spherical Monte Carlo photon code. The calculations were carried out at various energies from 12 keV to 100 keV and out to 10 mean-free-paths. Even though the calculations for the fluence used to calculate the build-up factors were performed using the density of air at an altitude of 22,860 meters, this had no effect on the build-up factors since the energy build-up factor is independent of altitude when it is reported as a function of mean-free-path. Comparison to Krumbein's calculations is shown in Figs 108, 109 and 110. For 20 keV, the percent differences range from 7.5% to 17%. For 40 keV, the percent differences range from 18% to 32%. For 100 keV, the percent differences range from 12% to 27%. These differences can be accounted for from the different cross sections used and by taking into account the error produced in the calculation by the moments method.

One of the most extensive calculations using a Monte Carlo code to solve the x-ray air transport problem in air was performed by Shelton and Keith (Ref 17). This calculation was performed by the HAT code. The results are presented in comparison to the moments method calculation in Figs 111-118. For 20 keV, the percent differences are from -8% to -69%. For 40 keV, the percent differences are from -2% to -413%. For 60 keV, the percent differences are from -8% to -76%. For 90 keV, the percent differences are from 3% to -70%. For 120 keV, the percent differences are from 7% to



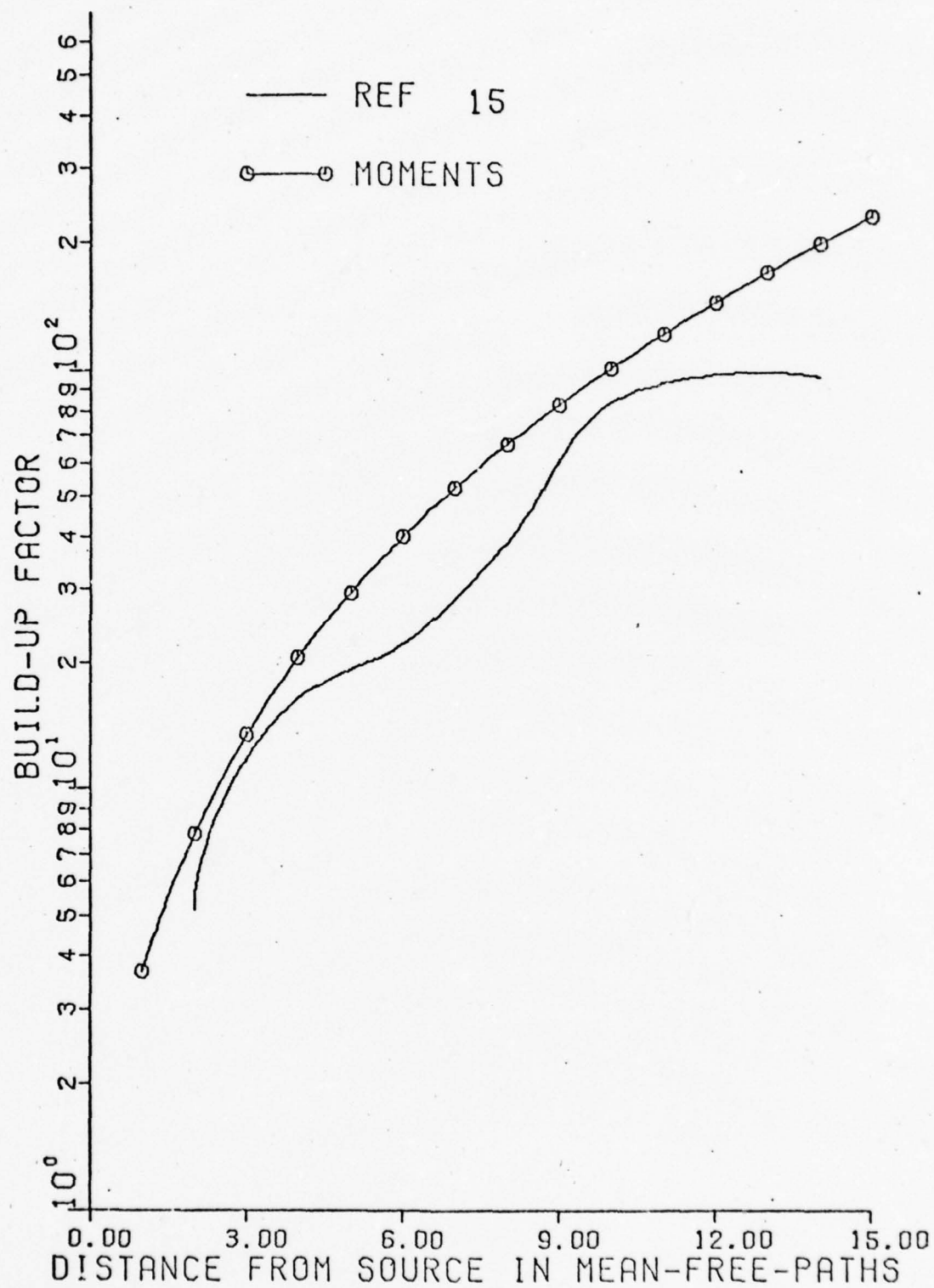


FIG. 107 COMPARISON OF ENERGY BUILD-UP FACTORS  
FOR 60 KEV



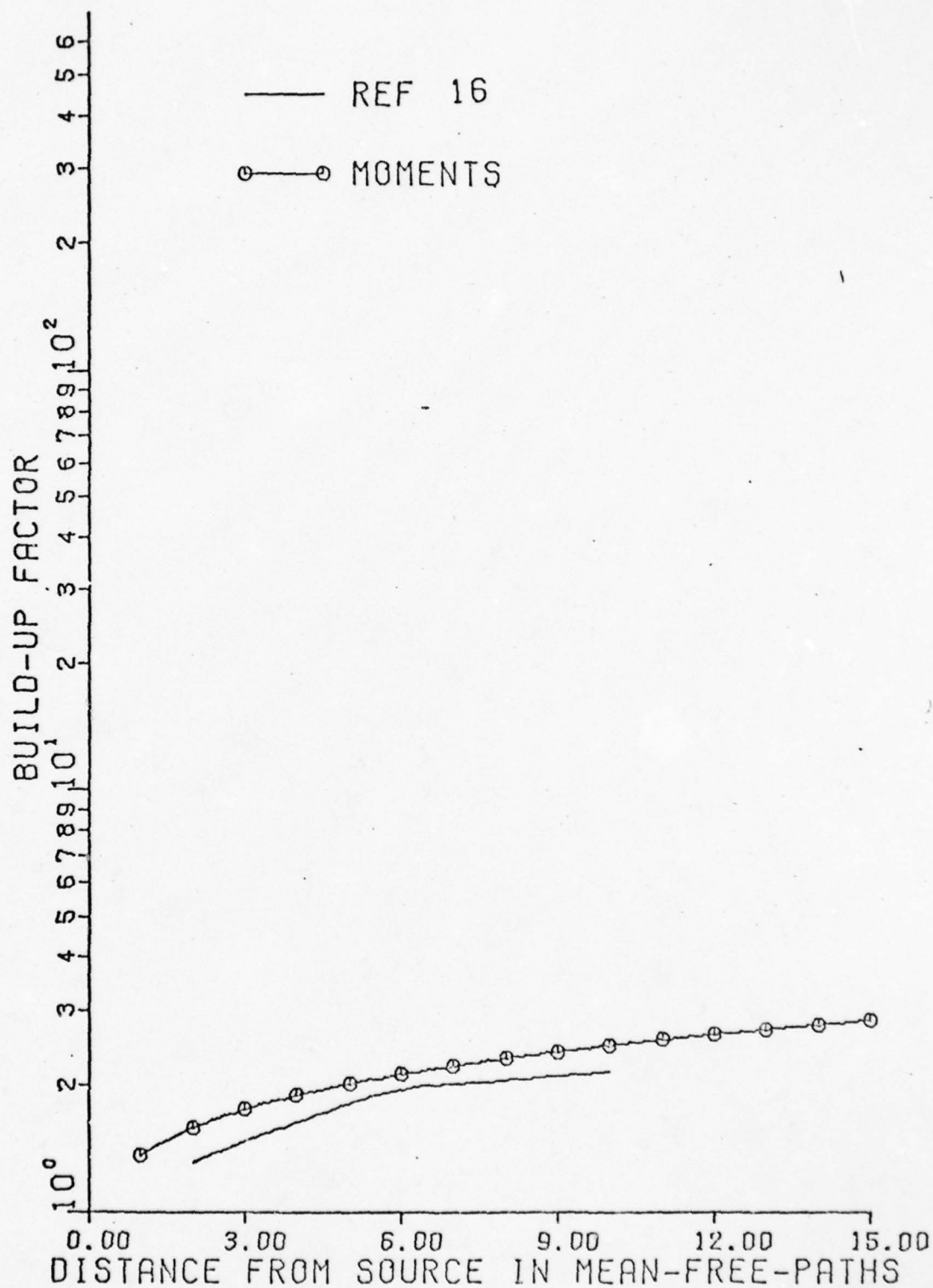


FIG. 108 COMPARISON OF ENERGY BUILD-UP FACTORS  
FOR 20 KEV

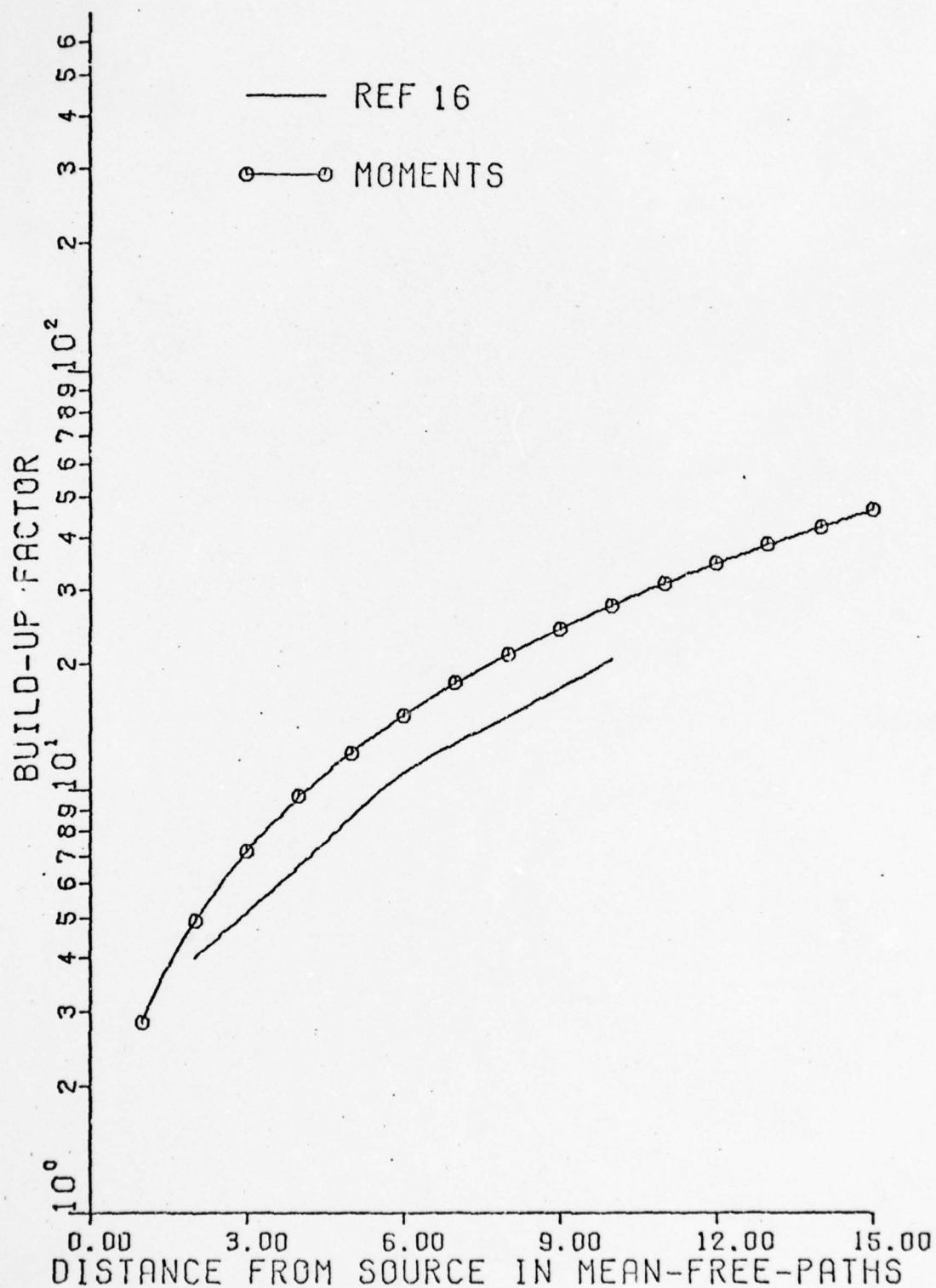


FIG. 109 COMPARISON OF ENERGY BUILD-UP FACTORS  
FOR 40 KEV

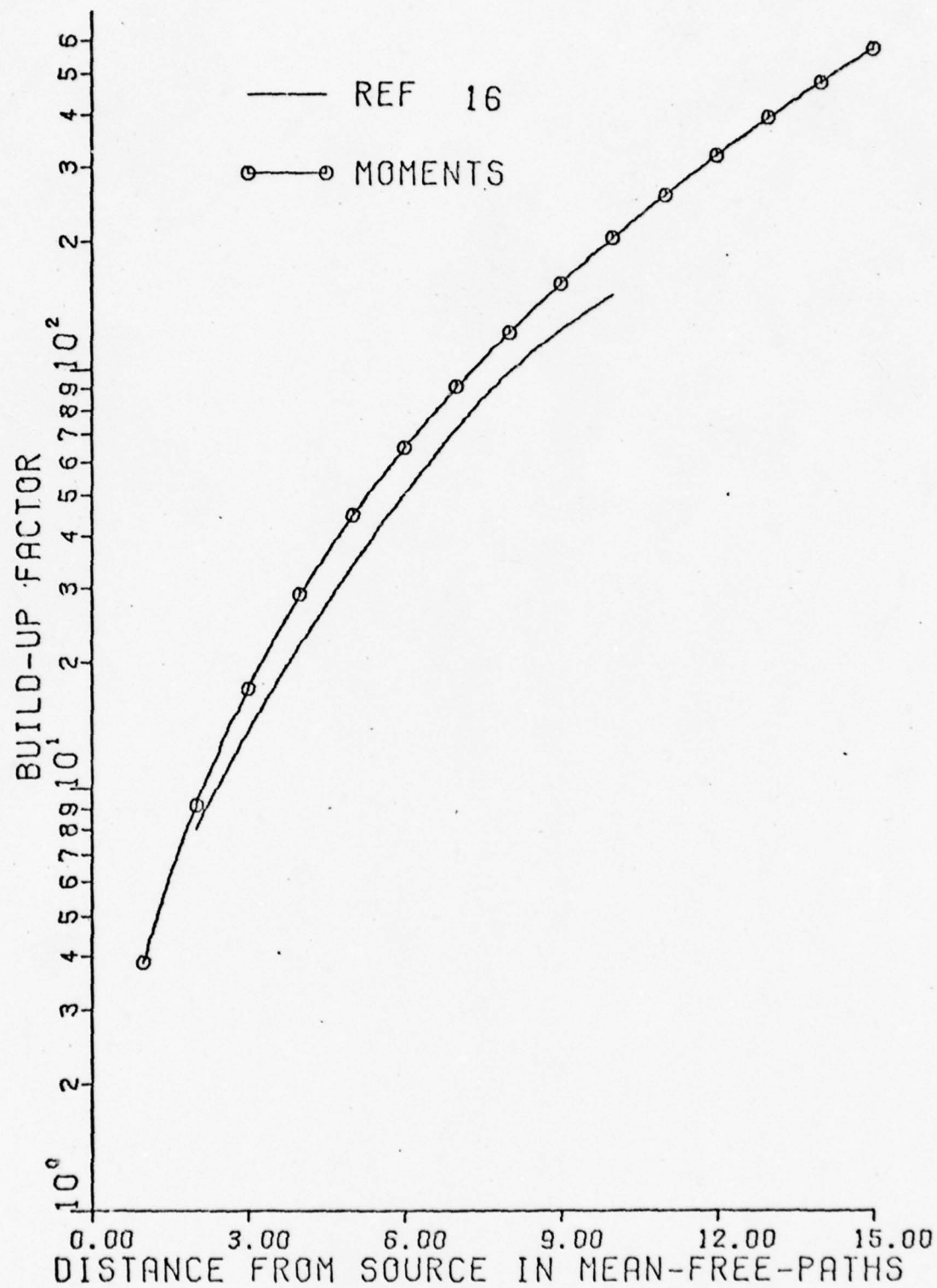


FIG. 110 COMPARISON OF ENERGY BUILD-UP FACTORS  
FOR 100 KEV

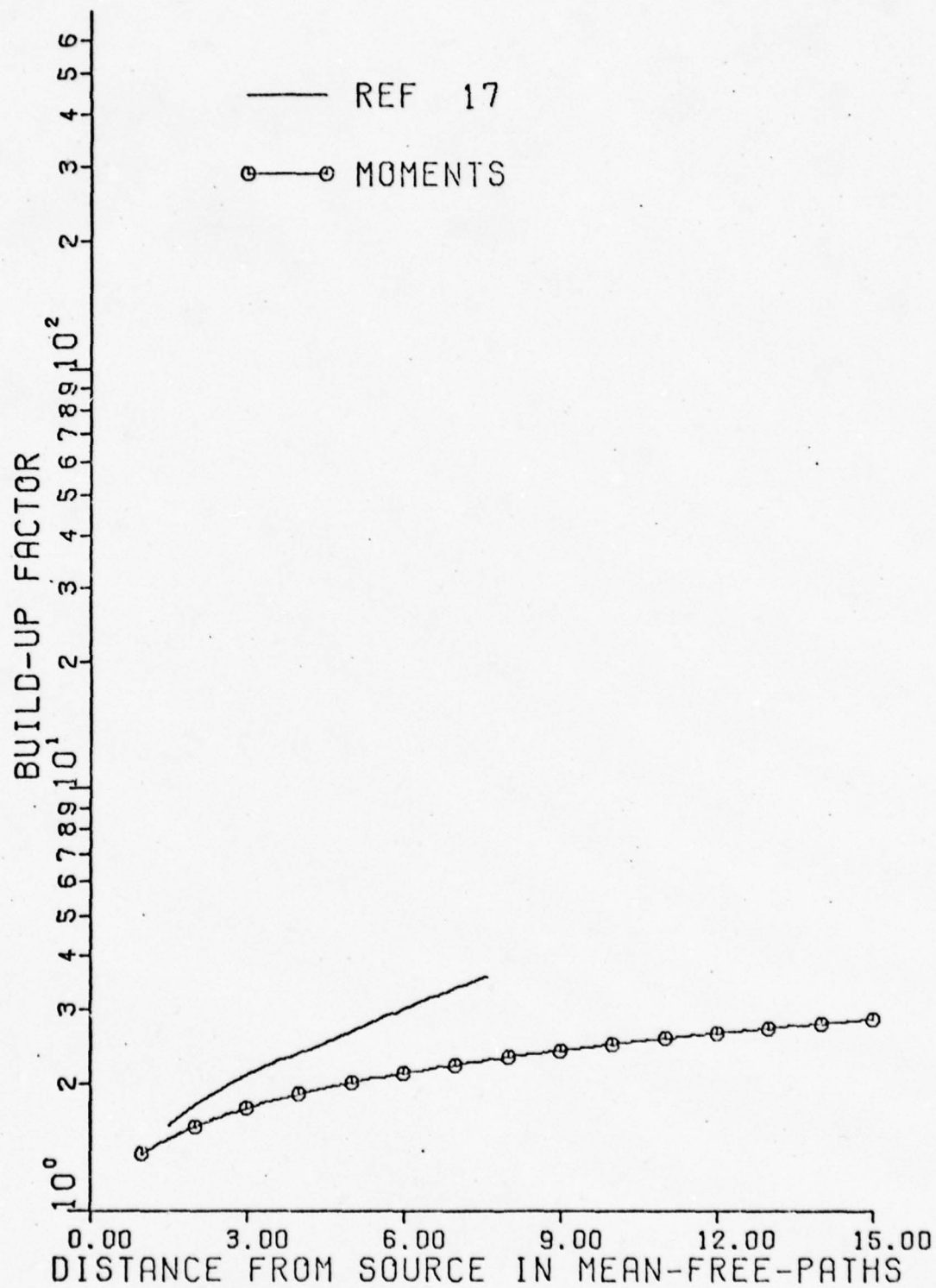


FIG. 111 COMPARISON OF ENERGY BUILD-UP FACTORS  
FOR 20 KEV

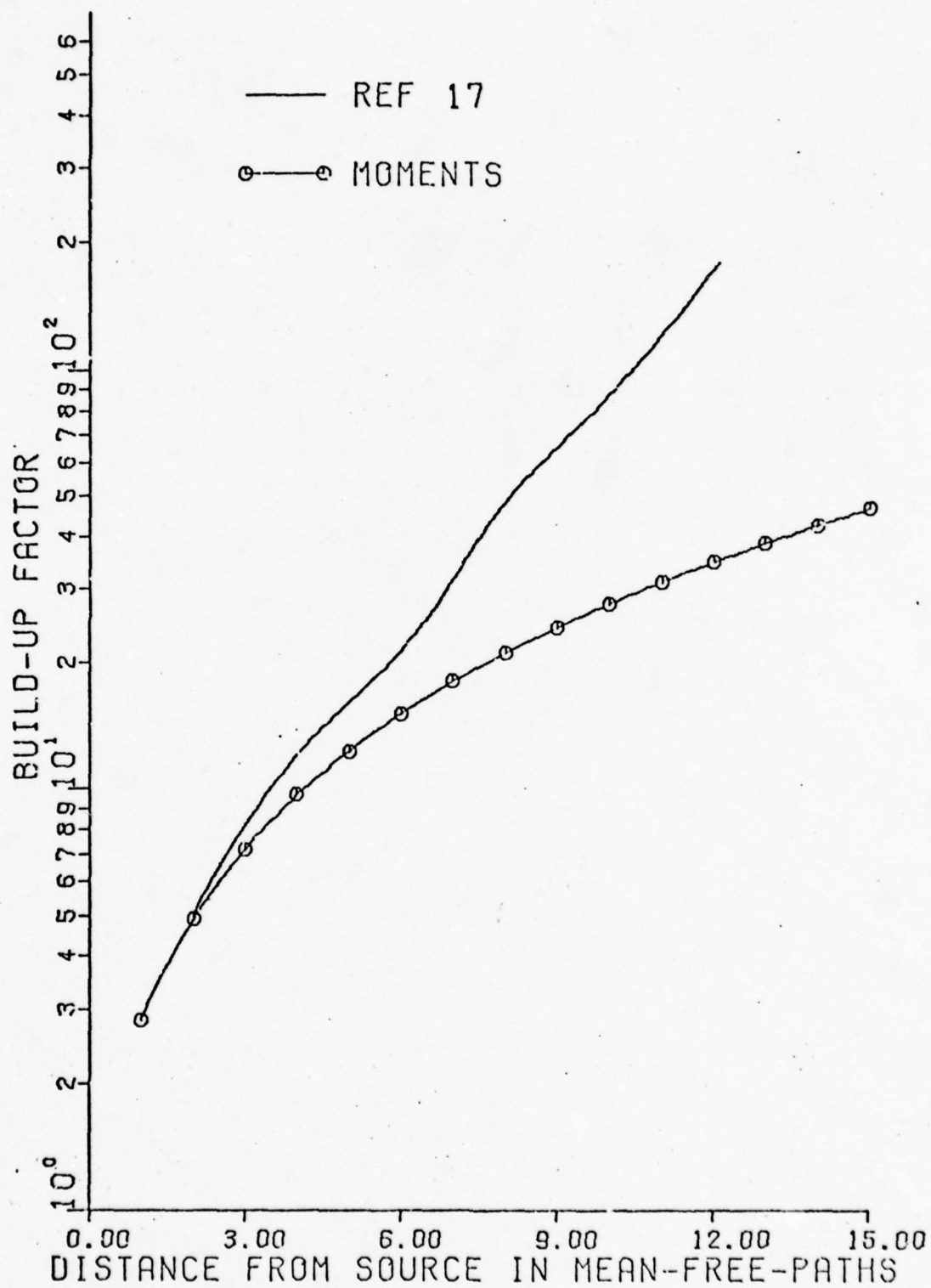


FIG. 112 COMPARISON OF ENERGY BUILD-UP FACTORS FOR 40 KEV



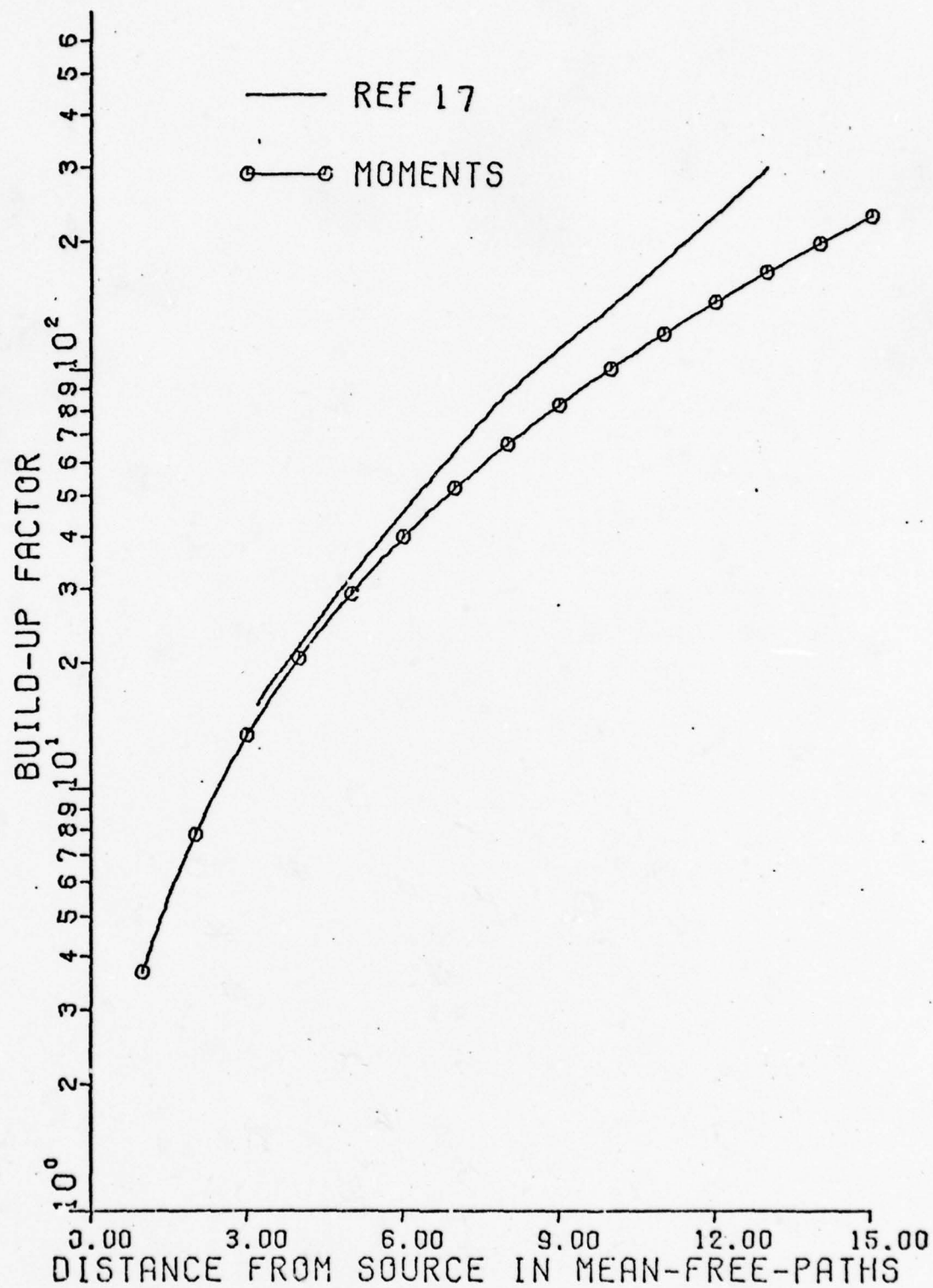


FIG. 113 COMPARISON OF ENERGY BUILD-UP FACTORS  
FOR 60 KEV

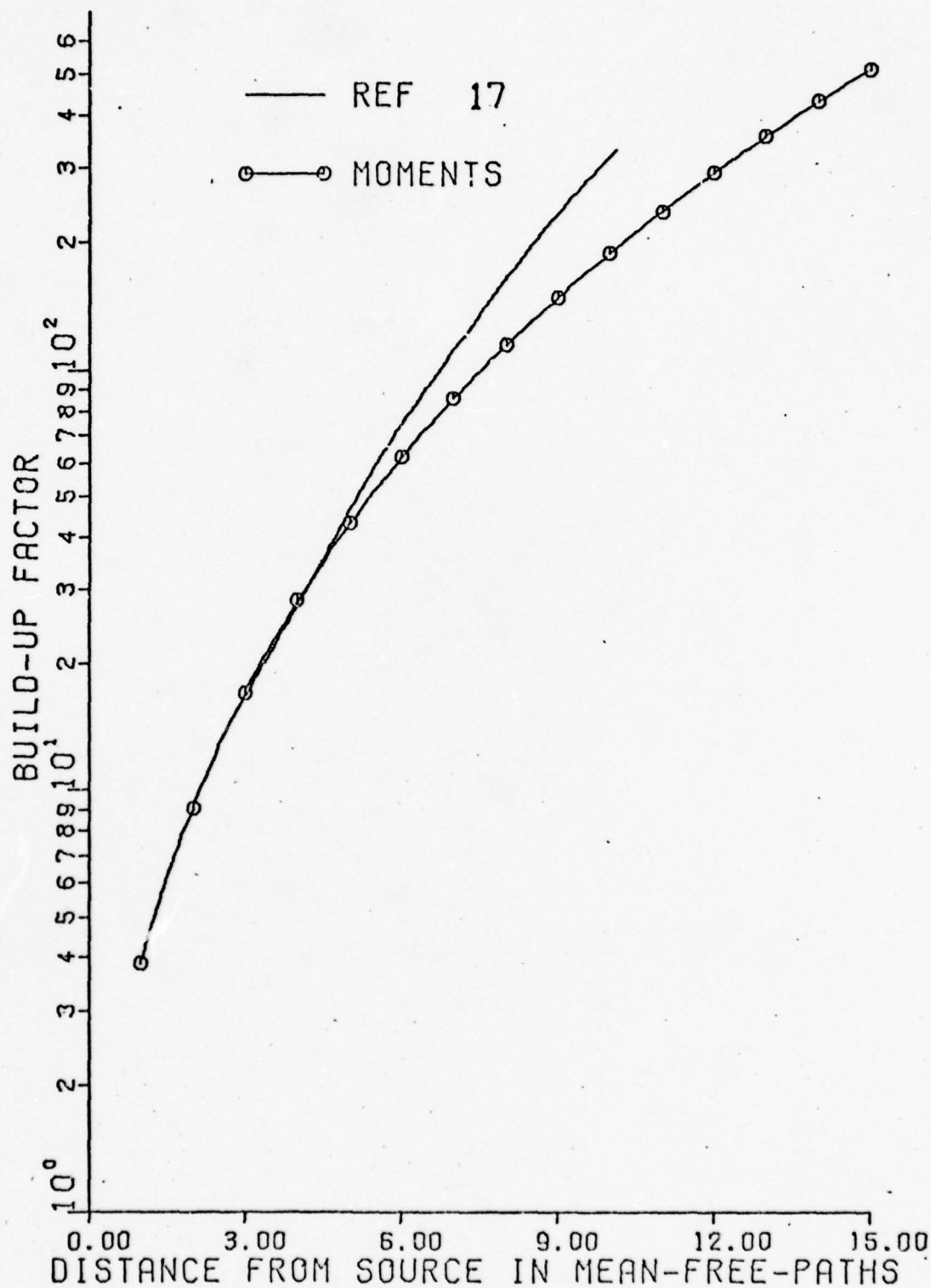


FIG. 114 COMPARISON OF ENERGY BUILD-UP FACTORS  
FOR 50 KEV

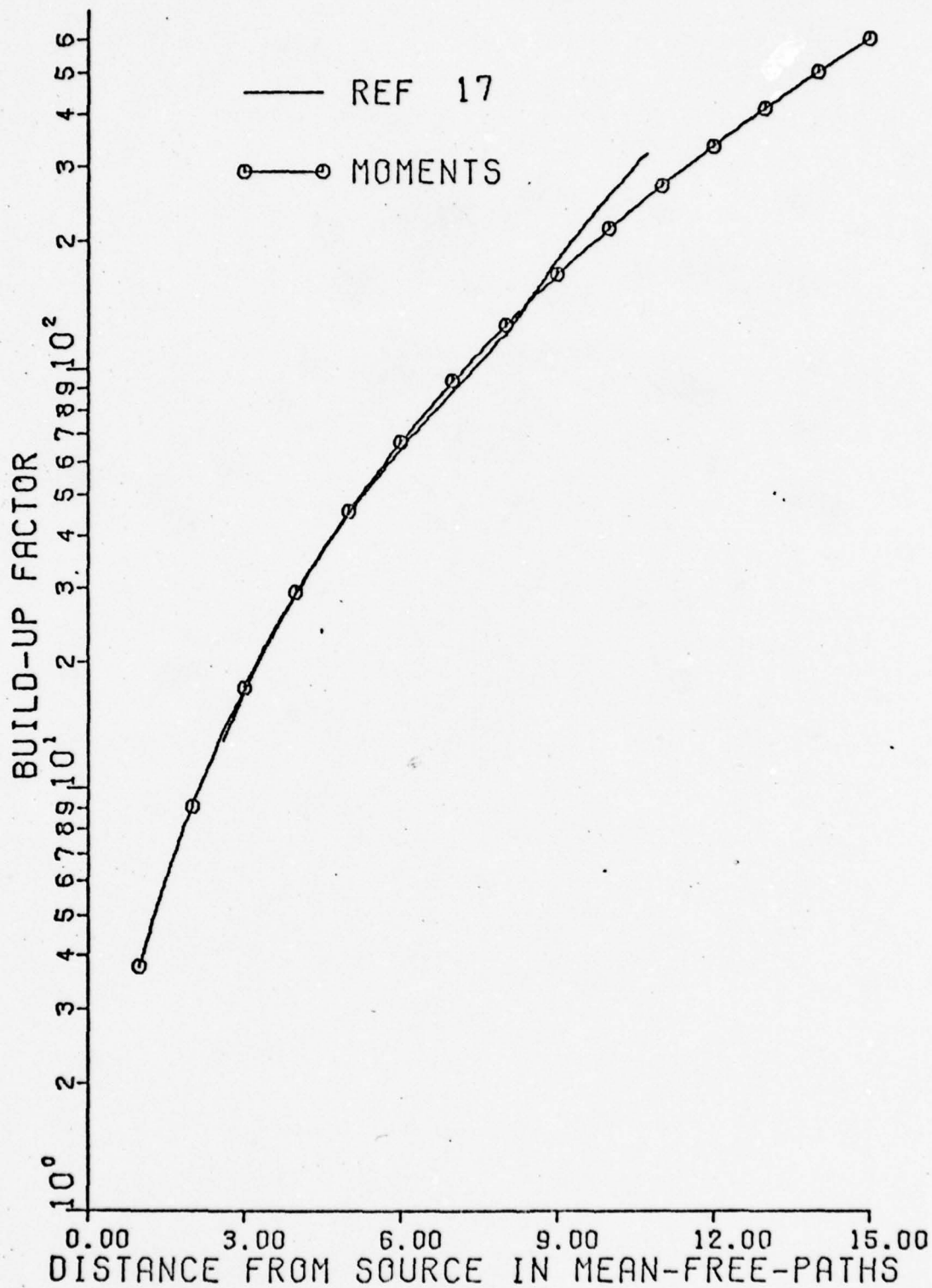


FIG. 115 COMPARISON OF ENERGY BUILD-UP FACTORS  
FOR 120 KEV

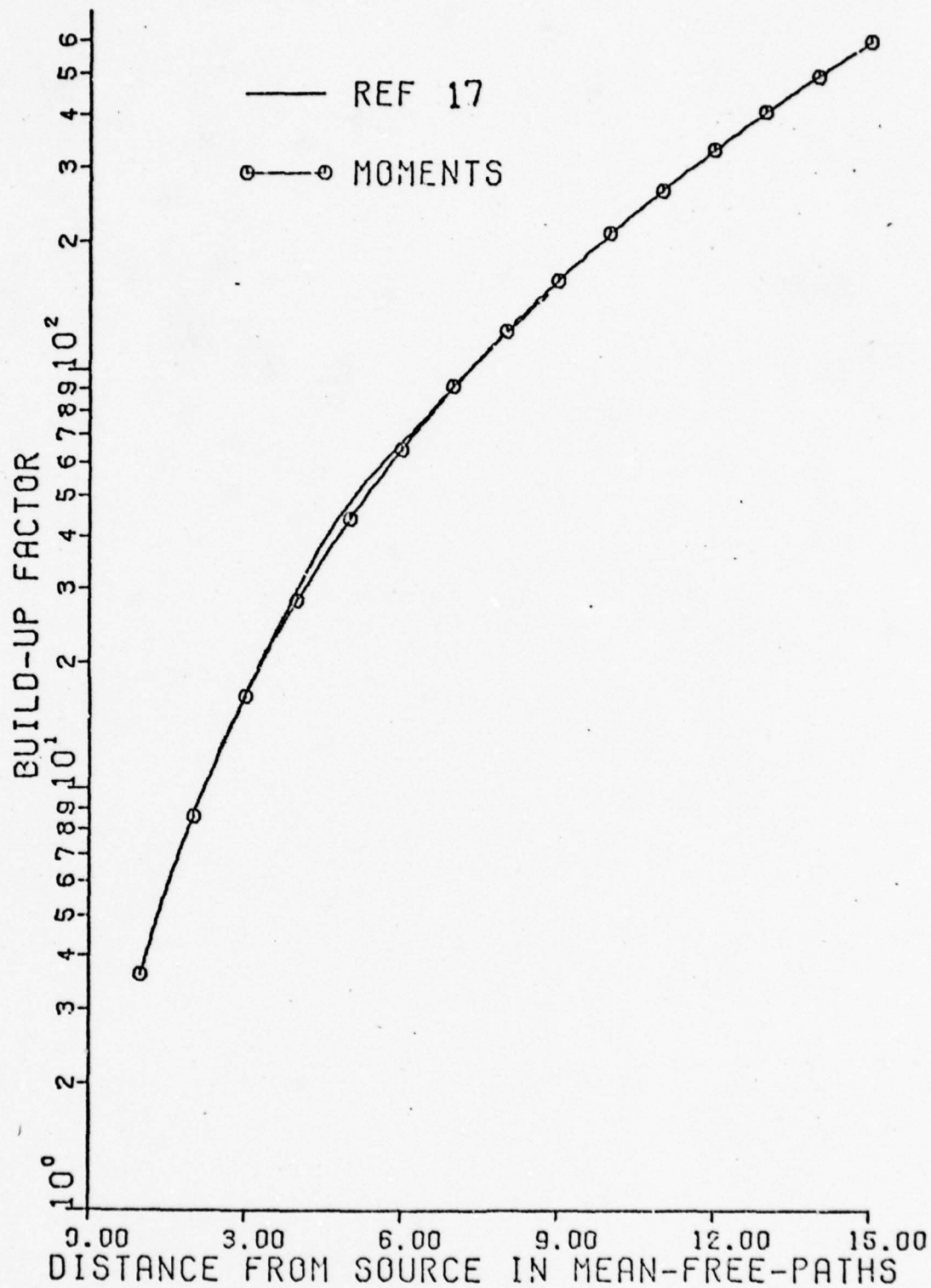


FIG. 116. COMPARISON OF ENERGY BUILD-UP FACTORS FOR 150 KEV

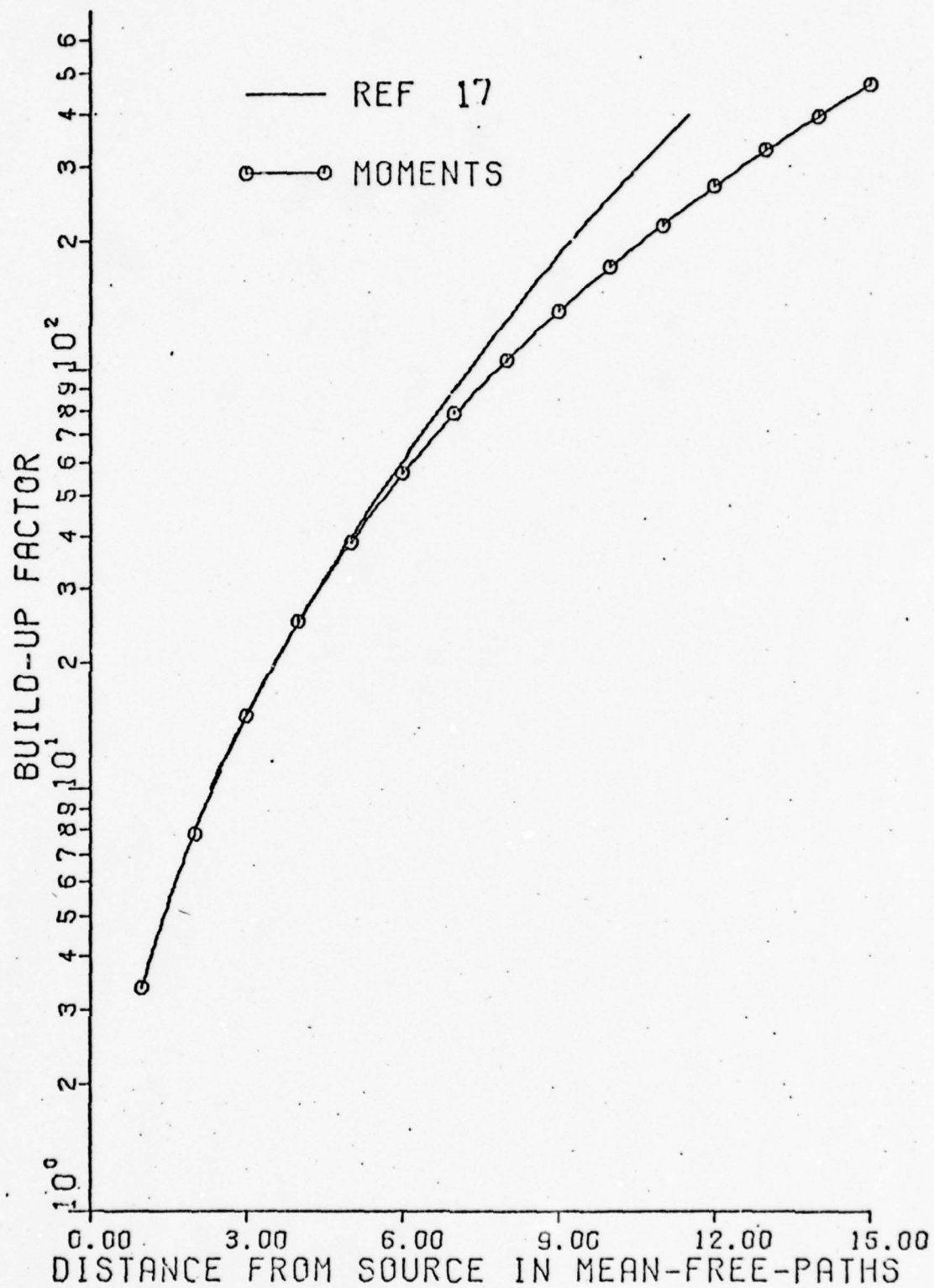


FIG. 117 COMPARISON OF ENERGY BUILD-UP FACTORS FOR 200 KEV



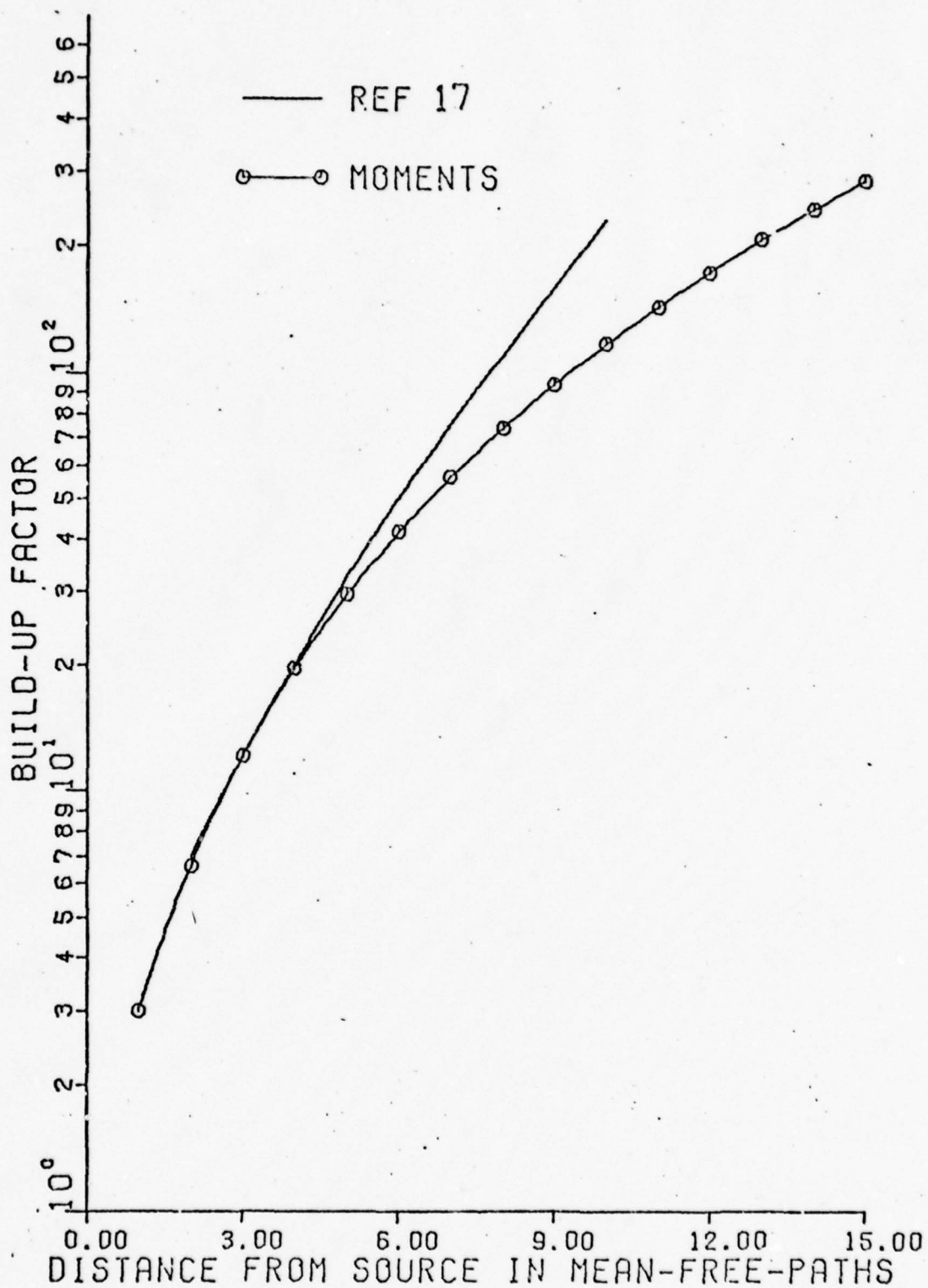


FIG. 118 COMPARISON OF ENERGY BUILD-UP FACTORS FOR 300 KEV

-27%. For 150 keV, the percent differences are from 5% to -9%. For 200 keV, the percent differences are from 1% to -63%. For 300 keV, the percent differences are from -2% to -96%. The differences go up as range increases in all cases except 150 keV. The absence of smooth curves in the range verses build-up factor semi-log graphs indicates sizable statistical variation in the build-up factors calculated by this Monte Carlo code. This can account for the large amount of disagreement at some ranges and energies.

Discrete Ordinates. Because of the limited amount of published results of discrete ordinates calculations, only one comparison of the moments method calculation to discrete ordinates will be presented. Dupree (Ref 18) used DTFXRAY to perform a limited calculation at 100 keV. Since energy fluence was obtained for only three distances, a table of results along with the results of the moments method and the percent differences are presented as Table II. The results are in great disparity. The erratic agreement is due to either the limited and truncated discrete ordinates calculation, which was a  $P_3S_8$  or opposite maximum error in the discrete ordinates and moments method.

Bigelow. Because the program used by Bigelow was the same one that was used for this study, comparison would not be in order. But using the same input, the exact results were obtained, showing that the program was working as programmed and any error calculations performed by Bigelow are applicable to this study. When recent cross sections for energy range from 1 keV to 100 keV were used, deviation in results occurred at small energies.

Table II

Comparison of Energy Build-up Factors for 100 keV

Mean-free-paths	Discrete Ordinates	Moments Method	Percent Difference
2	4.80	9.12	47%
4	13.6	29.0	53%
10	97.6	205.	52%

## VI Conclusion

### Purpose and Scope

The purpose of this report is to provide a complete set of monoenergetic build-up factors which are used to simplify the x-ray air transport problem. To compute these build-up factors, a moments method program was used. The program PHOTDIS was chosen and run on a CDC 6600. The energies considered were from 14 keV to 1000 keV. The ranges considered were from one to 15 mean-free-paths.

### Results and Discussion

The results were presented in a set of graphs for each energy. The intrinsic accuracy of the program estimated by convergence analysis performed by Bigelow was found to be a maximum of 20%. Comparison to others found the results of the moments method calculation to be higher than some Monte Carlo calculations and lower than others. For 10 mean-free-paths, this is shown in Fig 119. To facilitate use of the data presented, selected energies are presented together in Figs 120 and 121.

### Recommendations and Summary

Because of the limited time and the nature of the program, experimentation with different number of moments and the number of polynomials used in the reconstruction could not be performed. It is recommended that any other extensive study that computes build-up factors using the moments method should vary the number of moments and reconstruction polynomials.

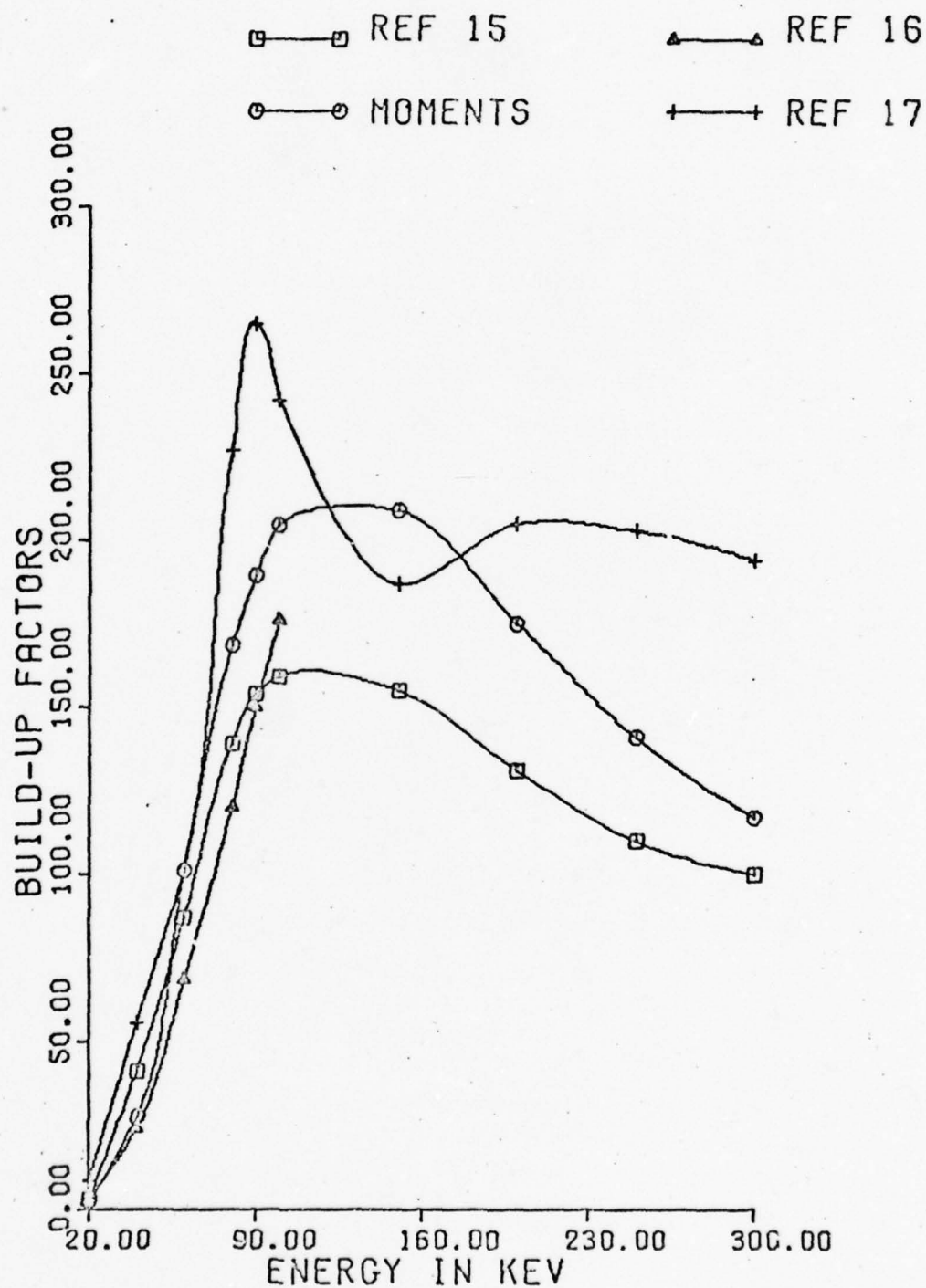


FIG. 119 COMPARISON OF ENERGY BUILD-UP FACTORS  
AT 10 MEAN-FREE-PATHS



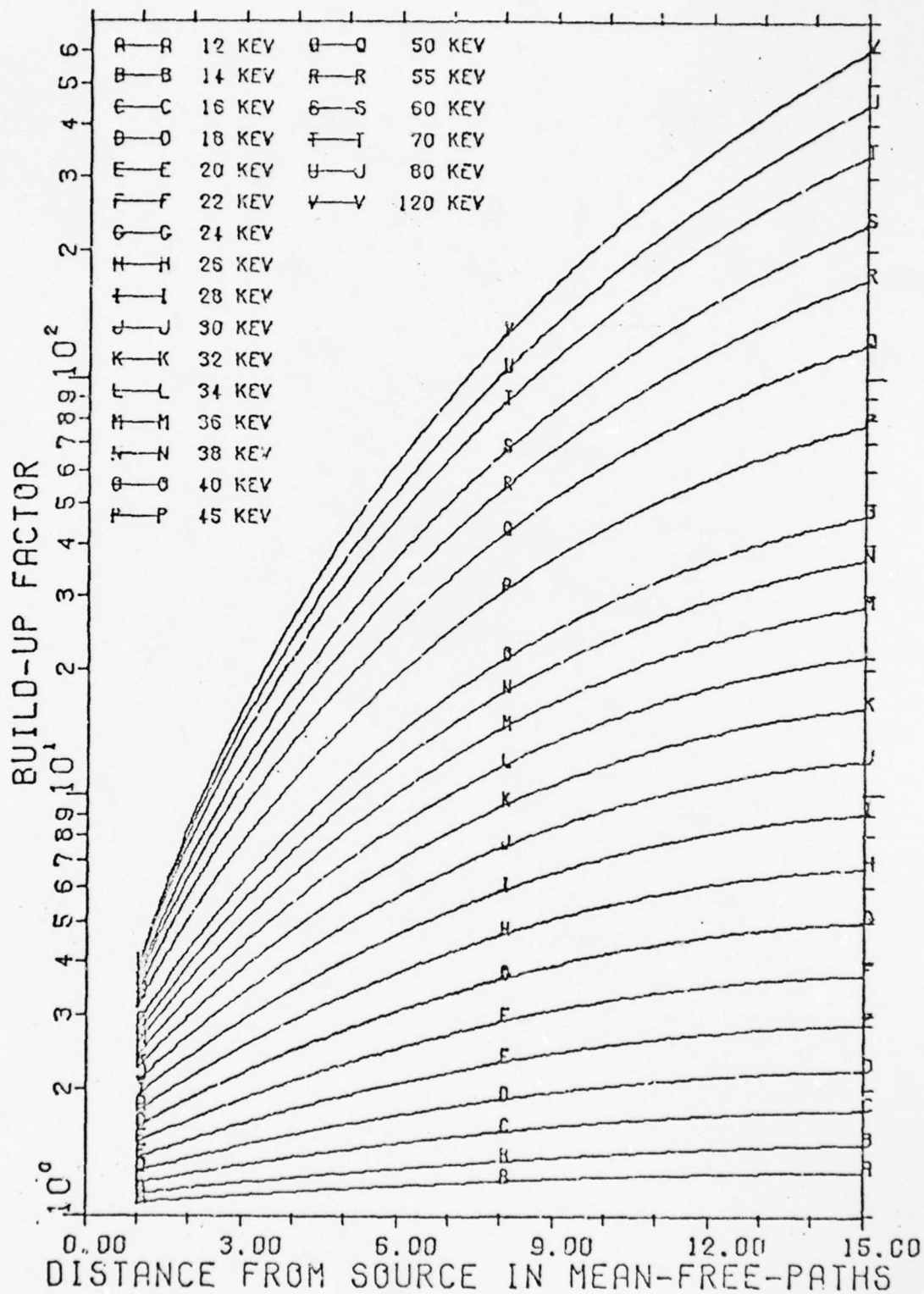


FIG. 120 ENERGY BUILD-UP FACTORS FOR  
12-120 KEV



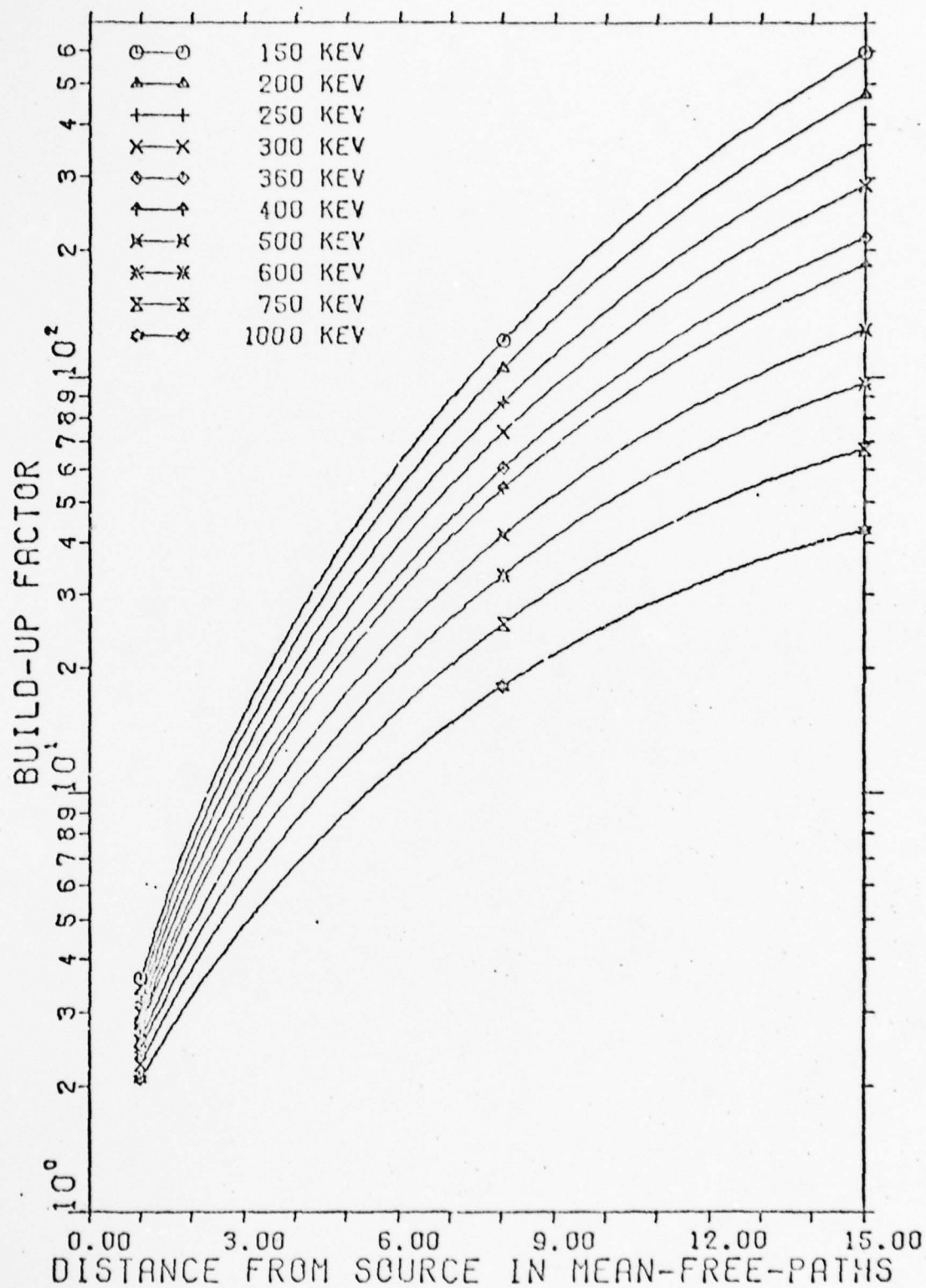


FIG. 121 ENERGY BUILD-UP FACTORS FOR  
150-1000 KEV

### Bibliography

1. Bigelow, Winfield S. Photon Transport from a Point Source in the Atmosphere. Thesis Number GNE/PH/68-3. Wright-Patterson AFB, Ohio, Air Force Institute of Technology, July 1968.
2. Shulstad, Raymond A. An Evaluation of Mass Integral Scaling as Applied to the Atmospheric Radiation Transport Problem. Report Number AFWL-TR-76-221. Kirkland AFB, N.M., Air Force Weapons Laboratory. Dec 1976.
3. Futterer, Arnold T. Atmospheric Transport of Radiation Including Abstracts of Selected Computer Codes. Report Number NDL-TR-119. Edgewood Arsenal, Md., U.S. Army Nuclear Defense Laboratory. Jan 1969.
4. Jordan, T.M. The MASTER Program File, Methods and Models. Report Number AFWL-TR-76-197. Santa Monica Calif., Experimental and Mathematical Physics Consultants. May 1977.
5. Woolson W., et al. DART - A Monte Carlo Code for Atmosphere Transport of X-ray and Gamma Rays. Report. La Jolla Calif., Science Applications Inc. Dec. 1974.
6. Sargis, D.A., et al. DART-II: A Monte Carlo Code for High Altitude Transport of Gamma Rays and X-rays. Report Number SAI-75-641-LJ. La Jolla Calif., Science Applications Inc. Jan. 1976.
7. X-ray Transport - IV (Monte Carlo Air Transport Code). Report Number KN-65-116(R). Colorado Springs, Colo., Kamen Nuclear. April 1965.
8. Straker, E.A. et al. The MORSE Code - a Multigroup Neutron and Gamma-Ray Monte Carlo Transport Code. Report Number ORNL-4585. Oak Ridge, Tenn., Oak Ridge National Laboratory. Sept 1970.
9. Sargis, D.A., et al. HAM, a Version of the MORSE Code for High Altitude Transport. Report Number SAI-74-646-LJ. La Jolla Calif., Science Applications Inc. May 1975.
10. Zerby, C.D., et al. PHOTRAN - a General Purpose Photon Transport Program in Complex Geometry, Volume I. Report Number AFWL-TR-65-171, Vol I. Tarrytown N.Y., Union Carbide Research Institute. March 1965.
11. Zerby, C.D., et al. PHOTRAN - a General Purpose Photon Transport Program in Complex Geometry, Volume II. Report Number AFWL-TR-65-171, Vol II. Tarrytown N.Y., Union Carbide Research Institute. March 1965.
12. Ladd, D.E., et al. PHOTRAN - a General Purpose Photon Transport Program in Complex Geometry, Volume IV. Report Number AFWL-TR-65-171, Vol IV. White Plains N.Y., Union Carbide Corporation. Jan. 1968.
13. McMaster, W.H., et al. Compilation of X-ray Cross Sections. Report Number UCRL-50174, Sec II, Rev. 1. Livermore Calif., Lawrence Radiation Laboratory of the University of California.
14. Marotta, C.R. Updated Master Library Tape for PHOTRAN. Report Number AFWL-TR-67-11. Tarrytown N.Y., Union Carbide Corporation Space Science and Engineering Laboratory. May 1967.
15. Banks, Morman E. and Wayne A. Coleman. Transport of Photons Through Air Using Source-Energy Band Structure from 300 keV to 2 keV. Report Number BRL-1557. Aberdeen Proving Ground Md., Ballistic Research Laboratory. April 1972.

16. Krumbein, A.D. et al. "Buildup Factors for Point Monoenergetic Low Energy Photon Sources in Air". Transaction of the American Nuclear Society. 9:342 (1966).
17. Shelton, Frank H. and Jonnie R. Kieth. Time Dependent X-ray Air Transport (U). Report Number KN-717-68-4. Colorado Springs, Colo., Kamen Nuclear. May 1968. (S/RD)
18. Dupree, S.A. and H.A. Sandmeier. Photon Transport Calculations Using the Method of Discrete Ordinates Volume I. Theoretical Considerations. Report Number NWEF 1035. Albuquerque, N.M., Navel Weapons Evaluation Facility. May 1969
19. Taylor, J.J. Application of Gamma Ray Build-up Data to Shield Design. Report Number WAPD-RM-217. Westinghouse Electric Corporation, Atomic Power Division. Jan 1954.

## APPENDIX A

### Solution of the Boltzmann Transport Equation by the Moments Method

#### Reduction of the Boltzmann Transport Equation

From Eq (5), the Boltzmann Transport Equation integrated over all time for spherical coordinates can be extracted:

$$\frac{\partial F(r, E, \mu)}{\partial r} + \frac{1-\mu^2}{r} \frac{\partial F(r, E, \mu)}{\partial \mu} + \mu^t F(r, E, \mu) = \iint F(r, E, \mu') \mu^s(\mu_0; E' \rightarrow E) dE' d\mu' + S(r, E, \mu) \quad (11)$$

where

$\mu$  is the cosine of the angle  $\theta$  in spherical coordinates.

Since the virgin fluence can be calculated without resort to computers by Eq (1), the fluence in Eq (11) is the scattered fluence.

To expand the functions in Eq (11), a set of polynomials is needed. Legendre polynomials conform to the requirements for expansion polynomials. These polynomials have the following properties:

$$\int_{-1}^{+1} P_n(x) P_m(x) dx = \frac{2n+1}{4\pi} \delta_{mn} \quad (12)$$

$$f(x) = \sum_{n=0}^{\infty} f_n P_n(x) \frac{2n+1}{4\pi} \quad (13)$$

$$f_n = \int_{-1}^{+1} f(x) P_n(x) dx \quad (14)$$

Therefore, the expansion of the fluence  $F$ , the Scatter cross section  $\mu^s$ , and the source  $S$  in Legendre polynomials is

$$F(r, E, \mu) = \sum_{n=0}^{\infty} \frac{2n+1}{4\pi} F_n(r, E) P_n(\mu) \quad (15)$$

$$\mu^s(\mu_0; E' \rightarrow E) = \sum_{m=0}^{\infty} \frac{2m+1}{4\pi} s_m(E' \rightarrow E) P_m(\mu_0) \quad (16)$$



$$S(r, E, \mu) = \sum_{m=0}^{\infty} \frac{2m+1}{4\pi} S_m(r, E) P_m(\mu) \quad (17)$$

Substituting Eqs (15), (16) and (17) into Eq (11) yields

$$\begin{aligned} \sum_{n=0}^{\infty} \frac{\partial F_n(r, E)}{\partial r} P_n(\mu) \frac{2n+1}{4\pi} + \sum_{n=0}^{\infty} \frac{1-\mu^2}{r} \frac{\partial P_n(\mu)}{\partial \mu} F_n(r, E) \frac{2n+1}{4\pi} \\ + \sum_{n=0}^{\infty} \mu^t F_n(r, E) P_n(\mu) \frac{2n+1}{4\pi} = \sum_{n=0}^{\infty} S_n(r, E) P_n(\mu) \frac{2n+1}{4\pi} \end{aligned} \quad (18)$$

$$+ \iint \left( \sum_{n=0}^{\infty} F_n(r, E') P_n(\mu') \frac{2n+1}{4\pi} \right) \left( \sum_{m=0}^{\infty} \mu_m^s(E' \rightarrow E) P_m(\mu_0) \frac{2m+1}{4\pi} \right) d\mu' dE'$$

By rearranging the scattering integral (the second term on the right side), it becomes:

$$\int \left[ \left( \sum_{n=0}^{\infty} F_n(r, E') \frac{2n+1}{4\pi} \right) \left( \sum_{m=0}^{\infty} \mu_m^t(E' \rightarrow E) \frac{2m+1}{4\pi} \right) \int_0^2 \int_{-1}^{+1} P_n(\mu') P_m(\mu_0) d\mu' d\phi' \right] dE'$$

By using the addition theorem on the double integral above, the integral becomes

$$\int_0^{2\pi} \int_{-1}^{+1} \left\{ P_m(\mu) P_m(\mu') + 2 \sum_{k=1}^m \frac{(m-k)!}{(m+k)!} P_m^k(\mu) P_m^k(\mu') \cos[k(\phi - \phi')] \right\} P_n(\mu') d\mu' d\phi'$$

Upon performing the integrals

$$\frac{4\pi}{2n+1} P_m(\mu) \delta_{mn}$$

So the scattering integral in Eq (18) becomes

$$\int_0^E \left[ \left( \sum_{n=0}^{\infty} F_n(r, E) \frac{2n+1}{4\pi} \right) \left( \sum_{m=0}^{\infty} \mu_m^t(E' \rightarrow E) \frac{2m+1}{4\pi} \right) \frac{4\pi}{2n+1} P_m(\mu) \delta_{mn} \right] dE'$$

which equals

$$\int_0^E \sum_{n=0}^{\infty} F_n(r, E) \frac{2n+1}{4\pi} \mu_n^t(E' \rightarrow E) P_n(\mu) dE'$$

Putting the last term into Eq (18), the full equation becomes



$$\begin{aligned} & \sum_{n=0}^{\infty} \frac{\partial F_n(r, E)}{\partial r} P_n(\mu) \frac{2n+1}{4\pi} + \sum_{n=0}^{\infty} \frac{1-\mu^2}{r} \frac{\partial P_n(\mu)}{\partial \mu} F_n(r, E) \frac{2n+1}{4\pi} \\ & + \sum_{n=0}^{\infty} \mu^n F_n(r, E) P_n(\mu) \frac{2n+1}{4\pi} = \int_0^E \sum_{n=0}^{\infty} F_n(r, E') \mu^n S_n(E' \rightarrow E) \frac{2n+1}{4\pi} P_n(\mu) dE' \quad (19) \\ & + \sum_{n=0}^{\infty} \frac{2n+1}{4\pi} S_n(E) \delta(r) P_n(\mu) \end{aligned}$$

By multiplying each term of Eq (19) by  $2\pi P_\ell(\mu) d\mu$  and integrating each term from -1 to +1, the following equation is obtained:

$$\begin{aligned} & \sum_{n=0}^{\infty} \frac{2n+1}{2} \frac{\partial F_n(r, E)}{\partial r} \int_{-1}^{+1} P_n(\mu) P_\ell(\mu) d\mu \\ & + \sum_{n=0}^{\infty} \frac{2n+1}{2r} F_n(r, E) \int_{-1}^{+1} (1-\mu^2) \frac{\partial P_n(\mu)}{\partial \mu} P_\ell(\mu) d\mu + \mu^n F_\ell(r, E) = S_\ell(E) \delta(r) \quad (20) \\ & + \int_0^E F_\ell(r, E') \mu^n S_\ell(E' \rightarrow E) dE' \end{aligned}$$

To simplify Eq (20), the recursion relations for Legendre polynomials must be employed:

$$P_m(\mu) = \frac{1}{2m+1} \left[ (m+1)P_{m+1}(\mu) + mP_{m-1}(\mu) \right] \quad (21)$$

$$(1-\mu^2) \frac{\partial P_m(\mu)}{\partial \mu} = m \left\{ P_{m-1}(\mu) - \frac{1}{2m+1} \left[ (m+1)P_{m+1}(\mu) + mP_{m-1}(\mu) \right] \right\} \quad (22)$$

By substituting Eq (21) into the first term of Eq (20) and by substituting Eq (22) into the second term of Eq (20) and performing the integration, the final  $P_\ell$  equation is obtained:

$$\begin{aligned} & \frac{\ell+1}{2\ell+1} \frac{\partial F_{\ell+1}(r, E)}{\partial r} + \frac{\ell}{2\ell+1} \frac{\partial F_{\ell-1}(r, E)}{\partial r} + \frac{(\ell+1)(\ell+2)}{2\ell+1} \frac{F_{\ell+1}(r, E)}{r} \\ & - \frac{\ell(\ell-1)}{2\ell+1} \frac{F_{\ell-1}(r, E)}{r} + \mu^n F_\ell(r, E) = S_\ell(E) \delta(r) + \int_0^E F_\ell(r, E') \mu^n S_\ell(E' \rightarrow E) dE' \quad (23) \end{aligned}$$

It is necessary to introduce the definition of the moments of a function f:

$$M_n = \int_0^\infty r^n f(r) 4\pi r^2 dr \quad (24)$$

where  $M_n$  is the  $n$ th moment of the function  $f$ . To obtain the moments of the fluence in Eq (23), it is essential to multiply each term in Eq (23) by  $r^n 4\pi r^2 dr$  and integrate from zero to infinity:

$$\begin{aligned} & \frac{\ell+1}{2\ell+1} \int_0^\infty r^n \frac{\partial F_{\ell+1}(r,E)}{\partial r} 4\pi r^2 dr + \frac{\ell}{2\ell+1} \int_0^\infty r^n \frac{\partial F_{\ell-1}(r,E)}{\partial r} 4\pi r^2 dr \\ & + \frac{(\ell+1)(\ell+2)}{2\ell+1} \int_0^\infty r^n \frac{F_{\ell+1}(r,E)}{r} 4\pi r^2 dr - \frac{(\ell-1)\ell}{2\ell+1} \int_0^\infty r^n \frac{F_{\ell-1}(r,E)}{r} 4\pi r^2 dr \quad (25) \\ & + \mu_\ell^t \int_0^\infty r^n F_\ell(r,E) 4\pi r^2 dr = \int_0^E \int_0^\infty r^n \mu_{S_\ell}^t F_\ell(r,E) 4\pi r^2 dr dE + \int_0^\infty r^n S_\ell(E) \delta(r) 4\pi r^2 dr \end{aligned}$$

Using the moments definition, Eq (24), the following equation is extracted:

$$\begin{aligned} & \frac{\ell+1}{2\ell+1} \int_0^\infty r^n \frac{\partial F_{\ell+1}(r,E)}{\partial r} 4\pi r^2 dr + \frac{\ell}{2\ell+1} \int_0^\infty r^n \frac{\partial F_{\ell-1}(r,E)}{\partial r} 4\pi r^2 dr \\ & + \frac{(\ell+1)(\ell+2)}{2\ell+1} M_{\ell+1,n-1} - \frac{(\ell+1)\ell}{2\ell+1} M_{\ell-1,n-1} + \mu_\ell^t M_{\ell n} = S_\ell(E) + \int_0^E M_{\ell n} \mu_{S_\ell}^t dE \quad (26) \end{aligned}$$

where  $M_{\ell n}$  is the  $n$ th moment of the  $\ell$ th expansion coefficient. By applying integration by parts to the first two terms of Eq (26), they become

$$- \frac{\ell+1}{2\ell+1} (n+2) M_{\ell+1,n-1} - \frac{\ell}{2\ell+1} (n+2) M_{\ell-1,n-1}$$

So the full moments equation is

$$\begin{aligned} & \left[ -\frac{\ell+1}{2\ell+1} (n+2) + \frac{(\ell+1)(\ell+2)}{2\ell+1} \right] M_{\ell+1,n-1} + \left[ \frac{-\ell}{2\ell+1} (n+2) - \frac{(\ell+1)\ell}{2\ell+1} \right] M_{\ell-1,n-1} \\ & + \mu_\ell^t M_{\ell n} = S_\ell(E) + \int_0^E M_{\ell n} \mu_{S_\ell}^t dE \quad (27) \end{aligned}$$

Rearranging and combining terms, the recursion equation for the moments is

$$\mu_\ell^t M_{\ell n} = \int_0^E \mu_{S_\ell}^t M_{\ell n} dE + S_\ell(E) + \frac{\ell^2 + 4\ell + 1 - n}{2\ell+1} M_{\ell+1,n-1} + \frac{\ell^2 + 2\ell - 2 - n}{2\ell+1} M_{\ell-1,n-1} \quad (28)$$

The integral is evaluated by numerical quadrature. With Eq (28), all the moments can be calculated. But only moments where  $\ell-n$  is even or  $\ell-n$  is odd are related. Also moments where  $\ell-n$  are negative have no physical significance.

### Reconstruction of the Fluence

Even though Eq (28) is for the scattered contribution to the fluence, the once scattered fluence can also be calculated directly using (Ref 1:12)

$$F^1(r, E, \mu) = \frac{S_T u(l - \cos \alpha) u^S(E_0 \rightarrow E)}{8\pi^2 r (\sin \alpha) (\sin \theta)} \left\{ \exp \left[ -r \left( \mu^t(E_0) \frac{\sin \theta}{\sin \alpha} + \mu^t(E) \frac{\sin(\alpha - \theta)}{\sin \alpha} \right) \right] \right\} \quad (29)$$

where

$F^1$  is the once scattered fluence

$$\alpha = \cos^{-1} \left[ 1 + (m_0 c^2 / E_0) - (m_0 c^2 / E) \right]$$

$u(x)$  is the unit step function =  $\begin{cases} 0 & \text{for } x < 0 \\ 1 & \text{for } x > 0 \end{cases}$

$E_0$  is the source energy

$S_T$  is the total source strength

$m_0$  is the mass of an electron

Therefore, all that is needed to find the total fluence is the multiscattered fluence. This fluence can be calculated from the multiscattered moments given by

$$M_{ln}^m = M_{ln} - M_{ln}^1 \quad (30)$$

where

$M_{ln}^m$  is the multiscattered moments

$M_{ln}^1$  is the once scattered moment calculated from the once scattered fluence

To find the multiscattered fluence from its moments, a moments reconstruction must be performed. The first step is to define the expansion function of the moments,  $G$ , which is

$$G_{ln} = S_l(E) \sum_{j=0}^N (-1)^j \frac{(2+j+l)! n!}{(2j+2l)! (n-j)! j!} M_{l, l+2j}^m \quad (31)$$

Using the available moments, the expansion function's values can be used to calculate the expansion coefficients,  $F_l^m(r, E)$  for the multiscattered fluence:

$$F_{\ell}^m(r, E) = \frac{y^{\ell} e^{-y}}{4\pi r^2} \sum_{n=0}^N G_{\ell n} W_n(y) \quad (32)$$

where

$$W_{n+1}^{\ell} = \frac{1}{2(n+1)} \left[ (2n + 2\ell + 1 - y) W_n^{\ell} + y \frac{dW_n^{\ell}}{dy} \right] \quad (33)$$

and  $W_0^{\ell} = 1$ . It should be noted that in Eq (31), only the moments where  $\ell-n$  are positive and even are needed to calculate the expansion function.

The multiscattered fluence is

$$F_{\ell}^m(r, E, \mu) = \sum_{l=0}^L \frac{2\ell+1}{4\pi} F_{\ell}^m(r, E) P_{\ell}(\mu) \quad (34)$$

So the total fluence is

$$F(r, E, \mu) = F^0(r, E, \mu) + F^1(r, E, \mu) + F^m(r, E, \mu) \quad (35)$$

where  $F^0(r, E, \mu)$  is the virgin fluence calculated from Eq (1),  $F^1(r, E, \mu)$  calculated from Eq (29) and  $F^m(r, E, \mu)$  calculated from Eq (34). The build-up factor is given by the following equation:

$$B = \frac{F(r, E, \mu)}{F^0(r, E, \mu)} \quad (36)$$



## APPENDIX B

### Sample Input and Program Listing

#### Sample Input

The sample input listed on pages 151-154 is the input used in this study. This listing is the data input into unit 5. Unit 4 inputs the number of energies to run, the energies and the ranges in mean-free-paths.

#### Program Listing

The program listed on pages 155-177 is the version of PHOTDIS used in this study. This program is exactly the same as the program used by Bigelow (Ref 1) except for format of input and output. Output is on units 2,3, and 6. Unit 2 is output for input of a plotting program used to generate the plots on pages 16-120. Units 3 and 6 are printed output. Much intermediate output is eliminated for this study, since fluence, moments and convergence analysis are not desired. This program, run on a CDC 6600 takes 48 central processor seconds and 260 input-output seconds per energy using five space points.



NITROGEN 7. 2. 0.7808400E 00

0.1000000E-30	0.7000000E 01
0.5540000E 00	0.5200000E 01
0.1330000E 01	0.3300000E 01
0.1300000E 01	0.1300000E 01
0.2550000E 01	0.1700000E 01
0.3310000E 01	0.1800000E 01
0.3380000E 01	0.1200000E 01
0.4320000E 01	0.1000000E 01
0.5310000E 01	0.0000000E 00
0.5370000E 01	0.0000000E 00
0.6540000E 01	0.3000000E 00
0.7300000E 01	0.3000000E 00
0.1231000E 02	0.2700000E 00
0.2000000E 02	0.1000000E-01
0.7000000E 02	-0.0000000E 00
0.1000000E 03	-0.0000000E 00
0.1000000E 32	-0.0000000E 00
1.000	7.89500E 04 2.12400E-01
1.500	2.60900E 04 5.15700E-01
2.000	1.14700E 04 2.12800E-01
3.000	3.44300E 03 1.38100E 00
4.000	1.43000E 04 1.85400E 00
6.000	4.00700E 02 2.68700E 00
8.000	1.59400E 02 2.85600E 00
10.000	7.73100E 01 3.09500E 00
15.000	2.04500E 01 3.15400E 00
20.000	7.89900E 00 3.85100E 00
30.000	2.05600E 00 3.20200E 00
40.000	7.91700E-01 3.21100E 00
60.000	2.07500E-01 3.19900E 00
80.000	8.10200E-02 3.14900E 00
100.000	3.93300E-02 3.40200E 00
150.000	1.08000E-02 3.06300E 00
200.000	4.40000E-03 2.83300E 00
300.000	1.28500E-03 2.46600E 00
400.000	5.51900E-04 2.21300E 00
500.000	2.91700E-04 2.02200E 00
600.000	1.75500E-04 1.87100E 00
800.000	8.07300E-05 1.64400E 00
1000.000	4.52300E-05 1.47800E 00
0.14998E 04	0.25000E-04 0.12008E 01
0.15000E 04	0.25000E-04 0.12008E 01
0.20000E 04	0.15000E-04 0.10238E 01
0.30000E 04	0.56000E-05 0.10463E 00
0.40000E 04	0.35000E-05 0.67064E 00
0.50000E 04	0.23000E-05 0.17875E 00
0.60000E 04	0.23000E-05 0.11121E 00
0.80000E 04	0.15000E-05 0.11767E 00
0.10000E 05	0.12500E-05 0.35532E 00
0.15000E 05	0.80000E-05 0.26225E 00
0.20000E 05	0.55000E-05 0.20995E 00
0.30000E 05	0.10000E-05 0.15211E 00

0.40000E 05	0.10000E-30	0.12033E 00
0.50000E 05	0.10000E-30	0.10002E 00
0.60000E 05	0.10000E-30	0.85831E-01
0.80000E 05	0.10000E-30	0.07192E-01
0.10000E 03	0.10000E-30	0.15404E-01
OXYGEN	8. 2.	0.2094760E 00
0.1000000E-30	0.9000000E 01	
0.6540000E 00	0.6400000E 01	
0.1330000E 01	0.3900000E 01	
0.1930000E 01	0.2400000E 01	
0.2630000E 01	0.2000000E 01	
0.3310000E 01	0.1500000E 01	
0.3830000E 01	0.1000000E 01	
0.4540000E 01	0.1300000E 01	
0.5310000E 01	0.1200000E 01	
0.5970000E 01	0.1100000E 01	
0.6640000E 01	0.9000000E 00	
0.7300000E 01	0.8000000E 00	
0.1251000E 02	0.5000000E-01	
0.2000000E 02	-0.0000000E 00	
0.7000000E 02	-0.0000000E 00	
0.1000000E 03	-0.0000000E 00	
0.1000000E 32	-0.0000000E 00	
1.000	1.22100E 05	1.17300E-01
1.500	4.15700E 04	3.61700E-01
2.000	1.67300E 04	6.30400E-01
3.000	5.73500E 03	1.22000E 00
4.000	2.45100E 03	1.77000E 00
5.000	1.24000E 03	2.17100E 00
6.000	7.06500E 02	2.54000E 00
8.000	2.85100E 02	3.06300E 00
10.000	1.40000E 02	3.35400E 00
15.000	3.79200E 01	3.84400E 00
20.000	1.43100E 01	4.08000E 00
30.000	3.92100E 00	4.27800E 00
40.000	1.52500E 00	4.30900E 00
50.000	7.35000E-01	4.27100E 00
60.000	4.05400E-01	4.20300E 00
80.000	1.59500E-01	4.04200E 00
100.000	7.76200E-02	3.87800E 00
150.000	2.15300E-02	3.51900E 00
200.000	8.80700E-03	3.23500E 00
300.000	2.56000E-03	2.62000E 00
400.000	1.10200E-03	2.52900E 00
500.000	5.85900E-04	2.31000E 00
600.000	3.52200E-04	2.13800E 00
800.000	1.51500E-04	1.87800E 00
1000.000	9.02500E-05	1.08900E 00
0.15000E 04	0.45000E-04	0.13721E 01
0.20000E 04	0.22000E-04	0.11701E 01
0.30000E 04	0.12500E-04	0.91959E 00
0.40000E 04	0.85000E-05	0.76644E 00
0.50000E 04	0.52000E-05	0.66143E 00

0.60000E 04	0.43000E-05	0.18424E 00
0.60000E 04	0.32000E-05	0.17734E 00
0.10000E 05	0.23000E-05	0.16607E 00
0.15000E 05	0.13000E-05	0.29972E 00
0.20000E 05	0.20000E-06	0.23994E 00
0.30000E 05	0.10000E-30	0.17384E 00
0.40000E 05	0.10000E-30	0.13752E 00
0.50000E 05	0.10000E-30	0.11431E 00
0.60000E 05	0.10000E-30	0.98095E-01
0.80000E 05	0.10000E-30	0.76731E-01
ARGON	19.	1. 0.9340000E-02
0.1000000E-30	0.1900000E 02	
0.6640000E 00	0.1121000E 02	
0.1330000E 01	0.1030000E 02	
0.1900000E 01	0.3200000E 01	
0.2650000E 01	0.6900000E 01	
0.3310000E 01	0.5300000E 01	
0.3900000E 01	0.4800000E 01	
0.4640000E 01	0.4000000E 01	
0.5310000E 01	0.3400000E 01	
0.5970000E 01	0.2300000E 01	
0.6640000E 01	0.2400000E 01	
0.7300000E 01	0.2200000E 01	
0.1201000E 02	0.1370000E 01	
0.2000000E 02	0.8000000E 00	
0.7000000E 02	-0.0000000E 00	
0.1000000E 03	-0.0000000E 00	
0.1000000E 32	-0.0000000E 00	
1.000	2.13000E 05	4.81700E-01
1.500	7.43400E 04	9.33500E-01
2.000	3.40500E 04	1.45500E 00
3.000	1.11000E 04	2.45300E 00
3.201	9.25700E 03	2.02700E 00
3.202	9.16500E 04	2.02700E 00
4.000	5.22300E 04	3.32200E 00
5.000	2.30900E 04	4.03900E 00
6.000	7.97200E 03	5.11100E 00
10.000	4.20300E 03	6.18200E 00
15.000	1.27000E 03	7.35200E 00
20.000	5.31300E 02	8.07000E 00
30.000	1.52200E 02	8.74800E 00
40.000	5.20500E 01	8.98600E 00
50.000	3.08400E 01	9.04000E 00
60.000	1.74100E 01	8.99900E 00
80.000	7.07300E 00	8.78000E 00
100.000	3.52300E 00	8.10000E 00
150.000	1.01200E 00	7.80300E 00
200.000	4.23900E-01	7.20800E 00
300.000	1.28300E-01	6.31100E 00
400.000	5.64400E-02	5.67100E 00
500.000	3.04200E-02	5.18600E 00
600.000	1.90000E-02	4.85700E 00
800.000	8.80000E-03	4.22200E 00
1000.000	5.04000E-03	3.79700E 00

0.12000E 04	0.27700E-02	0.30853E 01
0.20000E 04	0.17500E-02	0.26317E 01
0.30000E 04	0.95500E-03	0.20683E 01
0.40000E 04	0.67200E-03	0.17242E 01
0.50000E 04	0.49500E-03	0.14882E 01
0.60000E 04	0.39500E-03	0.13145E 01
0.80000E 04	0.28100E-03	0.10740E 01
0.80000E 04	0.28100E-03	0.10740E 01
0.90000E 04	0.26100E-03	0.10740E 01
0.90000E 04	0.23100E-03	0.10740E 01
0.90000E 04	0.23100E-03	0.10740E 01
0.90000E 04	0.23100E-03	0.10740E 01
0.90000E 04	0.23100E-03	0.10740E 01
0.90000E 04	0.23100E-03	0.10740E 01
2		
0.00000E 00		
0.25471E 20		
0.20032E 03		
3 40 1		
5 21 1		
6 5 19		
0.3000000E 24		
0.0050 41 91 115 5 81 111 331		
1 21 31 41 51 331		
1.00 0.99 0.98 0.97 0.94 0.92 0.90 0.88 0.85 0.82 0.80		
0.79 0.59 0.40 0.00 -0.20 -0.40 -0.60 -0.80 -1.00		



```
PROGRAM PHOTDIS( INPUT, OUTPUT, TAPE5, TAPE6, TAPE8, TAPE3, TAPE4, TAPE3,
1TAPE2)
```

```
$$$$$$$$$ SUBROUTINES USED BY THIS PROGRAM $$$$$$$$$$
```

```
SIG.....CALCULATES TOTAL MACROSCOPIC CROSS SECTION
AKERN.....CALCULATES DIFFERENTIAL SCATTERING CROSS SECTION
              (SCATTERING KERNEL)
POLKER.....CALCULATES PRODUCT OF LEGENDRE POLYNOMIAL AND SCAT-
              TERING KERNEL
ONCE .....EVALUATES PART OF THE ONE-SCATTER FORMULA, EQ (21)
WXPAN.....USES RECURSION RELATION TO CALCULATE COEFFICIENTS FOR
              THE EXPANSION POLYNOMIALS ( EQ (54) )
BATA.....CALCULATES EXPANSION COEFFICIENT OF EQ (27)
FIRST.....CALCULATES ANGULAR DISTRIBUTION OF ONCE-SCATTERED PHO-
              TONS, ALSO ALL-ANGLE FIRST SCATTER, AND FIRST SCATTER
              ENERGY DENSITY
SPACE.....INTERLINKAGE OF THE MOMENTS
INC.....CONTROLS INDEXING OF ARRAY
TORIAL.....CALCULATES FACTORIALS
```

```
COMMON PHOT(3,40), ENERG(3,40), INCO(3,40), ETA(3,17), CAPK(3,17), DN(3
1), DN7(3), NXS, NEL, TOLE, TCLK, PIE, RZERO, LMAX, XMUMU, XMULAM, TEMP, YIY, DM
2U, SIGMAG, SINHL, SIGO, ONE, XLNCK, L, N, LP, NP, XLANG, BETA, JZERO,
3NTRANS, NHU, XLAMO, GARB, NYP, NCUT, FACTOR, 3SCAT(10,19),
5SIGMAT(331), LAMBDA(331), ONESC(5,33,21), ALANG1(5,33), ALENG(5), XMU(
621), Y(5), PHU(2,21), VIRGIN(5), ALENG4(5), A(10,19)
```

```
DIMENSION APRAY(10,19,25), DELTAB(10,19), ONEP(5,33,21), SUMN(10,5,33
1), PC(10), PO(10), PLNK(10), PLNKM1(10), PLNKM2(10), PLNKM3(10), Z(3), NAT
30MS(3), HORD(3,2), HC(9), D(9), BONE(10,19), INTEG(10,19), BS(10,19), BSM
41(10,19), BS42(10,19), BSM3(10,19), BONEP(10,19), NSUMND(
510), IC04(16)
```

```
REAL LAMBDA, INCO, NATOMS, INTEG
INTEGER G, G1, G2
```

```
DATA CLITE/2.997925E10/, FORPIE/12.56637/
```

```
RECURSION RELATION FOR LEGENDRE POLYNOMIALS
```

```
ALEGRC(X, ARG, POLY1, POLY0) = ((2.*X+1.) * ARG * POLY1 - X * POLY0) / (X+1.)
```

```
*****
```

```
READ(4,1007) J03C
WRITE(3,2013)
WRITE(6,2013)
DO 999 JOR=1, J03C
FACTOR=511.006
DO 996 NSTUF=1, 10
```



```

995 NSUMND(NSTUF)=1
    ALPHA=1.
    NPOINT=1
C
C INPUT CROSS SECTIONS FOR NITROGEN, OXYGEN AND ARGON. ETA AND
C CAPK ARE PARAMETERS USED TO DETERMINE THE BOUND-ELECTRON CORRECTIO
C TO THE KLEIN-NISHINA DIFFERENTIAL CROSS SECTION FORMULA
C
DO 180 I=1,3
  READ(5,1010)(WORD(I,J),J=1,2),Z(I),NATOMS(I),DN(I)
  READ(5,1000)(ETA(I,K),CAPK(I,K),K=1,17)
  READ(5,1002)(ENERG(I,K),PHOT(I,K),INCO(I,K),K=1,40)
180 CONTINUE
C
C IPASS=2 .....WAVELENGTH MESH PARAMETERS TO BE INPUT
C      =1 OTHERWISE
  READ(5,1007)IPASS
C ALTITUDE AND PARTICLE DENSITY
  READ(5,1005)ALT
  WRITE(3,1105)ALT
  READ(5,1005)DENSITY
C ENERGY ABOVE WHICH NO CORRECTION IS TO BE MADE TO THE KLEIN-
C NISHINA SCATTERING LAW
  READ(5,1005)ENKN
  XLNCK=FACTOR/ENKN+.0001
C JND=2 FOR PHASE II (RECONSTRUCTION) ONLY
C      =1 OTHERWISE
  READ(5,1001)NFL,NXS,JND
C NYP=1,5 ... NUMBER OF SPACE POINTS
C LEND=1 ...ANGULAR PHOTON DENSITY IS TO BE CALCULATED
C      =2 CALCULATE THE ALL-ANGLE DENSITY ONLY
  READ(5,1001)NYP,NHU,LEND
C NSTOP/2= NUMBER OF MOMENTS TO BE USED INITIALLY IN RECONSTRUCTION
C OF THE ALL-ANGLE DENSITY...NADD/2= NUMBER OF MOMENTS TO BE ADDED
C TO THE RECONSTRUCTION EACH TIME THROUGH UNTIL NMAX/2 IS REACHED...
  READ(5,1001)NSTOP,NADD,NMAX
C EZERO = SOURCE ENERGY ***** QZERO = SOURCE STRENGTH
  READ(5,1000)QZERO
  READ(4,1100)EZERO
  IF(EOF(4) .NE. 0.) GO TO 500
C
C *****
C
C $$$$ UNITS ... IN GENERAL, CGS UNITS...ENERGIES IN KEV
C
629 IND=1
    LPJ=1
    PIE=3.14159
    RZERO=7.9398E-26
    TOLE=.0001
    TOLK=.0001
181 LMAX=NMAX/2
183 LMAXP=LMAX+1
    NHAXP=NMAX+1

```

```

NSTOPP=NSTOP+1
DO 72 I=1,NEL
DN(I)=DENSTY*DN(*)*NATOMS(I)
DNZ(I)=DN(I)*Z(I)
DO 72 K=1,17
CAP=1.-CAPK(I,K)/Z(I)
IF(CAP)131,131,132
131 CAPK(I,K)=0.1E-30
GO TO 72
132 CAPK(I,K)=CAP
72 CONTINUE
XLAMO=FACTOR/EZERO
G=1

C
C DETERMINE THE WAVELENGTH MESH TO BE USED IN CALCULATION OF MOMENTS
C NTRANS .....STEP SIZE SHIFTS FROM .02 TO .04
C NDL ... SHIFT FROM .04 TO .08
C NDLP24 ... ALL MOMENTS REQUIRED FOR INTEGRATION CAN BE STORED IN
C ARRAY (MOMENTS FOR 25 VALUES OF THE WAVELENGTH)
C NCTOT ... 1*NUMBER OF INTEGRATION STEP SIZE CHANGES
C NCUT ... NUMBER OF MESH POINT AT THE FIRST SCATTER CUT OFF
C NOCUT ... NUMBER OF MESH POINT WHERE SECOND SCATTER CUTS OFF
C NBIGGP ... NUMBER OF POINTS IN THE WAVELENGTH MESH
C NC ... LOCATIONS OF STEP SIZE CHANGES
C
GO TO(403,791),IPASS
403 D(1)=.02
NC(1)=1
NC(2)=21
NTRANS=21
NC(3)=71
NC(4)=331
NCTOT=4
NDL=71
NDLP24=95
NCUT=61
NOCUT=91
NBIGGP=331
GO TO 404

C
C *****
C
791 READ(5,1012)D(1),NTRANS,NDL,NDLP24,NCTOT,NCUT,NOCUT,NBIGGP
READ(5,1011)(NC(I),I=1,NCTOT)

C
C *****
C
C SET WAVELENGTH VALUES FOR THE MESH AND CALCULATE CORRESPONDING
C TOTAL CROSS SECTIONS (CM**-1)
C
404 ID=1
NCC=NC(2)
DELTA=D(1)

```



NSKIP=1

C FIND WHETHER DISCONTINUITY AT FIRST SCATTER CUT OFF IS WITHIN THE  
C RANGE OF INTEGRATION AND LOCATE THE LOWER LIMIT OF THE INTEGRAL  
C

IF(MCTR .GE. NCUT) GO TO 300  
301 NGS=1  
IF(MCTR-NCUT) 305, 305, 303  
300 JUMP=2  
XLAMG2=LAMBDA(MCTR)-2.  
DO 304 NGS=NCUT, MCTR  
TEST=XLAMG2-LAMBDA(NGS)  
IF(ABS(TEST)-1.E-05) 305, 305, 610  
610 IF(TEST) 305, 305, 304  
304 CONTINUE  
303 NDISCO=2  
XLAMG2=LAMBDA(MCTR)-2.  
NGS=1  
IF(XLAMG2-XLAMO) 305, 305, 313  
313 DO 307 NGS=2, NCUT  
TEST=XLAMG2-LAMBDA(NGS)  
IF(ABS(TEST)-1.E-05) 305, 305, 312  
312 IF(TEST) 305, 305, 307  
307 CONTINUE  
305 LIMLOW=NGS  
GO TO 302  
306 LIMLOW=NGS-1  
302 NBKSP=NGS-LIMLOW

C  
C POSITION TAPE 9 TO READ IN MOMENTS ... LOOKING FOR THE MOMENTS  
C CORRESPONDING TO THE LOWER LIMIT OF THE INTEGRAL  
C

IF(NBKSP .GT. LIMLOW) GO TO 750  
751 DO 752 I=1, NBKSP  
752 BACKSPACE 9  
GO TO 753  
750 REWIND 9  
READ(9) NRIGGP, LMAXP, NMAXP  
753 READ(9) NSS, ((NS(LP, NP), LP=1, LMAXP), NP=1, NMAXP)  
IF(NSS .NE. LIMLOW) GO TO 753  
CALL POLKER(P0, XLAMO, XLG)  
IF(LIMLOW .NE. 1) GO TO 354  
DO 355 LP=1, LMAXP  
355 PLNK(LP)=P0(LP)  
GO TO 310  
354 CALL POLKER(PLNK, LAMBDA(LIMLOW), XLG)

C  
C FIND WHERE DELTA LAMBDA CHANGE IS THAT IS CLOSEST TO MCTR  
C  
310 DO 502 ID=1, NCTOT  
IF(MCTR-NC(ID)) 317, 317, 502  
502 CONTINUE



C SUBDIVIDE THE INTEGRAL SO THAT SEGMENTS ARE FORMED WHICH HAVE  
 C NO CHANGE IN STEP SIZE WITHIN THEM AND NO DISCONTINUITY  
 C LNDSEG IS THE MESH POINT AT THE END OF SUCH A SEGMENT  
 C

```

317 NCC=NC(ID-1)
    IF(NCC-1) 336, 336, 319
336 LNDSEG=MCTR
    GO TO 555
319 IF(LAMBDA(NGG-1)-LAMBDA(NCC)) 264, 261, 262
262 IF(LAMBDA(NGG-2)-LAMBDA(NCC)) 264, 263, 264
261 NSKIP=3
    LSEG=NCC-4
    ASSIGN 266 TO NSK
    GO TO 572
263 NSKIP=2
    LSEG=NCC-2
    ASSIGN 266 TO NSK
    GO TO 572
264 NSKIP=1
    ASSIGN 267 TO NSK
572 NPOINT=1
    J=1
    DO 562 ID=1, NCTOT
    IF(NC(ID)-LIMLOW) 562, 562, 563
562 CONTINUE
563 NCC=NC(ID)
    IF(MCTR-NCC) 571, 570, 570
571 NCC=MCTR
570 GO TO(550, 600, 600), NSKIP
600 IF(LSEG-NCC) 561, 560, 560
560 LNDSEG=NCC
    GO TO 564
561 LNDSEG=LSEG
564 GO TO(565, 567), NOTSCO
567 IF(NCUT-LNDSEG) 566, 566, 565
566 LNDSEG=NCUT
    NOTSCO=1
565 CONTINUE
    IF(LIMLOW-NCUT) 311, 314, 311
314 DO 315 LP=1, LMAXP
    DO 315 NP=1, NMAXP
315 BS(LP, NP)=BS(LP, NP)-DELTA8(LP, NP)
311 IF(LIMLOW-LSEG) 569, 568, 569
568 J=2
    NPOINT=4
    LNDSEG=MCTR
569 LIML=LIMLOW+J
    DELTA=LAMBDA(LIML)-LAMBDA(LIMLOW)
328 XLL=LAMBDA(LIMLOW)
    GO TO(339, 340), J
339 NPOINT=LNDSEG-LIMLOW+1
  
```

CALCULATE THE CONTRIBUTION TO INTEG FROM THIS SEGMENT



C  
C THIS CONTROL SECTION CONTROLS THE COURSE OF THE INTEGRATION OF THE  
C SEGMENT IT SETS UP THE PARTICULAR COMBINATION OF INTEGRATION  
C SCHEMES TO BE USED

340 IF(9-NPOINT)203,209,210  
210 GO TO(250,202,207,204,205,206,207,208),NPOINT  
202 ASSIGN 260 TO IST  
GO TO 222  
203 ASSIGN 260 TO IST  
GO TO 225  
204 ASSIGN 260 TO IST  
GO TO 228  
205 ASSIGN 204 TO IST  
GO TO 222  
206 ASSIGN 204 TO IST  
GO TO 225  
207 ASSIGN 204 TO IST  
GO TO 228  
208 ASSIGN 206 TO IST  
GO TO 225  
209 LLSIMP=NPOINT-3  
IF((NPOINT/2)\*2-NPOINT)211,212,212  
211 LSIMP=4  
GO TO 213  
212 LSIMP=7  
ASSIGN 213 TO IST  
GO TO 228  
213 ASSIGN 259 TO IST  
GO TO 228  
259 IF(LSIMP-LLSIMP)215,204,204  
215 ASSIGN 259 TO IST  
LSIMP=LSIMP+2  
GO TO 225

C  
C END OF THE CONTROL SECTION FOR A SPECIFIC SEGMENT  
C  
C THIS SECTION IS USED ONLY AFTER NDLP24 HAS BEEN REACHED  
C

761 DELTA=.08  
XLL=LAMBDA(NGG-25)  
ASSIGN 228 TO IST  
ASSIGN 781 TO ITRAP  
ASSIGN 764 TO IFOR  
CALL POLKER(PO,XLAMO,XLG)  
CALL POLKER(PLNK,XLL,XLG)  
DO 767 LP=1,LMAXP  
DO 767 NP=1,NMAXP  
767 9S(LP,NP)=ARRAY(LP,NP,G)

C  
C TRAPEZOIDAL RULE  
C

222 XLM1=XLL  
XLL=XLM1+DELTA

```

IF (ABS (XLL-XLG) -.00001) 217,218,218
217 LAST=2
218 DO 271 LP=1,LMAXP
    PLNKM1(LP)=PLNK(LP)
    DO 271 NP=1,NMAXP
271 BS(M1(LP,NP)=BS(LP,NP)
    CALL POLKER(PLNK,XLL,XLG)
    GO TO ITRAP, (781,783)
781 G=INC(G)
    DO 782 LP=1,LMAXP
    DO 782 NP=1,NMAXP
782 BS(LP,NP)=ARRAY(LP,NP,G)
    GO TO 250
783 GO TO(220,221), LAST
220 READ(9)NGEE,((BS(LP,NP),LP=1,LMAXP),NP=1,NMAXP)
    GO TO 250
221 DO 272 LP=1,LMAXP
C
C AVOID TRUNCATION AT UPPER LIMIT OF INTEGRAL
C (NOTICE THAT THIS DOES NOT APPLY WHEN THE KLEIN-NISHINA FORMULA IS
C BEING USED)
C
IF (XLG .GT. XLNCK) PLNK(LP)=PLNKM1(1)
DO 272 NP=1,NMAXP
272 BS(LP,NP)=0.
250 H=DELTA*XLG/2.
    DO 349 LP=1,LMAXP
    DO 349 NP=1,NMAXP
    IF (LP-NP) 350,351,349
350 LPNP=LP+NP
    IF ((LPNP/2)*2-LPNP) 349,351,351
351 INTEG(LP,NP)=INTEG(LP,NP)+H*(PLNKM1(LP)*BS(M1(LP,NP)/XLM1+PLNK(LP)*
1BS(LP,NP)/XLL)
349 CONTINUE
    GO TO IST, (204,206,213,259,260,228,342)
C
C SIMPSON'S RULE
C
225 XLM2=XLL
    XLM1=XLM2+DELTA
    XLL=XLM1+DELTA
    IF (ABS (XLL-XLG) -.00001) 542,543,543
542 LAST=2
543 DO 273 LP=1,LMAXP
    PLNKM2(LP)=PLNK(LP)
    DO 273 NP=1,NMAXP
273 BS(M2(LP,NP)=BS(LP,NP)
    READ(9)NGEE,((BS(M1(LP,NP),LP=1,LMAXP),NP=1,NMAXP)
    CALL POLKER(PLNK1,XLM1,XLG)
    CALL POLKER(PLNK,XLL,XLG)
    GO TO(223,224), LAST
223 READ(9)NGEE,((BS(LP,NP),LP=1,LMAXP),NP=1,NMAXP)
    GO TO 251

```

```

224 DO 274 LP=1,LMAXP
    IF(XLG .GT. XLNCK) PLNK(LP)=PLNKM1(1)
    DO 274 NP=1,NMAXP
274 BS(LP,NP)=0.
251 H=DELTA*XLG/3.
    DO 346 LP=1,LMAXP
    DO 346 NP=1,NMAXP
    IF(LP-NP) 347, 348, 346
347 LPNP=LP+NP
    IF((LPNP/2)*2-LP*P) 346, 348, 348
348 INTEG(LP,NP)=INTEG(LP,NP)*H*(PLNKM2(LP)*BSM2(LP,NP)/XLM2+4.*PLNKM1
1(LP)*BSM1(LP,NP)/XLM1+PLNK(LP)*BS(LP,NP)/XLL)
346 CONTINUE
    GO TO IST, (204,206,213,259,260,228,342)

C
C FOUR POINT RULE
C
228 XLM3=XLL
    XLM2=XLM3+DELTA
    XLM1=XLM2+DELTA
    XLL=XLM1+DELTA
    IF(ABS(XLL-XLG)-.00001) 544,545,545
544 LAST=2
545 DO 275 LP=1,LMAXP
    PLNKM3(LP)=PLNK(LP)
    DO 275 NP=1,NMAXP
275 BSM3(LP,NP)=BS(LP,NP)
    CALL POLKER(PLNKM2,XLM2,XLG)
    CALL POLKER(PLNKM1,XLM1,XLG)
    CALL POLKER(PLNK,XLL,XLG)
    GO TO IFOR, (764,269)
764 G=INC(G)
    G1=INC(G)
    G2=INC(G1)
    DO 768 LP=1,LMAXP
    DO 768 NP=1,NMAXP
    BSM2(LP,NP)=ARRAY(LP,NP,G)
    BSM1(LP,NP)=ARRAY(LP,NP,G1)
768 BS(LP,NP)=ARRAY(LP,NP,G2)
    G=G2
    IF(LAST .EQ. 2) ASSIGN 342 TO IST
    GO TO(252,227),LAST
269 READ(9)NGEE,((BSM2(LP,NP),LP=1,LMAXP),NP=1,NMAXP)
    GO TO(257,573),LAST
573 GO TO NSK,(266,257)
266 NSKIP=NSKIP-1
    ASSIGN 267 TO NSK
    GO TO 259
267 READ(9)NGEE,((BSM1(LP,NP),LP=1,LMAXP),NP=1,NMAXP)
    GO TO(258,574),LAST
574 GO TO(258,270),NSKIP
    NSKIP=NSKIP-1
    GO TO 257

```

```

268 GO TO(226,227),LAST
226 READ(9)NGEE,((BS(LP,NP),LP=1,LMAXP),NP=1,NMAXP)
GO TO 252
227 CONTINUE
DO 276 LP=1,LMAXP
IF(XLG.GT.XLNC<) PLNK(LP)=PLNKM1(1)
DO 276 NP=1,NMAXP
276 BS(LP,NP)=0.
252 H=DELTA*XLG*3./9.
DO 343 LP=1,LMAXP
DO 343 NP=1,NMAXP
IF(LP-NP)344,345,343
344 LPNP=LP+NP
IF((LPNP/2)*2-LPNP)343,345,345
345 INTEG(LP,NP)=INTEG(LP,NP)+H*(PLNKM3(LP)*BSM3(LP,NP)/XLM3+3.*PLNKM2
1(LP)*BSM2(LP,NP)/XLM2+3.*PLNKM1(LP)*BSM1(LP,NP)/XLM1+PLNK(LP)*BS(L
2P,NP)/XLL)
343 CONTINUE
GO TO IST, (204,206,213,259,260,228,342)
C
C IS THIS THE LAST SEGMENT IN THE INTEGRAL...
C
260 GO TO(341,342),LAST
342 MCTR=MCTR+1
H=H/XLG
GO TO 501
341 LIMLOW=LNDSEG
C
RETURN TO CALCULATE THE NEXT SEGMENT
C
GO TO 572
C
C CALCULATE MOMENTS IN THE DESIRED PORTION OF THE L,N PLANE
C
501 LL=0
NN=0
L=0
N=0
20 NP=N+1
LP=L+1
651 IF(NGG-2)365,366,365
366 DETER=PO(LP)*LAMBDA(NCUT)
DELTAB(LP,NP)=SPACE(N,L,SIGO,DETER,DELTAB(L,N),DELTAB(LP+1,N),SIGM
1AT(NCUT))
365 SIGMAG=SIGMAT(NGG)
OTERM=XLG*PO(LP)
STERM=OTERM+INTEG(LP,NP)
BSCAT(LP,NP)=SPACE(N,L,SIGO,STERM,BSCAT(L,N),BSCAT(LP+1,N),SIGMAG)
1/(1.-H*PLNK(LP)/SIGMAG)
BONE(LP,NP)=SPACE(N,L,SIGO,OTERM,BONE(L,N),BONE(LP+1,N),SIGMAG)
BONEP(LP,NP)=BSCAT(LP,NP)-BONE(LP,NP)
26 IF(N-NMAX)16,17,17
16 IF(L)19,19,18
18 L=L-1

```



```

N=N+1
GO TO 20
19 LL=LL+1
NN=NN+1
L=LL
N=NN
GO TO 20

C
17 CONTINUE

C
C USE OF ARRAY FOR MOMENTS STORAGE REDUCES RUN TIME
C

IF(NGG .LT. NDL) GO TO 765
DO 762 LP=1,LMAXP
DO 762 NP=1,NMAXP
762 ARRAY(LP,NP,G)=BSCAT(LP,NP)
G=INC(G)
IF(NGG .LT. NDL*24) GO TO 765
ASSIGN 761 TO IGO
GO TO 766
765 WRITE(9)NGG,((BSCAT(LP,NP),LP=1,LMAXP),NP=1,NMAXP)
766 IF(NGG .LT. NOUT) GO TO 754
NOUT=NOUT+10
WRITE(8)NGG,((BONEP(LP,NP),LP=1,LMAXP),NP=1,NMAXP)
ENERGY=FACTOR/LAMBDA(NGG)
430 CONTINUE
754 IF(NGG .LT. NRIGGP) GO TO 361
REWIND 8
126 DO 438 NG=1,33
DO 438 IY=1,5
DO 438 LP=1,10
DO 780 NP=1,19
780 A(LP,NP)=0.
438 SUMN(LP,IY,NG)=0.

C
C $$$$ $$$$
C BEGIN PHASE II
C $$$$ $$$$
C
C RECONSTRUCTION OF THE PHOTON DENSITY DISTRIB FROM ITS
C MOMENTS BY THE POLYNOMIAL METHOD
C
624 NGCUT=(NCUT-1)/10

C
C *****
C
C NMU= ANGULAR VARIABLES (COS(THETA) )
C NYP= NUMBER OF SPACE POINTS (MEAN FREE PATHS)
C
READ(5,1003)(X4U(MU),MU=1,NMU)
READ(4,1004)(Y(IY),IY=1,NYP)
IF(EOF(4) .NE. 0.) GO TO 500

C
C *****

```



```

DO 44 MJ=1,NMU
PMU(1,MJ)=1.
44 PMU(2,MJ)=XMU(MJ)
412 IND=2
NUNIT=8
C
C UNCOLLIDED PHOTON DENSITY
C
630 DO 48 IY=1,NYP
YIY=Y(IY)
VIRGIN(IY)=QZERO*EXP(-YIY)*(SIGO/YIY)**2/(CLITE*FORPIE)
48 CONTINUE
C
C ONCE-SCATTERED PHOTON DENSITY
C
GARB= QZERO*SIGO/(CLITE*FORPIE )
CALL FIRST
NGST=NGCUT
ASSIGN 631 TO KST
GO TO 630
631 CONTINUE
DO 710 NG=1,NGCUT
NGG=1+10*NG
ENERGY=FACTOR/LAMBDA(NGG)
710 CONTINUE
C
DO 414 IY=1,NYP
DO 414 NG=1,NGMAX
DO 424 MU=1,NMU
424 ONESCT(IY,NG,MU)=0.
414 SUMN(1,IY,NG)=0.
DO 415 NP=1,NMAXP
415 A(1,NP)=0.
C
408 LSTOP=NSTOP/2
IF(LEND.EQ.2) LSTOP=0
105 LSTOPP=LSTOP+1
NEXT=(NSTOP+2)/2
433 CONTINUE
436 CONTINUE
C
C RECONSTRUCTION OF THE LEGENDRE EXPANSION COEFFICIENTS
C
DO 140 LP=1,LSTOPP
L=LP-1
TWOL=L+
XL=L
101 NEND=NEXT-L
106 NSTARP=NSUMND(LP)
IF(NEND-NSTARP)139,138,188
188 DO 621 NP=NSTARP,NEND
READ(NUNIT)NBIGGP,LMAXP,NMAXP
N=NP-1

```

```

C      CALCULATE COEFFICIENTS OF THE EXPANSION POLYNOMIALS
C
      CALL WXPAN
43     DO 39 NG=1,NGMAX
        NGG=1+10*NG
C
C      BRING MULTIPLE-SCATTER MOMENTS IN FROM OFF LINE STORAGE
C
410    READ(NUNIT)NGS,((BSCAT(LPP,NPP),LPP=1,LMAXP),NPP=1,NMAXP)
      IF(NGS-NGG)410,409,409
409    XLAMG=LAMBDA(NGG)
      CALL BAITA
      DO 39 IY=1,NYP
        YIY=Y(IY)
        WSUM=0.
        DO 38 I=1,NP
          WSUM=WSUM+A(LP,I)*YIY**(I-1)
          BWPR=BETA*WSUM
39     SUMN(LP,IY,NG)=SUMN(LP,IY,NG)+BWPR
      REWIND NUNIT
621    CONTINUE
      NSUMND(LP)=NEND+1
C
C      OUTPUT SUMN FOR USE IN CONVERGENCE ANALYSIS
C
      DO 119 NGGG=1,NGMAX
        NGG=1+10*NGGG
119    CONTINUE
189    CONTINUE
      IF(NSTOP-NMAX)140,120,120
120    CONTINUE
      IF(L-1)46,46,45
45     LPJ=2
C
C      USING RECURSION RELATION FOR LEGENDRE POLYNOMIALS
C
      DO 47 MJ=1,NMU
        TEMP=PMU(2,MJ)
        PMU(2,MJ)=ALEGRG(XL,XMU(MJ),TEMP,PMU(1,MJ))
47     PMU(1,MJ)=TEMP
        GO TO 117
46     LPJ=LP
117    CONTINUE
      DO 742 IY=1,NYP
        YIY=Y(IY)
C
C      ALPHA=1 .... CALCULATING THE WEIGHT FUNCTION
C
      FACT=YIY*ALPHA
      WT=SIGOSQ*FACT**(L-2)*ALPHA**2
      WT=WT*EXP(-FACT)
      DO 411 NG=1,NGMAX
        NGG=1+10*NG

```

```

      WTSUM=WT*SUMN(LP,IY,NG)

C
C   RECONSTRUCTION OF THE ANGULAR DEPENDENCE ... THE FIRST TERM IN
C   THIS EXPANSION IS THE ALL-ANGLE DENSITY/(4*PIE)
C
      DO 40 MJ=1,NMU
      ONEP(IY,NG,MU)=ONEP(IY,NG,MU)+(TWOL+1.)*WTSUM*PMU(LPJ,MU)/FORPIE
40    CONTINUE
      IF(L.EQ.0)    SUMN(1,IY,NG)=WTSUM
411  CONTINUE
      IF(L.NE.0)    GO TO 742
      TSUM=(LAMBDA(11)-XLAMO)*SUMN(1,IY,1)/2.
      NG1=1
      NG2=2
      NGG1=11
      NGG2=21
740  DLM=LAMBDA(NGG2)-LAMBDA(NGG1)
      TSUM=TSUM+DLM*(SUMN(1,IY,NG1)/LAMBDA(NGG1)+SUMN(1,IY,NG2)/LAMBDA(N
1GG2))/2.
      IF(NG2.EQ.NGMAX)    GO TO 741
      NG1=NG2
      NG2=NG2+1
      NGG1=NGG2
      NGG2=NGG2+10
      GO TO 740

C
C   MULTIPLY-SCATTERED PHOTON ENERGY DENSITY

741  ALENGM(IY)=TSUM*FACTOR
742  CONTINUE
140  CONTINUE
      IF(NSTOP-NMAX)115,116,116
115  NSTOP=NSTOP+NADD
      NSTOPP=NSTOP+1
      GO TO 408
116  CONTINUE
      DO 748 IY=1,NYP

C
C   COMBINE MULTIPLY-SCATTERED AND ONCE-SCATTERED PHOTON ENERGY
C   DENSITIES TO OBTAIN THE ENERGY DENSITY DUE TO ALL SCATTERED PHO-
C   TONS
C
748  ALENG(IY)=ALENG(IY)+ALENGM(IY)

C
C   CALCULATE UNCOLLIDED ENERGY DENSITY AND ENERGY DENSITY BUILD-UP
C   FACTOR
C
      DO 760 IY=1,NYP
      VIRGE=VIRGIN(IY)*EZERO
760  ALENGM(IY)=(ALENG(IY)+VIRGE)/VIRGE
      CONTINUE
989  WRITE(3,1103) (Y(IND),IND=1,NYP)
      WRITE(2,1101) (Y(IND),IND=1,NYP)

```

```

988 WRITE(6,1104) EZERO, (ALENGH(IND), IND=1, NYP)
   WRITE(2,1101) EZERO
   WRITE(2,1101) (ALENGH(IND), IND=1, NYP)
   JO=1
744 DO 145 NG=1, NGMAX
   NGG=1+10*NG
   XLAMG=LAMBDA(NGG)
   ENERGY=FACTOR/XLAMG
   IF(JO .EQ. 1) GO TO 745
   DO 746 IY=1, NYP
   IF(NG .LE. NGOUT) SUMN(1,IY,NG)=SUMN(1,IY,NG)+ALANG1(IY,NG)
746 CONTINUE
   GO TO 145
745 DO 743 IY=1, NYP
743 SUMN(1,IY,NG)=SUMN(1,IY,NG)*XLAMG**2/FACTOR
145 CONTINUE
   IF(JO .NE. 1) GO TO 747
   JO=2
   GO TO 744
747 CONTINUE
   ASSIGN 990 TO KST
   NGST=NGMAX
680 DO 124 NG=1, NGST
   NGG=1+10*NG
   ENERGY=FACTOR/LAMBDA(NGG)
   DO 124 MU=1, NMU
   ONEP(IY,NG,MU)=ONEP(IY,NG,MU)*FACTOR/(ENERGY**2)
124 CONTINUE
   GO TO KST, (990, 631)
990 RFWIND 5
999 CONTINUE
   WRITE(3,2013)
   WRITE(6,2013)
500 STOP
C
1100 FORMAT(F6.1)
1101 FORMAT(5F8.4)
1102 FORMAT(4H FOR, F7.1, 12H KEV, 1 HFP= , F7.3, 7H METERS)
1103 FORMAT(33X, 16H BUILT UP FACTORS, //, 10X, 11H ENERGY (KEV), 14X, 27H
1103 1REE-PATHS FROM SOURCE, /, 21X, 5(5X, F6.3))
1104 FORMAT(13X, F6.1, 4X, 5(2X, F9.4))
1105 FORMAT(15H THIS RUN IS AT, F7.0, 7H METERS)
C
1000 FORMAT(2(E14.7, 2X))
1001 FORMAT(3(I2, 2X))
1002 FORMAT(3(E12.5, 1X))
1003 FORMAT(12(F3.2, 1X))
1004 FORMAT(10F7.3)
1005 FORMAT(E12.5)
1007 FORMAT(I2)
1010 FORMAT(2A6, 4X, F4.0, 3X, F3.0, 3X, E13.7)
1011 FORMAT(3I4)
1012 FORMAT(F6.4, 7I4)

```



2000 FORMAT (/,22X,8H ONE MFP=,F7.3,6H METERS,/, (15X,5(5X,F7.3)))  
 2001 FORMAT (///,3H L=,I2)  
 2002 FORMAT ( 3X,E11.4,1X,5(1X,E11.4))  
 2004 FORMAT (14H COS(THETA)=MU,6X,11H FOR LAMBDA=,E12.5,9H (ENERGY=,E12.5  
 1,5H KEV),//)  
 2005 FORMAT (/,I3,2X,10E11.4,/, (5X,10E11.4))  
 2006 FORMAT (24X,38H VIRGIN COMPONENT OF THE PHOTON DENSITY,/,50H WAVELEN  
 1GTH(CU) MEAN-FREE-PATHS FROM SOURCE,/, (15X,5(5X,F7.3),/))  
 2008 FORMAT (24X,28H MULTIPLY-SCATTERED COMPONENT,/,28X,32H PHOTONS PER(CM  
 1\*\*3\*KEV\*STERADIAN))  
 2009 FORMAT (///,24X,20H TOTAL PHOTON DENSITY)  
 2010 FORMAT (///,42H WAVELENGTH DISTANCE FROM SOURCE,/,50H (C  
 1COMPTON UNITS) (IN MFP'S OF VIRGIN PHOTONS))  
 2011 FORMAT (////,50H (4\*PI\*E\*\*2/(Y\*\*L\*EXP(-Y)))\*LEGENDRE EXPANSION COE  
 1FFICIENTS,/,15X,57H (FOR L=0, MOMENTS THRU N=  
 2,I2,17H WERE UTILIZED ))  
 2012 FORMAT (24X,34H ALL-ANGLE SCATTERED PHOTON DENSITY,/,24X,27H (PHOTONS  
 1 PER CM\*\*3 PER KEV),/,50H ENERGY(KEV) MEAN-FREE-PATHS FR  
 20M SOURCE,/, (15X,5(5X,F7.3),/))  
 2013 FORMAT (1H1)  
 2014 FORMAT (///,20X, 11H FOR LAMBDA=,E12.5,9H (ENERGY=,E12.5  
 1,5H KEV),//)  
 2015 FORMAT (20X,44H CALCULATION OF A PHOTON DENSITY DISTRIBUTION,///,24H  
 1 SOURCE/ POINT ISOTROPIC,/,1X,E14.7,22H PHOTONS PER SECOND AT,1X,E  
 214.7,4H KEV,///,60H MEDIUM/ INFINITE, HOMOGENEOUS, ISOTROPIC, COMPT  
 30N SCATTERER,/,9X,43H ICAL STANDARD ATMOSPHERE AT AN ALTITUDE OF ,E  
 412.5,7H METERS,/,9X,18H PARTICLE DENSITY= ,E12.5,10H PER CM\*\*3,/,9X  
 5,14H CONSTITUENTS/ ,7X,41H ATOM DENSITY ELECTRON DENSITY  
 6)  
 2016 FORMAT (15X,2A6,7X,E13.7,11X,E13.7)  
 2017 FORMAT (9X,43H THE MEAN-FREE PATH OF UNCOLLIDED PHOTONS IS,F7.3,7H M  
 1ETERS,/,  
 2 82X,5H TOTAL,/,30X,12H ENERGY (KEV),8X,  
 316H WAVELENGTH (CU)\*,11X,22H CROSS-SECTION (CM\*\*2),/)  
 2018 FORMAT (24X,I3,3X,3(E12.5,12X))  
 2019 FORMAT (50H \* 1 CU (COMPTON UNIT) =COMPTON WAVELENGTH OF THE ELEC  
 1TRON,/,38H ENERGY(KEV)=511.006/WAVELENGTH(CU))  
 2020 FORMAT (///,35X,46H MOMENTS OF THE LEGENDRE EXPANSION COEFFICIENTS,/  
 1 ,5X,65H (THOSE FOR N-L GREATER  
 6 THAN ZERO OR ODD HAVE NOT BEEN CALCULATED),/,50X,10H (N VS ))  
 2021 FORMAT (///,31H FOR MULTIPLY-SCATTERED PHOTONS)  
 2022 FORMAT (///,26H FOR ALL SCATTERED PHOTONS)  
 2023 FORMAT (24X,21H ONE-SCATTER COMPONENT,/,28X,32H PHOTONS PER(CM\*\*3\*KEV  
 1\*STERADIAN))  
 2024 FORMAT (18X,20H ONE-SCATTER CUT-OFFS,///,43H WAVELENGTH MU  
 1 ,//)  
 2027 FORMAT (35H ANALYTICAL ALL-ANGLE FIRST SCATTER,//)  
 2031 FORMAT (47H ALL-ANGLE, ALL-ENERGY SCATTER--KEV/CM\*\*3,/,5(2X,E  
 114.7))  
 2034 FORMAT (24X,43H ALL-ANGLE MULTIPLY-SCATTERED PHOTON DENSITY,/, (15X,5  
 1(5X,F7.3),/))  
 2035 FORMAT (///,44H ENERGY BUILD-UP FACTORS AT THE SPACE POINTS,/,14X,  
 15(1X,E11.4))  
 2040 FORMAT (16A5)



```
041 FORMAT(15A5,///)
END
```

C  
C  
C  
C

```
SUBROUTINE SIG(ENERGY,SIGMA)
COMMON PHOT(3,40),ENERG(3,40),INCO(3,40),ETA(3,17),CAPK(3,17),DN(3
1),DNZ(3),NXS,NEL,TOLE,TOLK,PIE,RZERO,LMAX,XMUMU,XMULAM,TEMP,YIY,DM
2U,SIGMAS,SINTHL,STGO,ONE,XLNCK,L,N,LP,NP,XLAMG,BETA,DZERO,
3NTRANS,NMU,XLAM0,GARB,NYP,NCUT,FACTOR,BSCAT(10,19),
5SIGMAT(331),LAMBDA(331),ONESCT(5,33,21),ALANG1(5,33),ALENG(5),XMU(
621),Y(5),PMU(2,21),VIRGIN(5),ALENG4(5),A(10,19)
REAL INCO,INCOH
```

C  
C  
C

```
ARITHMETIC STATEMENT FUNCTION FOR LOG-LOG INTERPOLATION
```

```
ALINTP(X,X1,Y1,X2,Y2)=EXP(ALOG(Y1)+ALOG(X/X1)*ALOG(Y2/Y1)/ALOG(X2/
1X1))
```

C

```
SIGMA=0.
DO 58 I=1,NFL
CONVF=DN(I)*1.E-24
IF(ENERGY-TOLF)52,62,63
62 PHOTO=PHOT(I,1)*CONVF
INCOH=0.
GO TO 68
63 DO 66 K=2,NXS
IF(ABS(ENERGY-ENERG(I,K))-TOLE)65,65,64
64 IF(ENERGY-ENERG(I,K))67,65,66
65 PHOTO=PHOT(I,K)*CONVF
INCOH=INCO(I,K)*CONVF
GO TO 68
66 CONTINUE
67 PHOTO=CONVF*ALINTP(ENERGY,ENERG(I,K-1),PHOT(I,K-1),ENERG(I,K),PHOT
1(I,K))
INCOH=CONVF*ALINTP(ENERGY,ENERG(I,K-1),INCO(I,K-1),ENERG(I,K),INCO
1(I,K))
68 SIGMA=SIGMA+PHOTO+INCOH
RETURN
END
```

C  
C  
C  
C

```
SUBROUTINE AKERN(AKERNL,XLP,XL)
COMMON PHOT(3,40),ENERG(3,40),INCO(3,40),ETA(3,17),CAPK(3,17),DN(3
1),DNZ(3),NXS,NEL,TOLE,TOLK,PIE,RZERO,LMAX,XMUMU,XMULAM,TEMP,YIY,DM
2U,SIGMAS,SINTHL,STGO,ONE,XLNCK,L,N,LP,NP,XLAMG,BETA,DZERO,
3NTRANS,NMU,XLAM0,GARB,NYP,NCUT,FACTOR,BSCAT(10,19),
5SIGMAT(331),LAMBDA(331),ONESCT(5,33,21),ALANG1(5,33),ALENG(5),XMU(
621),Y(5),PMU(2,21),VIRGIN(5),ALENG4(5),A(10,19)
ALINTP(X,X1,Y1,X2,Y2)=EXP(ALOG(Y1)+ALOG(X/X1)*ALOG(Y2/Y1)/ALOG(X2/
1X1))
```

```

      IF(XL-XLP-2.00001) 85,85,6
85  IF(XL .GT. XLNCK) GO TO 5
853 R=XLP/XL
      D=XL-XLP
      DNZK=0.
      DO 854 I=1,NEL
854 DNZK=DNZK+DN7(I)
      GO TO 55
5  IF(ABS(XL-XLP)-1.E-05) 6,6,53
6  AKERNL=0.
      RETURN
53 R=XLP/XL
      D=XL-XLP
      DUMMY=137.*SORT(1.+R*(R+2.+D+D))/XLP
      IF(DUMMY-TOLK) 6,6,55
55 DNZK=0.
      DO 54 I=1,NEL
C
C  INTERPOLATION TO FIND THE CORRECTION FACTOR (CAPKAY)
C
      DO 57 K=2,17
      IF(ABS(DUMMY-ETA(I,K))-TOLK) 58,58,59
59 IF(DUMMY-ETA(I,K)) 60,58,57
57 CONTINUE
60 CAP1=CAPK(I,K-1)
      CAP2=CAPK(I,K)
      IF(CAP1-CAP2) 61,61,61
61 CAPKAY=ALINTP(DUMMY,ETA(I,K-1),CAP1,ETA(I,K),CAP2)
      GO TO 54
58 CAPKAY=CAPK(I,K)
54 DNZK=DN7K+DN7(I)*CAPKAY
56 AKERNL=PIE*RZERO R**2*(R+XL/XLP-D-D*D)*DNZK
      RETURN
      END
C
C
C
      SUBROUTINE POLKER(P,XLAMP,XLAMG)
      COMMON PHOT(3,40),ENERG(3,40),INCO(3,40),ETA(3,17),CAPK(3,17),DN(3
1),DNZ(3),NXS,NEL,TOLE,TCLK,PIE,RZERO,LMAX,XHUMU,XMULAM,TEMP,YIY,DY
2U,SIGMAG,SINTHL,SIGC,ONF,XLNCK,L,N,LP,NP,XXXXX,BETA,DZERO,
3NTRANS,NMU,XLAMG,GARB,NYP,NCUT,FACTOR,3SCAT(10,19),
5SIGMAT(331),LAMGDA(331),ONESCT(5,33,21),ALANG1(5,33),ALENG(5),XMU(
621),Y(5),PHI(2,21),VIRGIN(5),ALENGH(5),A(10,19)
      DIMENSION P(20)
      CALL AKERN(P(1),XLAMP,XLAMG)
      ARG=1.+XLAMP-XLAMG
      P(2)=P(1)*ARG
      DO 184 L=2,LMAX
      XL=L
184 P(L+1)=((2.*XL+1.)*ARG*P(L)-XL*P(L-1))/(XL+1.)
      RETURN

```

C  
C  
C  
END

SUBROUTINE ONCE  
COMMON PHOT(3,40),ENERG(3,40),INCO(3,40),FTA(3,17),CAPK(3,17),DN(3  
1),DNZ(3),NXS,NEL,TOLE,TOLK,PIE,RZERO,LMAX,XMUMU,XMULAM,TEMP,YIY,DM  
2U,SIGMAG,SINTHL,SIGO,ONE,XLNCK,L,N,LP,NP,XLAMG,BETA,ZZERO,  
3NTRANS,NMU,XLAMO,GARB,NYP,NCUT,FACTOR,BSCAT(10,19),  
5SIGMAT(331),LAMBDA(331),ONESCT(5,33,21),ALANG1(5,33),ALENG(5),XMU(6  
21),Y(5),PMU(2,21),VIRGIN(5),ALENGM(5),A(10,19)  
XM=XMUMJ  
IF(XMUMU.EQ.1.) XMUMU=0.99999  
IF(XMUMU.LT.XMULAM) GO TO 488  
SINTHR=SQRT(ABS(1.-XMUMU\*\*2))  
ONE=TEMP\*EXP(-YIY\*(SINTHR+SIGMAG\*(XMUMU\*SINTHL-XMULAM\*SINTHR)/SIGO  
1)/SINTHL)/SINTHR  
XMUMU=XM  
RETURN  
488 ONE=0.  
RETURN  
END

C  
C  
C  
C

SUBROUTINE FIRST  
COMMON PHOT(3,40),ENERG(3,40),INCO(3,40),FTA(3,17),CAPK(3,17),DN(3  
1),DNZ(3),NXS,NEL,TOLE,TOLK,PIE,RZERO,LMAX,XMUMU,XMULAM,TEMP,YIY,DM  
2U,SIGMAG,SINTHL,SIGO,ONE,XLNCK,L,N,LP,NP,XLAMG,BETA,ZZERO,  
3NTRANS,NMU,XLAMO,GARB,NYP,NCUT,FACTOR,BSCAT(10,19),  
5SIGMAT(331),LAMBDA(331),ONESCT(5,33,21),ALANG1(5,33),ALENG(5),XMU(6  
21),Y(5),PMU(2,21),VIRGIN(5),ALENGM(5),A(10,19)  
REAL LAMBDA  
DO 488 IY=1,NYP  
YIY=Y(IY)  
ALEN=0.  
NG=1  
NGG=1  
NGC=11  
730 ASSIGN 731 TO JON  
XLAMG=LAMBDA(NGG)  
SIGMAG=SIGMAT(NGG)  
IF(NGG.EQ.1) XLAMG=XLAMO+.0001  
IF(NGG.EQ.NCUT) XLAMG=LAMBDA(NCUT)-.001  
CALL AKERN(XKER,XLAMO,XLAMG)  
XMULAM=1.-XLAMG\*XLAMO  
SINTHL=SQRT(ABS(1.-XMULAM\*\*2))  
TEMP1=GARB\*XKER/SINTHL  
TEMP=TEMP1/YIY  
ASSIGN 703 TO ION  
ONETOT=0.  
MU=1

XMU1=1.  
 XMUMU=1.  
 DMU=0.0001

C  
 C  
 C  
 C

CALCULATION OF ANGLE-DEPENDENT ONCE-SCATTERED AND INTEGRATION  
 TO FIND ALL-ANGLE DENSITY

CALL ONCE  
 WON=ONE  
 701 XMUMU=XMUMU-DMU  
 IF(XMUMU .LE. XMJLAM) GO TO ION,(703,702)  
 705 CALL ONCE  
 ONETOT=ONETOT+DMU\*(ONE+WON)/2.  
 IF(XMUMU .LE. 0.99901) DMU=0.001  
 IF(XMUMU .LE. 0.99001) DMU=0.01  
 IF(XMUMU .LE. 0.90001) DMU=0.02  
 IF(XMUMU .LE. 0.80001) DMU=0.10  
 707 IF(NGG .NE. NGC) GO TO 700  
 IF(ABS(XMU(MU)-XMU1) .GT. 0.0001) GO TO 700  
 ONESCT(IY,NG,MU)=WON/(2.\*PIE)  
 IF(MU .EQ. NMU) GO TO 706  
 MU=MU+1  
 700 WON=ONE  
 XMU1=XMUMU  
 GO TO 701  
 703 XMUMU=XMUMU+DMU  
 IF(DMU .GT. 0.01) DMU=0.01  
 CHECK=ABS(XMUMU-XMULAM)  
 IF(CHECK .LT. 0.01001) DMU=0.001  
 IF(CHECK .LT. 0.00101) DMU=CHECK  
 XMUMU=XMUMU-DMU  
 IF(DMU .GE. CHECK) ASSIGN 702 TO ION  
 GO TO 705  
 702 IF(NGG .NE. NGC) GO TO 498  
 XMUMU=XMU(MU)  
 CALL ONCE  
 GO TO 707  
 706 ALANG1(IY,NG)=ONETOT\*XLAMG\*\*2/FACTOR

C  
 C  
 C

FIND ALL-ANGLE ENERGY DENSITY DUE TO ONCE-SCATTERED PHOTONS

NG=NG+1  
 NGC=NGC+10  
 498 CONTINUE  
 GO TO JON,(731,732, 734,735,736,737)  
 731 ASSIGN 732 TO JON  
 NGG=NGG+1  
 ONET=ONETOT/XLAMG  
 DLM=LAMBDA(NGG)-XLAMG  
 GO TO 730  
 732 ALEN=ALEN+DLM\*(ONET+ONETOT/XLAMG)/2.  
 IF(NGG .LT. NTRANS) GO TO 731  
 733 NGG=NGG+10



```

      ONET1=ONETOT/XLAMG
      ASSIGN 734 TO JON
      GO TO 730
734  ASSIGN 735 TO JON
      ONET2=ONETOT/XLAMG
      NGG=NGG+10
      GO TO 730
735  ASSIGN 736 TO JON
      ONET3=ONETOT/XLAMG
      NGG=NGG+10
      DLM=LAMBDA(NGG)-XLAMG
      GO TO 730
736  ASSIGN 737 TO JON
      ALEN=ALEN+      (ONET1+3.*(ONET2+ONET3)+ONETOT/XLAMG)*3.*DLM/8.
738  NGG=NGG+2
      DLM=LAMBDA(NGG)-XLAMG
      ONET=ONETOT/XLAMG
      GO TO 730
737  ALEN=ALEN+      (ONET+ONETOT/XLAMG)*DLM/2.
      IF(NGG.LT. NCUT) GO TO 738
      ALENG(IY)=ALEN*FACTOR
488  CONTINUE
      RETURN
2025 FORMAT(1X,E12.5,5X,F6.3)
      END

```

C  
C  
C  
C

```

SUBROUTINE WXPAN
COMMON PHOT(3,40),ENERG(3,40),INCO(3,40),ETA(3,17),CAPK(3,17),DN(3
1),DNZ(3),NXS,NEL,TOLE,TOLK,PIE,RZERO,LMAX,XMU4U,XMULAM,TEMP,YIY,DM
2U,SIGMAS,SINTHL,SIGO,ONE,XLNCK,L,N,LP,NP,XLAMG,BETA,DZERO,
3NTRANS,XMU,XLAMG,GARR,NYP,NCUT,FACTOR,SCAT(10,19),
5SIGHAT(331),LAMBDA(331),ONESCT(5,33,21),ALANG1(5,33),ALENG(5),XMU(
621),Y(5),PMU(2,21),VIRGIN(5),ALENGM(5),A(10,19)
      IF(N)41,41,42
41  A(LP,1)=1.
      RETURN
42  NIP=N
      N=N-1
      TWONP=2*NIP
      CON=2*(L+N)+1
      A(LP,NIP+1)=-A(LP,NIP)/TWONP
      IF(N)185,185,185
186  DO 37 I=1,N
      IM=I-1
      XI=N-IM
      II=NIP-IM
37  A(LP,II)=((CON+XI)*A(LP,II)-A(LP,II-1))/TWONP
185  A(LP,1)=CON*A(LP,1)/TWONP
      N=N+1
      RETURN
2005 FORMAT(/,I3,2X,10F11.4,/,/(5X,10E11.4))

```



END

C  
C  
C  
C

SUBROUTINE BAITA

COMMON PHOT(3,40),ENERG(3,40),INCO(3,40),FTA(3,17),CAPK(3,17),DN(3  
1),DNZ(3),NXS,NFL,TOLE,TCLK,PIE,RZERO,LMAX,XMUMU,XMULAM,TEMP,YIY,DM  
20,SIGMAG,SINTHL,SIGO,ONE,XLNCK,L,N,LP,NP,XLAMG,BETA,QZERO,  
3NTRANS,NMU,XLAM0,GARB,NYP,NCUT,FACTOR,3SCAT(10,19),  
5SIGMAT(331),LAMBDA(331),ONESCT(5,33,21),ALANG1(5,33),ALENG(5),XMU(6  
21),Y(5),PHU(2,21),VIRGIN(5),ALENG4(5),A(10,19)

CLITE=2.997925E+10

SUMJN=0.

DO 36 JP=1,NP

J=JP-1

LP2J=LP+J+J

TERMJ=TORIAL(LP2J-1)\*BSCAT(LP,LP2J)

TERMJ=TERMJ/TORIAL(J+J+L+L)

TERMJ=TERMJ/TORIAL(N-J)

TERMJ=TERMJ/TORIAL(J)

JJ=J/2

IF(JJ\*2.EQ.J) GO TO 36

TERMJ=-TERMJ

36 SUMJN=SUMJN+TERMJ

BETA=QZERO\*TORIAL(N)\*SUMJN/(CLITE\*XLAMG)

RETURN

END

C  
C  
C  
C

FUNCTION SPACE(N,L,SIGO,DETERM,DE1,DE2,SIGH)

XL=L

XN=N

LP=L+1

XLP=LP

LEND=1

LLND=1

TERM=0.

IF(L-N)550,551,551

551 LEND=2

550 IF(L)650,650,651

650 LLND=2

651 IF(N)134,134,133

133 GO TO(652,653),LLND

652 TERM=XL\*(XN+XLP)\*DE1

653 GO TO(552,553),LEND

552 TERM=TERM+XLP\*(XN-XL)\*DE2

553 DETERM=DETERM+TERM\*SIGO/(XN\*(XL+XLP))

134 SPACE=DETERM/SIGH

RETURN

END

C  
C

```
FUNCTION INC(K)
K=K+1
IF(K.GT. 25)  K=1
INC=K
RETURN
END
```

C  
C  
C

```
FUNCTION TORIAL(K)
IF(K)32,32,33
32  TORIAL=1.
    RETURN
33  KTOR=1
    DO 34  IT=1,K
34  KTOR=KTOR*IT
    TORIAL=KTOR
    RETURN
END
```

### VITA

Gary Michael Kalansky was born on 14 September 1955 in Pittsburgh, Pennsylvania, the son of Michael Kalansky and Helen Jastszemska Kalansky. He graduated with honors from Steel Valley High School, Munhall Pennsylvania in June 1973. He graduated Cum Laude from Duquesne University, Pittsburgh, Pennsylvania in May 1977 receiving a Bachelor of Science in Physics. He received a reserve commission as a Second Lieutenant in June 1977 and entered the Air Force Institute of Technology in August 1977.

Permanent Address:      143 Bellwood Drive  
                                 Mumhall, Pennsylvania 15120

UNCLASSIFIED

SECURITY CLASSIFICATION OF THIS PAGE (When Data Entered)

REPORT DOCUMENTATION PAGE		READ INSTRUCTIONS BEFORE COMPLETING FORM
1. REPORT NUMBER AFIT/GNE/PH/78D-18	2. GOVT ACCESSION NO.	3. RECIPIENT'S CATALOG NUMBER
4. TITLE (and Subtitle)  X-RAY BUILD-UP FACTORS		5. TYPE OF REPORT & PERIOD COVERED  MS Thesis
7. AUTHOR(s)  Gary M. Kalansky 2nd Lt.		6. PERFORMING ORG. REPORT NUMBER
9. PERFORMING ORGANIZATION NAME AND ADDRESS  Air Force Institute of Technology (AFIT-EN) Wright-Patterson AFB, Ohio 45433		8. CONTRACT OR GRANT NUMBER(s)
11. CONTROLLING OFFICE NAME AND ADDRESS  Air Force Institute of Technology (AFIT/EN) Wright-Patterson AFB OH 45433		10. PROGRAM ELEMENT, PROJECT, TASK AREA & WORK UNIT NUMBERS
14. MONITORING AGENCY NAME & ADDRESS (if different from Controlling Office)		12. REPORT DATE December 1978
		13. NUMBER OF PAGES 179
		15. SECURITY CLASS. (of this report)  Unclassified
		15a. DECLASSIFICATION/DOWNGRADING SCHEDULE
16. DISTRIBUTION STATEMENT (of this Report)  Approved for public release; distribution unlimited		
17. DISTRIBUTION STATEMENT (of the abstract entered in Block 20, if different from Report)		
18. SUPPLEMENTARY NOTES  Approved for public release; IAW AFR 190-17  JOSEPH P. HIPPS, Major, USAF Director of Information		
19. KEY WORDS (Continue on reverse side if necessary and identify by block number)  Photon Transport Build-up Factors X-ray Transport Moments Method Atmospheric Radiation Transport		
20. ABSTRACT (Continue on reverse side if necessary and identify by block number)  This report is a compilation of time integrated x-ray energy build-up factors from a monoenergetic point source in infinite homogeneous air. These factors were computed by the use of PHOTDIS, a moments method computer code, and performed on a CDC 6600. This code was chosen after a literature search and a review of many computer models. Energies from 12 keV to 1000 keV and ranges from 1 mean-free-path to 15 mean-free-paths are considered. All results are presented on semi-log graphs with each graph containing one energy. This program is estimated to have an error of at most 20%. The results are		

DD FORM 1 JAN 73 1473

EDITION OF 1 NOV 65 IS OBSOLETE

UNCLASSIFIED

SECURITY CLASSIFICATION OF THIS PAGE (When Data Entered)



UNCLASSIFIED

SECURITY CLASSIFICATION OF THIS PAGE(When Data Entered)

compared to Monte Carlo and Discrete Ordinates calculations. Even though the moments calculations do not completely agree with any of the Monte Carlo calculations, the moments calculation agree with the average of the Monte Carlo calculations. A complete derivation of the moments method from the Boltzmann Transport Equation is also included.

UNCLASSIFIED

SECURITY CLASSIFICATION OF THIS PAGE(When Data Entered)